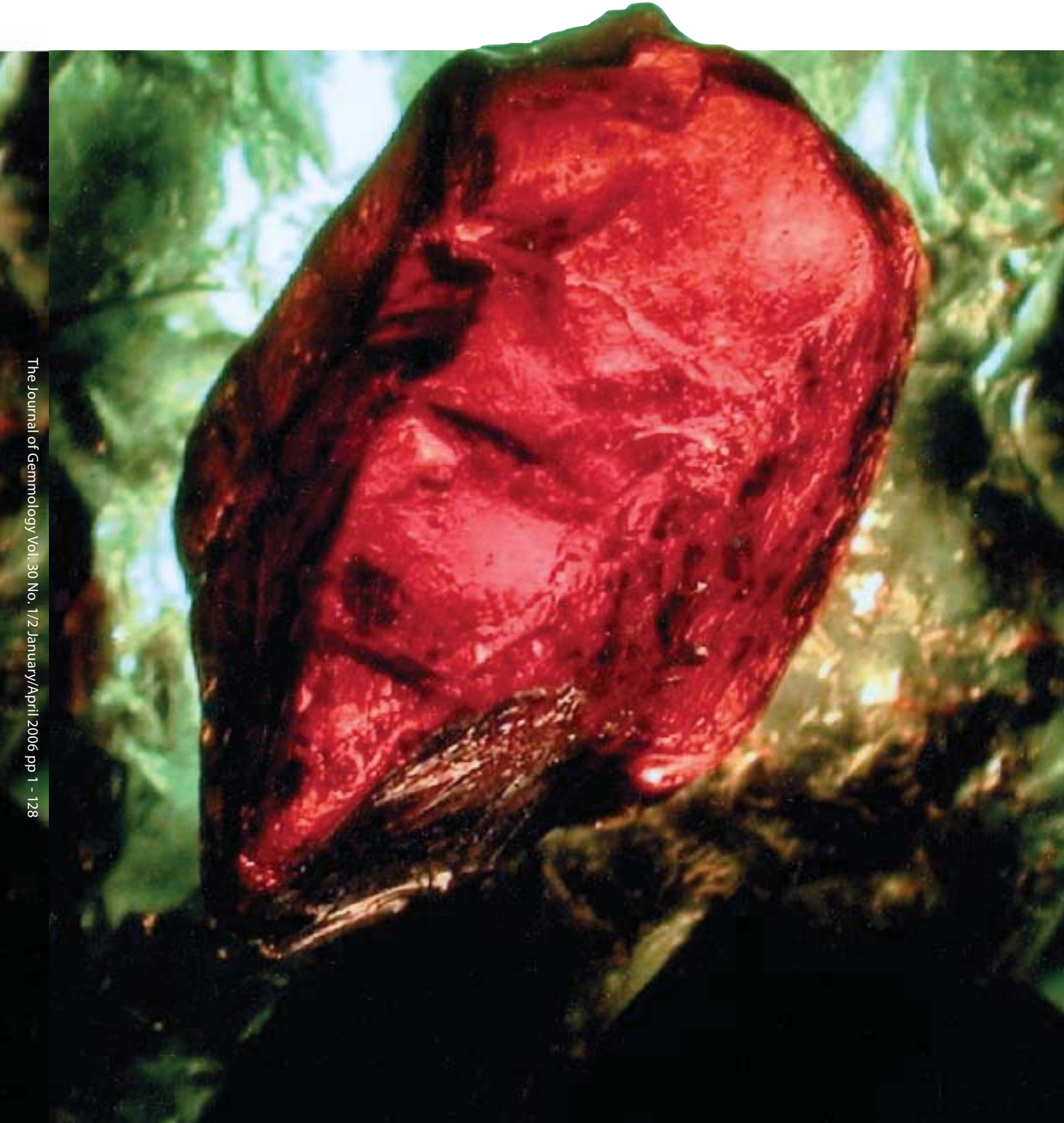




The Journal of
Gemmology

Volume 30 No. 1/2
January/April 2006



The Journal of Gemmology Vol. 30 No. 1/2 January/April 2006 pp 1 - 128

The Gemmological Association and Gem Testing Laboratory of Great Britain

Registered Charity No. 1109555

27 Greville Street, London EC1N 8TN

Tel: +44 (0)20 7404 3334 | Fax: +44 (0)20 7404 8843

e-mail: information@gem-a.info | Website: www.gem-a.info

President: E A Jobbins

Vice-Presidents: N W Deeks, R A Howie, D G Kent

Honorary Fellows: Chen Zhonghui, R A Howie, K Nassau

Honorary Life Members: H Bank, D J Callaghan, E A Jobbins, J I Koivula, I Thomson, H Tillander

Chief Executive Officer: J M Ogden

Council: A T Collins – Chairman, P Barthaud, S Burgoyne, T M J Davidson, S A Everitt, E A Jobbins, M McCallum, M J O'Donoghue, E Stern, P J Wates

Members' Audit Committee: A J Allnutt, J W Collingridge, P Dwyer-Hickey, J Greatwood, G M Green, B Jackson, D J Lancaster, C H Winter

Branch Chairmen: Midlands – P Phillips, North East – M Houghton and S North, North West – D M Brady, Scottish – B Jackson, South West – R M Slater

Examiners: C Abbott, A J Allnutt MSc PhD FGA, L Bartlett BSc MPhil FGA DGA, He Ok Chang FGA DGA, Chen Meihua BSc PhD FGA DGA, Prof A T Collins BSc PhD, A G Good FGA DGA, D Gravier FGA, J Greatwood FGA, S Greatwood FGA DGA, G M Green FGA DGA, G M Howe FGA DGA, B Jackson FGA DGA, B Jensen BSc (Geol), T A Johnes FGA, L Joyner PhD FGA, H Kitawaki FGA CGJ, R J Lake FGA DGA, Li Li Ping PhD FGA DGA, M A Medniuk FGA DGA, T Miyata MSc PhD FGA, C J E Oldershaw BSc (Hons) FGA DGA, H L Plumb BSc FGA DGA, N R Rose FGA DGA, R D Ross BSc FGA DGA, J-C Ruffli FGA, E Stern FGA DGA, S M Stocklmayer BSc (Hons) FGA, Prof I Sunagawa DSc, M Tilley GG FGA, R K Vartiainen FGA, P Vuillet à Ciles FGA, C M Woodward BSc FGA DGA

The Journal of Gemmology

Editor: Dr R R Harding

Assistant Editors: M J O'Donoghue, P G Read

Associate Editors: Dr C E S Arps (Leiden), G Bosshart (Horgen), Prof A T Collins (London), J Finlayson (Stoke on Trent), Dr J W Harris (Glasgow), Prof R A Howie (Derbyshire), E A Jobbins (Caterham), Dr J M Ogden (London), Prof A H Rankin (Kingston upon Thames), Dr J E Shigley (Carlsbad), Prof D C Smith (Paris), E Stern (London), Prof I Sunagawa (Tokyo), Dr M Superchi (Milan)

Production Editor: M A Burland

The Usambara effect and its interaction with other colour change phenomena

Asbjørn Halvorsen

NORPLAN, Underground Construction Technology Division, Ski, Norway
Email: asbjorn.halvorsen@norplan.com

Abstract: *The Usambara effect, colour change with change in path length of light through a material, is found to interact with the alexandrite effect, colour change with change in spectral distribution of light. This article provides insight into the interaction between the Usambara effect and other colour change phenomena. In colour change studies of the past more focus has been placed on the alexandrite effect, but old studies also show awareness of the Usambara effect. This contribution provides a review of previous work and updating of earlier interpretation of this effect in the light of new observations. Epidote and kornepupine are introduced as new colour change minerals, and the Usambara effect is discussed in synthetic alexandrite and chlorophyll.*

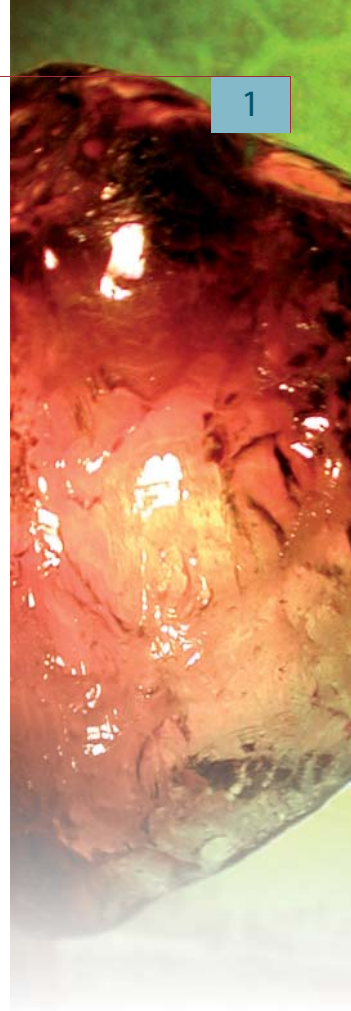
Keywords: *absorption-modified dispersion, alexandrite effect, concentration effect, fluorescence, thermochromy, Usambara effect*

Introduction

“Let us rather recognise that even relatively simple observations can still provide us with unexpected and awe-inspiring phenomena.”

This statement by Dr Kurt Nassau in the preface to the 2001 edition of *Physics and Chemistry of Color* referred to the Usambara effect and some other new discoveries. The Usambara effect is named after the verdant Usambara Mountains, south of the Uмба area in Tanzania, and was introduced by Halvorsen and Jensen (1997a,b). They had studied a peculiar colour change from green to red in chromiferous tourmaline from Nchongo in the Uмба area (Figure 1) and

concluded that this depended primarily on the path length of light through the stone, modified by type of illumination and varying with pleochroic directions. This effect seemed to be hardly known to gemmologists. Nassau responded to the article by Halvorsen and Jensen (1997a) with a Letter to the Editor (Nassau, 1997). He advised that this effect was well known in the field of organic dyes and expressed his surprise that it had not been observed previously in minerals. Further, he expressed expectation that now, when attention had been drawn to these effects, they would very likely also be



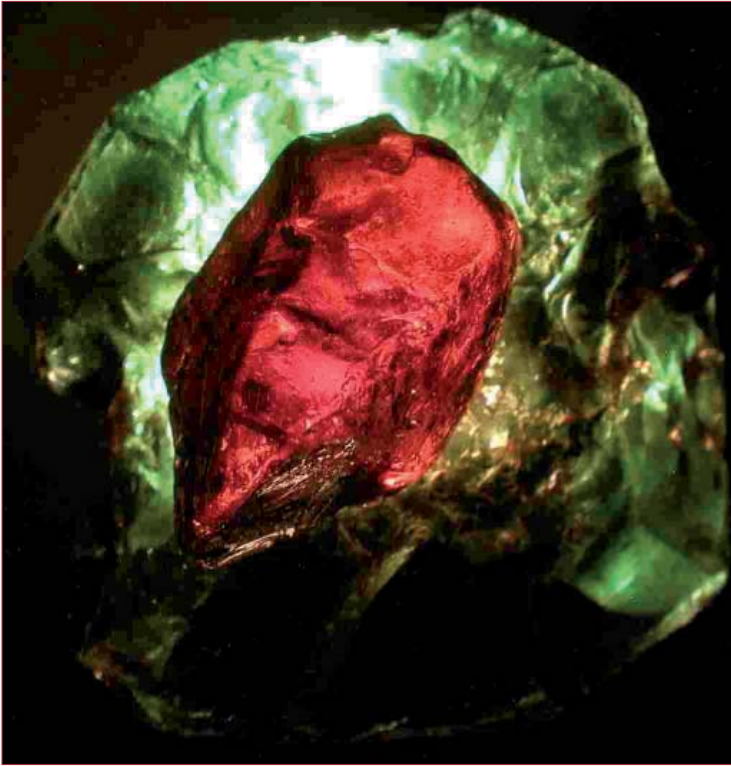


Figure 1: A green UE tourmaline turns red when placed on top of another green UE tourmaline.

observed in other minerals. In a colorimetric study of the same tourmalines, Liu *et al.* (1999a) suggested that the Usambara effect is a complex phenomenon, including effects of both path length and type of illumination.

The optical behaviour of the Nchongo tourmalines is extreme. After having studied a cut stone from this locality, Nassau (*pers. comm.*, 2002) commented: "I cannot think of any other stone that would show such clear-cut contrasting colours." This colour change behaviour is also found in some other minerals and man-made materials, e.g. plastics (Nassau, 2001). Most striking is maybe the similarity with colour change found in chlorophyll – the main colorant in nature.

The aim of this paper is to place the Usambara effect in the wider context of other colour change phenomena and to update understanding of it by description and discussion of new observations. Much of this is based on a detailed study of Nchongo tourmaline, but first there is a review of previous investigations of colour change phenomena.

Colour change phenomena in minerals – previous investigations

Colour change effects are reversible effects where radical changes in colour (hue) of a mineral are observed as result of environmental changes. A common attribute for most colour change minerals is transmission spectra with two pronounced transmission peaks, i.e. dichromatic spectra. In this study, the following causes of colour change are discussed:

- | Change in spectral composition of light – *alexandrite effect*
- | Change in path length of light through a material – *Usambara effect*
- | Change in temperature – *thermochromy*
- | Change in the direction of light in relation to the optic axes of an anisotropic mineral – *pleochroism*
- | Change in concentration of light absorbing impurities – *concentration effect*

Throughout this paper UE is used as abbreviation for *Usambara effect* and AE for *alexandrite effect*.

Alexandrite effect (AE)

Gem minerals changing colour between daylight and incandescent light have been known and appreciated for centuries. Such colour change was first observed in a mineral found in the emerald mines at Tokowaia in the Urals (Wörth, 1842; Kokscharow, 1861). According to Gübelin and Schmetzer (1982) and other recent authors, alexandrite was discovered in 1830. Of the older authors, only Wörth (1842) seems to inform on when this happened: the mineral was first found in the Tokowaia mines in 1833. This was claimed to have happened on the birthday of Alexander Nikolajewitsch, later Tsar Alexander II, and the Finnish explorer and mineralogist Nils Nordenskiöld suggested that the new mineral be named *alexandrite*. The colours were described as emerald green in daylight and reddish violet in candlelight which were linked by Nordenskiöld to the red and green Russian military colours.

The name *alexandrite* was also used by Wörth, who examined the new mineral in St Petersburg in 1833 and found it to be chrysoberyl, a beryllium aluminium oxide (Wörth 1842; Kokscharow, 1861). Kokscharow gave Gustav Rose the credit for the first comprehensive crystallographic description of alexandrite (i.e. chrysoberyl). Rose (1842) described in detail the mineral deposits in the Urals. In an emerald green chrysoberyl he found dichroism to be influenced by type of light: in transmitted light a hyacinth colour was observed in one direction in the crystal. This colour was seen only in strong sunlight or candlelight, not in normal daylight. Wörth (1842) described observations done in overcast daylight: green colour in one direction and red perpendicular to this. He found that by changing the proportions of green and red in the light, the colour of the mineral changed. When illuminated by candle light or by a low sun, the red rays dominated the green rays and the observed colour was red. Both Rose and Wörth concluded that the chrysoberyl was coloured by chromium oxide. Chemical analyses by Awdejew (1842) showed a chromium oxide content of 0.36%.

Another mineral known for colour change (in addition to strong pleochroism) is tourmaline. Bank and Henn (1988) reported change from green in daylight to brownish red or red in artificial light in tourmalines from Tanzania, and although their searches for previous examples of tourmalines with the AE had proved fruitless, such tourmalines from the Urals had been described a century earlier by Cossa and Arzruni (1883). This tourmaline was found in chrome-iron deposits near Sysert, south of Yekaterinburg, associated with emerald, uvarovite, demantoid and a new mineral, chrome mica. The detailed description includes results of chemical, crystallographic and optical analyses. In daylight, prismatic crystals of tourmaline were yellowish brown when illuminated parallel to the optic axis and blue green perpendicular to this. In incandescent light the colours were orange reddish brown to ruby red and weak green, respectively. Cossa and Arzruni suggested

that the new tourmaline variety was a perfect counterpart to alexandrite; they also claimed that previously only alexandrite was known for such colour change. Gustav Rose had donated samples of Ural chromian tourmaline to the Museum of Natural History in Berlin in 1829, but did not observe the colour change behaviour in these. The relevant passage of Cossa and Arzruni (1883), translated from German, is:

“Two minerals that have been unknown till now deserve attention: a beautiful emerald green chrome mica and a deep green chrome tourmaline. The latter was certainly seen, collected and described by G. Rose, but the true nature of this remained however hidden for this sharp observer. Prof. Websky recognised at the first glance that this mineral contained chrome. This was also confirmed by the observation of the beautiful dichroism, till now only known for alexandrite, and the pronounced partial transparency for certain parts of the spectrum. This property was especially clear by use of lamp light; these red rays were transmitted nearly unimpaired in the tourmaline, which appeared intense ruby-red.”

The British Museum also received a sample of the Ural chromian tourmaline from Arzruni. Dunn (1977) examined this sample, a dravite with a Cr_2O_3 content of 5.96%, but did not comment on any colour change behaviour.

According to Gübelin and Schmetzer (1982), White *et al.* (1967) introduced the term *alexandrite effect*. This denotation had, however, already been used by Neuhaus (1960), who presented typical absorption spectra for several chromium-containing minerals, all with two absorption maxima, and classified them (*Figure 2*) as:

- 1 Red group, with absorption maximum I at ~ 540 to ~ 570 nm and maximum II at ~ 390 to ~ 415 nm, mainly *oxides*.
- 1 Green group, with maximum I at $> \sim 580$ to $> \sim 650$ nm and maximum II at $> \sim 420$ to $> \sim 460$ nm, mainly *silicates*.
- 1 Transition group, including AE minerals, with maxima in general located between the maxima of the red and green groups.

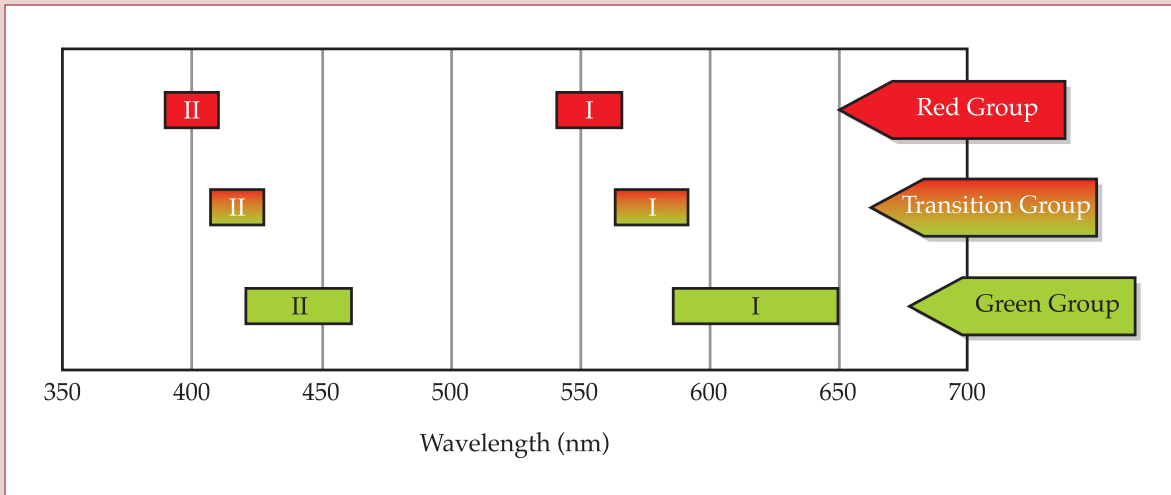


Figure 2: Chromium-containing minerals classified as three spectral groups according to Neuhaus (1960), with location of absorption maxima I and II for the three groups.

In 1970 Crowningshield reported a rare garnet from Tanzania, which was found to be an isomorphous mixture of pyrope and spessartine, and appeared blue-green in daylight and purple-red in incandescent light. However, garnets with green to red colour change were not as rare as Crowningshield suggested, as similar garnets had been found in the Czech Republic (Fiala, 1965) and Norway (Carstens, 1973).

In a study of colour change in man-made crystalline chromium compounds, White *et al.* (1967) found the AE in ruby with 20 wt% Cr_2O_3 , appearing pink in incandescent light and green in daylight. Schmetzer *et al.* (1980) described the AE in chrysoberyl, garnet, corundum and fluorite. Bank and Henn (1988) mentioned that such colour change was also known in alexandrite, garnet, corundum, spinel, zircon, fluorite, kyanite and diaspore. Bernstein (1982) described the AE in monazite from North Carolina, showing yellow-orange in daylight, reddish-orange in incandescent light and pale green in fluorescent light. He also listed other AE minerals, including coquimbite in addition to those listed by Bank and Henn (1988).

Liu *et al.* (1994, 191) described the AE as “change in colour appearance with differences in lighting” and stated that they had observed approximately 40 gem minerals displaying this behaviour. They introduced four categories of colour change that all met a

requirement of at least 20 calculated absolute hue-angle change between different light sources in the CIELAB colour space. This concept was further elaborated by Liu *et al.* (1999b).

Usambara effect (UE) Chrysoberyl and tourmaline

Early awareness of the UE is found in the descriptions by Haidinger (1849) and Kokscharow (1861) of Ural chrysoberyl. Haidinger observed the trichroic colours using a dichroscope loupe. In daylight, variations of green were observed, and under lamplight he described colour 1 (lightest tone) as orange-yellow, colour 2 (darkest tone) as emerald green and colour 3 (medium tone) as reddish violet. A remarkable observation was that the latter colour was dichromatic, i.e. having two colour maxima. In thin sections colour 3 was green with an addition of violet, and in thick sections reddish violet. Haidinger recorded the strange phenomenon of colour 2 also being green in lamplight, i.e. not influenced by change in illumination, but being dominated by the red with a lighter tone (see Discussions with Dr Kurt Nassau below). Also Cossa and Arzruni (1883) seemed to observe the UE. Their main concern in regard to colour change in the Ural tourmaline was change in pleochroic colours with type of illumination. They also described how the

pleochroic colours varied from thin to thick sections of the mineral, with reference to code numbers in Radde's International Colour Scale. Regrettably it has not been possible to trace illustrations or explanations for these colour codes.

The early researchers apparently had a good understanding of the factors affecting colour change in minerals, and of the interaction between these. Wörth (1842) concluded that chromium oxide was the colouring agent in alexandrite. He had found that a solution of chromium in hydrochloric acid or in sulphuric acid transmitted both green and red rays and had demonstrated for other researchers how the colour in crystallised bodies (presumably laboratory-grown crystals) coloured by chromium, was affected by pleochroism. According to Wörth, Nordenskiöld later found the same properties in the Ural chrysoberyl. Wörth also reported in detail how the pleochroic colours are influenced by type of illumination.

In a paper on colouring in minerals, Kennard and Howell (1941, 407) used the term 'polychromatism' with reference to "the fact that the hue and saturation of the colour, in isotropic as well as anisotropic materials, are dependent on both the concentration of the absorbing substance and the depth or thickness of the medium traversed." As an example of a strongly polychromatic mineral, they mentioned ferric oxide (hematite), with hues ranging from yellow through red to nearly black. They did not mention colour change caused by change in illumination. Polychromatism was the term used by Webster (1994) to describe green to red colour change in chrome alum solutions, caused by either increase in concentration or sample thickness. Haidinger (1849) and Kokscharow (1861) also used this denotation for a UE type of colour change in alexandrite.

Webster (1961) described tourmalines from the Gerevi Hills, Tanzania, which appeared red under a Chelsea colour filter. In a thorough description of the optical behaviour and physical properties of this mineral, he used the term '*dichromatism*' to describe the property such that in transmitted light, thinner sections of a dark stone appeared green and thicker

sections red. The depth of the red seen through a Chelsea filter, as well as the strength of dichroism, varied in proportion with the depth of the green. In a dark green stone, the thinner sections showed strong dichroism in light and dark green colours, while thicker sections showed light and dark red dichroic colours. Under a SW UV lamp the tourmaline showed mustard yellow fluorescence and under high intensity light a dim red glow. Webster did not comment on the influence of type of illumination on the colour change in these tourmalines. In 1997 Halvorsen and Jensen were not familiar with Webster's observations, but their observations (*op. cit.*, 1997a) were very similar. Based on spectral analyses, and in agreement with chemical analyses by Basset (1955), Webster concluded that the vanadium content exceeded that of chromium, and that the vanadium content in dark stones was higher than in light stones. Basset did not describe colour change in the tourmaline. This is understandable in view of the apparently poor quality of sample material, as indicated in his description. Bank and Henn (1988) referred to Webster (1961), but did not mention any colour change as a result of changes in path length. Also Crowningshield (1967) found that some very small Tanzanian chromian tourmaline samples appeared bright red under the Chelsea colour filter. On the basis of an absorption spectrum he inferred the presence of chromium. Crowningshield also did not observe any colour change, but his stones were very small. In a detailed description of many gem minerals from the Umba valley, Zwaan (1974) described a sample of emerald-green tourmaline from the Umba mine showing red in transmitted incandescent light but did not further explore the phenomenon. How can this pronounced colour change behaviour have avoided further focus in recent publications on gemstones from this region? UE tourmalines also occur in the John Saul ruby mine, Taita-Taveta District, Kenya (Simonet, 2000) which is located just north of the Umba area of Tanzania, about 95 km NNW of Nchongo. Emerald-green tourmalines with similar colour change behaviour have also been found in Madagascar (M.S. Krzemnicki, *pers. comm.*, 2004).

Garnet

Fiala (1965) described change from green in daylight to red-violet in incandescent light in pyropes from peridotites in the České Středočeské Mountains, close to Trebenice in the Czech Republic. The green colour in daylight was seen especially in small fragments – an observation indicating presence of the UE. C. Simonet (*pers. comm.*, 2000) observed the UE in garnets from Taita Hills, Kenya. He found that this type of colour change was much stronger in garnets than in tourmalines from this area, especially in daylight, and that many stones showed both AE and UE. In the trade, gem dealers he had met described the UE in many stones as dichroism and talked about dichroism in garnets.

Manson and Stockton (1984, 200) studied a selection of garnets exhibiting colour change between incandescent light and daylight equivalent illumination and observed that: “While all the stones show some change in colour between incandescent and daylight or fluorescent illumination, most also display a different colour when light is passed through the stone, as compared to internally reflected light from the same source.” They referred to the latter as colour shift and suggested: “Colour shift does not occur with a change in illumination, but rather with the relative amounts of light (from a single source of illumination) that a viewer observes either (1) passed through the stone or (2) internally reflected by a gemstone. The former reveals the stone’s body colour, the latter requires the viewer and illuminant to be on the same side of the gem, so that the internal reflections (which represent the reflected colour) may be observed.”

The observations by Manson and Stockton are similar to observations concerning UE tourmalines and are discussed below.

Concentration effect

Colour change with change in concentration of light-absorbing impurities is covered by the denotation ‘*polychromatism*’ (Kennard and Howell, 1941). In his study

of pyropes, Fiala (1965) found that the colour changed from orange-red to violet with Cr_2O_3 content increasing from 1.15% to 6.54%. Pyrope garnets showing an AE had previously been described from peridotites found on the island of Otterøy, close to Molde, Norway, changing from violet in daylight to wine red in incandescent light (Hysingjord, 1967 and 1971). Then, Carstens (1973) found that a more chromium-rich pyrope from the same location changed from blue-green in daylight to wine-red in incandescent light. This pyrope had a Cr_2O_3 content of 6.22%, while the one with colour change from violet to wine red had 3.72%. Carstens analysed absorption spectra for the green chromium-rich pyrope and a red chromium-poor pyrope (1.50% Cr_2O_3), finding a pronounced shift towards the red end of the spectrum for the two absorption peaks, as well as for the minimum between these, with increased Cr_2O_3 content. He concluded that the change from green to red in these garnets, being essentially solid solutions of pyrope, almandine and uvarovite, occurred at about 6-7% Cr_2O_3 . Orgel (1957) reported a similar colour change in laboratory-grown rubies which remained red with up to 8% Cr_2O_3 , turning progressively more and more green with increasing Cr_2O_3 content. This effect was also described by Thilo *et al.* (1955) and by Nassau (2001).

Thermochromy

This colour change phenomenon is related to crystallographic lattice distortions caused by change in temperature. Kenngott (1867) described colour change to green by heating of red corundum from Sri Lanka, and reversion to red by cooling. Thermochromy in corundum and spinel has been thoroughly discussed by Weigel (1923) on the basis of detailed spectral analyses and he found that the colour change in ruby was influenced by pleochroism. Thilo *et al.* (1955) concluded that the colour change with temperature in ruby is momentary and strictly reversible. They studied the colour behaviour of samples of synthetic corundum with variation in chromium content and measured the *grey*

point temperatures, at which a grey colour was observed on the transition between red and green. The lower the chromium content, the higher was the *grey point* temperature. With a Cr₂O₃ content of 5%, the *grey point* temperature for ruby was found to be of the order of 600 C. They also found that the *grey point* changed with type of light. At room temperature corundum with 17% Cr₂O₃ was grey in daylight and red in incandescent light. These findings were analysed by Orgel (1957) who described this optical behaviour of ruby as anomalous. Based on experimental data on chromium-containing solids, Poole (1964) suggested that thermochromy is a general property of solids containing Cr³⁺ ions. He assumed thermochromy to be present in chromium-containing minerals, including ruby, emerald, uvarovite, fuchsite and chrome diopside. Carstens (1973) found that his red pyrope with 1.50% Cr₂O₃ turned green when heated to about 200 C, while a violet pyrope with 3.72% Cr₂O₃ turned green at about 150 C. Neuhaus (1960) described thermochromy in chrome alum solutions.

The Usambara effect

Basic idea

Characteristic for UE is colour change as response to change in the light transmission path length. A green UE tourmaline may turn red in transmitted light when placed on top of another green UE tourmaline (Figure 1). When light is transmitted through a coloured mineral, certain frequencies are absorbed and the remaining frequencies combine to give the mineral its colour. Change in path length of transmitted light will affect the spectral power distribution. An increased path length will result in a general increase in absorption. The Lambert law, $I_{(z)} = I_0 \cdot \exp(-a \cdot z)$, defines the degree of absorption for a given path length z , where I_0 is the intensity of light entering the material, and $I_{(z)}$ is the intensity of the light after passing through a thickness z of material with absorption coefficient a . If the intensity of light is reduced to half on passing through material with thickness z , an increase in

material thickness (or path length) to $2z$ will reduce the intensity of transmitted light to a fourth. A crucial condition in regard to the UE is that the increase in absorption is higher for the higher frequencies than for the lower. With increased path length, the intensity of the red transmission is increased relative to the intensity of the green, and thereby the balance between the green and red transmissions is shifted towards red, a shift that can be observed as relatively sudden. The sensitivity of the human eye is highest in the green sector, for wavelengths between 500 and 510 nm (Kuehni, 1997), so if light transmitted through a mineral has transmission peaks of the same intensity in the green and red, the mineral will appear green. With a minor change towards red in the balance between the transmissions in the green and red, a mineral might still appear green, but if there is sufficient increase in red transmission, a sudden change to red may be observed (Poole, 1964).

Discussions with Dr Kurt Nassau

Extensive discussions between Nassau and the author covered various aspects of the UE and, concerning its definition, Nassau (*pers. comm.*, 1998) suggested:

“It is necessary here to distinguish between a colour change that involves a change in hue (or dominant wavelength or chromatic colour, etc.) and one that does not do so. The term Usambara effect is obviously intended to apply only to a change involving hue. Most materials will change colour without a change in hue when either the concentration of a light-absorbing impurity or the light path length is increased. If there is a change in the field (crystal or ligand), then the hue will change with the concentration, but not with the path length. Only when at least one transmission band extends significantly out of the visible region, as at the red end of the spectrum with your tourmaline, will there be a change of hue with either concentration or path length. It seems to me that only under these conditions should the former be termed “concentration dichroism” in dyes or the concentration effect

of colour-producing impurities in minerals. Similarly, only the latter should be termed the Usambara effect.”

In a discussion about causes for observed colour changes in UE tourmaline, Nassau (*pers. comm.*, 2000) commented:

“One interesting question which your discussion has raised in my mind is why it is so rare to see more than one of the pleochroic colours from a gemstone (without turning it or using a polariser): andalusite with both reddish and greenish colours is exceptional – some alexandrite also shows this effect, but less strongly, some zoisite with yellow flashes in the green, and green to almost black in tourmaline (not exactly a colour change). Even then, why do only some pleochroic materials show only some of their colours on being turned (without a polariser)? Ruby shows both its colours, but iolite shows only two of its three colours. I believe that I now know the answer: the reason lies in the fact that the ordinary ray colour is seen in all orientations. If the ordinary ray colour is intense and saturated, it will then hide the other colours in those orientations where one would expect to see them.”

This explanation is consistent with that given by Wörth (1842) and by Haidinger (1849) for their observations concerning alexandrite.

New observations, investigations and interpretations

The observations described below relate to UE tourmalines from Nchongo, unless otherwise specified. They are grouped according to the cause (tentative or proven) for the observed phenomena: *colour change due to change in path length of transmitted light, thermochromy, dispersion and visible-light-induced fluorescence*. Discussion and suggested explanations follow the observations.

Spectral analyses were carried out by K.A. Solhaug, Agricultural University of Norway, Ås, using an Ocean Optics SD 2000 spectrometer (*Figures 3, 10, 15 and 17*) and L.O. Björn, Lund University, Sweden, using an Optronics 754 spectroradiometer

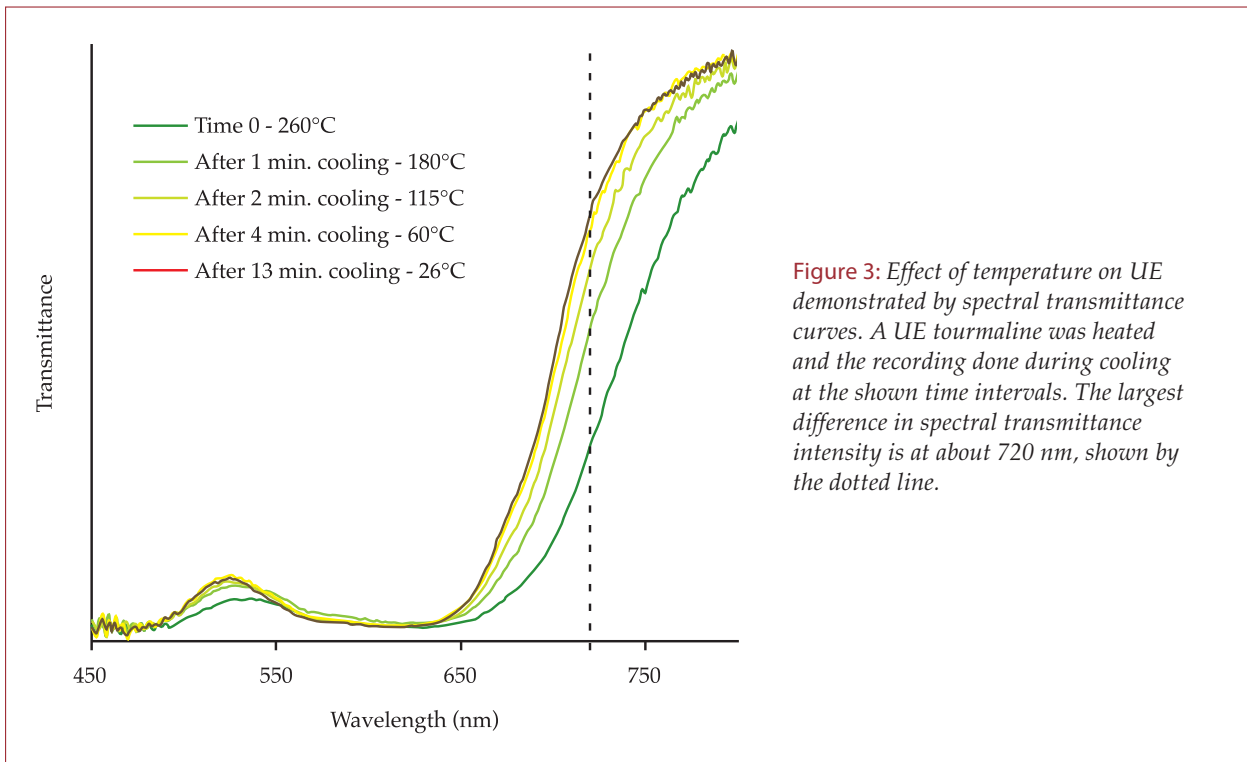
(*Figure 7*). Electron microprobe analyses were carried out by C.J. Stanley at the Natural History Museum, London, using a Cameca SX50. Fluorescence was measured by J. Kihle, Institute of Energy Technology, Oslo, Norway, using a customised Olympus BX-61 microscope at 10x magnification, fibre-optically connected to a modified Edinburgh Analytical Instrument CD900 excitation/emission spectrometer, excitation wavelength set to 405 nm.

Gemmological instruments utilised by the author include a Krüss refractometer, OPL dichroscope, dichromatic colour filters: Chelsea filter with transmissions in the deep red and in the yellow-green (570 nm). Hanneman Aqua filter with transmissions in deep red and in blue-green (490 nm). Fibre optic lamps had 20W and 150W tungsten halogen light sources. A Nikon Coolpix 990 camera was used to record images.

Change in path length of transmitted light

Observations

- I a The colour of a green UE tourmaline, illuminated from behind, shifts towards red when studied through green or blue UE sheets of plastic. The same happens when the tourmaline is studied through solutions of certain types of green and blue dyes for colouring Easter eggs.
- I b A certain orange-yellow sapphire placed on top of a green UE tourmaline turns deep red in transmitted light.
- I c Normally a green UE tourmaline appears red when studied through a Chelsea colour filter, and an even stronger red through a Hanneman Aqua filter. In a pale green UE tourmaline, the colour of a thicker part of the stone may turn red under a Chelsea filter, but not the thinner parts. The same effect is seen in tsavorites from Kalalani, Uмба area, which show more red in the thicker than in the thinner parts when studied through a Chelsea filter.
- I d An emerald green kornrupine crystal from Nchongo, Uмба area, shows a peculiar pleochroism.



Discussion

Dichromatic colour filters (e.g. Chelsea filter) have a colour changing effect similar to the UE. The colour change observed when a green tourmaline is placed on top of another green tourmaline is the same as that seen when one of the stones is replaced with a Chelsea filter. Placing the orange-yellow sapphire on top of a green UE tourmaline also results in relative increase in intensity of the combined red transmission due to superposition, with colour change to red.

Thermochromy

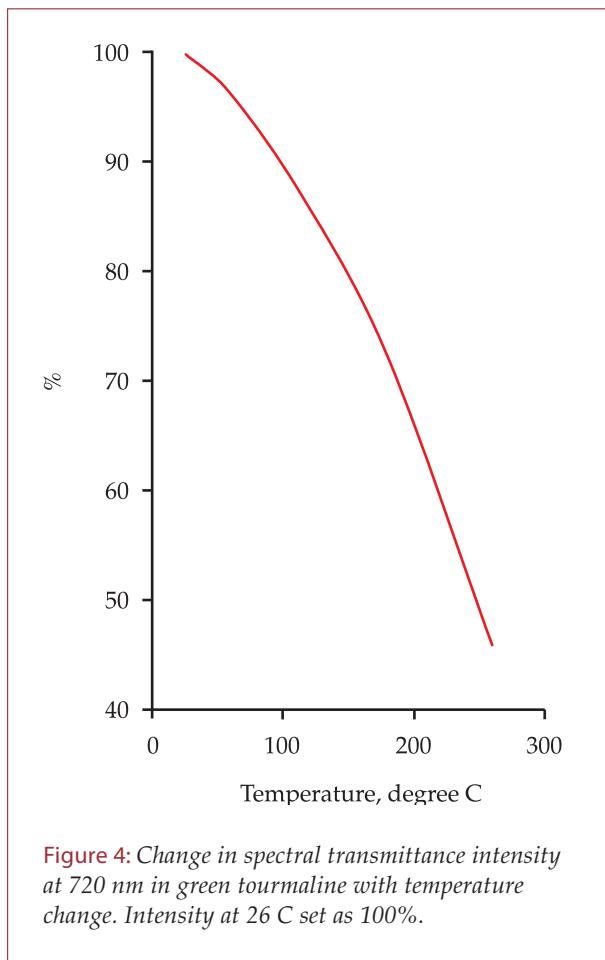
Observations

II When a UE tourmaline is moderately heated to about 250-300 C the red colour disappears and then reappears when the stone is cooled down. The return of the red colour is not spontaneous, but is seen first in the thickest part of the stone, then in the thinner parts. By measuring the temperature when the stone was cooling, its influence on colour could be observed at least down to 120-130 C. Also the red colour attributed to absorption-modified dispersion (see below) disappears when the stone is heated.

Discussion

This test was done after reading Carstens' (1973) descriptions of thermochromy in garnets with change in colour at 150 C. Observation II indicated that even lower temperatures than 150 could affect the colours involved in the UE in tourmaline. Spectral analyses were then done at different temperatures. To avoid influence of pleochroism and of change in light path length, all measurements had to be done without moving the sample. A heated stone was placed on the spectrophotometer and measurements conducted while the stone was cooling. With the available instrument set-up, measurement of temperature in the stone was not possible simultaneously with the transmittance recording. By repeating heating of the sample and then measuring the decreasing temperatures at the same time intervals as the spectra had been recorded, the corresponding temperatures could be estimated. These temperatures are linked to the spectra in Figure 3, and indicate the approximate range for this test. The change in spectral transmittance intensity is highest at the highest temperatures, but even down towards room temperature a

slight change can be observed. The largest change is indicated by a dotted line at about 720 nm. *Figure 4* shows the change in intensity at 720 nm with temperature change. It follows that temperature changes experienced under natural climatic conditions may affect the UE colour change in some stones.



Absorption-modified dispersion (AMD)

Observations

III a Light reflected from faceted UE tourmalines may contain red and green flashes, and the quantitative distribution of these colours will depend on size of the stone, colour saturation and illumination (*Figure 5*). Larger stones will show a higher proportion of red than small stones, but the red hue in a small stone seems identical to the red hue in a large stone cut from the same crystal. Red flashes have been observed

in faceted stones down to 0.2 ct. Study of such flashes under a loupe shows that the colour changes from strong red, often seen as a sharp band, at one end of a facet, through a central yellow transition zone, to a strong green band at the opposite end. The green hue in this *spectrum* may be a purer green than the transmittance colour. Such *dichromatic fire* may also be seen in other gem minerals with transmission spectra characterised by two transmission bands (dichromatic minerals). Examples are alexandrite, tanzanite, colour-change sapphires and tsavorite. Careful study of reflections in facets in rubies from the Umba area not only revealed the deep red colour, but also a thin, blue band close to the edge of a facet. In blue sapphires from Umba, thin red bands were observed, and the same feature was seen in the facets of deep blue spinel.

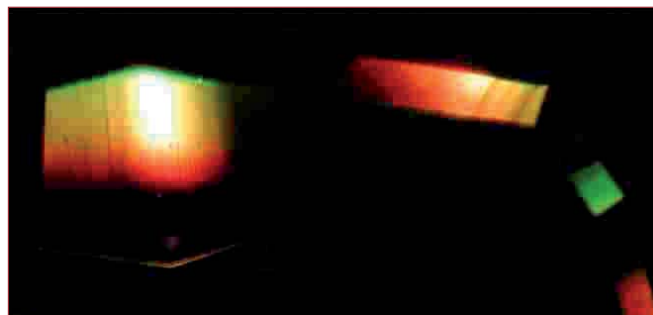


Figure 5: Dispersion colours in facets of 18 ct UE tourmaline.

III b In prismatic tourmaline crystals, viewed in the direction of the *c*-axis and illuminated from behind, a red colour may be seen along the crystal faces, while the central part of the crystal is green, see *Figure 6*. C. Simonet (*pers. comm.*, 2001) observed the same in tourmaline crystals from Taita Hills, Kenya. He did an electron microprobe traverse across the crystal to check the possibility that the red colour was caused by compositional zoning such as chromium variation, but such zoning was not found.



Figure 6: Red colour along contour of UE tourmaline crystal when viewed along c-axis and illuminated from behind. Photo by J. Kihle.

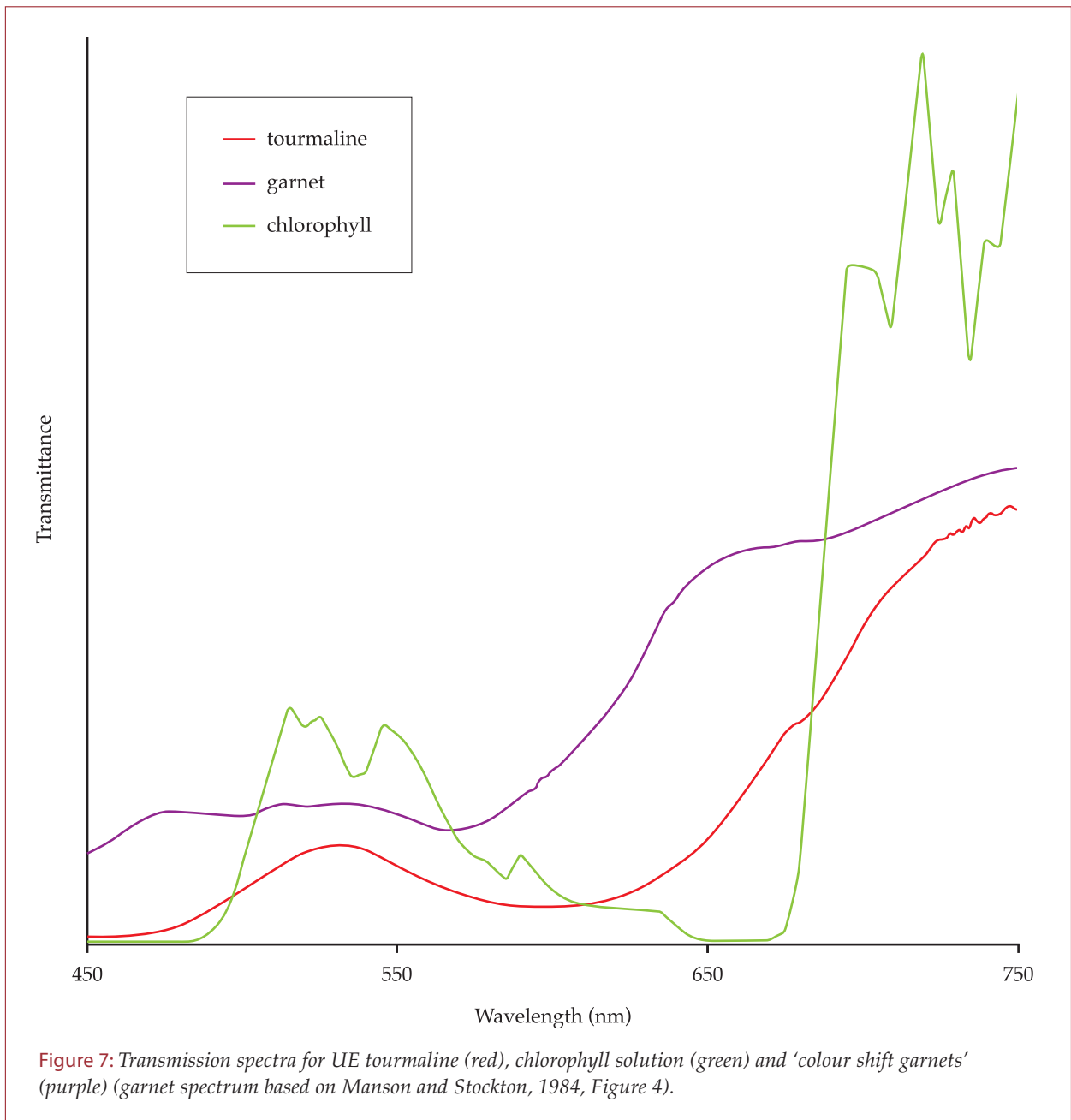
- III c A strong red colour may be observed at surface irregularities, such as edges and weathering grooves on rough stones and the roughly ground girdles of faceted stones. Red colour may also be seen associated with inclusions.
- III d Viewing a light bulb through the table of sizable faceted UE tourmalines held close to the eye reveals a pronounced red-green spectrum which consists of a sharp green band following the contour of one side of the bulb and a sharp red band along the contour of the opposite side. No distinct colours are seen in between. The green and the red bands have more or less the same width. If the stone is rotated, the green and the red bands shift towards each other and when the bulb is viewed parallel to the table the two bands appear next to each other. Crowningshield and Ellison (1951) introduced the Eyeball method for determination of optical properties and described spectral observations in various gemstones. In incandescent light the red in alexandrite was very strong and the blue-green was almost halved by a broad absorption band. In daylight,

the red was very weak while the blue-green was strong. In a UE tourmaline, the widths of red and green bands change somewhat with type of light, but possibly not as much as in alexandrite. The Eyeball method was described for faceted stones, but in UE tourmaline, spectral images can also be seen in rough stones and cabochons. Further, the light source does not need to be well defined: for example, looking at a variably-lit landscape through a faceted tourmaline held close to the eye reveals numerous spectral images related to light and dark points in the landscape. Also when a stone is moved away from the eye, the spectral images of a light source can be seen as red and green flashes in the stone.

- III e If a fibre-optic light is placed against the backsurface of a flat plate of UE tourmaline, a partial or full red rim may be seen at the edge of the circular fibre bundle. A full red circle seems to be dependent on a certain thickness of the stone, while a partly red, partly green circle is produced by stones of less thickness. Similar observations can be made when viewing the fibre optic light through a Chelsea filter, a chlorophyll solution, or through certain green or blue dyes.
- III f A remarkable observation was made when studying a flat, rough, deep green UE tourmaline. With the fibre optic light placed behind the stone in the direction of the short axis, the stone showed a deep green hue. With the light placed on the same side as the observer, an object such as a pencil held behind the stone could show a deep red hue, especially along the edges.

Discussion

Although dispersion has not traditionally been considered to be connected with change in the body colour of a mineral, it is still important in connection with the UE. A major part of the red flashes in a faceted



green UE tourmaline is apparently caused by dispersion. Dispersion in gemstones is described as *fire* and is most clearly observed in colourless or pale-coloured gems with strong dispersion. In more intensely coloured stones dispersion is normally masked. It is here postulated that minerals with dichromatic transmission spectra are exceptions and that these may show a conspicuous *dichromatic fire*, an apparently neglected quality criterion for gemstones. In minerals with dichromatic absorption spectra the appearance of dispersion seems to be different from what is normally seen in coloured gems. A UE tourmaline has

normally strong colour saturation and weak dispersion. Is it still possible that dispersion can be the cause of the colour change phenomena described above? It is possible that parts of the dispersion spectrum are being absorbed. In a colourless stone with no absorption, dispersion separates all the colours of the visible spectrum and is seen as *polychromatic fire*. In a coloured stone with one dominant transmission frequency, all the colours separated by dispersion are being inhibited, except for the transmitted colour, resulting in *monochromatic fire*. In a coloured stone with a transmission spectrum characterised by two colours of more or less

the same intensity, a *dichromatic fire* may be seen. Transmission bands may act as *windows* for dispersion colours of corresponding frequencies. Red dispersion rays escape through a red transmission window, and similarly green dispersion rays through a green transmission window. Any other dispersion colours are trapped by absorption.

Manson and Stockton (1984) suggested that the *colour shift* in their garnets required an absorption spectrum similar to that which produces the Alexandrite type of colour change, see *Figure 7*. They found the AE not to be the dominating effect and the colour shift was observed in transmitted light or by internal reflections. Is it possible that the *colour shift* observed in transmitted light was an effect of light path length (UE)? By colorimetric analyses of Manson and Stockton's absorption spectra, L.O. Björn (*pers. comm.*, 2004) has linked the change in colour with change in path length. The *colour shift* in reflected light was probably due both to UE and AMD.

AMD may take place also in UE materials with sample thickness too small to give a UE colour change. This prioritised appearance of AMD in relation to the UE can be seen in UE tourmalines, but is even better shown by the green and blue dyes showing the UE.

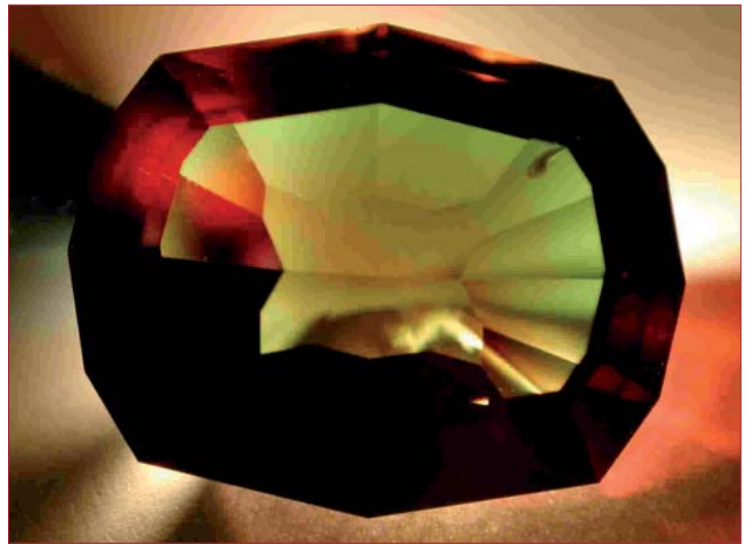


Figure 8: Red fluorescence caused by fibre optic light at upper left corner of 18 ct UE tourmaline.

Fluorescence induced by visible light

Observations

- IV a When fibre-optic light is placed against the surface of a UE tourmaline more than about 8mm long, a red, elliptical ray can be seen (*Figure 8*). The red ray extinguishes at a depth of 4 – 6 mm, and is somewhat chalky, different from the clear red caused by the UE.
- IV b A green UE tourmaline turns red when illuminated with high-intensity violet light (405 nm), see *Figure 9*.

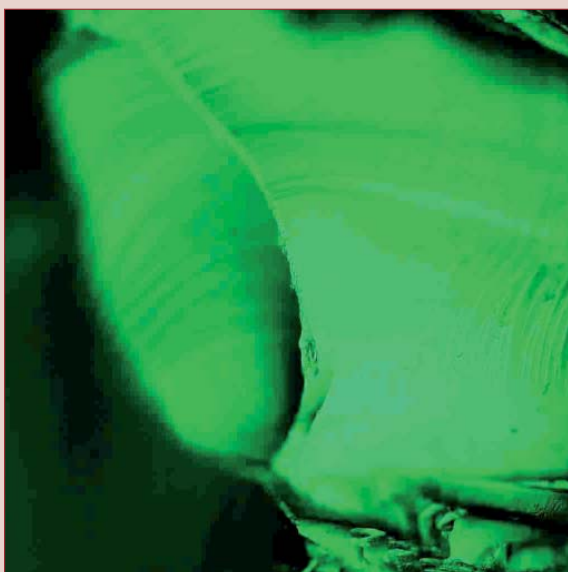


Figure 9: Colour change due to fluorescence: (a) green when illuminated with white light, and (b) red with 405 nm monochromatic light. 400x magnification. Photo by J. Kihle.

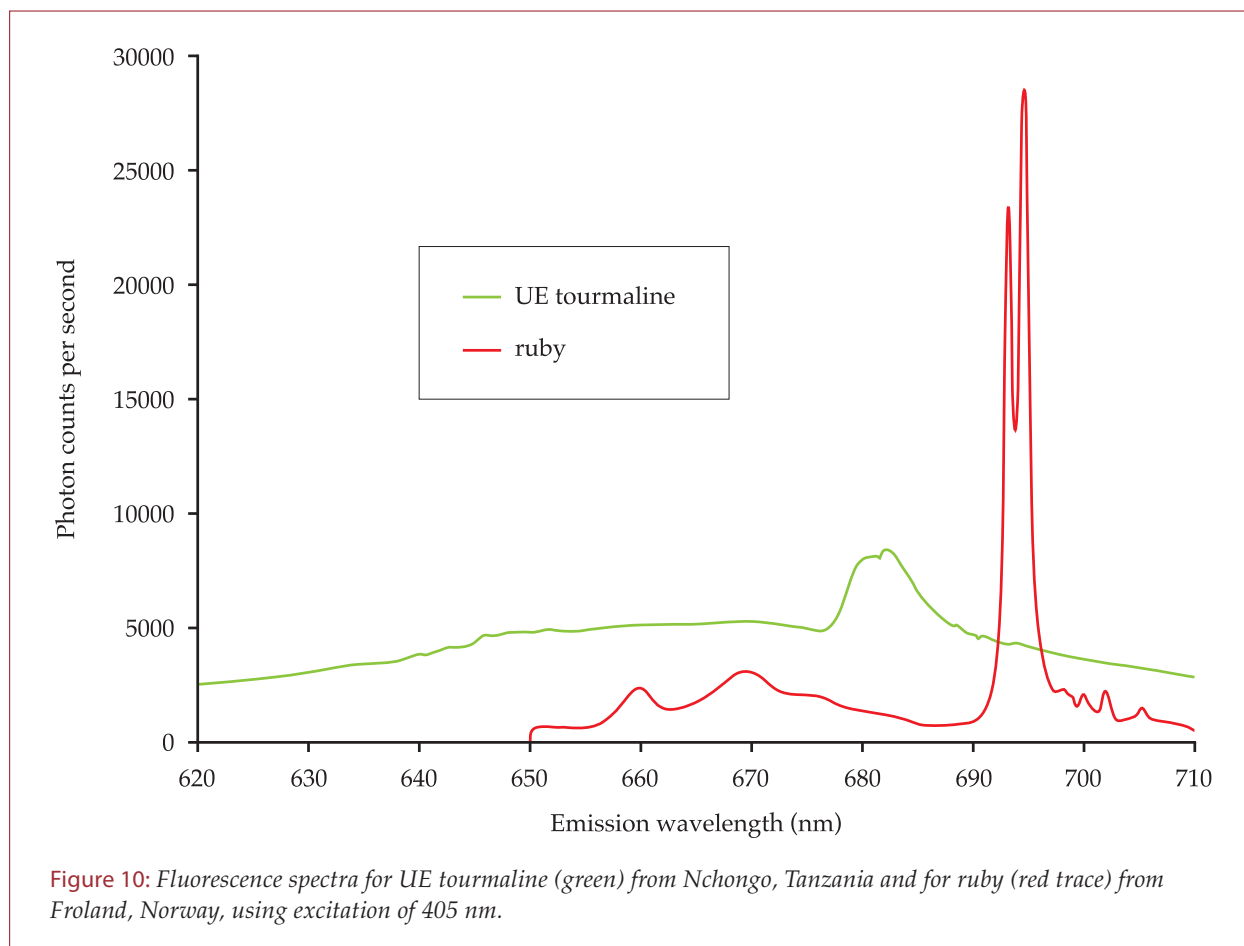


Figure 10: Fluorescence spectra for UE tourmaline (green) from Nchongo, Tanzania and for ruby (red trace) from Eroland, Norway, using excitation of 405 nm.

Discussion

In a fluorescence study of some UE tourmalines J. Kihle (*pers. comm.*, 2002) found a red luminescence when the tourmaline was excited by light in the violet part of the visible spectrum. The strongest luminescence was obtained with an excitation wavelength of around 405 nm, with a pronounced luminescence intensity peak at 682 nm, see Figure 10 where it may be compared with a fluorescence spectrum for ruby. When excited by 405 nm light, the luminescence intensity from the tourmaline is about 30% of that from the ruby.

The elliptical shape of the red luminescence ray obtained from green UE tourmalines using fibre-optic light, is probably caused by reduction in light intensity by absorption. Beyond a distance of 8-12 mm from the light source, the intensity is probably too low for inducing fluorescence. Increasing the intensity of the light is found to result in a deeper luminescence penetration.

Chemistry and colour in UE tourmalines

Halvorsen and Jensen (1997a) described the tourmalines in their study as calcium-bearing dravites and two analysed samples had 0.34 and 0.22 wt% Cr_2O_3 and about 0.05 wt% V_2O_5 . In various studies of tourmalines from East Africa, a topic for discussion has been the relative contents of Cr and V in green tourmalines and whether they should all be called chrome tourmalines. Schmetzer and Bank (1979) concluded that green tourmalines from East Africa are mainly coloured by vanadium and should be named *vanadium tourmalines*, but Simonet (2000) reported higher chromium than vanadium contents for three out of four green tourmalines from the Taita-Taveta District, Kenya. For the present study, the contents of Cr_2O_3 , V_2O_5 and FeO in a selection of cut UE tourmalines from Nchongo were analysed at the Natural History Museum, London, and the results are given in Table I. Corresponding transmission spectra are shown in Figure 11. Samples 2073 and 2045 with relatively high V_2O_5 – content

Table I: Contents of Cr_2O_3 , V_2O_5 and FeO in cut green UE tourmalines from Nchongo, Tanzania, based on electron microprobe analyses.

Sample ^a			Chromophores wt% ^b			Colour			Refractive indices		
No.	Weight ct	Cr_2O_3	V_2O_5	FeO	Hue, fluorescent light	Saturation ^a	Response to Chelsea filter	n_{ω}	n_{ϵ}	Δn	
2073	0.8	0.19	0.72	bdl	Bluish green	Very high	Mod. – strong	1.641	1.621	0.020	
2045	1.0	0.15	0.75	bdl	Bluish green	Very high	Mod. – strong				
2030	1.4	0.24	bdl	bdl	Bluish green	High	Mod.	1.643	1.624	0.019	
2060	2.45	0.12	0.14	bdl	Olive green	Medium	Mod.	1.643	1.622	0.021	
2063	4.1	0.19	bdl	bdl	Green	Medium	Mod.	1.645	1.629	0.016	
2062	1.5	0.15	bdl	bdl	Green	Medium	Mod.	1.645	1.634	0.011	
2078	1.15	0.08	bdl	0.16	Green	Medium – low	Weak	1.639	1.620	0.019	
2034	0.55	bdl	bdl	bdl	Green	Very low	Very weak	1.643	1.637	0.006	

N.B. a. Samples listed according to colour saturation: high to low, visually assessed.

b. Wt.% semi-quantitative from uncoated specimens, normalised to 3.5 wt.% H_2O and 10 wt.% B_2O_3 ; detection limits about 0.01 wt.%; bdl = below detection limit. Cameca SX50 electron microprobe, analyst: CJ Stanley.

(0.72 and 0.75 wt%), have a pleasant bluish-green hue, but are too dark for use as gems. Their spectra show a more distinct and broader absorption in the yellow-orange, compared to the other spectra. Sample 2078, with a measurable FeO content, shows a pure green colour. Apparently, red flashes in the light-coloured stones are caused by AMD and not by UE.

UE in plants

In nature, green is the dominant colour and chlorophyll the main colorant. Pigments in green plants are chlorophylls a and b with transmissions in green and red (Figure 7), similar to the transmissions in the UE tourmaline, and anthocyanins with transmission in red (see Appendix). The UE in different depths of chlorophyll solution in acetone are shown in Figure 12. A thin layer of this in a beaker is green in transmitted light. When the layer thickness is increased, the colour turns red. In addition to UE, AMD and visible light induced fluorescence in chlorophyll solution can also be observed.

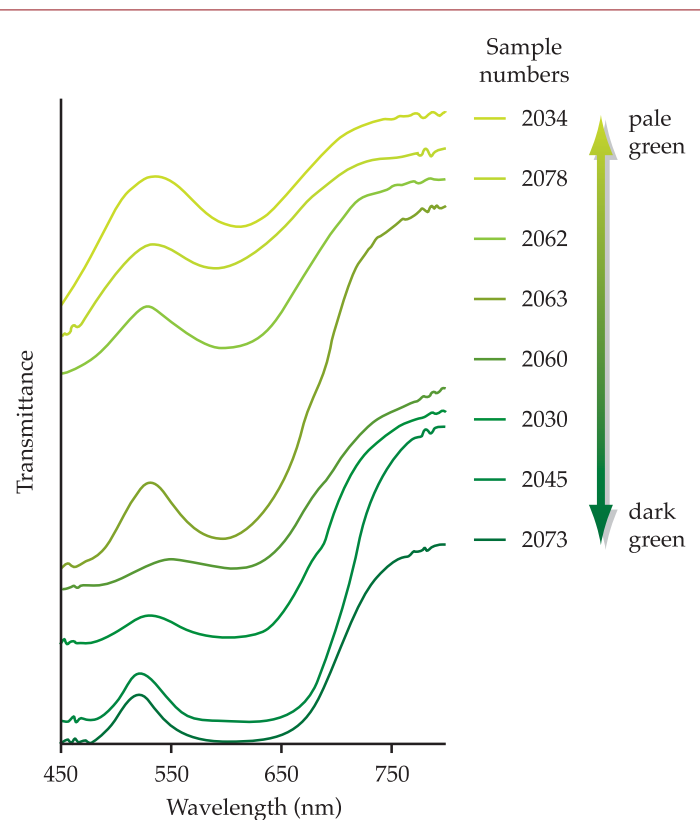


Figure 11: Transmission spectra for the eight UE tourmalines listed in Table I.

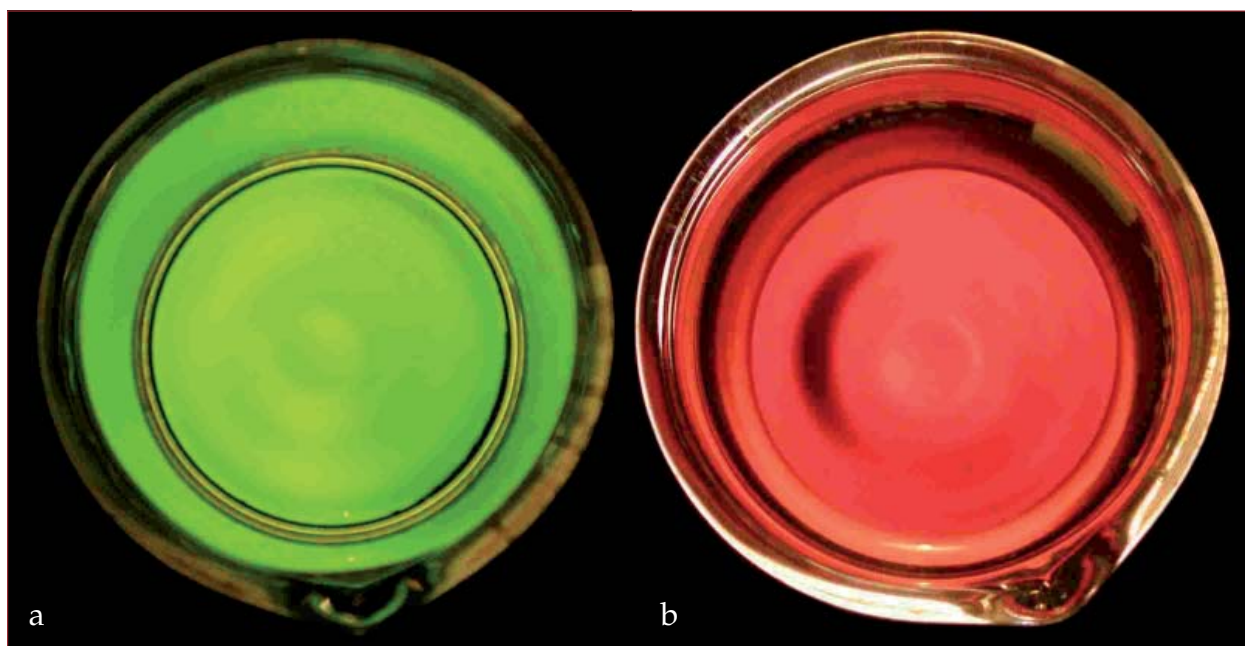


Figure 12: UE colour change in chlorophyll solution. a) green with liquid thickness 5 mm. b) red with liquid thickness 15 mm.



Figure 13: A deep green UE tourmaline appears red when placed on top of two or three leaves and illuminated from below.

Fluorescence spectra obtained with 405 nm excitation wavelength showed fluorescence peaks at 671 nm for the chlorophyll solution (cf. 682 nm for the UE tourmaline) with fluorescence intensity close to eight times as high for the chlorophyll.

A green UE tourmaline crystal may also turn red when illuminated by high-intensity light through two or three green leaves (Figure 13) which act as a colour filter, increasing the relative intensity of red.

UE in other minerals

Kornerupine

Kornerupine is a borosilicate with orthorhombic crystal symmetry. An emerald-green kornerupine crystal from Nchongo, Umba area, shows a peculiar pleochroism. Refractive indices are $n_{\gamma} = 1.681$ and $n_{\alpha} = 1.671$ and electron microprobe analysis showed a Cr_2O_3 content of 0.24-0.28 wt%. When viewed along the c -axis, the crystal apparently shows both UE and AE types of colour change. In incandescent light, green is seen in the short section of the crystal and brownish red in the longest section (Figure 14). Observation of both green and red colours along the c -axis could possibly be explained as result of change in light ray direction and influence of the strong pleochroism. The red seen in the c -direction is however strengthened when the kornerupine is placed on top of a UE tourmaline, a feature interpreted as presence of UE in the kornerupine. Under the dichroscope the kornerupine shows variations between bluish green and red perpendicular to the c -axis and variations of red along the c -axis. The colour observations are related to the vibration directions as follows: green in α direction, two shades of red in β and γ directions. In fluorescent light,

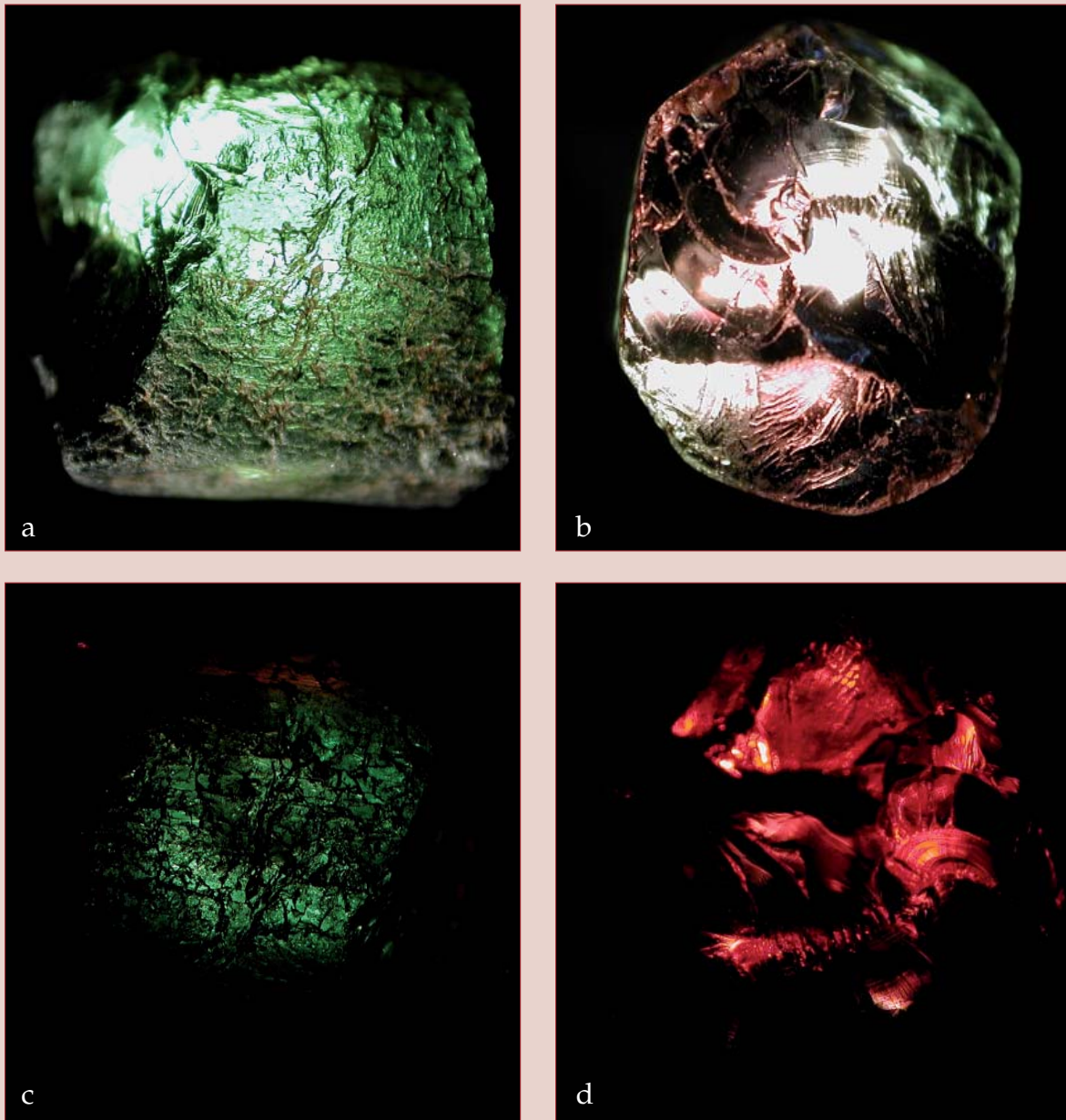


Figure 14: Pleochroism in kornepine crystals from Nchongo. Length along the *c*-axis varies from 6.5 mm to 11 mm. (a) Seen perpendicular to *c*-axis in transmitted incandescent light; (b) parallel to the *c*-axis; (c and d) same lighting, but with use of Hanneman Aqua filter.

the red colour is absent. Under a Hanneman Aqua filter, the red intensifies but the bluish green at right angles becomes an even darker pure green. With moderate heating the red colour disappears (thermochromy). AMD can also be observed. The transmission spectra in *Figure 15* are not considered as dichromatic spectra, but they demonstrate the distinct pleochroism of this crystal, with strong transmission in the green when measured perpendicular to the *c*-axis and strong transmission in the red parallel to the *c*-axis.

Epidote

Epidote from Tanganyika Massagati, a remote area north of Mahenge, Tanzania, changes colour from green to brownish red with increasing thickness (*Figure 16*). The red is intensified by a Chelsea filter. This colour change is also influenced by type of illumination. The transmission spectrum of this epidote (*Figure 17*) is dichromatic and resembles the UE tourmaline spectrum, with the green transmission at a slightly higher

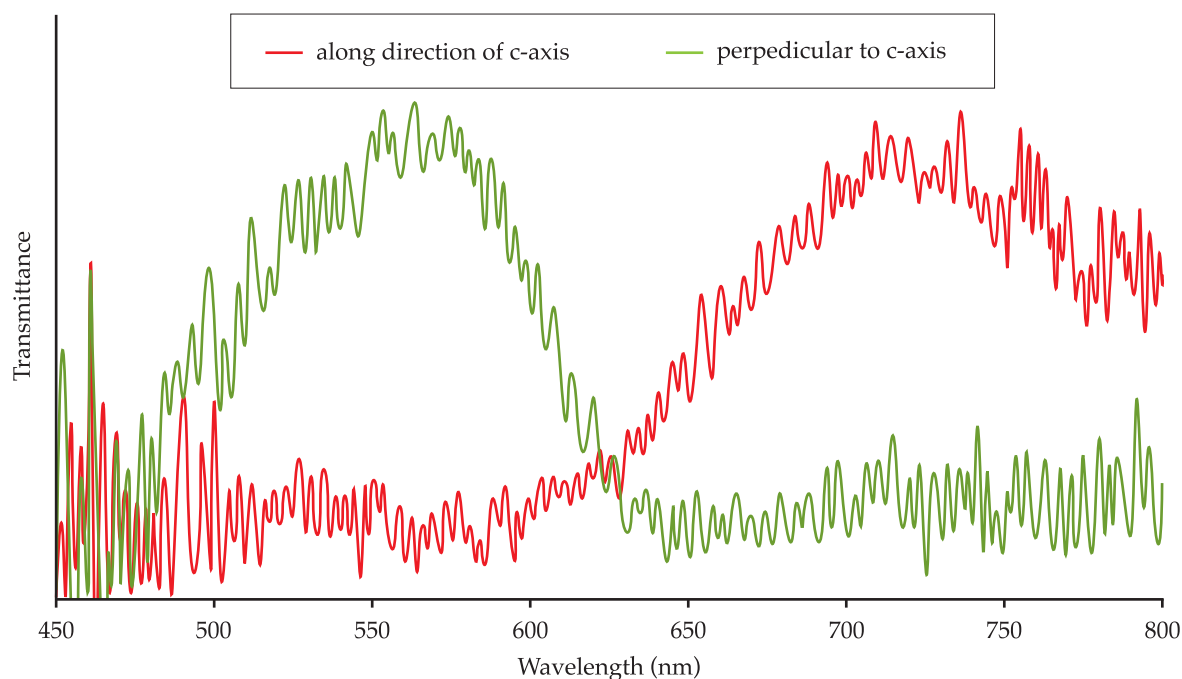


Figure 15: Transmission spectra for kornerupine from Nchongo, Uмба area, along the direction of (red) and perpendicular to (green) the *c*-axis.



Figure 16: UE in epidote crystal fragments from Tanganyika Massagati. (a) Green with 4 mm thickness. (b) Brownish red with 8 mm thickness. In (a) AMD is visible as tiny red spots at irregularities. Both (a) and (b) are viewed into a 001 cleavage face.

wavelength. This spectrum was obtained from a {001} cleavage fragment, with light travelling in the XZ plane, perpendicular to the Y axis. No detectable chromium or vanadium was found by electron microprobe analyses; its refractive indices are $n_{\gamma}=1.765$ and $n_{\alpha}=1.732$.

Alexandrite

Alexandrite is not only appreciated as a gemstone. Synthetic alexandrite is also important as tunable solid-state laser material. Three rods of such alexandrite with lengths 70-80 mm were obtained from Northrop Grumman Space Technology. The Cr contents of the rods were 0.076% (light colour), 0.123% (medium colour) and 0.308% (dark colour). All rods show deep red along the long axis, both in incandescent light and in daylight. However, a 10 mm thick slice cut from the medium-coloured rod appeared greenish blue viewed along the length (Figure 18). In the long rod of medium colour, variations between dark, greyish rose and red along the long axis, and along the same axis in the 10 mm piece, variations between greyish yellow and greenish blue are visible under the dichroscope.

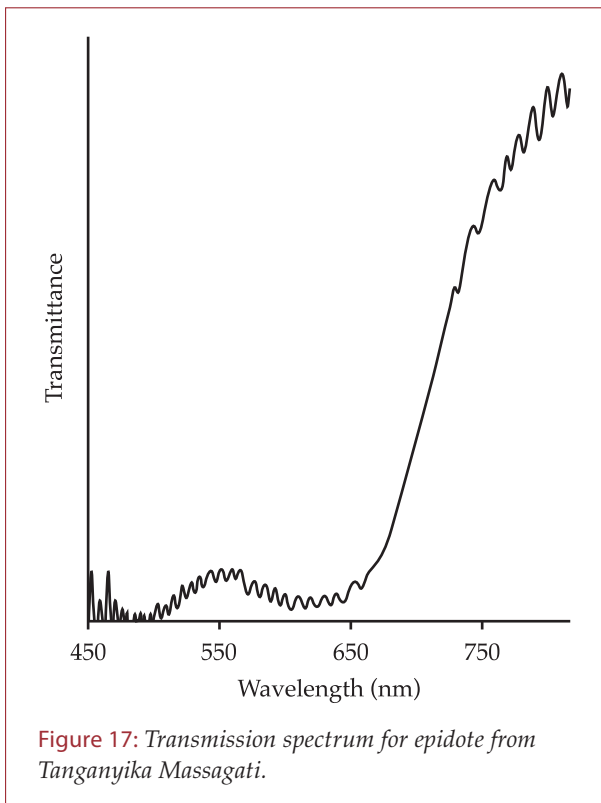


Figure 17: Transmission spectrum for epidote from Tanganyika Massagati.

Prediction of UE colour change by colorimetric analyses

The author of a recent book on colorimetric studies in the field of biology (Björn, 2002) has developed an interesting method for prediction of UE colour change by analyses of transmission spectra using computer programmes which can be downloaded from the internet (L.O. Björn, *pers. comm.*, 2004). A description of this method may be requested from the present author. The materials studied include chlorophyll, UE tourmaline, alexandrite and colour change garnet,

see Figure 7. The predicted colour changes correspond well with the observed colour changes, particularly the change from green to red with increase in path length for UE tourmaline and for alexandrite. This method for UE colour change prediction can be extended to AE colour change by considering the spectral distribution of illumination.

Concluding remarks

Based mainly on observations and analyses of the Nchongo tourmalines, this study has provided insight into the complex colour phenomena in minerals with spectra characterised by two colour maxima (dichromatic minerals). In addition to AE and UE, the phenomena of thermochromy, visible-light-induced fluorescence and absorption-modified dispersion (AMD) have been described and discussed. AMD is a tentative explanation for certain colour phenomena in dichromatic materials and needs further verification. Colour change behaviour is also described for the minerals epidote and kornerupine. As a curiosity, the colour change behaviour of chlorophyll is briefly described and the use of green leaves as a colour filter, which can change the colour of UE tourmaline, is shown.

The study has also provided insight into the interaction between the various colour phenomena. It is concluded that the AE is affected by the UE and they may both interact with other described colour phenomena. Haidinger (1849) and Cossa and Arzruni (1883)

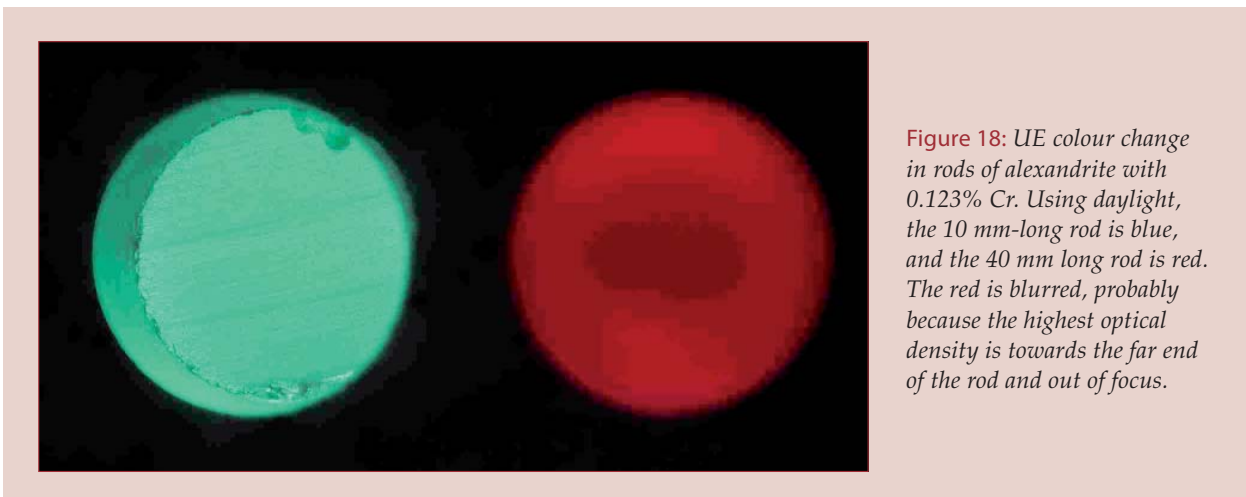


Figure 18: UE colour change in rods of alexandrite with 0.123% Cr. Using daylight, the 10 mm-long rod is blue, and the 40 mm long rod is red. The red is blurred, probably because the highest optical density is towards the far end of the rod and out of focus.

described interaction between AE and UE. The observation by Fiala (1965) of green colour in small pyrope fragments indicates the same. Haidinger (1849), Kokscharow (1861), Cossa and Arzruni (1883), and Farrel and Newnham (1965) described interaction between AE and pleochroism, by different degrees of colour change along the different optic axes. In the kornerupine described in this paper, AE was found in only one direction. C. Simonet (*pers. comm.*, 2000) observed this feature in kyanite from Kenya. Haidinger (1849) noted that one of the trichroic colours in alexandrite was not affected by whether the source was daylight or incandescent light. Weigel (1923), Thilo *et al.* (1955), Orgel (1957) and Carstens (1973) described interaction between AE, concentration effect and thermochromy. The above observations indicate interaction between thermochromy and UE, as well as AMD and pleochroism. Neuhaus (1960) suggested that AE colour change observations should be conducted at a constant temperature, and that observations of thermochromy should be carried out with constant spectral distribution of light. This study shows that understanding the interaction between the various colour change phenomena is essential for understanding the features of any one stone. In particular, the influence of UE should be considered in studies of AE. Colour change in minerals is complex and its understanding requires a holistic approach.

Acknowledgements

I wish to thank Kurt Nassau, Cedrik Simonet, Brenda Jensen and Lars Olof Björn for valuable discussions, and Brenda also made useful comments about the structure and content of this paper. Ulf Kapborg is thanked for providing the alexandrite rods from Northrop Grumman Space Technology, USA. Multiconsult, Norway is thanked for financial support and Chris Stanley, Lars Olof Björn, Knut Asbjørn Solhaug and Jan Kihle provided analyses relating to the colour change experiments. Thanks also to Ada Eckhoff and other librarians for their persistence in the search for old publications.

Appendix

UE in plants

When the leaves open in the spring some trees look reddish, as anthocyanins may be the dominating pigments in the early phase of the leaves, before the chlorophylls become dominant and green is the observed colour. In the autumn a spectacular colour change may take place, with the green leaves turning yellow or red. The green chlorophyll then decreases to reveal the red, orange or red of the remaining anthocyanins. Chlorophyll is the main factor in photosynthesis, using the energy of sunlight for production of oxygen. Chlorophyll absorbs light in the violet-blue and in the orange-red and transmits in the green and red. Light absorption leads to formation of excited chlorophyll. This returns to the ground state by dissipation of energy through the photochemical process, conversion into heat and emission of fluorescence in the red. Chlorophyll is not only important for photosynthesis, but also as a communication device for trees and plants. Plants have a sort of *colour vision*, by being able to *sense* the frequencies of the light surrounding them (L.O. Björn, *pers. comm.*, 2004). When light is transmitted through a canopy of vegetation, selective absorption takes place. A plant can *sense* the ratio between short-wave (about 660 nm) and long-wave red light (about 730 nm) and be aware of any competing plants or trees and thereby adapt to its neighbourhood.

References

- Awdejew, von, 1842. Ueber das Beryllium und dessen Verbindungen. Chrysoberyl. *Annalen der Physik und Chemie von Poggendorff*, Bd. LVI, 118-21
- Bank, H., and Henn, U., 1988. Colour-changing tourmalines from East Africa. *J. Gemm.* 21(2), 102-3
- Bassett, H., 1955. A vanadiferous variety of tourmaline from Tanganyika. *Geol. Surv. Tanganyika Rec.*, 3, 93-6
- Bernstein, L.B., 1982. Monazite from North Carolina having the Alexandrite effect. *Am. Mineral.*, 67, 356-9
- Björn, L.O., 2002. *Photobiology. The science of light and life*. Kluwer Academic Publishers, Dordrecht
- Carstens, H., 1973. The red-green change in chromium-bearing garnets. *Contributions to Mineralogy and Petrology*, 41, 273-6

- Cossa, A., and Arzruni, A., 1883. Ein Chromturmalin aus den Chromeisenlagern des Urals. *Zeitschrift für Kristallographie und Mineralogie von P. Groth*, VII, 1-16
- Crowningshield, G.R., 1967. Chrome tourmaline from Tanzania. *Gems & Gemology*, 12(8), 242-4
- Crowningshield, G.R., 1970. A rare alexandrite garnet from Tanzania. *Gems & Gemology*, 13(5), 174-7
- Crowningshield, G.R., and Ellison, J.G., 1951. The determination of important optical properties without instruments. *Gems & Gemology*, 7(4), 120-4
- Dunn, P.J., 1977. Chromium in dravite. *Mineralogical Magazine*, 41, 408-10
- Farrel, E.F., and Newnham, R.E., 1965. Crystal field spectra of chrysoberyl, alexandrite, peridot and sinhalite. *Am. Mineral.*, 50, 1972-81
- Fiala, J., 1965. Pyrope of some garnet peridotites of the Czech massif. *Krystallinikum*, 3, 55-74
- Gübelin, E., and Schmetzer, K., 1982. Gemstones with alexandrite effect. *Gems & Gemology*, 18(4), 197-203
- Haidinger, W., 1849. Ueber den Pleochroismus des Chrysoberylls. *Annalen der Physik und Chemie von Poggendorff*, Bd. LXXVII, 228-36
- Halvorsen, A., and Jensen, B.B., 1997a. A new colour change effect. *J. Gemm.*, 25(5), 325-30
- Halvorsen, A., and Jensen, B.B., 1997b. Letter to the editor. *J. Gemm.*, 25(7), 491-2
- Hysingjord, J., 1967. Edel granat fra Otterøy ved Molde. *Geological Survey of Norway*, 255, 5-9
- Hysingjord, J., 1971. A gem garnet from the island of Otterøy near Molde, Western Norway. *J. Gemm.*, 12(7), 296-9
- Kennard, T.G., and Howell, D.H., 1941. Types of coloring in minerals. *Am. Mineral.*, 26, 405-21
- Kenngott, A., 1867. Über die alkalische Reaction einiger Minerale. *Neues Jahrbuch für Mineralogie, Geologie und Paläontologie*, 302-19
- Kokscharow, N.W., 1861. *Alexandrit. Materialien zur Mineralogie Russlands*, Bd., 4, 56-72, St. Petersburg
- Kuehni, R.G., 1997. *Color – An introduction to practice and principles*. John Wiley & Sons, Inc., New York
- Liu, Y., Shigley, J.E., Fritsch, E., and Hemphill, 1994. The "Alexandrite Effect" in gemstones. *Color Research and Application*, 19(3), 186-91
- Liu, Y., Shigley, J.E., and Halvorsen, A., 1999a. Colour hue change of a gem tourmaline from the Umba Valley, Tanzania. *J. Gemm.*, 26(6), 386-96
- Liu, Y., Shigley, J.E., Fritsch, E., and Hemphill, 1999b. A colorimetric study of the alexandrite effect in gemstones. *J. Gemm.*, 26(6), 371-85
- Manson, D.V., and Stockton, C.M., 1984. Pyrope-spessartine garnets with unusual color behaviour. *Gems & Gemology*, 20(4) 200-7
- Nassau, K., 1997. Letter to the editor, *J. Gemm.*, 25(7), 491
- Nassau, K., 2001. *The physics and chemistry of color*. 2nd ed. Wiley Interscience, Chichester
- Neuhaus, A., 1960. Über die Ionenfarben der Kristalle und Minerale am Beispiel der Chrom-färbungen. *Z. Krist.*, 113, 195-233
- Orgel, L.E., 1957. Ion compression and the colour of ruby. *Nature*, 179, 1348
- Poole, C.P., 1964. The optical spectra and color of chromium containing solids. *J. Phys. Chem. Solids*, 25, 1169-82
- Rose, G., 1842, *Mineralogisch-geognostische Reise nach dem Ural, dem Altai und dem Kaspische Meere*, Bd. II, Berlin
- Schmetzer, K., and Bank, H., 1979. East African tourmalines and their nomenclature. *J. Gemm.*, 16(5), 310-11
- Schmetzer, K., Bank, H., and Gübelin, E., 1980. The alexandrite effect in minerals: chrysoberyl, garnet, corundum, fluorite. *Neues Jahrbuch für Mineralogie Abhandlungen*, 138(2), 147-64
- Simonet, C., 2000. Geology of the Yellow Mine (Taita-Taveta District, Kenya) and other yellow tourmaline deposits in East Africa. *J. Gemm.*, 27(1), 11-29
- Thilo, E., Jander, J., and Seeman, H., 1955. Die Farbe des Rubins und der (Al,Cr)₂O₃-Mischkristalle. *Z. Anorg. Allgem. Chem.*, 279, 2-17
- Webster, R., 1961. Tanganyika tourmalines. *The Gemmologist*, 30(356), 41-54
- Webster, R., 1994. *Gems: their sources, description and identification*. 5th edition, P.G. Read (Ed.) Butterworth-Heinemann, Oxford
- Weigel, O., 1923. Über die Färbänderung von Korund und Spinell mit der Temperatur. *Neues Jahrbuch für Mineralogie, Geologie und Paläontologie*, 48, 274-309
- White, W.B., Roy, R., and Crichton, J.M., 1967. The 'alexandrite effect': an optical study. *Am. Mineral.*, 52 (5-6), 867-71
- Wörth, F. von, 1842. Untersuchung des Alexandrit, oder Chrysoberyll des Ural. *Schriften der Russisch-Kaiserlichen Gesellschaft für die gesammte Mineralogie zu St. Petersburg*. 1 (1), 116-27
- Zwaan, P.C., 1974. Garnet, corundum and other gem minerals from Umba, Tanzania. *Scripta Geologica* 20, 1-41

New Courses from Gem-A

ADVANCED DIAMOND GRADING COURSE

THREE-DAY PRACTICAL ADVANCED DIAMOND GRADING COURSE AND EXAM



- Use of the microscope to clarity grade and plot diamonds
- Colour grading and master stones
- Fluorescence grading
- Cut – measurements, proportions, symmetry and polish

Developed especially for Gem Diamond Diploma or Diamond Grading Certificate holders wishing to extend their knowledge of diamond grading.*

Tuesday 31 October to Thursday 2 November 2006

Introductory price: £675.00

* This course is for Gem Diamond Diploma or Diamond Grading Certificate holders.

PRACTICAL GEMMOLOGY CERTIFICATE

SIX-DAY PRACTICAL COURSE AND CERTIFICATED EXAM

Identical to the practical section of the Diploma in Gemmology course and exam, the course covers:

- Fashioned and rough gem materials, natural, synthetic, imitation and treated
- Use of the 10x lens and microscope for observation and identification of gem materials
- Detailed use of the refractometer, polariscope, spectroscope, dichroscope, Chelsea colour filter, UV and specific gravity
- Advice on examination technique



Practical Certificate holders who subsequently qualify in the Gemmology Diploma Theory Exam will be awarded the full Diploma in Gemmology*.

Wednesday 21 to Wednesday 28 June (weekdays only), exam 29 June 2006

Price £876.00** (includes Practical Handbook and instrument kit)

* Applicants must hold the Gem-A Foundation in Gemmology Certificate.

** Correspondence course students please phone for a special price.

Courses held at Gem-A's London Headquarters

Visit www.gem-a.info or call Claire on 020 7404 3334 for further information

Determination of the origin of blue sapphire using Laser Ablation Inductively Coupled Plasma Mass Spectrometry (LA-ICP-MS)

Ahmadjan Abduriyim and Hiroshi Kitawaki

Research Laboratory, Gemmological Association of All Japan, 5-25-11 Ueno Taitoku, Tokyo, 110-0005 Japan

Abstract: *Non-basalt-related and basalt-related sapphires can be distinguished on the basis of their trace element contents (sometimes called a chemical fingerprint), as determined with energy-dispersive X-ray fluorescence analysis. When using the oxide weight percent ratios of Cr_2O_3/Ga_2O_3 versus Fe_2O_3/TiO_2 these trace elements show two discrete populations. However, for blue sapphires originating from non-basalt-related deposits in the Isalo area of Madagascar, from Ratnapura, Sri Lanka and from Mogok, Myanmar, a nearly complete overlap is observed whereas the overlap for basalt-related sapphires from Bo Phloi, Kanchanaburi, Thailand, New South Wales, Australia, and ChangLe, Shandong, China, is less significant. LA-ICP-MS was applied to obtain ppm and ppb-level data for 'ultra-trace elements' such as Zn, Sn, Ba, Ta and Pb. The results clearly show that they differ for blue sapphires from the sources investigated. The combination of trace element and 'ultra-trace element' contents offers the potential for providing useful criteria in identifying the geographical origins of sapphires and other gemstones.*

Keywords: *chemical finger print, geographical origin determination, laser ablation-inductively coupled plasma mass spectrometry (LA-ICP-MS), trace and ultra-trace element, untreated sapphire.*

Introduction

Although determination of geographical origin of a gemstone is justified, in common with seeking the origin of other precious and rare objects, it should be regarded primarily as an opinion issued by a laboratory or gemmologist. It is commonly difficult to provide reliable evidence for such

opinions. They can either be well-based on detailed analytical data for each gemstone, on databanks and literature references, or they can be less well-based and range from unreliable and unprofessional guesses to plain wishful thinking. Nevertheless, origin information about a gemstone can have

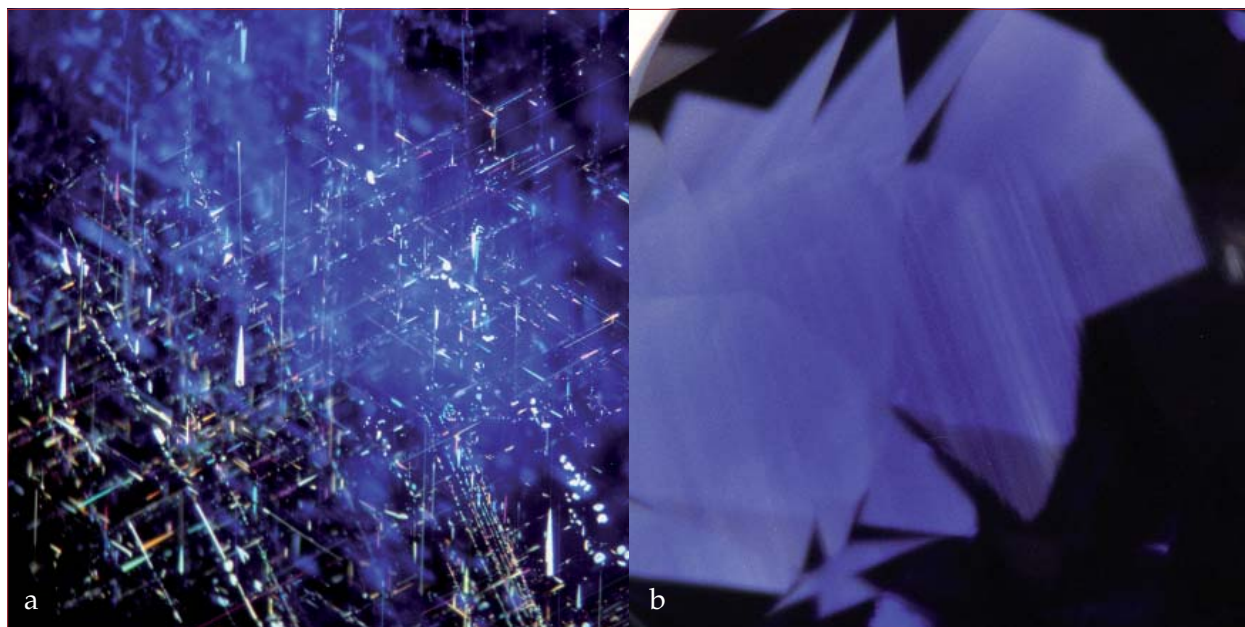


Figure 1: Rutile needles forming 'silk' (a), and colour zoning (b) are present in many Isalo sapphires.

historic and even archaeological importance, and for some jewellers it is a major factor in their daily trading. New analytical methods continuously have to be investigated for increased reliability of origin identification. The present paper describes such an effort.

Originally, the determination of sapphire origins focused on observation of internal features (Hughes, 1997) with later developments based on optical absorption spectrometry and chemical trace element analysis by X-ray fluorescence. With these methods, determination of geological occurrence, that is distinction between basalt-related origin (e.g. from Australia, China or Thailand) and non-basalt-related origin (e.g. from Sri Lanka, Myanmar or Madagascar) is now straightforward. However, distinction of sapphire origins in different countries but with a similar geological mode of occurrence – such as between Thailand and Australia, or between Madagascar, Sri Lanka and Myanmar – are much more difficult. When newly discovered blue sapphires from Madagascar came onto the gem market in the late 1990s, distinction between these and the more traditional sources in Sri Lanka and Myanmar often caused problems in the gem trade.

Recently, high-quality natural blue faceted sapphires from a new deposit at Isalo in the Ilakaka area of south-west Madagascar have become a commoner item in gem laboratories

for determination of their geographical origin than sapphires from Sri Lanka and Myanmar.

The Isalo sapphires come from secondary deposits associated with high-grade metamorphic and meta-sedimentary sources and have internal features similar to those in blue sapphires from Sri Lanka and Myanmar. Inclusions such as rutile needles, zircon with tension cracks, healed fissures and colour zoning are commonly seen in specimens from the Isalo area (Figure 1), but 'fingerprint' fluid inclusions (healed fissures) typical of Sri Lankan sapphires (Figure 2) have not been found.

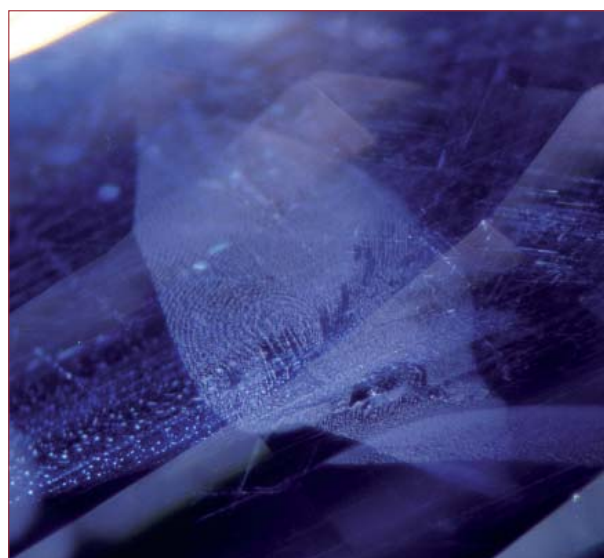
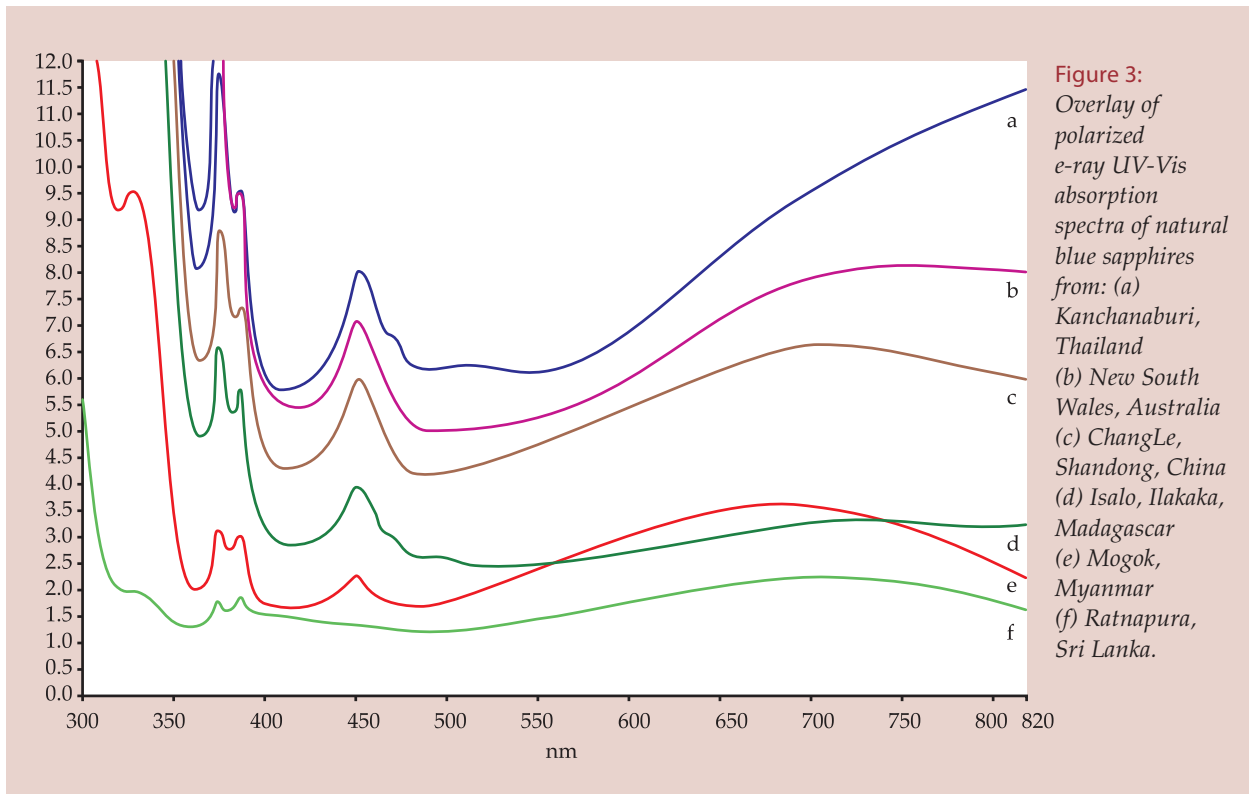


Figure 2: Fluid inclusion resembling a 'fingerprint' in sapphire from Sri Lanka.



The absorption spectra of Isalo blue sapphires are dominated by a broad pleochroic band between 500 and 800 nm with an e-ray absorption peak near 700 nm (due to charge transfer $\text{Fe}^{2+}/\text{Ti}^{4+}$), and a typical spectrum showing bands at 450 nm and 388 nm, a weak band at 377 nm and a band at 328 nm (all due to iron) with total absorption starting at about 300 nm, are shown in *Figure 3*. The polarised e-ray absorption spectrum of Isalo sapphire is different from the e-ray spectra of Sri Lankan and Myanmar sapphires.

Blue sapphires from Isalo can generally be distinguished from Sri Lankan and Mogok sapphires on the basis of colour, inclusions and absorption spectra. The aim of this study is to provide more compositional data and criteria from laser ablation (LA) and inductively coupled plasma mass spectrometry (ICP-MS) methods to be able to distinguish between these sapphires with more confidence. The compositional data are also compared to those of sapphires from the Bo Phloi district of Kanchanaburi, Thailand, from New South Wales, Australia, and from the ChangLe district of Shandong, China.

The sources of sapphires in Madagascar, Sri Lanka and Myanmar

Recent finds of significant quantities of gems in Madagascar, comparable to Sri Lanka and Myanmar, have had an important effect upon world gemstone supplies. The first finds of gem-quality blue sapphire were in the metamorphic skarns at Andranondambo, southern Madagascar, and mining started at the beginning of 1990 (Schwarz *et al.*, 1996) (*Figure 4*). Subsequently, dark blue sapphires associated with basaltic tuffs were found in the Diego Suarez area at the north end of the island and then a new large-scale secondary deposit containing sapphires of a range of colours was discovered in the Isalo/Ilakaka area of southwest Madagascar (Schmetzer, 1999). This deposit lies south of Isalo National Park and extends to Sakahara town; it contains high-saturation blue, pink and other colours of sapphires in large quantities, all deposited in a sedimentary basin. The primary geological source of these sapphires is not yet known, but sapphire placers

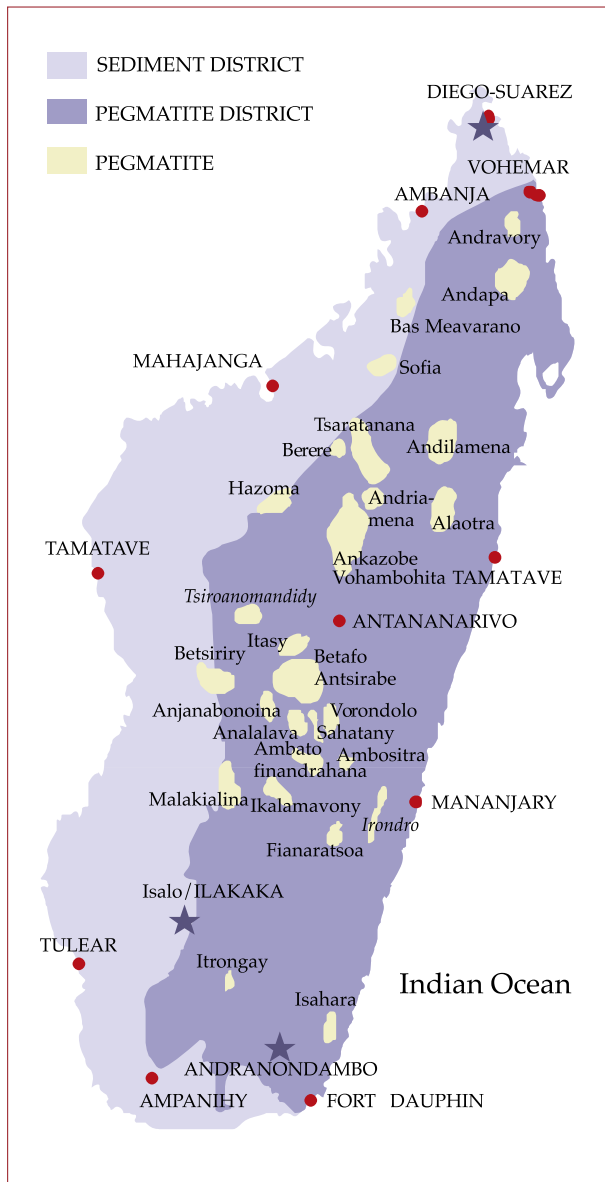
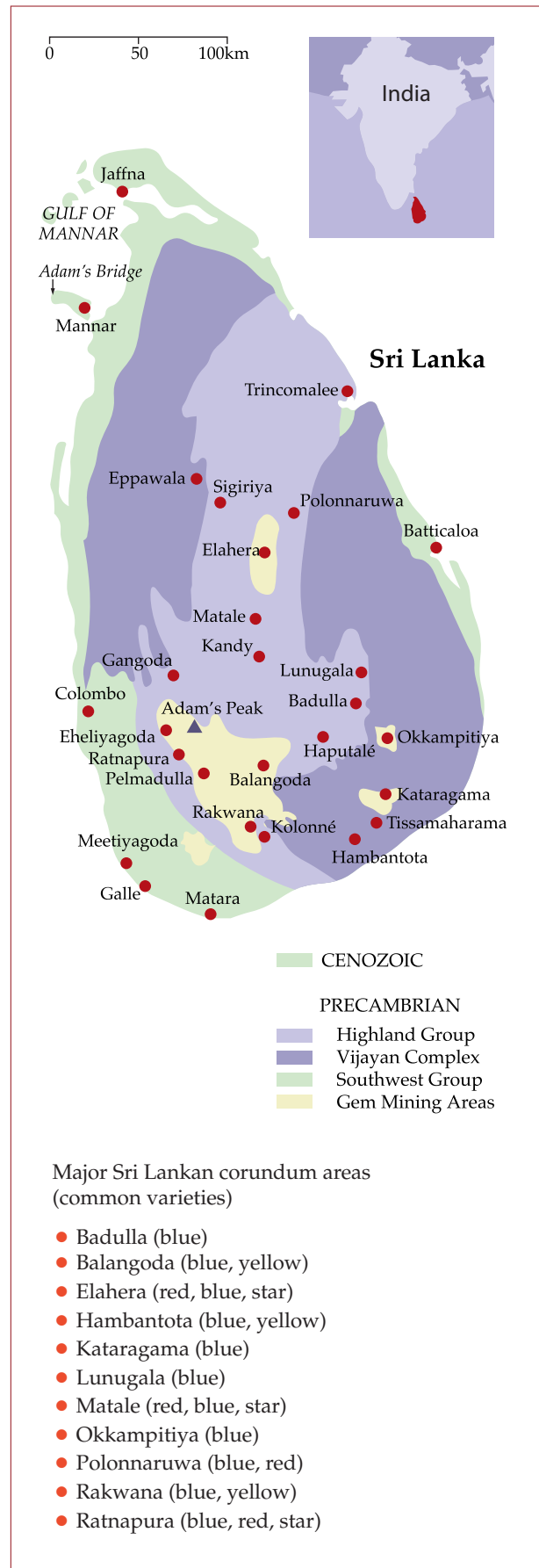


Figure 4: Map of Madagascar showing the corundum-producing areas of Isalo, Ilakaka, Andranondambo and Diego Suarez, and the broad regions where sedimentary or pegmatitic rocks predominate (modified after Pezzotta, 2001).

have probably originated from coarse-grained lenses and sedimentary strata of Permian and Mesozoic-age greywackes that themselves derived from possibly diverse sources of earlier metamorphic and pneumatolytic rocks and pegmatites.

In Sri Lanka, most of the main corundum deposits lie on the Highland, Vijayan and southwest groups of Precambrian metamorphic rocks (Cooray, 1967; Zoysa, 1981; Zwaan, 1982) (Figure 5). Colourless and sky blue to deep blue sapphires with habits of spindle-shaped hexagonal



Major Sri Lankan corundum areas (common varieties)

- Badulla (blue)
- Balangoda (blue, yellow)
- Elahera (red, blue, star)
- Hambantota (blue, yellow)
- Kataragama (blue)
- Lunugala (blue)
- Matale (red, blue, star)
- Okkampitiya (blue)
- Polonnaruwa (blue, red)
- Rakwana (blue, yellow)
- Ratnapura (blue, red, star)

Figure 5: Map of Sri Lanka showing the major gem-producing fields (modified after Zwaan, 1982).

bipyramids and flattened prisms with dominant pinacoid faces are mainly mined from secondary alluvial gravels, thought to be derived from a range of metasedimentary rocks including calc-silicates, marbles, quartzites, pelitic gneiss, khondalite and metamorphic rocks of igneous parentage, especially charnockites (orthopyroxene-bearing granites). Only a few dark opaque sapphires have been found *in situ*, and these have been in pegmatites

and gneisses. Mining is carried out in the Ratnapura, Elahera and Pelmadulla areas. The granulites and upper amphibolite metamorphic rocks derived from igneous rocks of the Vijayan and southwest groups are devoid of gems (Mathavan *et al.*, 2000).

Although rubies are the best-known gems from Myanmar, some of the world's finest blue sapphires have also come from the Mogok area (Figure 6). Sapphires from this area are tabular with pinacoid faces



Figure 6: Map of gem localities of Myanmar and Southeast Asia (modified after Hughes, 1997).

and probably originated in pegmatites, nepheline-corundum syenites and biotite gneisses, in contrast to the rubies which formed in contact- and regional-metamorphosed crystalline limestone (Hughes, 1997). Both sapphires and rubies occur in intimate association in virtually all alluvial deposits throughout the Mogok area, but the sapphires are found in quantity

at only a few localities, particularly 13 km west of Mogok, near Kathe (Halford-Watkins, 1935).

Although many Myanma blue sapphires show a more saturated blue than Sri Lankan sapphires, some are paler and do resemble those from Sri Lanka. Also, colours overlap with Madagascan sapphires and separation on this basis alone is not possible.

Gem mineral analysis methods

Standard methods of gem testing are increasingly being augmented by UV-visible-IR spectroscopy to analyse spectra, X-ray fluorescence (XRF) to obtain composition, and the electron probe micro-analyser (EPMA) to obtain detailed composition. Even these methods however may not lead to conclusive results and more sensitive analytical techniques are being developed. In mineral research samples are commonly dissolved by acid or are flux-melted using alkalis and brought into solution before they are analysed by Inductively Coupled Plasma-Atomic Emission Spectrometry (ICP-AES) or by Inductively Coupled Plasma-Mass Spectrometry (ICP-MS). Bringing the sample into solution, however, is both time-consuming and destructive. For analysis of small variations in composition EPMA with an element-mapping function can be used, but this method is also time-consuming in that the specimen has to be in an evacuated chamber and sensitivity to some elements is limited.

For gems, it is important to minimise any damage to a specimen under investigation, so Laser Ablation-Inductively Coupled Plasma-Mass Spectrometry (LA-ICP-MS), which can be used to analyse a solid sample in a very localized area with high sensitivity, offers new possibilities of obtaining trace element and ultra-trace element compositions of a gem mineral.

What is LA-ICP-MS?

LA-ICP-MS is a method of quantitatively and qualitatively analysing constituents of a sample by detecting a number of elements which have been evaporated from a tiny point on its surface. This is done by means of irradiation of the sample by a high-energy laser beam on its surface and the elements released are then ionised by high-frequency power which generates a plasma. The elements in the plasma can then be rapidly detected in minute amounts at the parts per billion (ppb) to parts per million (ppm) levels from atomic number 2, He (helium) upwards. A sample chamber does not need to be evacuated to carry out this analysis, and precise targeting of a specific area is possible with a narrow laser beam and a CCD camera. Measurements can be done on clean, rough or polished samples when using the fourth harmonic (266 nm) and the fifth harmonic (213 nm) of the tunable Nd-YAG (neodymium-doped yttrium aluminium garnet) laser or when using an excimer laser (193 nm). However, in order to obtain an acceptable result, one must allow that a minimum area on the gemstone of 100 μm^2 will suffer some damage. Guilong and Gunther (2001) were the first to use this method in seeking the origins of sapphires (*Figure 7a-b*).

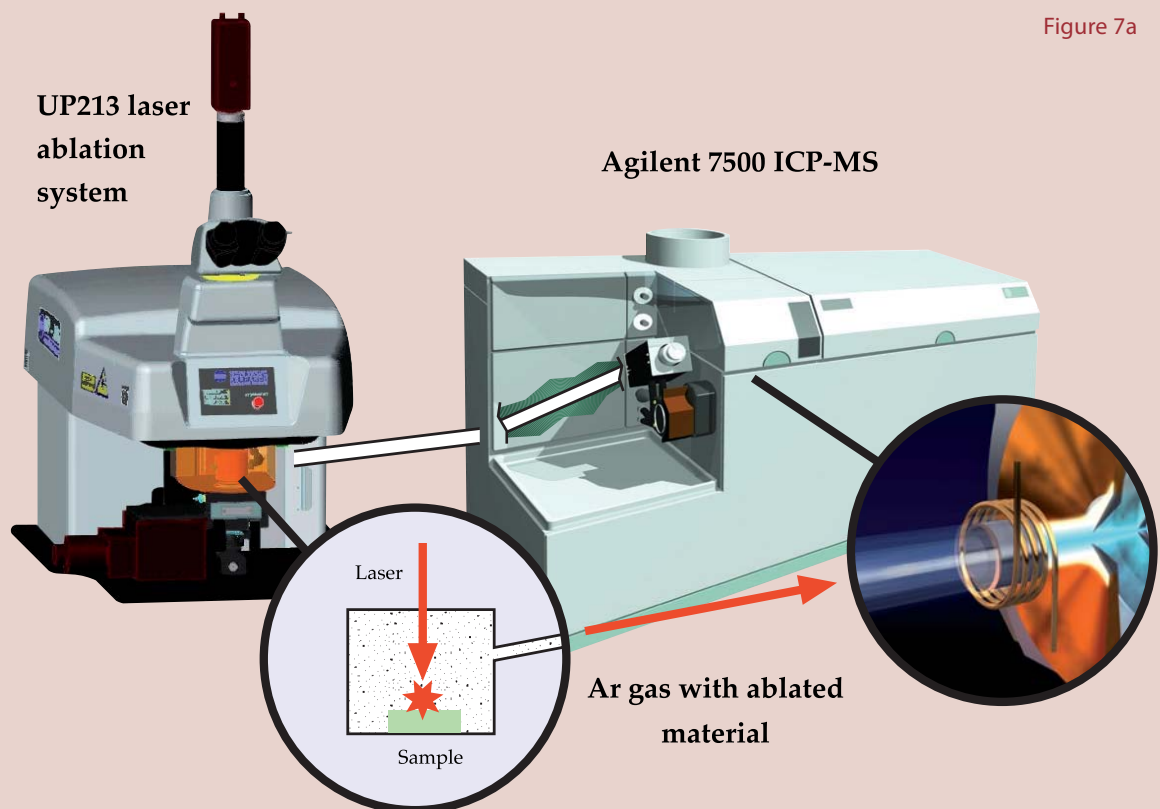


Figure 7a

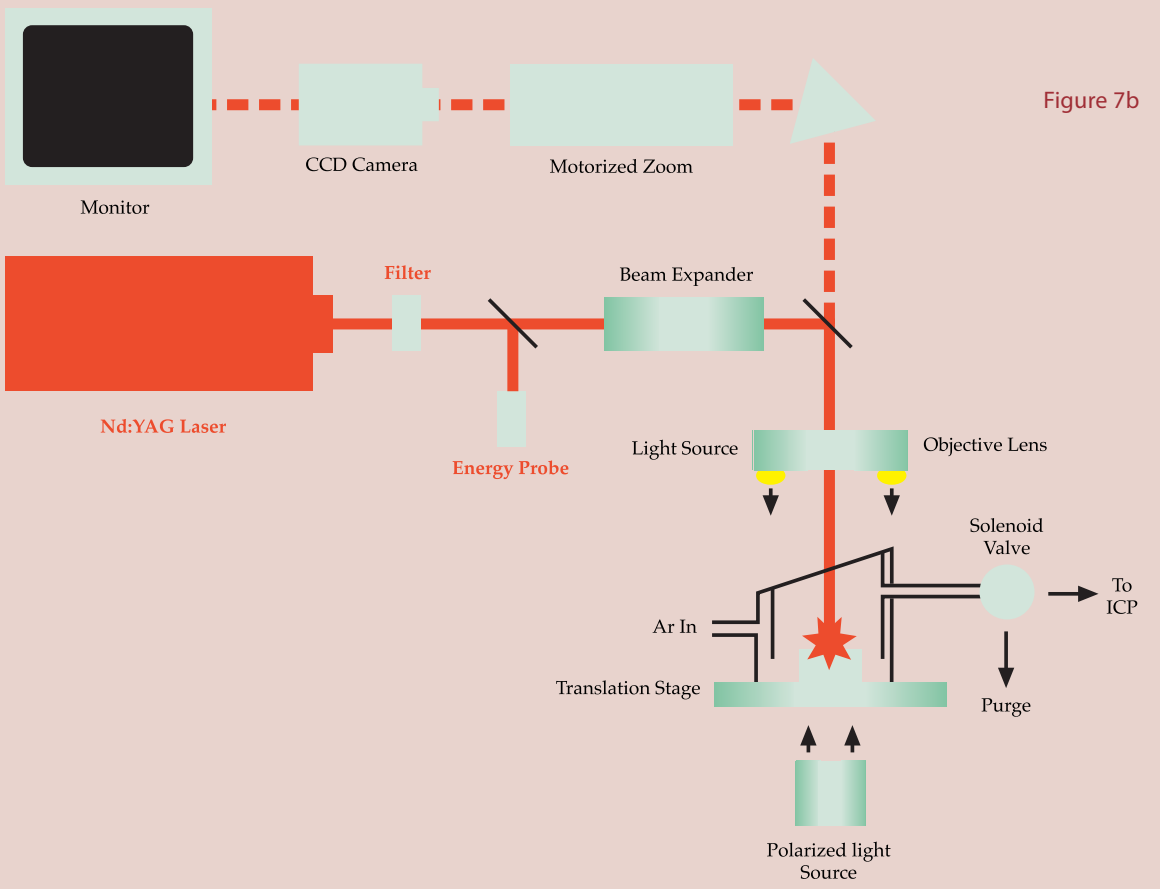


Figure 7b

Figure 7(a-b): Schematic diagrams showing the main elements of the Nd:YAG laser ablation system for ICP-MS



Figure 8: The LA-ICP-Mass Spectrometry system in the GAAJ Laboratory in Tokyo.

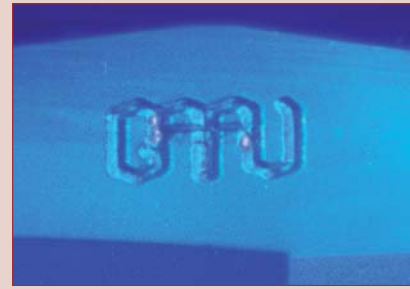


Figure 9: Laser logo mark of 'GAAJ' on the girdle of a blue sapphire in dark field illumination. The size of the mark is 80x230 μm with a laser line width of 16 μm and depth of 4~7 μm .

Measurements and samples

The Merchantek UP-213A/F made by New Wave Research and the model 7500a made by Agilent were used for the laser ablation system and for ICP-MS respectively (Figures 7 and 8). A concentration conversion factor on each element was made in this study to calculate its content because using calibration curves is less reliable. A standard sample multi-element glass NIST612 and internal standard of pure Al_2O_3 were used to calculate a concentration conversion factor, and this was used to convert the raw data obtained from the actual sample to quantitative values. After a laser analysis a trace of damage is left on the stone surface. However, this disadvantage was converted to an advantage by using the laser to generate sufficient material for analysis and at the same time inscribing the 'GAAJ' logo on the girdle; presence of the logo also proves that the test has been carried out (Figure 9). The width of the laser line is 16 μm , and the size of the mark is 80x230 μm with a depth of 4~7 μm ; it can barely be seen under a 10x loupe and resembles the inscription currently performed on diamonds. Conditions used are indicated in Table I. Each stone was subjected to laser ablation for 25 second periods in three runs, and ICP-MS data acquired for 40 second periods.

Table I: The settings and conditions used during LA-ICP-MS analysis

New Wave Research UV-213 A/F	Laser ablation parameters	Agilent	Plasma parameters
Wave length	213 nm	RF power	1500w
Pulse frequency	10Hz	Auxiliary gas flow rate	Ar 1.22ml/min and He 0.50ml/min
Laser energy	0.032mJ	ICP torch	Fassel torch 1.5mm id silica injector
Ablation pattern	'GAAJ' logo mark 16 μm wide line	Spray chamber	Water cooled
Scan speed	20 $\mu\text{m}/\text{sec}$	Sampler cone	Nickel. 1.1mm diameter
Laser warm up	5 sec	Skimmer core	Nickel. 0.8mm diameter
		Sampling depth	7mm
		Mass number	m/z=2 to 260
		Integration time	0.01 sec per point



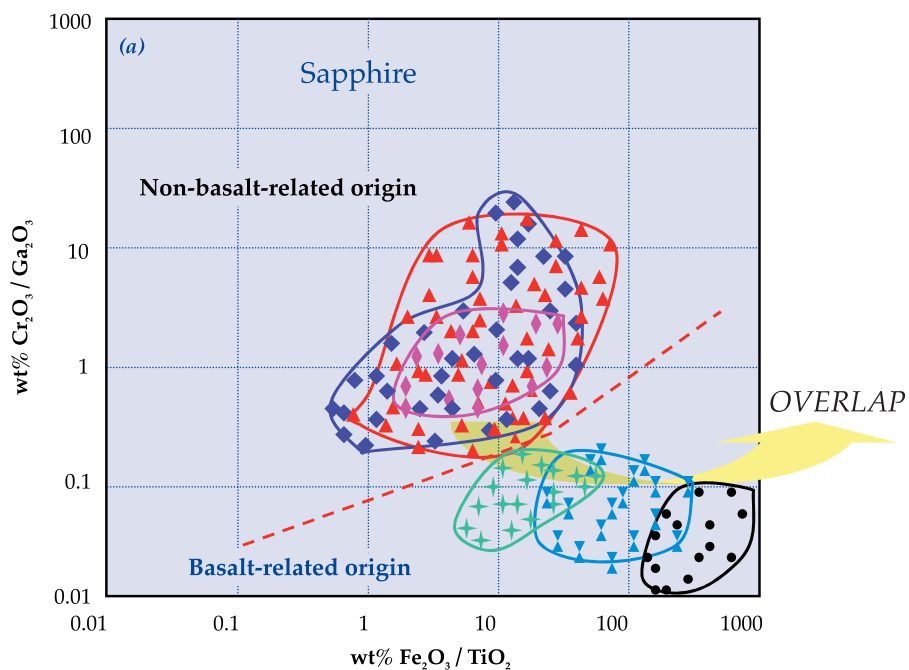
Figure 10: Blue sapphires (left to right and top to bottom: Madagascar, Sri Lanka, Myanmar, Thailand, Australia, China); all stones have natural colours and have not been heat-treated.

The sapphires analysed include 35 from Isalo, Madagascar, 30 from Ratnapura, Sri Lanka, and 15 from Mogok, Myanmar, all of which were non-heated-treated sapphires and came from non-basalt-related origins (Figure 10). Also, non-heat-treated sapphires from basalt-related origins in other localities such as Bo Phloi, Kanchanaburi, Thailand (6 stones), New South Wales, Australia (6 stones) and ChangLe, Shandong province, China (5 stones) were collected *in situ* from the mines. Details of the samples are given in Table II.

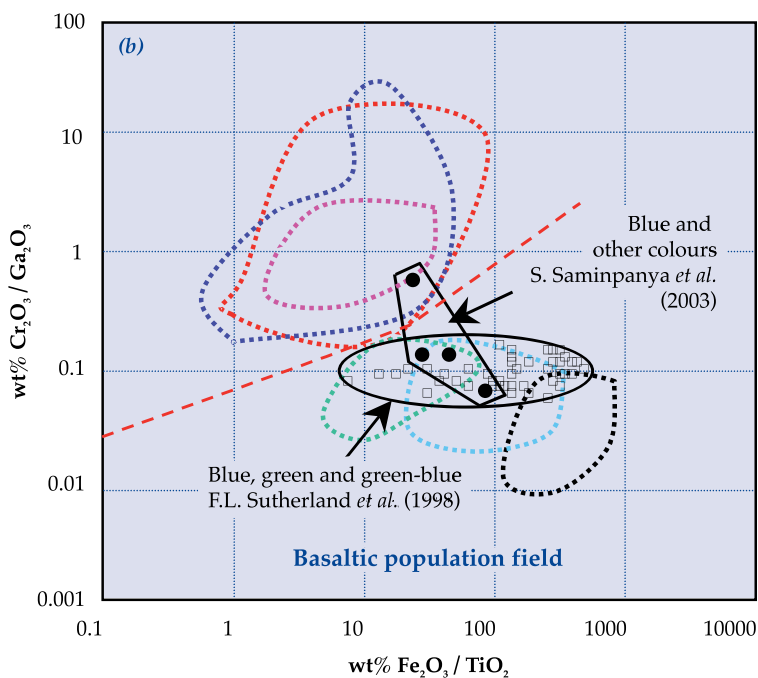
Descriptions of the different concentration ranges of the elements are as follows: ultra-trace elements ≤ 100 ppm < trace elements ≤ 10000 ppm (1%) < minor elements ≤ 100000 ppm (10%) < major elements $\leq 100\%$.

Table II: Details of sapphire samples from major gem-producing countries

Locality	Isalo, Ilakaka Madagascar	Ratnapura, Sri Lanka	Mogok, Myanmar	Bo Phloi, Kanchanaburi, Thailand	New South Wales, Australia	ChangLe, Shandong, China
Sample numbers	MD001-020 to M9-001-015	D027-502	B328-342	TH032-037	NS001-006	C125-127
Total of samples analysed	35	30	15	6	6	5
Colour	deep blue- light blue	blue- light blue	blue- light blue	dark blue- blue	dark blue- greenish blue	dark blue
Shape	mixed cut and cabochon	mixed cut	mixed cut	mixed cut	mixed cut	mixed cut
Weight (ct)	0.401-6.365	0.410-4.735	0.364-6.820	1.234-3.408	2.548-4.001	4.057-5.273
Fluorescence LW-UV	inert-weak red	inert-weak red	inert	inert	inert	inert
Fluorescence SW-UV	inert-very weak red	inert-very weak red	inert	inert	inert	inert



- | (a) Non-basalt-related Sapphire | Basalt-related Sapphire |
|---------------------------------|-----------------------------------|
| ▲ Isalo/Ilakaka, Madagascar | ★ Bo Phloi/Kanchanaburi, Thailand |
| ◆ Ratnapura, Sri Lanka | ▼ New South Wales, Australia |
| ◆ Mogok, Myanmar | ● ChangLe/Shandong, China |



- | (b) Comparison 'Basaltic' type Sapphires | |
|--|------------------------------|
| ● Kanchanaburi, Thailand | □ New South Wales, Australia |

Figure 11: (a) $\text{Cr}_2\text{O}_3/\text{Ga}_2\text{O}_3$ versus $\text{Fe}_2\text{O}_3/\text{TiO}_2$ ratios of blue sapphires from major gem-producing countries of the world. Group I consists of non-basalt-related sapphires with higher Cr and low Fe, Ti and Ga contents; Group II consists of basalt-related sapphires with high Ti, Fe, Ga and low Cr contents.

(b) Outlines of the fields detailed in (a) with sapphire data published by Sutherland *et al.* (1998) and Saminpanya *et al.* (2003) for comparison.

Results

LA-ICP-MS determinations of seventeen trace elements (^{23}Na , ^{24}Mg , ^{39}K , ^{47}Ti , ^{51}V , ^{53}Cr , ^{55}Mn , ^{57}Fe , ^{60}Ni , ^{63}Cu , ^{66}Zn , ^{69}Ga , ^{93}Nb , ^{118}Sn , ^{137}Ba , ^{181}Ta and ^{208}Pb) have been carried out on the 97 blue sapphires listed in *Table II* and the element contents in ppm are shown in *Table III* in order of atomic weight.

Results for Cr, Ga, Fe and Ti are plotted as oxide ratios in *Figure 11* to enable comparison with recent published work by Sutherland *et al.* (1998) and Saminpanya *et al.* (2003). Some of these previously reported data (from Bo Phloi; Kanchanaburi, Thailand, and New South Wales, Australia) are shown as black-bordered fields in *Figure 11b*.

By means of this diagram, two major groups of sapphires could be distinguished: the light to deep coloured non-basalt-related sapphires and the deep to dark coloured basalt-related sapphires (*Figure 11a*). The points representing non-basalt-related sapphires from Madagascar, Sri Lanka

and Myanmar lie in fields that completely overlap each other and so these chemical criteria cannot be used to separate sapphires from these three localities.

These trace element contents in basalt-related sapphires from three localities (Kanchanaburi, New South Wales and Shandong) in the second group lie in fields with less overlap. In comparison with previous data for similar localities (*Figure 11b*), our new data show a slightly wider range of Cr_2O_3 for New South Wales greenish-blue to dark blue sapphires and a wider range of $\text{Fe}_2\text{O}_3/\text{TiO}_2$ ratios in blue and dark blue Kanchanaburi sapphires.

For non-basalt-related sapphires, the above diagram is of no help in distinguishing Isalo, Ratnapura and Mogok sapphires. However, differences between sapphires from these three localities were first found in some of their ultra-trace element contents: specifically in Zn, Sn, Ba, Ta and Pb. The differences are summarized in *Table IV*.

Table III: Trace and ultra-trace element contents in parts per million of sapphires from major gem-producing countries obtained using LA-ICP-MS.

Locality	Madagascar	Sri Lanka	Myanmar	Thailand	Australia	China	
Number	MD001-020 to M9-001-015	D027-502	B328-342	Th032-037	NS001-006	C125-127	
Element	Na	bdl	bdl-55	14-49	bdl	bdl	bdl
	Mg	7-140	12.210	19-21	3-22	6-12	2-8
	K	bdl	bdl-7	bdl-4	bdl	bdl-5	bdl
	Ti	28-590	18-300	29-240	62-980	84-630	120-1200
	V	0.7-12	2-13	3-5	2-5	5-10	27-45
	Cr	2-66	3-120	4-31	0.3-0.6	0.7-7	<0.1-6
	Mn	<0.7	<0.7	<0.4	<0.4	<0.3-3	<0.3-9
	Fe	89-1160	180-1140	1030-1630	910-3670	1940-4660	1680-7230
	Ni	<0.4	<2	0.8-3	<0.2	<0.3	<0.2
	Cu	<0.2	<0.3	0.3-0.5	<0.5	<0.4	0.6-1
	Zn	bdl	bdl	1-15	bdl	bdl	bdl
	Ga	7-66	7-40	8-43	44-1000	55-130	88-190
	Nb	bdl	bdl	<0.2	bdl	bdl	bdl
	Sn	0.2-21	<2	0.5-2	<0.4	<0.3	<0.3
	Ba	bdl	bdl	0.1-2	bdl	bdl	bdl
	Ta	0.5-2	bdl	bdl	bdl	<0.1	bdl
Pb	bdl	bdl	0.2-2	bdl	bdl	bdl	

Note: '<' sign and 'bdl' are below the detection limit.

Table IV: Summary of distinctive element contents in sapphires.

Locality	Non-basalt-related origin	Detection limit ppm
Isalo, Ilakaka Madagascar	High Sn, high Ta, high Ga contents no Zn, no Ba, no Pb	Sn<0.1 Ta<0.01 Ga<0.5 Zn<1.01 Ba<0.05 Pb<0.13
Ratnapura Sri Lanka	no Zn, no Ba, no Ta, no Nb, no Pb low Sn (two samples)	Nb<0.01
Mogok Myanmar	Zn, Ba, Pb, and low Sn, Nb contents no Ta	
Locality	Basalt-related origin	Detection limit ppm
Bo Phloi, Kanchanaburi, Thailand	High Mg, low V contents	Mg<0.35 V<0.14
New South Wales, Australia	Low V contents	
ChangLe, Shandong, China	High V, high Cu, high Mn contents	Cu<0.21 Mn<0.40

Discussion

The Fe, Ti, Cr and Ga contents of sapphires obtained using LA-ICP-MS confirm the grouping of non-basalt-related and basalt-related sapphires when plotted on $\text{Cr}_2\text{O}_3/\text{Ga}_2\text{O}_3$ vs. $\text{Fe}_2\text{O}_3/\text{TiO}_2$ diagrams and reported by different workers.

The relative abundance of Ti, Fe and Ga in basalt-related corundums worldwide has been related or linked to plutonic crystallisation from a melt (Levinson and Cook, 1994) or alkaline Si- and Al-rich melts, either evolved from basaltic magma (Irving, 1986; Coenraads *et al.*, 1990) or derived from the melting of amphibolitised mantle (Sutherland, 1996; Sutherland *et al.*, 1998).

Isalo sapphires contain significant quantities of Ti, Fe, Ga and two elements closely related to granite, Sn and Ta. These sapphires were found in gem placer deposits in coarse-grained rocks of Permian and Mesozoic greywackes, which are considered to have been derived from metamorphic, pegmatitic and pneumatolytic rocks, reflecting a complex geological environment. But the presence of Sn and Ta suggests that the sapphires formed close to syenites or granites (see Aspen *et al.*, 1990 and Möller

et al., 1989). Saminpanya *et al.* (2003) also mentioned the presence of significant contents of the granitophile elements Ta, Nb and Sn in non-basalt-related Laos sapphires which originated from the Ban Huai Sai area. In contrast, the Ratnapura sapphires are notable for the absence of Zn, Ba, Pb, Ta and Nb with only two samples containing Sn above the detection limit. These sapphires have been mined from secondary deposits derived from various sources including the metasedimentary rocks: calc-silicates, marbles and pelitic gneisses, and metamorphic rocks of igneous parentage, particularly charnockites (orthopyroxene-bearing granites) (Cooray, 1994).

Mogok sapphires contain different quantities of Zn, Nb, Sn, Ba and Pb, the absence of Ta distinguishing them from Isalo sapphires. These contents suggest that Mogok sapphires were associated with nepheline-corundum syenite or syenitic gneiss which had been metasomatised by a felsic magma. A similar process was postulated for some Thai sapphires by Saminpanya *et al.* (2003) who explained that corundum-bearing syenitic gneiss was formed from Precambrian paragneiss through metasomatism by felsic or carbonatitic liquids at deep levels beneath Thailand.

The basalt-related blue and dark coloured sapphires from Bo Phloi, Kanchanaburi, New South Wales and ChangLe, Shandong, contain significant Ti, Fe and Ga. The ChangLe sapphires had the highest V contents of all the sapphires tested in this study. Generally, sapphires found in basaltic terrains are considered to have been carried to the Earth's surface by rapidly rising alkali basalt magmas and tuffs (Coenraads *et al.*, 1990; Guo *et al.*, 1992; Levinson and Cook, 1994). Experiments indicate that corundum crystals cannot be grown directly from melts of basaltic composition, and formation of corundum in a metamorphic environment is accepted by most researchers, although precise details are still unclear.

Chemical analysis is very important in the identification of gemstones. At present, the XRF method is entirely non-destructive and, in this respect, is more generally acceptable than LA-ICP-MS analysis, but its disadvantage is its limited sensitivity. This study has shown that trace and ultra-trace element analysis using LA-ICP-MS can be very useful for origin determination of gemstones. It can also be effective in detecting diffusion treatment and in identifying different parts of pearls. Trace and ultra-trace elements can show considerable variation across the surface of a sample, and to obtain a true picture, LA-ICP-MS analyses should be carried out around the girdle and on a number of facets. This study represents an initial stage in compiling trace element data which are useful in the gem trade and more data from more samples from more localities should now be collected.

Acknowledgements

The authors wish to thank Yasomi Hirano and Nilam Alawdeen for their field survey help and valuable advice about the Isalo/Ilakaka area of Madagascar and Ratnapura area of Sri Lanka, and our technical staff member Makoto Okano at GAAJ for assistance with this work. We are also grateful to Dr Ichiro Sunagawa and George Bosshart for critically reading and revising the draft of this manuscript.

References

- Aspen, P., Upton, B.G.J., and Dicken, A.P., 1990. Anorthoclase, sanidine and associated megacrysts in Scottish alkali basalts: high-pressure syenitic debris from upper mantle sources. *European Journal of Mineralogy*, 2, 503-17
- Coenraads, R.R., Sutherland, F.L., and Kinny, P.D., 1990. The origin of sapphires: U-Pb dating of zircon inclusions shed new light. *Mineralogical Magazine*, 54(1), 113-22
- Cooray, P.C., 1967. An introduction to the geology of Ceylon. *Spolia Zeylanica (Ceylon Journal of Science)*, 31(1), 1-324
- Cooray, P.C., 1994. The Precambrian of Sri Lanka; a historical review. *Precambrian Research*, 66, 3-18
- Guillong, M., and Gunther, D., 2001. Quasi non-destructive laser ablation-inductively coupled plasma-mass spectrometry fingerprinting of sapphire. *Spectrochimica Acta B*, 56, 1219-31
- Guo, J.F., Wang F.Q., and Yakoumelos G., 1992. Sapphires from Changle in Shandong Province, China. *Gems & Gemology*, 28(4), 255-60
- Halford-Watkins, J.F., 1935. Burma sapphires-locations and characteristics. *The Gemmologist*, 5(52), November, 89-98
- Hughes, R.W., 1997. *Ruby and Sapphire*. RWH Publishing, Boulder, 511pp
- Irving, A.J., 1986. Polybaric magma mixing in alkali basalts and kimberlites: Evidence from corundum, zircon and ilmenite megacrysts. Fourth International Kimberlite Conference Extended Abstracts. *Geological Society of Australia Abstracts Series*, 16, 262-4
- Levinson, A.A., and Cook, F.A., 1994. Gem corundum in alkali basalt: origin and occurrence. *Gems & Gemology*, 30(4), 253-62
- Mathavan, V., Kalubandara, S.T., and Fernando, G.W.A.R., 2000. Occurrences of two new types of gem deposits in the Okkampitiya gem field, Sri Lanka. *The Journal of Gemmology*, 27(2), 65-72
- Möller, P., Cern, P., and Saupe F., 1989. *Lanthanides, tantalum and niobium mineralogy, geochemistry, characteristics of primary ore deposit, prospecting, processing, and applications, Work papers*. Springer-Verlag, Berlin, 380pp
- Pezzotta, F. (Ed.), 2001. *Madagascar. A Mineral and Gemstone Paradise*. (Extra Lapis, English, No 1). Lapis International LLC, East Hampton, CT, 100pp
- Rankin, A.H., Greenwood, J., and Hargreaves, D., 2003. Chemical finger printing of some east African gem rubies by laser ablation ICP-MS. *The Journal of Gemmology*, 28(8), 473-82
- Saminpanya, S., Manning, D.A.C., Droop, G.T.R., and Henderson, C.M.B., 2003. Trace elements in Thai gem corundums. *The Journal of Gemmology*, 28(7), 399-415
- Schmetzer, K., 1999. Ruby and variously coloured sapphires from Ilakaka, Madagascar. *Australian Gemmologist*, 20(7), 282-4
- Schwarz, D., Petsch, E.J., and Kanis, J., 1996. Sapphires from the Andranondambo region, Madagascar. *Gems & Gemology*, 32(2), 80-99

- Schwarz, D., and Schmetzer, K., 2001. Rubies from the Vatomandry area, eastern Madagascar. *The Journal of Gemmology*, 27(7), 409-16
- Sutherland, F.L., 1996. Alkaline rocks and gemstones, Australia: a review and synthesis. *Australian Journal of Earth Science*, 43, 323-43
- Sutherland, F.L., Schwarz, D., Jobbins, E.A., Coenraads, R.R., and Webb, G., 1998. Distinctive gem corundum suites from discrete basalt fields: a comparative study of Barrington, Australia, and West Pailin, Cambodia, gemfields. *The Journal of Gemmology*, 26(2), 65-85
- Zoysa, E.G.G., 1981. Gem occurrences in Sri Lanka. *Journal of the Gemmological Society of Japan*. 8, 43-9
- Zwaan, P.C., 1982. Sri Lanka: the gem island. *Gems & Gemology*, 18(2), 62-71

Rubies with lead glass fracture fillings

Claudio C. Milisenda¹, Yoichi Horikawa², Yuji Manaka² and Ulrich Henn³

1. German Foundation for Gemstone Research (DSEF), Prof.-Schlossmacher-Str. 1, D-55743 Idar-Oberstein, Email: info@gemcertificate.com
2. Central Gem Laboratory, Miyagi Bldg, 5-15-14, Ueno, Taito-Ku, Tokyo 110-0005, Japan. Email: coloredstone@cgl.co.jp
3. German Gemmological Association (DGemG), Prof.-Schlossmacher-Str. 1, D-55743 Idar-Oberstein, Email: info@dgemg.com

Abstract: *Recently, a large number of relatively large faceted rubies showing an unusual inclusion pattern have appeared in the gem market. A detailed examination showed that the stones have been treated with a lead-bearing glass of high RI to improve the clarity. Under magnification, flash effects and bubble-like inclusions were visible and enabled straightforward detection of stones with this new type of modification. X-ray images (radiographs) also show evidence of fracture filling and lead can be detected by using X-ray fluorescence analyses. At present the majority of the stones tested have been from an occurrence at Andilamena in north-eastern Madagascar. However, the treatment can be applied to all types of fractured corundums.*

Keywords: *clarity enhancement, identification, Pb-glass, ruby*

Introduction

In recent months unusually large numbers of faceted, transparent to translucent rubies showing an unusual inclusion pattern have appeared in the gem market. The results of inquiries indicated that the majority of the stones originated from Madagascar.

A first Lab-Alert relating to these stones issued by the Research Laboratory of the Gemmological Association of All Japan (GAAJ) on 15 March 2004 described a lead-glass impregnated ruby with a weight of 13.22 ct. This was followed by short notes published by colleagues from the USA (e.g. AGTA-GTC Lab, 2004; Rockwell and

Breeding, 2004). A first detailed description of the treatment process was published by Pardieu (2005) on the AIGS website.

Since then we have examined approximately 150 stones weighing between 2.5 and 20 ct (*Figure 1*). After having tested the first stones in March 2004, we confirmed that their fractures and cavities had been filled with a lead-based glass to improve the clarity and informed the client about the result. The client then confirmed that the stones had been treated in Thailand and offered for sale with the suffix 'New Treatment' (in Thai: 'Paw Mai').



Figure 1: Faceted rubies from Madagascar with lead glass fracture fillings (weight between 4.03 and 12.58 ct).

Precursor material

Rubies rich in fissures and with a sufficient saturation of colour are the most suitable samples for treatment (Figure 2). At present most of such stones originate from a secondary deposit at Andilamena in north-eastern Madagascar. The occurrence was discovered in 2000 and is located in the Toamasina Province, about 50 km north of Lake Alaotra. Material from the mine is available by kilogram and includes cm-sized, partly rounded with tabular, prismatic or, rarely, rhombohedral crystal



Figure 2: Ruby crystals from Madagascar with a saturated colour and numerous cracks. Their appearance can be significantly improved with a high RI glass.

habits, and distinct striations on the basal and prism faces. From a geological point of view the corundum occurrences of northern Madagascar are related to late Mesozoic basalt flows in which both sapphires and rubies occur as xenocrysts. In addition to the Andilamena stones, heavily fractured rubies from Tanzania (Morogoro), Kenya and a star ruby from Madagascar (Figure 3) have been treated with Pb-glass and there may be similar rubies from other sources on the market.



Figure 3: Star ruby with lead glass fracture fillings from Madagascar (weight: 4.48 ct)

Treatment process

The treatment is a multi-step process involving simple heating and the use of different lead rich compounds to fill the fissures and cavities of the stones (Pardieu, 2005; Themelis, 2005, *pers. comm.*).

First, the stones are preformed in order to remove the matrix and any other impurities that could affect the treatment. Then the stones are washed with hydrofluoric acid (75% HF). In the first stage of the heating process in an electrical furnace at temperatures between 900° and 1400°C, additional impurities are removed from the fissures. This temperature range may not affect any rutile inclusions present. Next the stones are heated with various chemical additives.

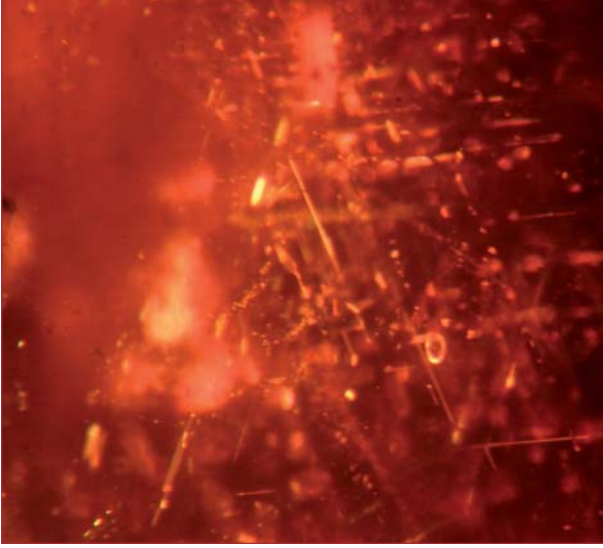


Figure 4: The presence of oriented unaltered rutile needles suggests that the rubies have not been treated at high temperatures (immersion, reflected light, field of view 3 mm).

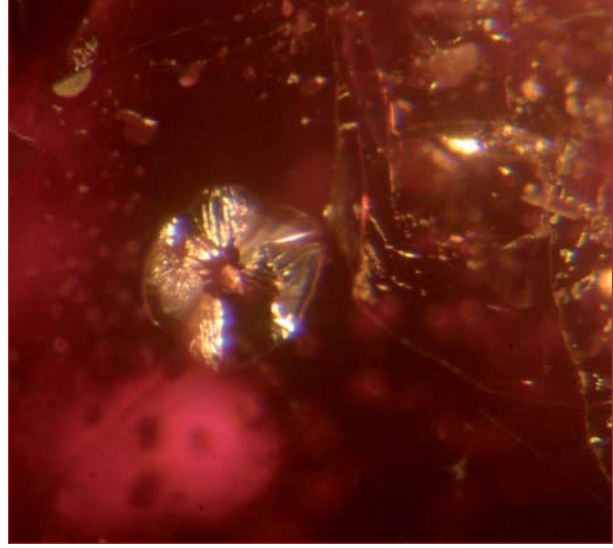


Figure 5: Mineral inclusions surrounded by discoidal tension cracks are indications of thermal enhancement (immersion, reflected light, field of view 2 mm).

Several chemical components may be used and various compositions are currently being tested. At present the composition is mainly a mixture of silica and lead but a number of other components such as sodium, potassium, calcium, tungsten, germanium and in particular metal-halides may be added to the powder and enter the glass composition as well. The composition of high refractive index glass and the process of filling fractures in minerals are published in European patent Application No. 1069087A1 (2001). It describes a glass composition having an RI of more than 1.75 and includes at least two metal-oxides or hydroxides (e.g. PbO and Bi₂O₃), one metal-halide or oxyhalide (e.g. PbF₂ or PbCl₂) and a glass-forming and stabilising component (e.g. SiO₂). The resulting glasses are colourless but can be coloured by adding small amounts of chromophores such as Cr₂O₃, Fe₂O₃, or others.

The stones are embedded in the powder along with some oil and placed in a crucible. The powder will melt in a furnace open to the atmosphere at temperatures between 850° and 1100°C and form a glass of high liquidity which enters microcavities in the stones and enhances their clarity.

The second heating process can be repeated several times until the best appearance can be obtained. Then the stones are faceted and polished. Some stones may be heated again with chemicals probably to make sure all microcavities are filled; this in turn means that the stones can take a better polish and their lustre is improved.

Identification criteria

If the term 'new treatment' is mentioned in the context of the corundum gem trade then, automatically, beryllium-diffusion comes to mind, a treatment in which the specimens are subjected to a high temperature. However, some samples in our batch of 150 showed crystallographically oriented and unaltered rutile inclusions (*Figure 4*), a feature which generally is viewed as an indication that a stone was not subjected to high temperatures. However, other stones contained mineral inclusions surrounded by tension cracks (*Figure 5*) which are typically found in stones that have been thermally enhanced, but not necessarily at very high temperature.

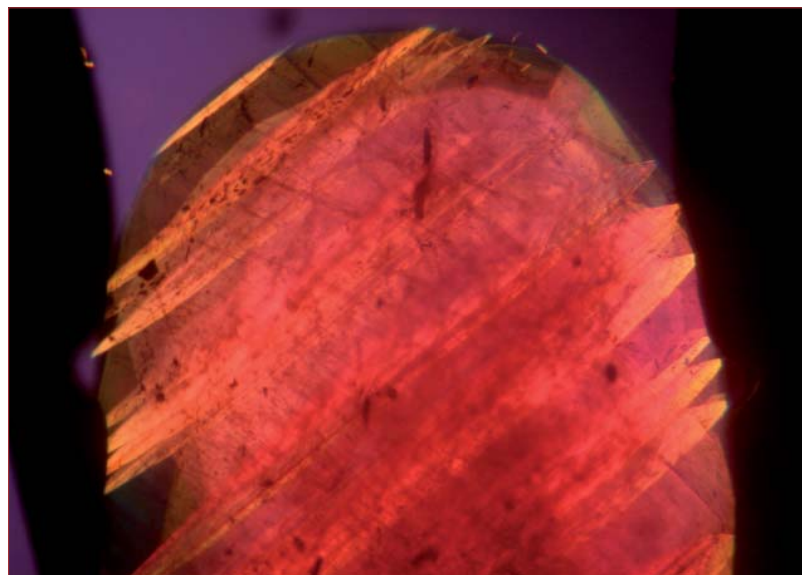


Figure 6: Lamellar twinning and boehmite tubes are commonly observed in rubies from East Africa (immersion, crossed polars, field of view 4 mm).

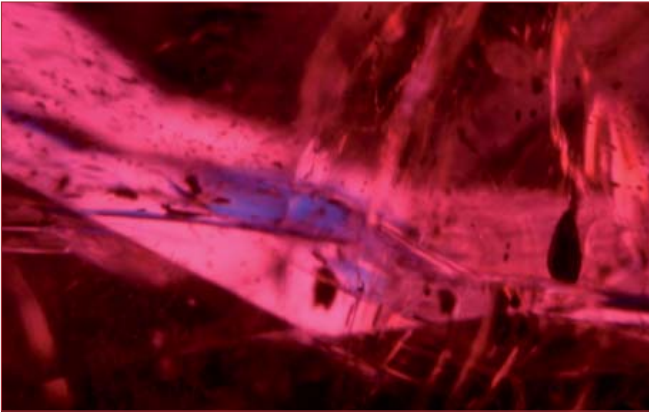


Figure 7: Blue flash effect in a fracture-filled ruby from Madagascar (dark field illumination).

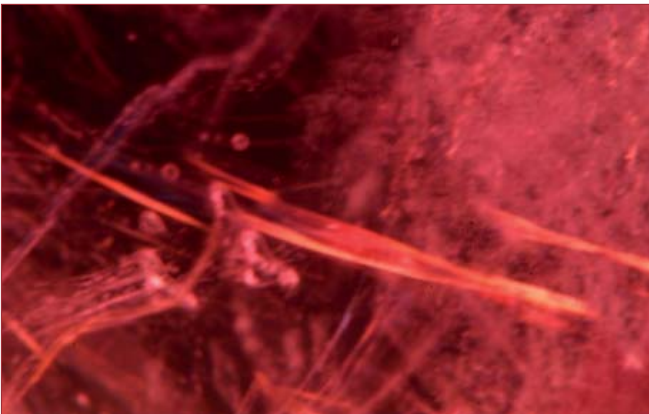


Figure 8: Orange flash effect in a fracture-filled ruby from Madagascar (dark field illumination).

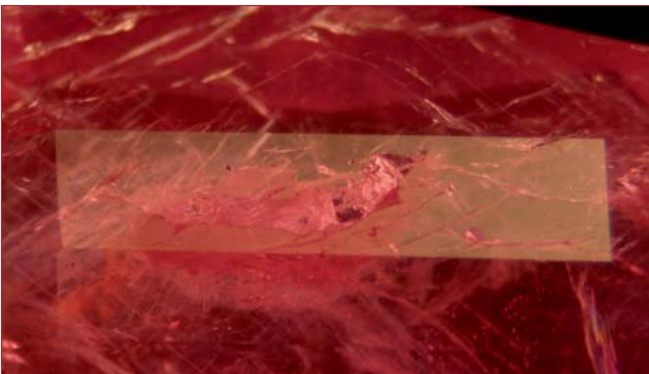


Figure 9: Open fracture in a clarity-enhanced ruby from Madagascar (dark field illumination).

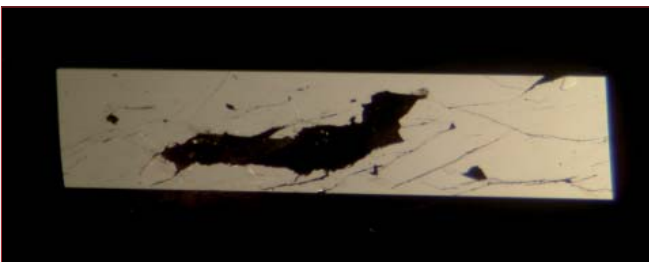


Figure 10: The same open fracture when viewed in reflected light.

Depending on their composition Pb-based glasses may have a melting point below 600°C (Themelis, 1992; Pfaender, 1997) a temperature that will not affect rutile inclusions but may affect minerals with a significantly lower melting point than rutile.

Most of the stones examined had an inclusion pattern typical of East African rubies including those from Madagascar. They showed a distinct twinning (Figure 6), and contained boehmite tubes and rutile needles in addition to other birefringent mineral inclusions and dust-like particles. The identification of the treatment process is quite straightforward for a trained gemmologist, especially for those familiar with the process used by the Israeli companies Yehuda and Koss to enhance the clarity of diamonds. Such treated stones first appeared in the mid 1980s and are known as 'Yehuda diamonds' and 'Koss-diamonds' in the trade. The presence of a high RI glass within the microcavities can be detected in both diamonds and rubies by the 'flash-effect'. In dark field illumination the glass-filled cavities will show blue to purple or orange colour flashes, that can best be seen when viewed parallel to the fissures (Figures 7 and 8). Fractures which contain foreign glassy substances of lower refractive indices such as the flux-assisted healed fissures of rubies from Mong Hsu in Myanmar, do not produce these flashes.

Washing the stones in HF after final cutting will dissolve the surface-reaching glass and leave behind open cavities (Figures 9 and 10).

Flat bubble-like inclusions also form a characteristic and diagnostic inclusion pattern (Figure 11) and larger fracture-filled areas are more visible in immersion (Figure 12).

X-ray images and X-ray-fluorescence analyses (EDXRF) can also confirm the presence of Pb-bearing glass. Because of the lead content the glass is less transparent to X-rays than the ruby host and as a result the filled areas appear darker on an X-ray image (Figure 13). Figure 14 a, b and c shows EDXRF spectra taken from fillings in the fractures of three different stones and all indicate the presence of lead.



Figure 11: Flat, bubble-like inclusions are a typical feature of lead glass fracture fillings in rubies (immersion, transmitted light, field of view approx. 1 mm).

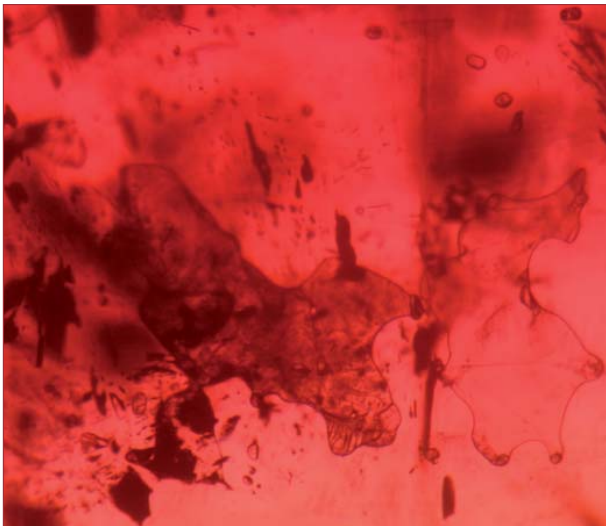


Figure 12: Larger filled fracture in a ruby from Madagascar (immersion, transmitted light, field of view approx. 2 mm).

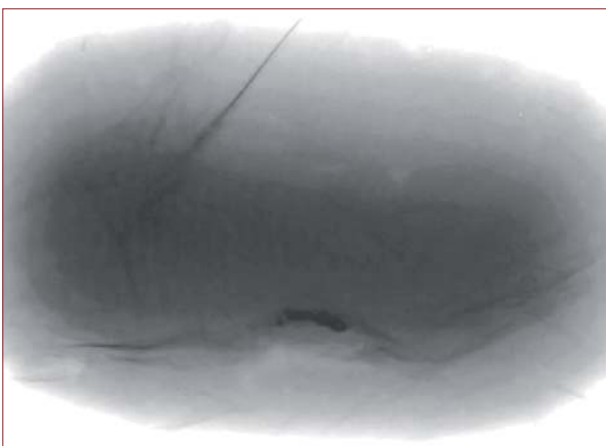


Figure 13: Lead glass is less transparent to X-rays and, therefore, filled fractures appear darker on images than the corundum host.

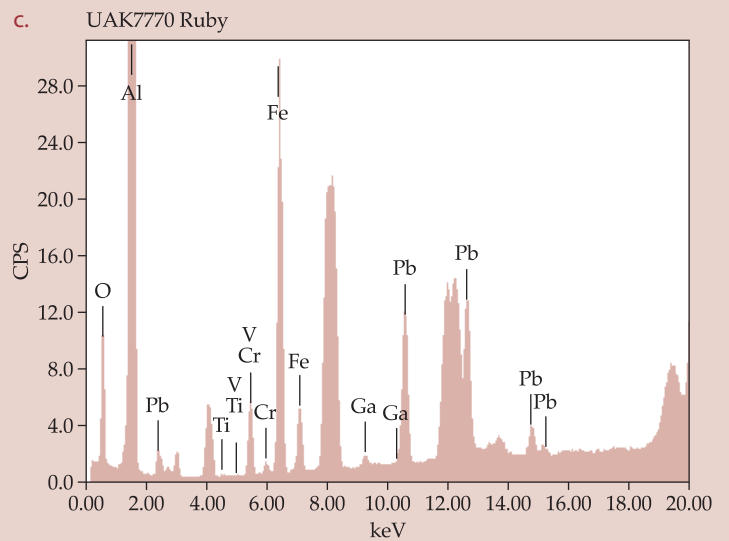
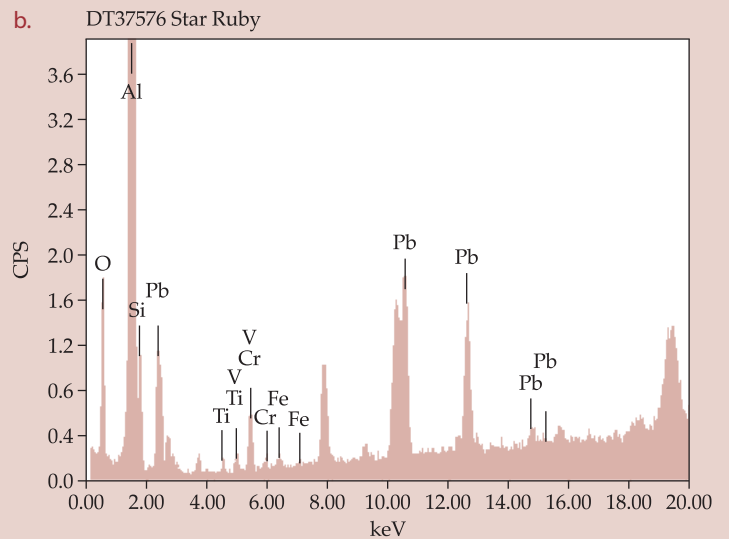
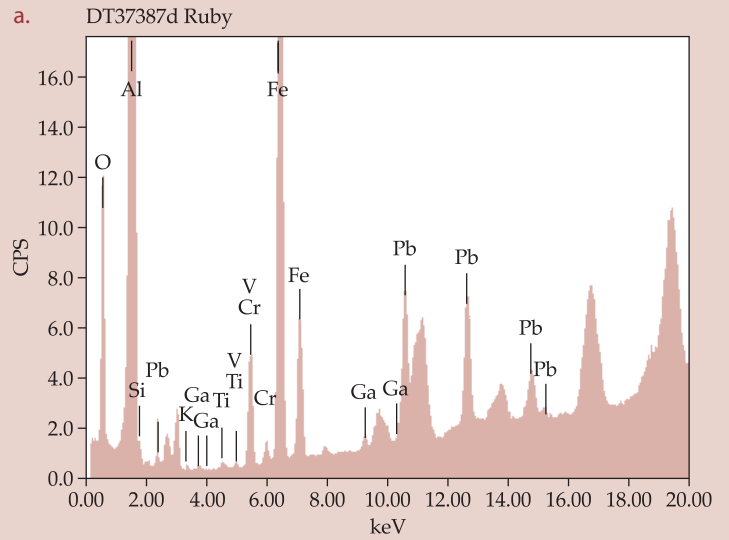


Figure 14a-c: X-ray fluorescence spectra indicating the elements present in glass filling fractures in three rubies. The presence of lead (Pb) is confirmed.

Conclusion

The filling of fractures in rubies with glass-like substances has been known for many years.

In the past the fractures were healed predominantly with a flux-based melt (borax) and the temperature used was relatively high ($\geq 1200^{\circ}\text{C}$), which commonly altered the inclusion pattern significantly (e.g. notably by reshaping or dissolving any rutile needles) and thus was indicative of the heating process.

In contrast, the lead-bearing melt can be induced into fissures at significantly lower temperatures ($\leq 1000^{\circ}\text{C}$) and, as a result, the inclusion pattern at first sight may not necessarily indicate that the stones have been heated.

However, the new treatment process of filling fractures in rubies by using a glass of distinctly higher refractive index than that produced by the borax fluxes and one that is almost the same as that of corundum significantly increases a stone's clarity. Therefore, this clarity enhancement needs to be specifically mentioned in any gemstone report of such a stone.

References

- GAAJ Lab Alert, 2004. Lead glass impregnated ruby. <http://www.gaaj-zenhokyo.co.jp/researchchroom/kanbetu/2004/gaaj-alert-040315en.html>
- AGTA Gemstone Update, 2004. New Ruby Treatment Arrives in the United States. <http://www.agta.org/consumer/news/200407002rubytreatment.htm>
- Pardieu, V., 2005. Lead glass filled/repared rubies. <http://www.aigslaboratory.com/Filearticle/55.pdf>
- Pfaender, H.G., 1997. *Schott-Glaslexikon*. 5th edn. MVG-Verlag, Landsberg am Lech
- Rockwell, K.M. and Breeding, C.M., 2004. Lab Notes: Rubies, Clarity enhanced with a lead glass filler. *Gems & Gemology* 40(3), 247-9
- Themelis, T., 1992. *The heat treatment of ruby and sapphire*. Gemlab Inc., Houston TX

A note on a pearl attached to the interior of *Crassostrea virginica* (Gmelin, 1791) (an edible oyster, common names, American or Eastern oyster)

Kenneth Scarratt¹, Carol Pearce² and Paul Johnson²

1. GIA Research (Thailand)

2. GIA Laboratory, New York, USA

Abstract: This report describes an egg-shaped non-nacreous pearl attached to the interior of a *Crassostrea virginica* (Gmelin, 1791) (in the position of the adductor scar); the State shell of Connecticut, Mississippi and Virginia, commonly known as the American or Eastern oyster. The pearl is said to have been discovered when the owner opened (shucked) an oyster for eating. The pearl is hollow and together with the shell has a gross weight of 28.204 grams. The pearl measures approximately 13.00 x 10.88 mm. The mollusc, UV/visible and Raman spectra, and microradiography results are described.

Keywords: *Crassostrea virginica*, Eastern oyster, mollusc, Raman spectra, USA

Introduction

When envisioning the growth of a pearl within an oyster, it is the nacre-producing pearl oysters of the family *Pteriidae* that generally come to mind. These winged or pearl oysters include *Pteria penguin*, *Pinctada radiata*, *Pinctada maxima* (gold-lipped pearl oyster) *Pinctada margaritifera* (black-lipped pearl oyster), *Pinctada fucata* and numerous others (Anonymous, 2004).

The family *Ostreidae* is composed of edible oysters and is most commonly known throughout the world as a popular source of seafood. The shell is porcellanous (non-nacreous) and the pearls produced from

these edible oysters generally have little beyond curiosity value (Anonymous, 2005). This report describes one such interesting non-nacreous pearl attached to the interior of *Crassostrea virginica* (Gmelin, 1791) (Figure 1 and Table I) in the position of the adductor muscle scar (Carriker, 1996).

Crassostrea virginica, the American or Eastern oyster, is native to the Western Atlantic coast of North America from the Gulf of St. Lawrence in Canadian waters southward around Florida (Anonymous, 2003), and all along the Gulf of Mexico, the Caribbean and the coasts of Venezuela, Brazil





Figure 1: The pearl featured in this report is attached to the interior of *Crassostrea virginica* (Gmelin, 1791) in the position of the adductor scar (photo Elizabeth Schrader © GIA).

and Argentina. It is common in estuaries and coastal areas of reduced salinity, and has been introduced along the Pacific coast in California and Washington, also in Hawaii, Australia, England, Japan and possibly other areas, but generally has not become established in most of these localities. The species still occurs naturally in some areas as extensive reefs on hard to firm bottoms; it is very important commercially and is widely cultivated in many areas (Carriker and Gaffney 1996; Wallace, 2001).

The shell is made up of two valves, the upper one flat and the lower convex, with variable outlines and a rough outer surface. The oyster spends most of its life attached with a sticky substance to various shells, rocks, and roots. Initial attachment is by a slender, near-transparent byssus thread.

Table 1: Taxonomic Hierarchy

Kingdom	<i>Animalia</i>
Phylum	<i>Mollusca</i>
Class	<i>Bivalvia</i>
Order	<i>Ostreoida</i>
Family	<i>Ostreidae</i>
Genus	<i>Crassostrea</i>
Species	<i>Crassostrea virginica</i>

This is followed by adhesion of the left valve to the substrate with a tanned protein similar to that of the periostracum. Both the thread and the adhesive are produced by the byssal gland.

After the oyster becomes sessile (permanently attached), it is invariably attacked by oyster drills, starfish and other enemies. The American, Eastern (or common) oyster reaches a length of 2 to 6 inches (5-15 cm). These oysters are harvested in artificial beds on both coasts of the United States: on the Atlantic especially in the regions of the Delaware and Chesapeake bays and in the waters off Long Island, and in the Gulf Coast off Louisiana; in the Pacific off the state of Washington. Prepared beds are usually seeded with veligers or young sessile oysters called spats. In warm waters they mature in 1½ years; in cooler waters the period of growth is about 4 to 5 years. They are usually transplanted several times before harvest to enhance their food supply and stimulate growth.

Pearls in edible oysters are not unknown, examples similar to the one described herein are on view in the pearl exhibit in the American Museum of Natural History, New York (specimen number 268828) (Figure 2) and described on the AMNH website (Anonymous, 2005). However, the pearl described herein seems to be unusually large and elegantly shaped. As with the AMNH examples this pearl is attached in the area of the adductor scar.



Figure 2: A specimen of *Crassostrea virginica* (Gmelin, 1791) containing a pearl in the position of the adductor scar. On view in the pearl exhibit in the American Museum of Natural History, New York. Photograph by Denis Finnin © AMNH.

A natural pearl from *Crassostrea virginica*

Materials and methods

Analytical techniques employed included: microscopy using gemmological microscopes at magnifications ranging from 15 to 60 x; UV/visible spectra were recorded in reflectance mode using a Zeiss MCS 500/501 spectrometer over the range between 250 and 800 nm; Raman data were obtained using the Renishaw Raman system 1000 spectrometer incorporating a 514 nm argon ion laser; microradiographs were produced using a Faxitron X-ray unit at 90 kV and 3 ma.

Results

Appearance and chemical composition

This pearl is egg-shaped with an uneven and mottled surface. It is attached in the area of the adductor scar to the inside of the shell of an Eastern (edible) oyster and like the shell is non-nacreous.

While the subject of the chemical composition of pigments in all types of oyster shells (and the pearls they produce)

is of great interest to the gemmologist, this area of gemmological investigation is far from being fully characterised. However, for *Crassostrea virginica* there are significant published data for gemmologists to note. According to Stenzel (1971) "Oysters living in warm and tropical regions have darker, more vivid, more varied and more extensive colorations than those living in cooler climates. The inner surfaces of the valves of northern populations of *Crassostrea virginica* living north of Cape Cod, for example, are characterized by whitish to grayish yellow colors, and adductor muscle scars are grayish-red purple to very dusky red purple. The inner valve surfaces of the same species living in the northern part of the Gulf of Mexico possess large areas of light brown to grayish purple and only a few patches of whitish color. Their adductor muscle scars have approximately the same colors. It is therefore generally possible to distinguish by pigmentation individuals from at least the extremes of their range". Also, "Carriker *et al.* (1982) observed that strongly pigmented areas on the surface of the right valve of *Crassostrea virginica* grown in controlled laboratory conditions contained low concentrations of magnesium, aluminum, silicon, and titanium" (Carriker, 1996).

Structure

In examining 'collectable' items, regardless of value, one has to be aware of possible 'fakes'. In this instance apart from confirming the pearl's authenticity, one of the other concerns might be whether or not the 'item' had been 'created' by adhering the pearl artificially to the shell.

During a careful microscopic examination of this pearl no indications of it being a manufactured product were observed; no layered (banded) shell-like structures were observed in the pearl and no artificial adhesion to the shell. The structures observed on parts of the surface of the pearl and the shell's internal surfaces resemble those seen in some other non-nacreous shells and pearls (e.g. *Mercenaria mercenaria*); having a slightly rippled appearance.

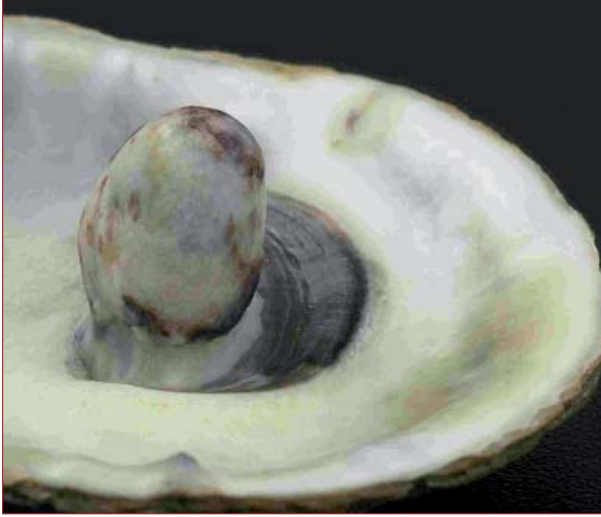


Figure 3: Non-nacreous pearl attached to the interior of *Crassostrea virginica* in the position of the adductor scar (photo Elizabeth Schrader © GIA).



Figure 4: Non-nacreous pearl attached to the interior of *Crassostrea virginica* in the position of the adductor scar (photo Elizabeth Schrader © GIA).

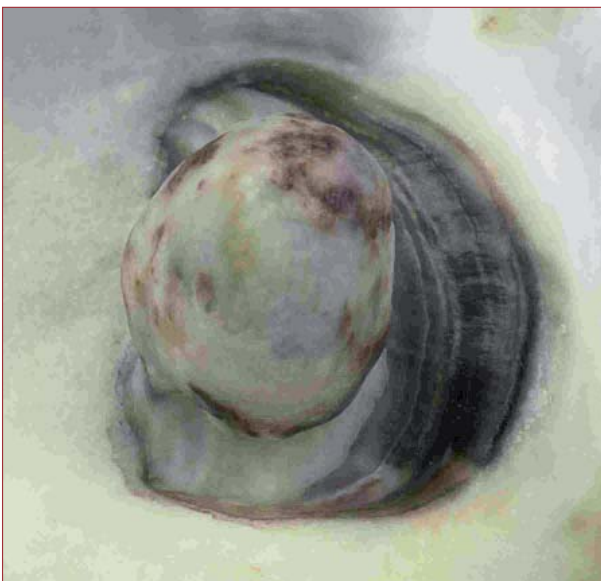


Figure 5: Non-nacreous pearl attached to the interior of *Crassostrea virginica* in the position of the adductor scar (photo Elizabeth Schrader © GIA).

The purple area in the region of the adductor scar was unusually translucent, and a close examination of this area and the pearl prompted an image in the mind's eye of "an iceberg (the pearl) floating in a purple translucent sea". Also 'floating' atop the purple area are a small number of calcitic globules (Figures 3, 4 and 5).

A detailed account of the shell microstructure is set out by Carriker (1996). Raman data presented later which indicates that calcite rather than aragonite is the main component of the examined pearl and shell, confirms the comments of Carriker and Palmer (1979) quoted by Carriker (1996): "From homogeneous aragonitic prodissoconch II valves, the shell metamorphoses abruptly beyond the metamorphic line to prismatic calcite (externally) and foliated calcite (internally). The reason for the sharp transition in shell mineralogy from aragonite to calcite, while islands of aragonite remain in muscle scars and residual fibers in the ligament, is unclear."

Microradiography

While being the most powerful technique in the arsenal of the gemmologist when distinguishing natural from cultured pearls, microradiography relies upon the differences in X-ray absorbance between the alternating crystalline and organic layers that are generally present within a nacreous pearl (natural or cultured) (Kennedy, 1998; Akamatsu *et al.*, 2001) but these differences are not necessarily obvious in non-nacreous pearls. Non-nacreous pearls tend to have a structure that consists of dense closely packed crystal arrays without large amounts of organic material being present. Therefore in general, non-nacreous pearls are opaque to X-rays and only occasionally show the presence of organic material by microradiography. Fortunately the pearl in this *Crassostrea virginica* shell revealed considerable information about its growth history despite being encumbered also by the shell.

The microradiographs are shown in Figures 6 and 7 and reveal that the pearl is not only egg-like in its external form, but also show clearly that it is egg-like internally

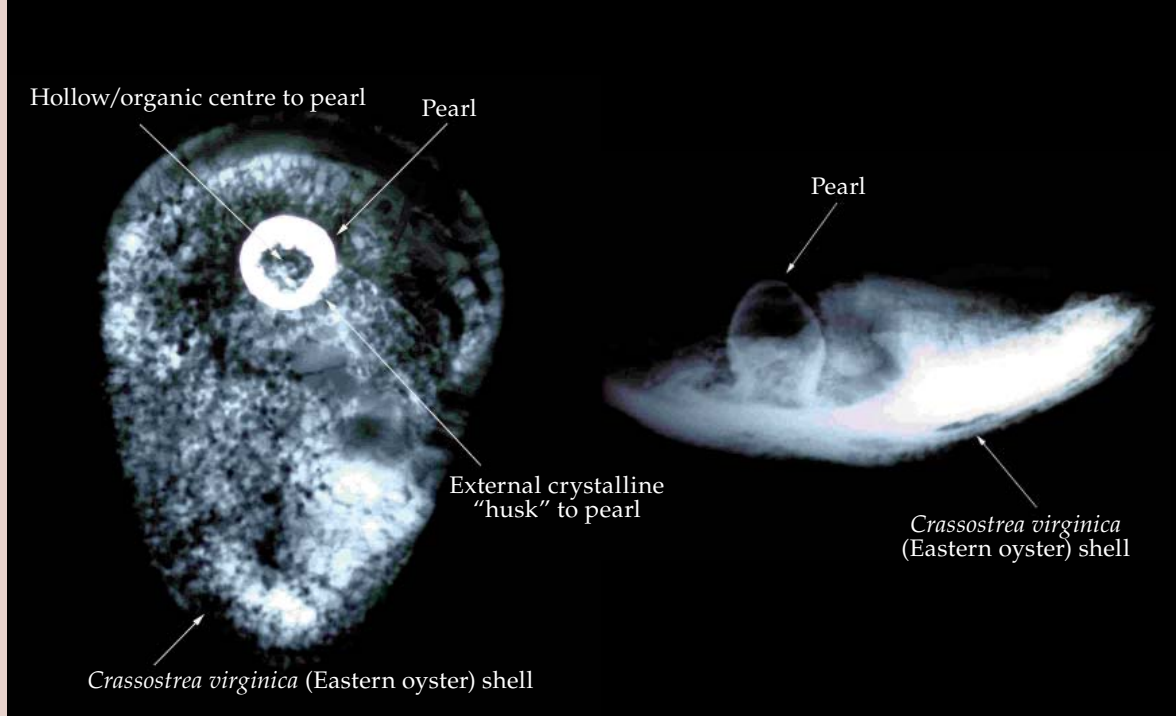


Figure 6: Microradiographs showing the *Crassostrea virginica* shell and pearl from above (left) and in profile (right). The shell and pearl structures are indicated by the annotations. Photo reproduction by Elizabeth Schrader © GIA.

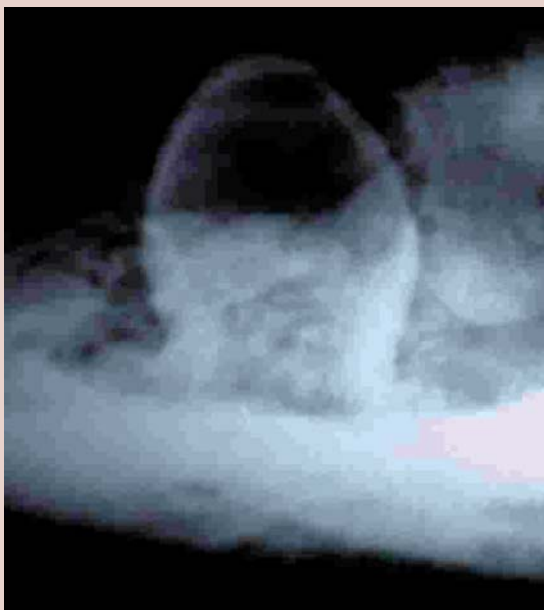


Figure 7: A close-up view of the microradiograph in Figure 6 concentrating on the pearl alone and revealing an organic core. Photo reproduction by Elizabeth Schrader © GIA.

– being composed of a relatively thin ‘shell’ of calcium carbonate (calcite) surrounding a large organic core. These microradiographs indicate that if the pearl were to be removed from the shell there would be a high likelihood of damage. Also, from its position in the shell and its organic core, it is very likely that during growth the pearl encased at least a portion of the adductor muscle.

Raman and UV/visible spectra

Raman spectra (Kiefert *et al.*, 2001) were collected from the purple portions only of the pearl. All spots examined produced similar spectra with peaks located at 311, 501, 666, 914, 941, 1029, 1145, 1308, and 1574 cm^{-1} (Figure 8).

These peaks are currently unassigned. Other peaks located at 1088, 711 and 279 cm^{-1} which we can attribute to calcite (Traub *et al.*, 1999, Li and Chen, 2001; Huang *et al.*, 2003, Kiefert *et al.*, 2004) were also noted. The spectrum for this pearl differs from those recorded for the non-nacreous pearls produced by *Strombus gigas* (the conch pearl) and the *Melo volutes* (the melo pearl) where peaks attributable to carotenoids are invariably present if these pearls are coloured, and where it is the peaks normal for aragonite (rather than calcite) at 1085 and 703 cm^{-1} that dominate. However, the presence of calcite rather than aragonite compares well with the spectra produced by the scallop pearl from *Nodipecten (Lyropecten) subnodosus* (Scarratt and Hänni, 2004).

The Raman spectrum of the pearl was compared with the Raman spectrum produced from the white area on the interior of the *Crassostrea virginica* shell to which it is attached (Figure 9). The white area produced a Raman spectrum typical of aragonite with peaks at 703 and 1085 cm^{-1} that were

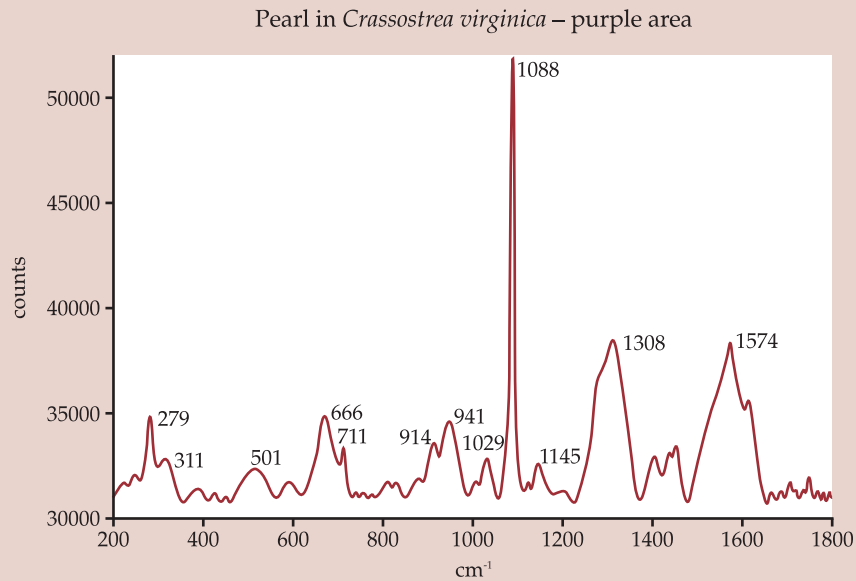


Figure 8: The Raman spectrum recorded for a purple area on the pearl adhering to the *Crassostrea virginica* shell. Characteristic peaks associated with calcite are recorded at 279, 711 and 1088 cm^{-1} the other peaks are unassigned.

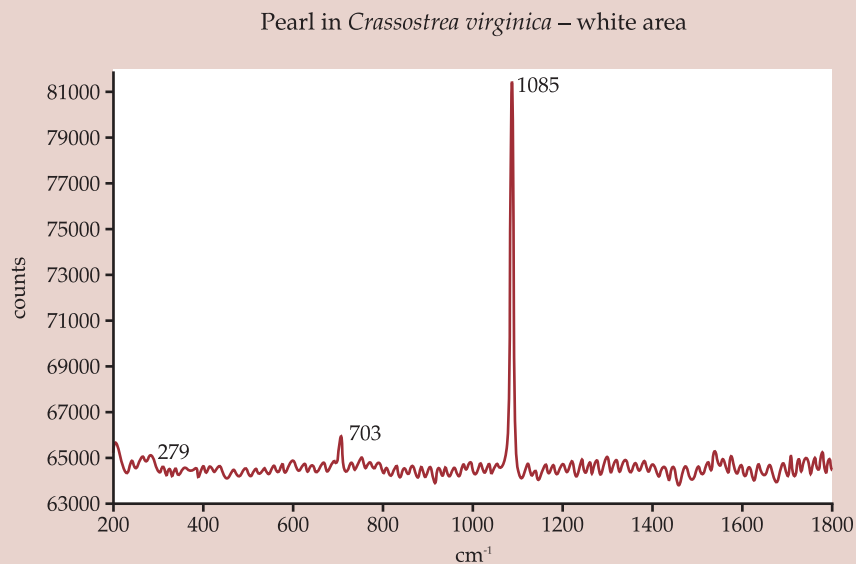


Figure 9: The Raman spectrum recorded for a white area on the inside of the pearl containing *Crassostrea virginica* shell described in this report. Peaks characteristic of aragonite at 1085, 703 and 279 cm^{-1} are recorded.

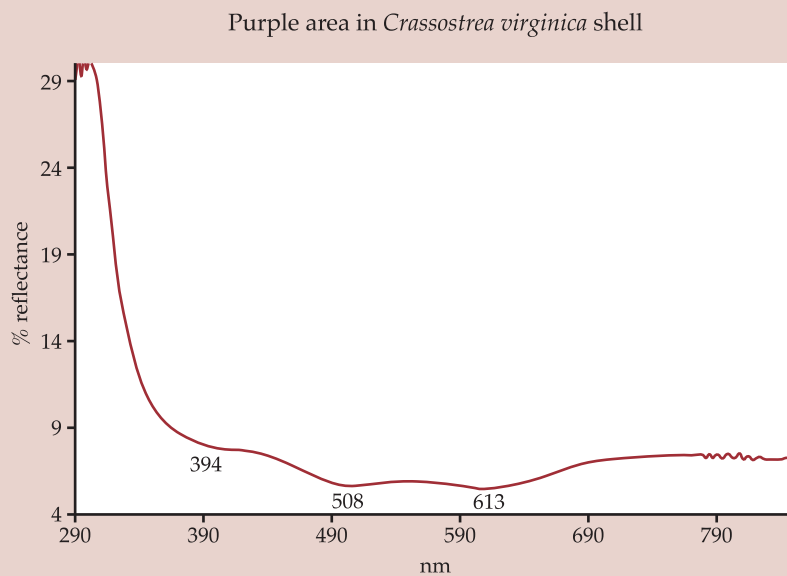


Figure 10: The UV/visible spectrum recorded for a purple area on the pearl within the adductor scar of the *Crassostrea virginica* shell. Broad low reflectance features were noted centred at 394, 508 and 613 nm.

unaccompanied by any unassigned peaks present in the purple areas of the pearl itself.

UV/visible spectra were recorded in reflectance mode for the purple area within the adductor scar on the interior of the *Crassostrea virginica* shell (Figure 10). Broad low reflectance features are centred at 394, 508 and 613 nm.

Discussion

While pearls from *Crassostrea virginica* have previously been reported, the examination of this pearl has for the first time recorded the Raman and UV/visible spectra for the shell and pearl. Radiographs have also revealed that the pearl has a large organic core and that its position within the shell indicates that the pearl has encased at least a portion of the adductor muscle. Clearly, unless great care is taken, damage to the pearl might occur if an attempt were made to remove it from the shell. Although such pearls may be regarded merely as interesting or curious and great conversational pieces, their investigation and recording allows those who are fascinated by the products of molluscs to understand the full range of the pearl family.

Acknowledgements

Several individuals were generous with their time and expertise during the preparation of this paper. Firstly the owner Anthony Dellagrotta, took the trouble to inform Antoinette Matlins of the existence of this item and Ms Matlins generously passed the information on to the authors. Both individuals took time from their busy schedules to bring it to New York City for examination. It is to Elizabeth Schrader of GIA that the authors owe the excellent macro photography. To Dr Lore Kiefert (Laboratory Director at AGTA-GTC) the authors are indebted for allowing the use of the Zeiss MCS spectrometer for the recording of UV/visible spectra. To Kathleen Moore the authors are greatly indebted for providing the image of the two examples in the AMNH

pearl exhibit. Finally the authors are indebted to those authors and editors responsible for the particularly lucid work: *The Eastern Oyster: Crassostrea Virginica* (Kennedy, V. S., *et al.*, 1996), a truly excellent reference text about the fascinating world of this mollusc.

References

- Anonymous, 2003. Eastern oyster, *Crassostrea virginica*. Florida Fish and Wildlife Conservation Commission, Florida Marine Research Institute
- Anonymous, 2004. *Gems & Gemology* data depository: Expanded localities for cultured pearls, natural pearls, and calcareous concretions.a. <http://www.gia.edu/pdfs/pearls2.pdf>. 2005, July
- Anonymous, 2005. Pearls (Pearls in the Half-Shell?) <http://www.amnh.org/exhibitions/pearls/marine/halfshell.html>. 2005, April
- Akamatsu, S., Zansheng, T., Moses, T.E., and Scarratt, K., 2001. The current status of Chinese freshwater cultured pearls. *Gems & Gemology*, 37(2), 96-113
- Carriker, M.R., 1996. The Shell and Ligament. In: *The Eastern Oyster Crassostrea virginica*, Kennedy, V.S., Newell, R.I.E., Eble, A.F. (Eds), Maryland Sea Grant College, College Park, 75-168
- Carriker, M.R., and Gaffney, P.M., 1996. A catalogue of selected species of living oysters (Osteacea) of the world. In: *The Eastern Oyster: Crassostrea virginica*, Kennedy, V.S., Newell, R.I.E., Eble, A.F. (Eds), Maryland Sea Grant College, College Park, 1-18
- Carriker, M. R., and Palmer, R.E., 1979. Ultrastructural morphogenesis of prodissoconch and early dissoconch valves of the oyster *Crassostrea virginica*. *Proceedings of the National Shellfish Association*, 70, 102-28
- Carriker, M. R., Swann, C.P., and Ewert, J.W., 1982. An exploratory study with the proton microprobe of the ontogenetic distribution of 16 elements in the shell of living oysters (*Crassostrea virginica*). *Marine Biology*, 69, 235-46
- Huang Fengming, Yun Xinqiang, Yang Mingxing and Chen Zhonghui, 2003. Pearl cultivation in Donggou, Ezhou, Hubai, and cathodoluminescence of cultured pearls. *The Journal of Gemmology*, 28(8), 449-62
- Kennedy, S., 1998. Pearl Identification. *The Australian Gemmologist*, 20(2), 2-19
- Kennedy, V. S., Newell, R.I.E., and Eble, A.F. (Eds), 1996. *The Eastern Oyster: Crassostrea virginica*, University of Maryland Sea Grant Publications
- Kiefert, L., Hänni, H., and Ostertag, T., 2001. *Raman Spectroscopic Applications to Gemmology*, Handbook of Raman Spectroscopy, from the Research Laboratory to the Process Line, H. G. M. E. I. R. Lewis, Marcel Dekker, New York/Basel
- Kiefert L., Moreno, D.McL., Arizmendi, E., Hänni, H., and Elen, S., 2004. Cultured Pearls from the Gulf of California, Mexico. *Gems & Gemology*, 40(1), 26-38

- Li Liping and Chen Zhonghui, 2001. Cultured Pearls and colour-changed cultured pearls: Raman spectra. *Journal of Gemology*, 27(8), 449-55.
- Scarratt, K., and Hänni, H., 2004. Pearls from the lion's paw scallop. *The Journal of Gemmology*, 29(4), 193-203
- Stenzel, H. B., 1971. *Mollusca 6, Bivalvia*, Geological Society of America, New York
- Traub, J., Zucker, B., Content, D., and Scarratt, K., 1999. *Pearl and the Dragon. A Study of Vietnamese Pearls and a History of the Oriental Pearl Trade*. Content, Derek J. Rare Books, Incorporated,
- Wallace, R. K., 2001. *Cultivating the Eastern Oyster, Crassostrea virginica*. Southern Regional Aquaculture Center Publication, 432

A short review of the use of 'keshi' as a term to describe pearls

Professor Dr H. A. Hänni

SSEF Swiss Gemmological Institute, Basel, Switzerland, Email: gemlab@ssef.ch

Abstract: *The original term 'keshi' describes tiny mantle pearls that developed without a tissue transplant during the production of Akoya cultured pearls. The term is now often used for gonad-grown cultured pearls that have formed from mantle tissue grafts under conditions where a bead has been rejected. A discussion of the term 'keshi' in its original and recent application is given. The formation of original and recent keshi cultured pearls is explained, with radiographs and cross sections of recent keshis. Current pearl trade use of the term is discussed. An alternative term to keshi – a beadless cultured pearl – is proposed. Recent Chinese freshwater cultured pearls with beads and the potential increase in numbers of beadless cultured pearls are discussed.*

Keywords: *beadless cultured pearls, bead rejection, Keshi cultured pearl, Keshi pearls*

Introduction

In earlier gemmological literature the term 'keshi' was traditionally used for small, near-round nacreous pearls deriving from Akoya shells that have undergone operations for producing beaded cultured pearls (Henn, 2001; Strack, 2001). The keshi pearls are characterised as unexpected by-products or even natural pearls (Webster, 1983, p. 538) and enjoy thus a close-to-natural identity. In the CIBJO nomenclature rules (CIBJO, 1998), the term 'keshi' appears under cultured pearls. We have noted that over approximately the last ten years, the term 'keshi' has increasingly often been used for pearls which do not come from the Akoya oyster (Figure 1) and are significantly larger. In fact today the name 'keshi pearl' is applied to a great number of large, well-shaped to off-shaped South Sea and Tahiti cultured pearls. This article reviews the background of



Figure 1: *Beadless cultured Tahiti pearl – a so-called keshi – mounted as a pendant, with its radiograph showing a large irregular cavity (dark area). Length of the pearl 22 mm. Photo © H.A.Hänni, SSEF.*

this new application of an old term to recent production of cultured pearls and discusses gemmological terminology and trade usage.

Comments on how Japanese keshis formed

An early description of the term 'keshi' in the western gemmological literature can be found in Taburiaux (1983, 1985). Keshi pearls have been found sporadically in Japanese Akoya shells during harvesting the beaded cultured pearls, and they are usually around 2 mm or smaller (*Figure 2*).



Figure 2: Keshi pearls from Japanese Akoya production. The smaller ones are mantle pearls which grew as a reaction to damage at the edge of the shell and in the mantle epithelium incurred during handling. The small size is consistent with the short period of time between the operation and the harvesting. The oblong and bigger ones are gonad grown, as a consequence of a lost bead. Length of the gauge is 1 cm. Photo © H.A.Hänni, SSEF.

It is interesting that these original keshi pearls were found in the mantle tissue, and not in the gonads that had received the mantle tissue transplant. They therefore cannot owe their formation directly to the transplanted epithelium. That they are always small has to be related to the age of the shell, or more correctly, with the length of time between the handling of the shells and harvesting of the crop. The following thoughts are deduced from the author's own observations and reflections and are

presented without having consulted the extensive professional literature in Japanese; should any of the ideas be similar, apologies are offered.

The formation of a natural pearl is in most cases the consequence of an injury to the external mantle tissue (Gübelin, 1946; Hänni, 2002). The subsequent healing of that injury may lead to the formation of a cyst, i.e. a pearl sac lined with external mantle tissue. Further production of calcium carbonate leads to the concretion, which may consist of or be coated with nacre, i.e. the pearl. Very small natural pearls are sometimes called poppy seed pearls (Landmann *et al.*, 2001, p 61). They are in fact the natural counterpart to the original keshis in *Pinctada martensii*, the classical Japanese oyster for beaded cultured pearls.

To explain a keshi pearl in the mantle, we should therefore look for an injury which dates back a sufficient number of years to account for the size of the small pearl encountered at the harvest of the Akoya cultured pearls. Since the growth period for Akoya cultured pearls is approximately one year to get a relatively thin nacre overgrowth on the bead, we can thus assume that the injury occurred during the handling of the shells from the sea to the operation table and back again to the sea. The very thin and fragile edge of the shell may have received a blow or have been damaged. The subsequent healing of such involuntary damage may well be the start of what is to become the so-called keshi pearl. In the short time between the operation (when the injury happened) and the harvest, a 2 mm pearl is perfectly well imaginable. When the keshis are retrieved from the shells during harvesting of the Akoyas, other concretions are also collected that have grown from tissue grafts that have accidentally lost the bead (*Figure 2*). Such formations include gonad-grown concretions that occur from tissue grafts that have lost the bead. They are small, randomly shaped, beadless cultured pearls, also of a size consistent with the short period of growth allowed for the Akoya process (i.e. operating on a mature *Pinctada martensii* oyster to produce beaded cultured pearls and harvesting them after a few months).

Requirements for the formation of a cultured pearl

Over about the past hundred years, the growth of (cultured) pearls that do not adhere to the shell has been stimulated by the transfer of a small piece of mantle tissue (mantle epithelium) from a sacrificed donor oyster into the body of a living oyster. The sites in the body where the grafts of tissue are most successful are the mantle or the gonad (the reproductive organ). The mantle tissue is the organ which lines and builds the shells, while the gonad is situated deep in the shell. To carry out the operation, the living oyster shell is opened about one centimetre and the tissue transplant is inserted with or without a bead.

In order to produce a cultured pearl, a small number of technical conditions must be selected (some of these options are independent from each other):

- one may work with freshwater or seawater oysters
- the cultured pearl may grow in the mantle or in the gonad, i.e. the tissue can be transplanted into the mantle or into the gonad
- the cultured pearl may or may not have a bead
- the donor oyster and receiver oyster may or may not be of the same species.

Should one decide to have mantle-grown cultured pearls, the first operation would include only the tissue transplant – the young oysters have a mantle that is too thin to house a bead – and their first (or only) product will be a beadless CP. With time both the pearl sacs and the shell rim grow larger so that the CPs virtually slide into the shell.

Should one decide to have gonad-grown cultured pearls, one has the choice to add a bead (beading) to the mantle tissue transplant (grafting). To start the formation of a CP, the grafting is indispensable but the beading is optional. In many circumstances, using one or both of these terms presents a much clearer picture than using the term ‘nucleation’ where either could be meant.

Understanding the formation of the product

Over the past several years large pearls that carry the name ‘keshi’ have become more common in trade fairs, in advertisements and in jewellery shops. They come mainly from cultured pearl (CP) farms using *Pinctada maxima* and *Pinctada margaritifera* shells, i.e. from salt-water oysters. Although the formation of small by-products in these shells, as in the Japanese Akoya, is possible, these so-called ‘keshis’ differ in size and mostly also in shape from the original. Commonly these large ‘keshis’ are found in the gonad tissue, and not in the mantle of the shell (Clinton Schenberg, *pers. comm.*, 1998; Dora Fourcade, *pers. comm.* 2003; Andy Müller, *pers. comm.*, 2005).

‘Keshi’ pearls from Australia, Tahiti or from the Philippines, are completely different from the keshi pearls as found in the Akoya oyster. Through the study of X-ray pictures of such so-called keshi pearls we can distinguish two types among them. Type 1 has a growth characteristic which is very similar to that of a beadless CP, such as the freshwater CPs from China. The shape is round to oval and a trace of a relatively small cavity is visible in the centre (Hänni, 2002). Most type 2 pearls have a flattened baroque shape with a distinct central cavity visible on the X-ray picture. The similar appearance of the central cavities in pearls of both types to central cavities in beadless freshwater CPs offers an explanation for their formation. The following comments are based on our observations and follow discussions with cultured pearl specialists D. Fourcade in 2003, A. Müller in 2002 and C. Schenberg in 1998.

Type 1: In the course of the production of beaded cultured pearls, it may happen that the oyster rejects the bead nucleus, although the tissue transplant is already grafted into the gonads. The mantle tissue will thus form a pearl sac and secrete calcium carbonate from its inner surface, and in this way produce a beadless cultured pearl. Because the piece of mantle tissue was placed into the gonad, this cultured pearl will grow in the gonad and later be harvested from there. Such formations are well known from all oysters that are commonly used for bead-cultured pearl production such as *Pinctada maxima* and *Pinctada margaritifera* (South Sea and Tahiti) (Figure 3).



Figure 3: South Sea *Pinctada maxima* (left) and Tahiti *Pinctada margaritifera* (right) beadless cultured pearls as grown after rejection of the bead after the first operation (tissue transplant and bead implant). Largest pearl is about 8 mm long. Photo © H.A.Hänni, SSEF.

Type 2: After a first CP with bead is harvested from one of the above-mentioned shells the already-present pearl sac is ready to take a second bead (second nucleation). Such a second bead nucleus is of the size of the previously harvested pearl and is placed in its former position. Since the inner surface of the pearl sac is still productive and will continue to precipitate nacre, the second bead will soon be covered with an overgrowth. There is thus no need for a second grafting or tissue transplant. Often, however, the bead is rejected from the pearl sac immediately after its introduction. The pearl sac then collapses since it is unsupported by a bead, but on its surface nacre is still being produced, forming a flattened to baroque shaped beadless CP. After the normal growth period, this product is harvested with the other CPs of the 'second generation' (Figure 4).

We can assume that beadless CPs may be formed in the gonads of operated shells when the first or second introduction of a bead is unsuccessful. In both situations, the formation is caused by the mantle tissue formerly transplanted (grafted) into the gonads. In a cross section through beadless CPs from saltwater oysters the structure is clearly visible. In type 1 the central cavity is small and more equidistant from the pearl's surface. In type 2 the surface continues to precipitate calcium carbonate, forming a



Figure 4: South Sea *Pinctada maxima* (left) and Tahiti *Pinctada margaritifera* (right) beadless cultured pearls as grown after rejection of the second bead (after collection of first cultured pearl and second bead implant). Larger pearl is about 15 mm long and 4.5 mm thick. Photo © H.A.Hänni, SSEF.



Figure 5: Cross sections through four beadless South Sea cultured pearls. The pearl at the upper left is from a first crop (after rejection of the first bead) and the other three pearls are from a second crop (after rejection of the second bead) where larger pearl sacs had collapsed. Length of the pearl on the lower left is 18 mm. Photo © H.A.Hänni, SSEF.

crust around a collapsed sac and leaving an irregular and perhaps large gap in the centre, as seen in *Figure 5*. In *Table I* the different beadless cultured pearls and their origin and trade terminology are listed.

Identification of beadless cultured pearls

The identification of beadless cultured pearls is most readily done with X-ray shadow pictures, i.e. radiographs. The method is described in a number of books and professional papers (e.g. Hänni, 1997; Scarratt *et al.*, 2000). However, distinction of natural pearls from beadless cultured pearls

is not always easy. Usually the beadless cultured pearls are characterised by a mark on the radiograph indicating a relatively significant central cavity and a number of growth bands with slight undulations. Those beadless cultured pearls that are currently called ‘keshi’ (*Figure 4*) show quite significant central cavities as seen in the X-ray pictures in *Figure 6*. Beadless cultured pearls do not reveal the directional characteristics shown by CPs with nacre beads, so the Laue diffraction method (Hänni, 1983) is not useful. A separation between saltwater and freshwater beadless cultured pearls can be done by X-ray luminescence on the basis of the Mn content (Hänni *et al.*, 2005).

Table I: Identification and trade terms for beadless cultured pearls.

Shell type	Trade name	Identification
<i>Pinctada martensii</i> (Akoya)	keshi	beadless cultured pearl
<i>Pinctada maxima</i>	South Sea keshi	beadless cultured pearl
<i>Pinctada margaritifera</i>	Tahiti keshi	beadless cultured pearl
<i>Cristaria plicata</i>	freshwater pearl	beadless cultured pearl
<i>Hyriopsis cumingi</i>	freshwater pearl	beadless cultured pearl

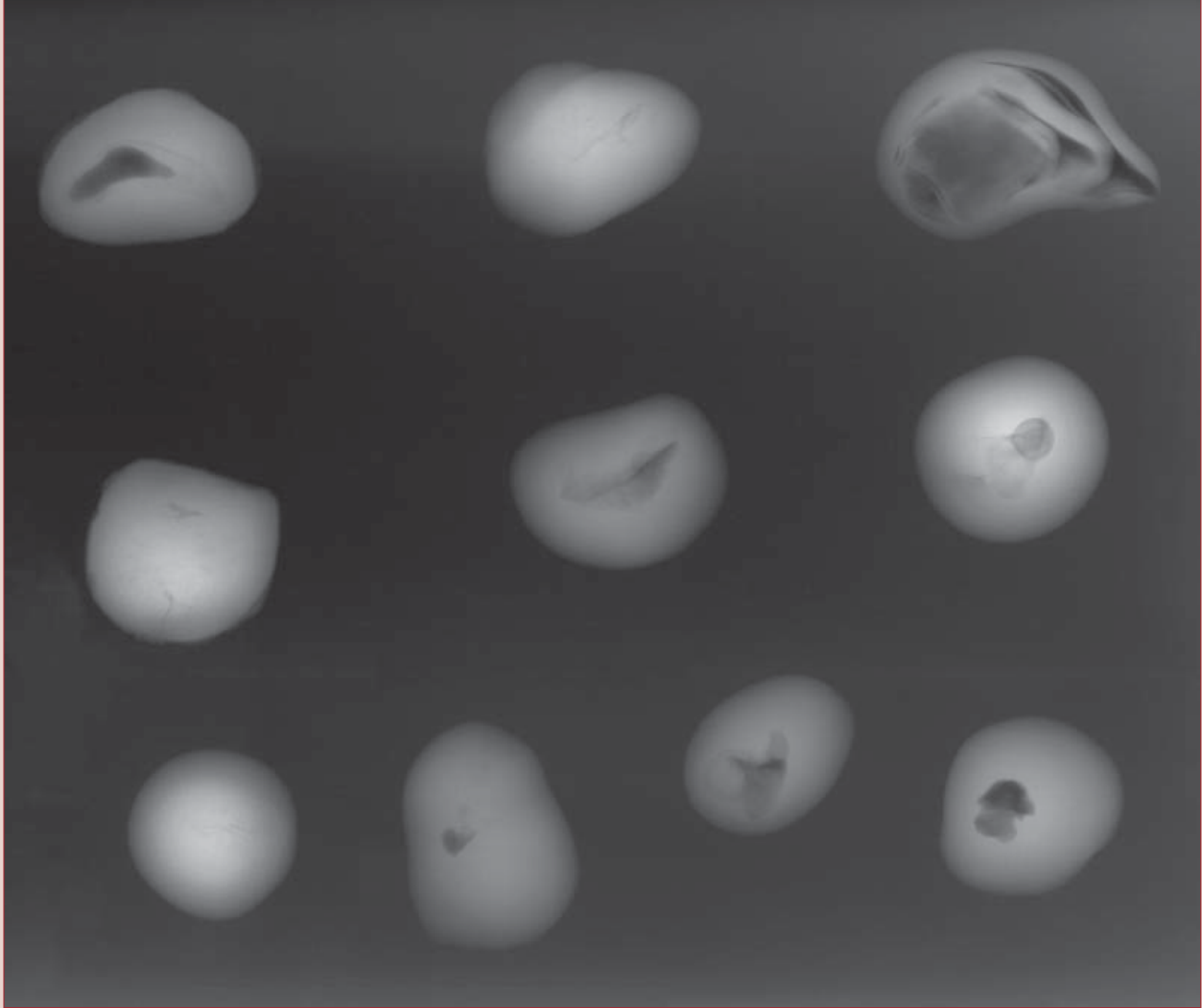


Figure 6: X-radiograph of a number of beadless South Sea cultured pearls called 'keshi' in the trade. Central cavities are visible in most pearls and show typical appearance. Photo © H.A.Hänni, SSEF.

Discussion of the recent use of the term 'keshi'

We have seen that the original application of the term 'keshi' is related to an injured rim of the shell in the mantle area. Original keshi pearls are thus 'mantle pearls', and not 'gonad pearls'. The more recent application of the term 'keshi' is related to concretions caused by mantle tissue transplants (grafts) into the gonads. However, the feeling in the pearl trade has always been more favourable to the term 'keshi' as such pearls were considered somehow to be more natural than straight cultured pearls. Such feeling and pressure from pearl traders led to the International Confederation of Jewellery, Silverware, Diamonds, Pearls and Gemstones (CIBJO) agreeing to the term 'keshi' for use in describing a seawater cultured pearl without

a nucleus (CIBJO, 1999). Descriptions in popular text books on pearls may introduce the same meaning of the expression that "something went wrong in the process of culturing pearl" (Matlins, 1999). In the same book it is made clear that the keshi is considered "not a natural pearl".

Although those in the pearl trade may call the 'gonad pearls' keshis, it is very questionable if it is scientifically helpful to equate these with the accidentally produced original keshi pearls. Their position in the gonads, the use of voluntarily grafted mantle tissue and their size are three major features of difference. So, while the keshis may strictly be by-products, since the producer wanted a fully round large beaded pearl rather than a baroque one, they cannot be considered as natural accidents since the tissue was transplanted into the gonads voluntarily. These 'gonad pearls' are

definitely cultured pearls since they derive from the tissue transplant. The author thinks that the terms 'beadless cultured pearl' or 'baroque beadless cultured pearl' would be acceptable names, which is furthermore correct in its statement, and that such pearls should not be called keshi pearls.

There is considerable danger in widening the term 'keshi' to include beadless CPs. Chinese production now consists largely of beadless (freshwater) CPs. Would the Tahiti and South Sea cultured pearl producers want the Chinese producers to market their pearls as keshis, merely because they are beadless? In one sense, the Chinese producers could even argue that their products grow in the mantle, just as the original keshis do. With the forthcoming production of beaded freshwater CPs from freshwater shells in China, we must also expect greater numbers of beadless CPs after bead rejection. The new production of large beaded CPs from the Chinese mussels is achieved by introducing a bead after the harvest of the first large beadless pearl (*Figure 7*). By this process the mussels can produce a second CP after only a short time, but one which is beaded. Since the mantle production of CPs can yield over 40 pearls in one mussel, intentionally flat beadless CPs can be produced simply by not inserting a bead into the empty pearl sacs. And inevitably, the number of flat beadless CPs resulting from rejection of the bead will also rise (*Figure 8*).

While studying a catalogue from a jewellery auction in Geneva in 1989, the author noticed the term 'keshi' in the description for a seven-strand pearl necklace, although an accompanying gemmological test report identified the pearls as natural. It seems that the cataloguer had chosen the term 'keshi' to refer to the slightly baroque shape of the pearls. So, although the term was used a long time ago, in this context it is potentially misleading; with this article the author would like to restore a clear meaning to the term 'keshi' so that trade and consumers do know what they can expect when it is applied.



Figure 7: Round freshwater beaded cultured pearls from China. These are grown as a second product in the mantle after the first (beadless) pearl has been collected. By inserting a bead into the pearl sac, a second large and round CP can be harvested shortly after the first crop. Photo © H.A. Hänni, SSEF.



Figure 8: The flat beadless freshwater cultured pearls. They represent pearls that have grown as a second product in the mantle after the first (beadless) pearl has been collected. Any bead that may have been inserted has been rejected, so there is no support for the pearl sac and it collapses into a flattened shape, which in turn leads to the flattened pearls. Photo © H. A. Hänni, SSEF.

Conclusion

The term 'keshi' as applied originally to small mantle pearls from the Japanese Akoya cultured pearl production is now used widely for cultured pearls from Tahiti and the South Seas. While the original product can be considered as an unintended by-product,

the pearls that are called keshi today in the market are large beadless cultured pearls. They are produced in the gonad and most are formed after a bead has been expelled after an unsuccessful implant. Although the term is approved in the trade, it is questionable whether these pearls should be named keshis. A term such as 'beadless cultured pearls' would explain more precisely what they really are.

Acknowledgements

The author is grateful to all those who have donated research material for the SSEF pearl research including Dora Fourcade (Pacific Perles, Papeete), Mrs M. Düby (Basel), Nick Paspaley (Darwin), Prof. Xinqiang Yuan (Wuhan), P. Fischer (Golay, Lausanne), T. Frieden (Thun) and Hans Schöffel (Stuttgart). My thanks go also to Dr M. S. Krzemnicki for his draft reading and thorough discussion of the present paper.

Editor's note: The nomenclatures surrounding gem materials are continuously being discussed and updated by CIBJO and other organisations. We believe it important to encourage debate and comment in this Journal, but the views expressed are those of the author concerned.

References

- CIBJO Pearl Commission., 1998. *CIBJO Pearl Book*. International confederation of jewellery, silverware, diamonds, pearls and stones. Distributed by UBOS, Bern, Switzerland
- Gübelin, E.J., 1946. *Perlen*. Max Daland, Zürich (distributed in Gübelin jewellery shops)
- Hänni, H.A., 1983. The influence of the internal structure of pearls on Lauegrams. *The Journal of Gemmology*, 18(5), 386-400
- Hänni, H.A., 1997. Über die Bildung von Perlmutter und Perlen. *Zeitschrift der Deutschen Gemmologischen Gesellschaft*, 46(4), 183-96
- Hänni, H.A., 2002. *Pearls*. Tutorial CD, SSEF Swiss Gemmological Institute, Basel, Switzerland, Email gemlab@ssef.ch
- Hänni, H.A., Kiefert, L., and Giese, P., 2005. X-ray luminescence, a valuable test in pearl identification. *The Journal of Gemmology*, 29(5/6), 325-9
- Henn, U., 2001. *Edelsteinkundliches Fachwörterbuch*. *Lexikon*. Deutsche Gemmologische Gesellschaft, Eigenverlag, Idar-Oberstein, ISBN 3-932515-24-2
- Landmann, N.H., Mikkelsen, P.M., Bieler, R., and Bronson, B., 2001. *B. Pearls – A natural history*. Harry N. Abrams Inc., New York, pp 232
- Matlins, A.L., 1999. *The pearl book*. 2nd ed. Gemstone Press, Woodstock, Vermont, ISBN 0-943763-28-2
- Müller, A., 1997. *Zuchtperlen, die ersten hundert Jahre*. Andy Müller and Golay Buchel Holding S.A., Lausanne, ISBN 4-9900624-1-8
- Scarratt, K., Moses, T.M., and Akamatsu, S., 2000. Characteristics of nuclei in Chinese freshwater cultured pearls. *Gems & Gemology*, 36(2), 98-109
- Strack, E., 2001. *Perlen*. Rühle-Diebener Verlag, Stuttgart, ISBN 3-00-008636-6
- Taburiaux, J., 1983. *La perle et ses secrets*. Hemmerlé Petit et Cie. Paris ISBN 2-9042-61-00-1
- Taburiaux, J., 1985. *Pearls, their origin, treatment and identification*. NAG Press, Ipswich, ISBN 0-7198-0151-6 (trans. of *La perle et ses secrets*)
- Webster, R., 1983. *Gems. Their sources, descriptions and identification*. Butterworths. & Co., London, ISBN 0-408-01148-3

A new type of Tairus hydrothermally-grown synthetic emerald, coloured by vanadium and copper

Dr Karl Schmetzer¹, Dr Dietmar Schwarz²,
Dr Heinz-Jürgen Bernhardt³ and Dr Tobias Häger⁴

1. Taubenweg 16, D-85238 Petershausen, Germany

2. Gübelin Gem Lab, Maihofstr. 102, CH-6006 Lucerne, Switzerland

3. Central Microprobe Facility, Ruhr-University, D-44780 Bochum, Germany

4. Institute of Gemstone Research, University of Mainz, D-55099 Mainz, Germany

Abstract: *Gemmological, chemical and spectroscopic properties of a new type of hydrothermally-grown synthetic emerald produced commercially by the Tairus company in Novosibirsk, Russia, are described. The results of chemical and spectroscopic examination in the UV-Vis range indicate that the samples are coloured by a combination of vanadium and copper; chromium contents are negligible. Infrared spectra show the presence of different types of water molecules and/or hydroxyl ions. Two major types of isomorphic replacement are present, octahedral substitution of aluminium by vanadium and tetrahedral substitution of silicon by aluminium with charge compensation by lithium on channel sites. Distinction of this new type of synthetic emerald from natural emerald can be made on the basis of distinct growth features visible through the microscope, and chemical and/or spectroscopic features may also be helpful.*

Keywords: *content of Cr, Cu, V; gemmological properties; IR spectra; synthetic emerald; Tairus; UV-Vis spectra*

Introduction

Since 1989, the year of its foundation, the Tairus company has become one of the world's largest producers of synthetic gem materials, mainly differently coloured varieties of the corundum and beryl families. Tairus is a Joint Venture between the Russian Academy of Sciences (Siberian Branch) of Novosibirsk and Tairus (Thailand) Co. Ltd of Bangkok.

In the past, a number of different types of synthetic emerald have been grown hydrothermally by Tairus. Emeralds coloured by a combination of chromium, iron, nickel and copper were produced by Tairus and elsewhere in Russia (see Granadchikova *et al.*, 1983; Schmetzer, 1988) in steel autoclaves without noble metal liners, and synthetic emeralds

coloured mainly by chromium were grown in autoclaves with noble metal insets or with teflon coating. A product which was marketed as 'internally clean' synthetic emerald was grown using specially oriented seed crystals (Koivula *et al.*, 1996; Schmetzer, 1996). With this special orientation of the seed, the Russian researchers tried to avoid the formation of easily detectable growth features.

In 2001, the Tairus company purchased Biron's growth technology (intellectual know-how and technical equipment) from Australia which was developed to produce synthetic emeralds whose colour is due to almost equal amounts of chromium and vanadium – in an attempt to resemble Colombian emeralds as closely as possible. After an intermediate production period in Thailand 2002, Biron type synthetic emerald is now produced by Tairus in Russia (W. Barshai, *pers. comm.* 2004).



Figure 1: Faceted samples of the new type of Tairus hydrothermally-grown synthetic emerald coloured by vanadium and copper; samples from 0.91 ct (centre, 5.0 × 7.0 mm) to 1.17 ct (right, 6.1 × 8.1 mm). Photo by M. Glas.

In 2004, a new type of synthetic emerald (Figure 1) was introduced by Tairus to the international market as 'Colombian Color Emerald'. The new development in synthetic emerald growth is attributed to Dr Dimitry Fursenko and his team, who worked on this project since 1999 and which culminated in September 2004 when the first rough crystals were cut (see <http://www.tairus.com/>). It is the purpose of the present paper to characterise this new type of hydrothermally-grown variety of synthetic beryl.

Crystal growth

The following section was produced using the information given and the photos submitted by the Russian scientists involved in the production of the new type of synthetic emerald in the laboratories of Tairus in Novosibirsk. Fursenko and his team are pictured in Figure 2a, and all research and development as well as commercial production is performed in the Tairus building in Novosibirsk (Figure 2b).



Figure 2a: The technology for the growth of the new type of synthetic emerald has been developed by Dr. Dimitry Fursenko (centre) and his team, Dr. Victor Thomas (right) and Ivan Fursenko (left). Courtesy of D. Fursenko.

Figure 2b: The commercial production as well as the scientific research is performed in the Tairus building in Novosibirsk, Russia. Courtesy of D. Fursenko.



Figure 3 a, b: The commercial production of the new type of Tairus synthetic emerald is performed in steel autoclaves with noble metal lining; height of the autoclaves about 50 cm, external diameter about 9 cm. Courtesy of D. Fursenko.

Commercial growth is performed in steel autoclaves (Figure 3 a, b) with a working chamber of 250 to 300 ml. A transparent model for demonstration (Figure 4a) shows the arrangement of seed plates and nutrient (Figure 4b). Colourless or very pale green natural beryl from the Ural mountains (cracked and purified) is used as the initial charge for crystal growth. The beryl nutrient, colour-causing dopants and components of the mineraliser (not shown) are placed into the lower part of the working chamber. Typical sizes of seed plates located in the upper part of the autoclave are 80 × 18 mm. Crystals are grown at a temperature near 600 °C and a pressure near 1.5 kbar. The temperature gradient in the autoclave is in the range of 50 to 100 °C. With these growth parameters, a growth rate of 0.3 mm per day is obtained. Typically, a synthetic emerald crystal (Figure 5) measures 80 × 18 × 14 mm, indicating a growth period of about 20 days.

Materials and methods

For this study, we examined ten hydrothermally-grown synthetic emeralds of the new type (Figure 6), which were purchased by one of the authors (DS) at Tairus, Bangkok, in 2004. They comprised four faceted stones (0.91 to 1.64 ct) and six platy rough crystals (2.86 to 10.70 ct). The rough crystals (thickness between 4 and 5 mm) had been sawn by the producer along the boundary of the seed and the grown emerald, in this way removing all residual parts of the seed plate. We were informed that our samples represent the commercial production after the final development of the growth technique.



Figure 4 a, b: A transparent autoclave model is used to demonstrate the arrangement of nutrient (below) and seed plates; components of colour-causing dopants and mineralizers are placed at the bottom of the autoclave (not shown). Courtesy of D. Fursenko.



Figure 5: A typical synthetic emerald crystal measures about $80 \times 18 \times 14$ mm. Courtesy of D. Fursenko.



Figure 6: Faceted and rough samples of the new type of Tairus hydrothermally-grown synthetic emerald coloured by vanadium and copper; rough crystal plate of 3.23 ct (12.7×6.6 mm), faceted stone of 1.16 ct (6.1×8.1 mm). Photo by M. Glas.

Standard gemmological methods were used to determine refractive indices (RI), optical character, specific gravity (SG) and fluorescence under long- and short-wave ultraviolet (UV) radiation. Standard microscopic techniques were used to examine the internal features under different lighting conditions, both with and without immersion liquids. The orientation of growth planes and colour zoning was performed with a horizontal (immersion) microscope with a specially designed sample holder and specially designed eye pieces (to measure angles).

For chemical characterisation, we first submitted all ten samples for qualitative energy-dispersive X-ray fluorescence (EDXRF) analysis using a Tracor Northern Spectrace 5000 system. Quantitative chemical data for the four faceted samples were determined by electron microprobe using a Cameca Camebax SX 50 instrument. Traverses with 10 point analyses each were performed across

the table facets of the four faceted gemstones. To obtain quantitative data for water and light elements (lithium and beryllium), slices were cut from two rough crystal plates and the powder obtained from these slices was used for wet chemical analyses. Lithium and beryllium contents were determined by atomic absorption spectroscopy (AAS), and the water content of the sample was analysed by Karl-Fischer titration.

Polarized UV-Vis absorption spectra (280 to 800 nm) from all ten samples were recorded with a Perkin Elmer Lambda 19 spectrophotometer. For the two samples for which the best orientation was obtainable (according to the determination of the optic axis by an immersion microscope combined with the results of UV-Vis spectroscopy), we also measured polarized absorption spectra in the near infrared (800 to 2500 nm; 12500 to 4000 cm^{-1}) with the Perkin-Elmer Lambda 19. Infrared spectroscopy in the mid-infrared range (4000 to 400 cm^{-1}) was performed using two different methods. For an overview of the complete range, a limited amount of powder was scraped from two rough samples for the preparation of KBr pressed pellets. For the measurement of polarized spectra in the mid-infrared, thin slices were sawn from two rough crystal plates with appropriate orientation (determined from immersion microscopy). These thin slices were polished to a thickness of about 0.3 mm to enable polarized measurement in the 4000 to 2000 cm^{-1} range (below 2000 cm^{-1} the thickness of these slices did not allow any reliable measurements). Both types of mid-infrared spectra were recorded using a Perkin Elmer FT-IR 1725X infrared spectrometer.

Solid particles on the rough surfaces of two synthetic-emerald crystals were analysed using an electron microprobe. For the identification of similar-appearing inclusions in one rough sample, this crystal was cut and polished in several steps until one of these inclusions was sufficiently exposed at the surface to enable an examination by electron microprobe and optical microscopy.

Results

Visual appearance and gemmological properties

All rough crystals had uneven, undulating surfaces parallel to the sawn plane (Figure 7), i.e. parallel to the original surface of the seed. This step-like surface consists of numerous faces of polycentrically growing synthetic emerald subindividuals. When examined with the unaided eye, all samples showed an intense, homogeneous, slightly bluish green colouration without any prominent colour zoning. The variation of colour within our ten samples was limited, indicating that these products came from an established production line.

Standard gemmological properties (Table I) show only small variation, and overlap those of natural emeralds from various localities, especially those of low alkali-bearing stones from Colombia. They are in the range commonly observed also for low iron-bearing or iron-free hydrothermally-grown synthetic emeralds.



Figure 7: Rough crystal plate of 7.52 ct the new type of Taurus hydrothermally-grown synthetic emerald coloured by vanadium and copper showing an uneven, undulating surface formed by numerous faces of subindividuals of synthetic emerald; size of plate about 16.5 × 7.5 mm, weight 7.52 ct. Photo by M. Glas.

The results of microprobe analyses of four faceted samples are presented in Table II. In addition to the major components of beryl, Al_2O_3 and SiO_2 , there are distinct amounts of vanadium and smaller percentages of chromium and copper. Traces of other transition metals and alkali elements are also present, while caesium, chlorine and fluorine were below the detection limit of the electron microprobe. Only a small variation within the three colour-causing trace elements, vanadium, chromium, and copper, was detected on traverses across the table facets of the cut synthetic emeralds (Table III).

Wet chemical analyses of powdered material from two samples showed the presence of distinct amounts of water and minor amounts of lithium (Table II). The values of Li_2O , BeO and H_2O did not show significant variation between the duplicate samples, so average values were used for the calculation of cation proportions and the crystal chemical formula, based on 36 oxygens, according to the general formula $\text{Be}_6\text{Al}_4\text{Si}_{12}\text{O}_{36}$ (see Deer *et al.*, 1986).

Isomorphic replacement of Be, Al, and Si in the beryl structure has been discussed in numerous papers, and summaries are given by Shatskiy *et al.* (1981), Aurisicchio *et al.* (1988), Lebedev *et al.* (1988), and Sherriff *et al.* (1991). According to these authors, beryls are subdivided into two groups, one with predominant octahedral aluminium substitution and the other with predominant tetrahedral beryllium substitution.

Table I. Gemmological properties of V-Cu-bearing Taurus synthetic emeralds

Colour	Homogeneous, very slightly bluish green
Pleochroism	Parallel c: bluish green Perpendicular c: yellowish green
RI	n_o 1.576 – 1.578 n_e 1.570 – 1.571
Birefringence	0.006 – 0.007
SG	2.68 – 2.69
UV fluorescence	Short wave: inert Long wave: inert

Chemical composition and formula

The results of qualitative X-ray fluorescence analysis indicate that there are no major differences between rough crystal plates and faceted synthetic emeralds.

Table II: Chemical composition of V-Cu-bearing Tairus synthetic emeralds

Microprobe analyses (average of 10 points on each emerald)				
Wt.%	A	B	C	D
SiO ₂	64.91	64.62	63.81	64.45
TiO ₂	0.01	0.01	0.01	0.01
Al ₂ O ₃	18.22	18.03	18.11	18.30
V ₂ O ₃	1.14	1.33	1.34	1.36
Cr ₂ O ₃	0.03	0.04	0.04	0.04
Fe ₂ O ₃ *	0.01	0.03	0.01	0.01
MnO	0.01	0.01	0.01	0.02
NiO	0.01	0.02	0.01	0.01
MgO	0.01	0.01	0.01	0.01
CuO	0.13	0.10	0.09	0.12
Na ₂ O	0.02	0.02	0.03	0.02
K ₂ O	0.01	0.02	0.02	0.02
Cs ₂ O	bdl	bdl	bdl	bdl
F	bdl	bdl	bdl	bdl
Cl	bdl	bdl	bdl	bdl
Wet chemical analyses (average of two powder samples)				
Li ₂ O	0.26	0.26	0.26	0.26
BeO	13.50	13.50	13.50	13.50
H ₂ O	1.48	1.48	1.48	1.48
Sum microprobe and wet chemical analyses	99.74	99.49	98.74	99.60

*Total iron as Fe₂O₃, bdl = below detection limit

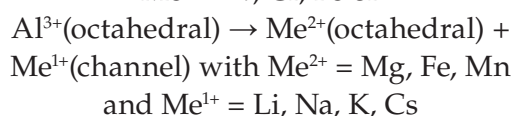
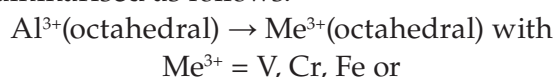
Number of ions based on 36 oxygens (excluding H ₂ O)				
Specimen	A	B	C	D
Si	11.888	11.875	11.816	11.834
Ti	0.002	0.002	0.002	0.001
Al	3.932	3.905	3.952	3.960
V	0.167	0.196	0.200	0.201
Cr	0.004	0.007	0.006	0.006
Fe	0.002	0.004	0.002	0.002
Mn	0.002	0.003	0.002	0.003
Ni	0.002	0.003	0.001	0.001
Mg	0.002	0.002	0.003	0.002
Sum Al octahedron	4.113	4.122	4.168	4.176
Cu	0.017	0.014	0.013	0.016
Be	5.941	5.960	6.006	5.955
Sum Be tetrahedron	5.956	5.974	6.019	5.971
Li	0.190	0.191	0.192	0.191
Na	0.005	0.008	0.009	0.007
K	0.003	0.005	0.005	0.005
Sum alkalis	0.198	0.204	0.206	0.203
H ₂ O	0.901	0.904	0.911	0.903

Average formula: $(\text{Be}_{5.96}\text{Cu}_{0.02}\text{Li}_{0.02})_{6}^{\text{tet}}(\text{Al}_{3.79}\text{V}_{0.21})_{4}^{\text{oct}}(\text{Si}_{11.85}\text{Al}_{0.15})_{12}^{\text{tet}}\text{O}_{36}(\text{Li}_{0.18}\text{H}_2\text{O}_{0.91})_{\text{channel}}$

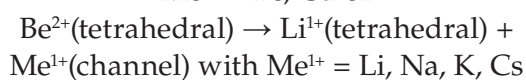
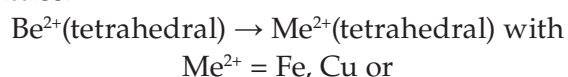
Table III: Chemical variation of colour-causing trace elements in V-Cu-bearing Tairus synthetic emeralds

Microprobe analyses (ranges of 10 point analyses each, data in wt.%)				
Specimen	A	B	C	D
V ₂ O ₃	1.09 - 1.21	1.24 - 1.41	1.30 - 1.40	1.30 - 1.43
Cr ₂ O ₃	0.01 - 0.05	0.02 - 0.08	0.02 - 0.06	0.02 - 0.07
CuO	0.09 - 0.17	0.07 - 0.014	0.06 - 0.14	0.07 - 0.15

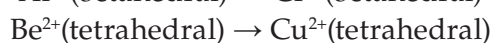
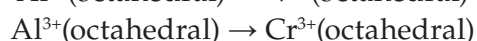
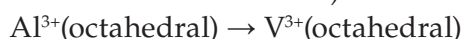
In octahedral sites in beryl, aluminium can be replaced by trivalent transition metals such as chromium, vanadium, and iron. Heterovalent isomorphic substitution is characterised by replacement of aluminium by divalent transition metals such as iron, manganese or by magnesium. For charge balance, alkalis enter channel sites of the beryl lattice and these substitutions can be summarised as follows:



In tetrahedral sites, beryllium can be replaced by divalent transition metals such as iron or copper. Heterovalent isomorphic substitution is characterised by replacement of beryllium by lithium. For charge balance, alkalis enter channel sites of the beryl lattice:

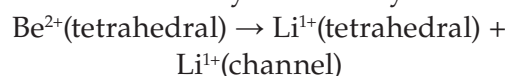


In the new type of Tairus synthetic emeralds, the major colour-causing trace elements are vanadium, chromium and copper, replacing aluminium on octahedral and beryllium on tetrahedral sites according to the following scheme (see spectroscopic properties and cause of colour):

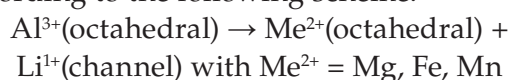


The results of chemical analyses show also a limited heterovalent isomorphic replacement of beryllium by lithium, because the sum of Be + Cu (sum Be tetrahedron

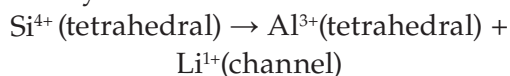
in *Table II*) is slightly smaller than the theoretical value of 6 apfu (atoms per formula unit). For charge balance, lithium also enters channel sites of the synthetic beryls:



In addition, the traces of bivalent magnesium, iron or manganese on aluminium sites need charge compensation according to the following scheme:



The analyses of the Tairus synthetic emeralds also show a small but distinct silicon deficiency (Si apfu smaller than 12) and some excess aluminium (sum Al octahedron in *Table II* larger than 4 apfu). An isomorphic replacement of Al and Si has been discussed in several papers (see, for example, Shatskiy *et al.*, 1981; Schmetzer and Bernhardt, 1994). Considering the different possibilities discussed and the necessity of charge balance, the following coupled isomorphic replacement scheme is consistent with analytical data:



Lithium has a complex function:

- a) it replaces beryllium in tetrahedral sites and
- b) it enters channel sites as charge compensator
 - b1) for bivalent magnesium, iron or manganese on aluminium sites,
 - b2) for lithium on beryllium sites and
 - b3) for aluminium on silicon sites, which is the major fraction of the three.

The amount of lithium determined experimentally is in good agreement with this complex function.

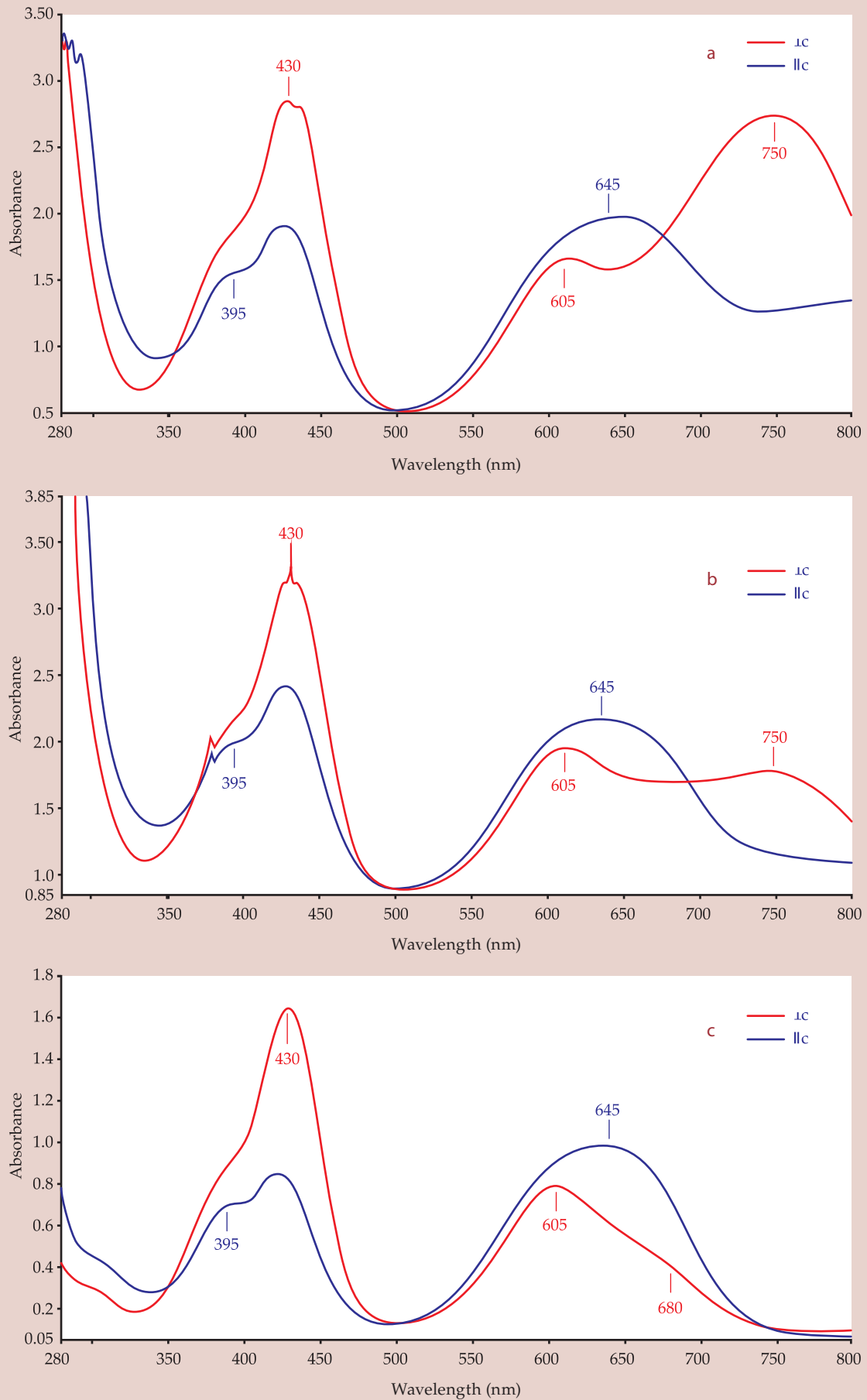


Figure 8: Polarized absorption spectra of two samples of the new type of Tairus hydrothermally-grown synthetic emerald coloured by vanadium and copper (a,b) compared with the spectra of a vanadium-bearing hydrothermally-grown Biron synthetic emerald (c).

Table IV: Spectral features related to transition metals in Tairus synthetic emerald

Absorption maximum (nm)	Polarisation E	Assignment
1180	⊥c	Cu ²⁺ on tetrahedral Be ²⁺ sites
920	∥c	
750	⊥c	
680 sh	⊥c *	Vanadium (?)
645	∥c	V ³⁺ on octahedral Al ³⁺ sites
605	⊥c	
430	⊥c > ∥c	
395	∥c > ⊥c	

sh = shoulder

* hidden by the Cu²⁺ band at 750 nm

As a result, the average crystal chemical formula for the four samples is calculated as given in Table II. The dominant isomorphous substitution in our Tairus synthetic emeralds is a replacement of aluminium by vanadium on octahedral sites. A heterovalent substitution of silicon by aluminium on tetrahedral sites with charge compensation by lithium on channel sites is also present.

Spectroscopic features of transition metals in beryl and cause of colour

Absorption spectra of samples of the new type of Tairus synthetic emerald (Figure 8 a,b) show numerous broad absorption bands in the UV-Vis-NIR range (Table IV). For an assignment of these absorption maxima, we have to consider the results of chemical analyses which indicate that the only significant colour-causing transition metals are vanadium and copper.

The position of absorption maxima at 1180, 920 and 750 nm is consistent with the spectra of copper-bearing hydrothermally-grown synthetic beryls (Solntsev *et al.*, 1976; Solntsev, 1981 a,b; Lebedev *et al.*, 1983, 1986; Rodionov *et al.*, 1987) and, consequently, these three broad absorption bands are assigned to Cu²⁺ on tetrahedral beryllium sites.

Absorption spectra of natural vanadium- and iron-bearing beryls from Brazil and Kenya (Wood and Nassau, 1968;

Schmetzer, 1978, 1982) are similar, but not completely identical to absorption spectra of hydrothermally-grown synthetic vanadium- and iron-bearing or to synthetic vanadium-bearing, iron-free beryls (Beckwith and Troup, 1973; Solntsev, 1981 a,b; Lebedev *et al.*, 1983, 1986). The differences in the 350 to 450 nm range are partly understandable by an overlap of the absorption bands due to vanadium and those due to iron, mostly in natural samples. Differences in the 600 to 700 nm range, on the other hand, are not completely understood at present.

If we focus only on the vanadium-related absorption bands of the spectra of the new type of Tairus synthetic emerald, these are identical with the spectra of vanadium-doped beryl crystals grown through gas-transport reactions (Rodionov *et al.*, 1987) as well as with the spectra of a vanadium-bearing, chromium- and iron-free sample grown by the Biron company in Australia for research purposes (Figure 8c; note: samples of the commercial production of Biron normally contained similar amounts of both, chromium and vanadium, see, for example, analyses by Mashkovtsev and Smirnov, 2004).

Comparing the pure vanadium spectrum of the Biron sample, it is evident that our spectra of the Tairus synthetic emerald samples are due to a superimposition of a 'pure' vanadium and a 'pure' copper spectrum. Thus, the absorption bands at 645, 605, 430 and 395 nm (Table IV) are assigned to V³⁺ on octahedral aluminium sites. The assignment of an additional shoulder at 680 nm (see Figure 8c), which is seen in the spectra of various natural and synthetic vanadium-bearing samples (Wood and Nassau, 1968; Beckwith and Troup, 1973; Schmetzer, 1978, 1982; Rodionov *et al.*, 1987) is rather uncertain. This shoulder might be due to vanadium cations which are not in the trivalent state.

Compared to vanadium, the relative amounts of chromium are small. Under these circumstances, the absorption bands of chromium are hidden by the much stronger absorption bands of vanadium (see Schmetzer, 1978, 1982; Schwarz and Schmetzer, 2002).

The bluish-green colour of the new Tairus samples is consistent with a combination of the yellowish-green colouration of a vanadium-bearing synthetic beryl sample and the blue colour of a copper-bearing hydrothermally-grown beryl (Figure 9). It is evident, that the colour of the pure vanadium-bearing yellowish-green sample is shifted to the desired bluish-green 'emerald' colour by the influence of the copper dopant of the synthetic beryl.



Figure 9: The slightly bluish green coloration of the new type of Tairus synthetic emerald (top, 7.52 ct, 16.5 × 7.5 mm) is caused by superimposition of the light blue colouration of a synthetic copper-bearing beryl (below left) and the yellowish-green colouration of a synthetic vanadium-bearing beryl (below right); the copper- and vanadium-doped samples are Russian research samples obtained by one of the authors in the early 1990s. Photo by M. Glas.

Infrared spectroscopy

Mid-infrared range (from 4000 to 400 cm⁻¹)

The spectra of the KBr pellets prepared with the emerald powder (Figure 10) show two absorption bands at 3697 and 3595 cm⁻¹. These spectra are consistent with infrared powder spectra of chromium-, iron-, nickel- and copper-bearing Russian hydrothermally-grown synthetic emeralds as described by Schmetzer (1988; see also the references cited therein). This general type of spectrum is identical for both lithium- and sodium-bearing synthetic beryl crystals (Shatskiy *et*

al., 1981; Vladimirova *et al.*, 1987).

In the mid-infrared the fundamental vibrations of molecules in the channels of the beryl structure as well as lattice vibrations are present. In our samples, no absorption bands related to chlorine (in the 2500 to 3100 cm⁻¹ range, Schmetzer *et al.*, 1997; Mashkovtsev and Solntsev, 2002; Mashkovtsev and Smirnov, 2004), to ammonium (in the 2500 to 3300 cm⁻¹ range, Mashkovtsev and Solntsev, 2002; Mashkovtsev and Smirnov, 2004; Mashkovtsev *et al.*, 2004) or to CO₂ (at 2360 cm⁻¹, Wood and Nassau, 1967, 1968; Charoy *et al.*, 1996; Mashkovtsev and Smirnov, 2004) were observed.

Polarized spectra (Figure 11) show two strong absorption bands at 3695 and 3596 cm⁻¹ and one weaker band at 3505 cm⁻¹ (polarization parallel to *c*) as well as two doublets at 3684, 3675 cm⁻¹ and 3605, 3593 cm⁻¹, a broad band at 3873 cm⁻¹ and two weak bands at 3558 and 3505 cm⁻¹ (polarization perpendicular to *c*). These spectra are identical with the spectra of chromium-, iron-, nickel- and copper-bearing Russian hydrothermally-grown synthetic emeralds grown for research purposes (Mashkovtsev and Lebedev, 1993) and with chromium-, iron-, nickel- and copper-bearing hydrothermally-grown synthetic emeralds of commercial Tairus production (Mashkovtsev and Solntsev, 2002; Mashkovtsev and Smirnov, 2004).

Using polarized infrared absorption spectra of alkali-bearing natural and alkali-free synthetic beryls and emeralds, two types of water molecules were characterized in channel sites of the beryl structure (Flanigen *et al.*, 1967; Wood and Nassau, 1967, 1968; Aines and Rossman, 1984). Type-I water molecules have their two-fold symmetry axis perpendicular to the *c*-axis of the beryl crystal and are not adjacent to alkali ions. Type-II water molecules have their two-fold symmetry axis parallel to the *c*-axis of the beryl crystal and are adjacent to alkali ions. Furthermore, comparing intensity ratios of the three main water absorption bands in the 3500 cm⁻¹ to 3800 cm⁻¹ range, it was concluded that one or more additional types of water

or hydroxyl group are present in beryl (Schmetzer, 1989; Schmetzer and Kiefert, 1990).

Subsequently, this general statement was confirmed by numerous researchers, but different assignments of various absorption bands in natural and synthetic alkali-bearing beryl and emerald samples have been given (Mashkovtsev and Lebedev, 1993; Aurisicchio *et al.*, 1994; Charoy *et al.*, 1996; Mathew *et al.*, 1997; Mashkovtsev and Solntsev, 2002; Mashkovtsev and Smirnov, 2004; Mashkovtsev *et al.*, 2004). In most cases, the doublets in the 3670 and in the 3600 cm^{-1} range are considered as overlaps of two different types of water maxima or as overlaps of water and hydroxyl bands.

In summary, we can conclude that the mid-infrared spectra of the new type of lithium-bearing hydrothermally-grown Tairus synthetic emeralds are due to three different types of water molecules or to two different types of water molecules and hydroxyl ions. The spectra are identical with those of older hydrothermally-grown synthetic beryls and emeralds (research samples and early commercial production) as well as with the spectra of previously produced types of synthetic emeralds grown by Tairus in Novosibirsk.

Near-infrared range (from 800 to 2500 nm; i.e. from 12500 to 4000 cm^{-1})

In the near-infrared numerous relatively broad to small absorption bands (Figure 12) are present in our samples. The two broad bands at 1180 and 920 nm have already been assigned to Cu^{2+} replacing Be^{2+} on tetrahedral lattice sites (see above).

In the spectrum with polarization E parallel *c* we observed absorption maxima at 1150, 1400, 1413, 1468, 1768, 1897, 2152 and 2460 nm; in the spectrum with E perpendicular to *c*, the absorption bands were found at 1366, 1410, 1420, 1430, 1835, 1898, 1961 and 2207 nm. Using the references cited above, all absorption bands are assigned to overtone and combination frequencies of both types of water and hydroxyl groups.

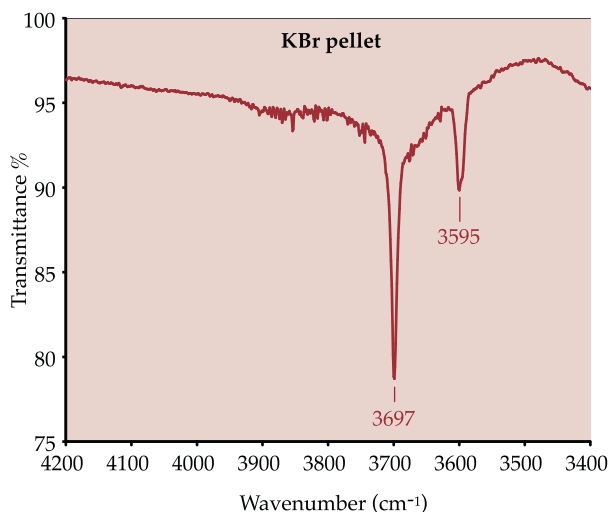


Figure 10: Mid-infrared absorption spectra of synthetic emerald powder (KBr pellet technique) in the range of fundamental water vibrations show two dominant absorption bands at 3697 and 3595 cm^{-1} which were assigned to two different types of water molecules in the beryl structure.

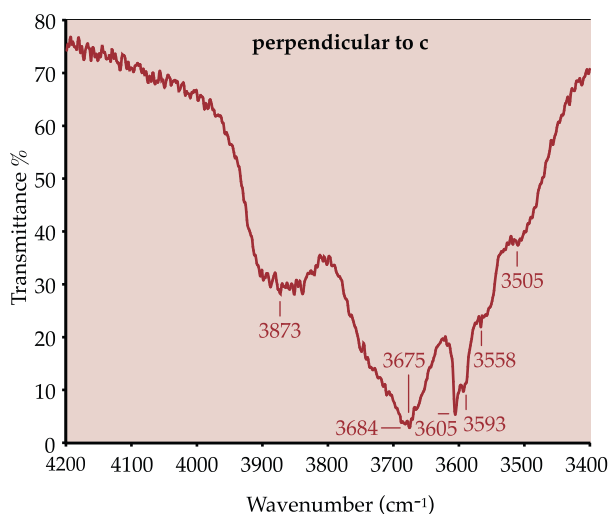
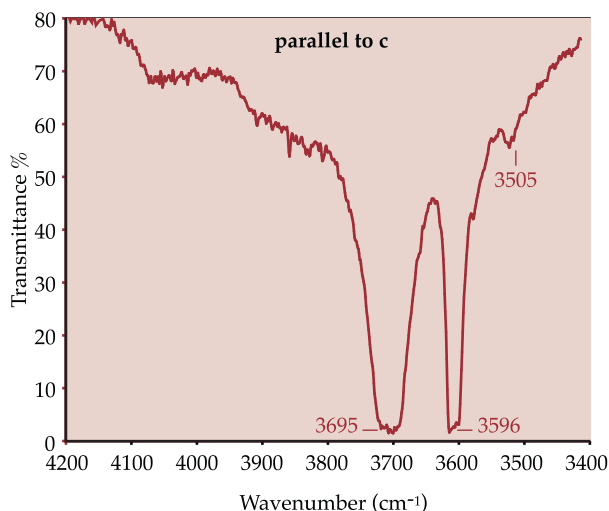


Figure 11: Polarized absorption spectra of a 0.3 mm thick oriented crystal plate in the mid-infrared range showing numerous absorption bands of different types of water molecules and/or hydroxyl ions.

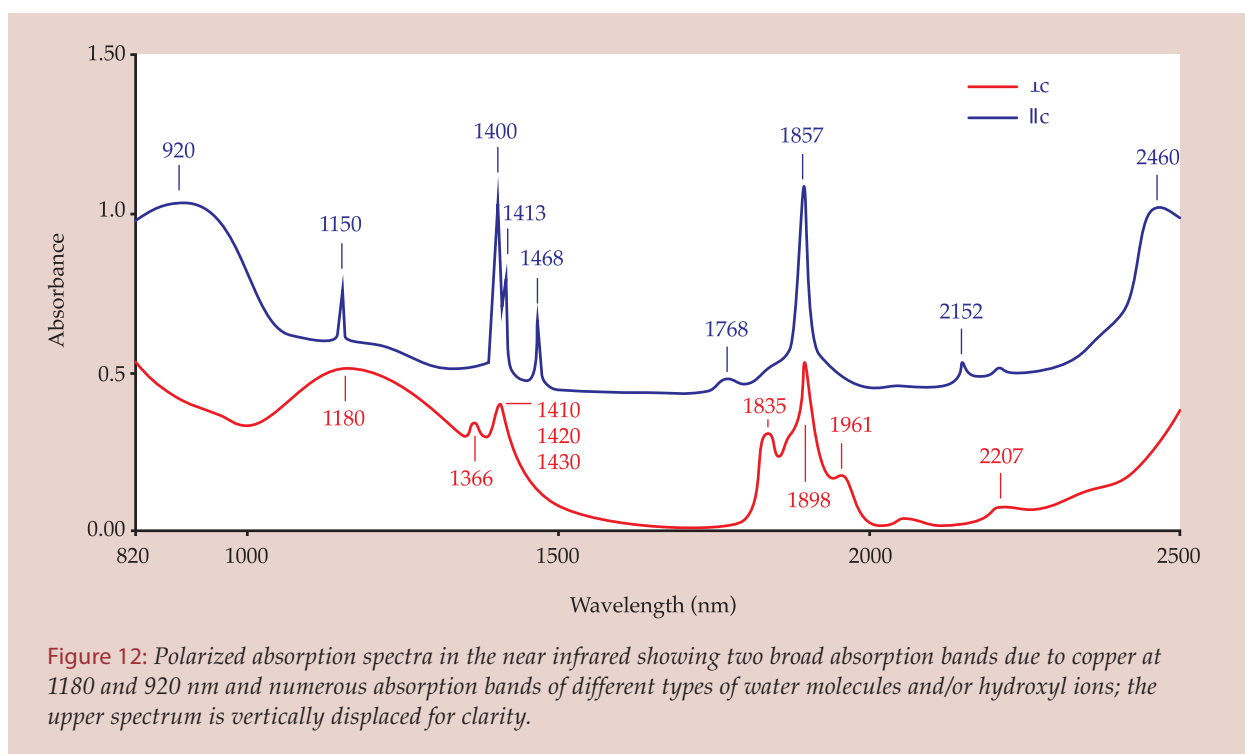


Figure 12: Polarized absorption spectra in the near infrared showing two broad absorption bands due to copper at 1180 and 920 nm and numerous absorption bands of different types of water molecules and/or hydroxyl ions; the upper spectrum is vertically displaced for clarity.

Microscopic characteristics

Structural properties

Neither rough nor faceted samples of the new type of Tairus hydrothermally-grown synthetic emerald showed residues of seed plates. All samples, however, contain step-like growth lines related to a weak colour zoning (*Figure 13*). In the rough samples, the sizes of the numerous steps within the growth lines increased from the sawn plane, which was next to the seed plate, towards the distant as-grown surface of the synthetic emerald crystal (*Figure 14*).

In both the rough and faceted samples, the angle between the step-like growth planes and the *c*-axis (representing the angle between seed plate and *c*-axis) was found to lie in a limited range between 28° and 30°. These results indicate that the synthetic emeralds were grown with seed plates cut with an angle to the *c*-axis slightly smaller than the characteristic angle of about 30°-32° which was for a long time used in growing synthetic emeralds in Russia (Schmetzer, 1988, 1996).

Almost perpendicular to the step-like growth lines, subgrain boundaries which are irregular and with a variety of orientations are present (*Figure 13, 14*). In one direction oblique to the step-like growth planes,



Figure 13: Faceted Tairus hydrothermally-grown synthetic emerald coloured by vanadium and copper; with step-like growth lines and colour zoning, and irregular subgrain boundaries almost perpendicular to the growth and colour zoning. Immersion, 40×. Photo by K. Schmetzer.



Figure 14: Rough crystal plate with step-like growth lines and colour zoning, irregular subgrain boundaries almost perpendicular to the growth and colour zoning. Immersion, 40×. Photo by K. Schmetzer.



Figure 15: Faceted Tairus synthetic emerald showing block structure between subparallel oriented subindividuals. Immersion, 60 \times . Photo by K. Schmetzer.

a characteristic block structure between subparallel oriented subindividuals is present (Figure 15). These microscopic features are characteristic for synthetic beryl and synthetic emerald, which is grown hydrothermally from seed plates cut oblique to the *c*-axis of the beryl crystal and non-parallel to possible natural faces of beryl (Klyakhin *et al.*, 1981; Granadchikova *et al.*, 1983; Lebedev and Askhabov, 1984; Lebedev *et al.*, 1986; Schmetzer, 1988).

Inclusions

Most of our Tairus synthetic emeralds were extremely clean. In one crystal and on the surface of two rough synthetic emerald plates, there are tiny opaque crystals or lamellae with a metallic lustre (Figure 16a).

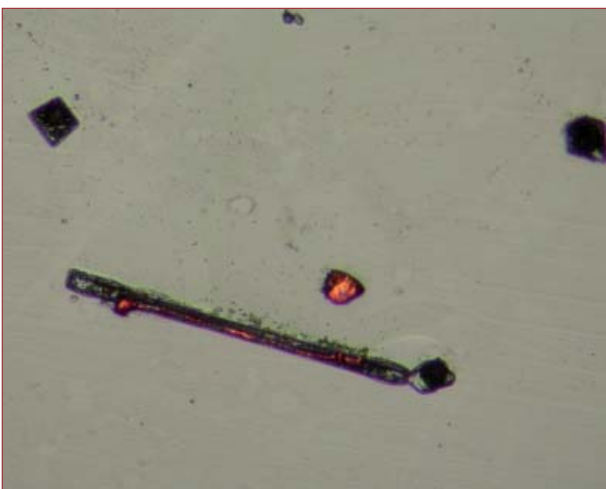


Figure 16a: On the surface of two Tairus hydrothermally-grown synthetic emerald plates we observed several crystals or lamellae of metallic copper. Reflected light, size of the lamella about 300 μm . Photo by H.-J. Bernhardt.

The solids on the surface of the rough crystal plates were identified using the electron microprobe as native copper. For the identification of the solid inclusions within a synthetic emerald plate, the sample was cut and polished until an octahedral crystal with metallic appearance (Figure 16b) was exposed at the surface; this inclusion was also identified as native copper. Only a few synthetic emerald samples contain small feathers consisting of liquid and two-phase inclusions.

Discussion

The ten samples of the new synthetic hydrothermally-grown beryl variety marketed by Tairus as 'Colombian Color Emerald' examined in the present study, reveal only small variability in their gemmological, chemical and spectroscopic properties. These data indicate – as announced by the producer – that our research material comprised samples of a commercial product grown by a finally developed technical process (see crystal growth).

According to the orientation of step-like growth structures and colour zoning, the orientation of the seed (about 28 -30° inclined to the *c*-axis) is only slightly different from the 'traditional' orientation used in Russia for commercial crystal growth of various types of synthetic emerald (about 30 -32°). A more

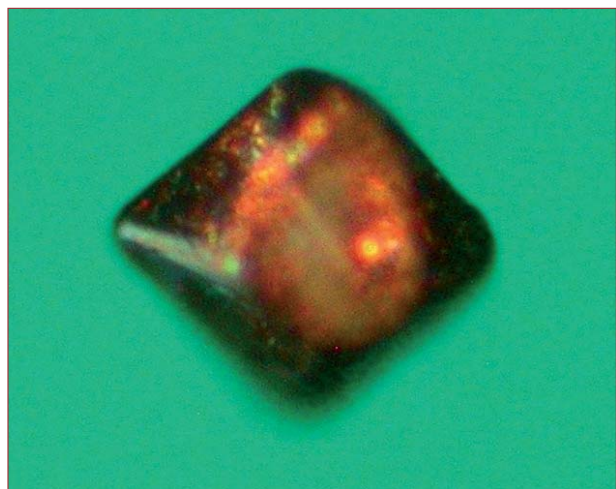


Figure 16b: This octahedral copper crystal inclusion in a Tairus synthetic emerald was exposed at the surface after cutting and polishing of the sample. Reflected light, diameter of the crystal about 55 μm . Photo by H.-J. Bernhardt.



Figure 17: Different types of hydrothermally-grown synthetic emeralds; upper line left: Biron (Australia) synthetic emerald coloured by chromium and vanadium (1.49 ct, 7.9 × 6.4 mm), centre: Russian synthetic emerald coloured by chromium (grown in an autoclave with noble metal liner), right: Russian synthetic emerald coloured by chromium, iron, copper, and nickel (grown in an autoclave without noble metal liner); lower line: two samples of the new type grown by Tairus coloured by vanadium and copper. Photo by M. Glas.

significant difference and the new scientific development in Novosibirsk is the formation and establishment of a growth medium in which both colour-causing trace elements, vanadium and copper, are incorporated in the required concentration as well as in the required valence state (mainly as V^{3+} and Cu^{2+}) into the beryl lattice. This suggests careful control of oxygen partial pressure in the autoclave, but, towards the end of the growth period, the partial pressure may change and enable the formation of native copper crystals both as inclusions and on the surfaces of crystals.

Gemmological properties of the material are in the range commonly observed for natural and hydrothermally-grown synthetic emeralds. Chemical and spectroscopic properties indicate that the synthetic beryls are coloured by a combination of vanadium and copper; chromium, which may derive from the natural colourless or slightly green beryl from the Ural mountains used as nutrient, is a very minor component. Infrared spectroscopy shows the presence of various types of water molecules and hydroxyl

groups, partly related to lithium in channel sites in the beryl structure.

Although experimental samples coloured by vanadium (yellowish green) or by copper (light blue) have been known for several decades, the new product is the first example of a synthetic bluish green 'emerald colour' synthetic beryl whose colour is caused by a combination of vanadium and copper, i.e. without any significant influence of chromium. The desired 'Colombian type' colouration of the new material closely matches the colour of other hydrothermally-grown synthetic emeralds on the market, for example synthetic emeralds coloured by:

- chromium,
- vanadium and chromium, or
- a combination of chromium, iron, copper and nickel (Figure 17).

The causes of colour and the definition of variously coloured natural and synthetic green beryls as 'emerald' was recently discussed by Schwarz and Schmetzer (2002). Considering that a practical definition of the term 'emerald' should include all materials accepted in general by the trade as emerald

without any need of a quantitative, time consuming chemical analysis (for example of chromium and/or vanadium contents in Colombian emeralds which show a great variability of chromium to vanadium ratios), the following suggestion was made: “Emeralds are yellowish green, green or bluish green, natural or synthetic beryls, which reveal distinct chromium and/or vanadium absorption bands in the red and blue-violet ranges of their absorption spectra.” Using this practical suggestion, the new material from Tairus is designated as synthetic emerald. The colour of the material underlines this designation, even if no distinct amounts of chromium are present in the synthetic beryls.

The distinguishing of the new type of Tairus synthetic emeralds from other emeralds can be carried out by microscopic examination on the basis of typical growth features such as step-like growth lines confined to colour zoning, irregular subgrain boundaries, and block structures between subparallel oriented subindividuals. In certain circumstances, spectroscopic and/or chemical data might also be helpful.

References

- Aines, R.D., and Rossman, G.R., 1984. The high temperature behaviour of water and carbon dioxide in cordierite and beryl. *American Mineralogist*, 69, 319-27
- Aurischio, C., Fioravanti, G., Grubessi, O., and Zanazzi, P.F., 1988. Reappraisal of the crystal chemistry of beryl. *American Mineralogist*, 73, 826-37
- Aurischio, C., Grubessi, O., and Zecchini, P., 1994. Infrared spectroscopy and crystal chemistry of the beryl group. *Canadian Mineralogist*, 32, 55-68
- Beckwith, P.J., and Troup, G.J., 1973. The optical and infrared absorption of V^{3+} in beryl ($Be_3Al_2Si_6O_{18}$). *Physica Status Solidi (a)*, 16, 181-6
- Charoy, B., De Donato, P., Barres, O., and Pinto-Coelho, C., 1996. Channel occupancy in an alkali-poor beryl from Serra Branca (Goiás, Brazil): Spectroscopic characterisation. *American Mineralogist*, 81, 395-403
- Deer, W.A., Howie, R.A., and Zussman, J., 1986. *Rock-forming minerals. Vol. 1B, Second Edition, Disilicates and Ring Silicates*. Longman Scientific & Technical, Harlow, England
- Flanigen, E.M., Breck, D.W., Mumbach, N.R., and Taylor, A.M., 1967. Characteristics of synthetic emeralds. *American Mineralogist*, 52, 744-72
- Granadchikova, B.G., Andreenko, E.D., Solodova, Yu.P., Bukin, G.V., and Klyakhin, V.A., 1983. Diagnostics of natural and synthetic emeralds. *Izv. Vyssh. Uchebn. Zaved., Geol. Razved.*, 26(10) 87-93 [in Russian]
- Koivula, J.I., Kammerling, R.C., DeGhionno, D., Reinitz, I., Fritsch, E., and Johnson, M.L., 1996. Gemological investigation of a new type of Russian hydrothermal synthetic emerald. *Gems & Gemology*, 32(1), 32-9
- Klyakhin, V.A., Lebedev, A.S., Il'in, A.G., and Solntsev, V.P., 1981. Growing of hydrothermal beryl. *Sintez i Vyrashchivanie Optich. Kristallov i Yuvelir. Kamnei, Novosibirsk 1981*, 45-66 [in Russian]
- Lebedev, A.S., and Askhabov, A.M., 1984. Regeneration of beryl crystals. *Zapiski Vsesoyuznogo Mineralogicheskogo Obshchestva*, 113(5), 618-28 [in Russian]
- Lebedev, A.S., Ilyin, A.G., and Klyakhin, V.A., 1983. Variétés de beryl “gemme” hydrothermal. *Revue de Gemmologie a.f.g.*, No. 76, 4-5
- Lebedev, A.S., Il'in, A.G., and Klyakhin, V.A., 1986. *Hydrothermally grown beryls of gem quality. In: Morphology and phase equilibria of minerals. Proceedings of the 13th General Meeting of the International Mineralogical Association, Varna 1982, Sofia 1986*, 403-11 [in Russian]
- Lebedev, A.S., Klyakhin, V.A., and Solntsev, V.P., 1988. Crystal-chemical characteristics of hydrothermal beryls. *Trudy Instituta Geologii i Geofiziki (Novosibirsk)*, 708, 75-94 [in Russian]
- Mashkovtsev, R.I., and Lebedev, A.S., 1993. Infrared spectroscopy of water in beryl. *Journal of Structural Chemistry* 33, 930-3
- Mashkovtsev, R.I., and Smirnov, S.Z., 2004. The nature of channel constituents in hydrothermal synthetic emerald. *Journal of Gemmology*, 29(4), 215-27
- Mashkovtsev, R.I., and Solntsev, V.P., 2002. Channel constituents in synthetic beryl: ammonium. *Physics and Chemistry of Minerals*, 29(1), 65-71
- Mashkovtsev, R.I., Stoyanov, E.S., and Thomas, V.G., 2004. State of molecules and ions in the structural channels of synthetic beryl with an ammonium impurity. *Journal of Structural Chemistry* 45(1), 56-63
- Mathew, G., Karanth, R.V., Gundu Rao, T.K., and Deshpande, R.S., 1997. Channel constituents of alkali-poor Orissan beryls: An FT-IR spectroscopic study. *Current Science*, 73(11), 1004-11
- Rodionov, A.Ya., Solntsev, V.P., and Weis, N.S., 1987. Crystallisation and properties of colored varieties of gas-transport beryl. *Trudy Instituta Geologii i Geofiziki (Novosibirsk)*, 679, 41-53 [in Russian]
- Schmetzer, K., 1978. *Vanadium III als Farbträger bei natürlichen Silikaten und Oxiden – ein Beitrag zur Kristallchemie des Vanadiums*. Dissertation, Universität Heidelberg, 277 pp
- Schmetzer, K., 1982. Absorptionsspektroskopie und Farbe von V^{3+} -haltigen natürlichen Oxiden und Silikaten – ein Beitrag zur Kristallchemie des Vanadiums. *Neues Jahrbuch für Mineralogie Abhandlungen*, 144(1), 73-106
- Schmetzer, K., 1988. Characterisation of Russian hydrothermally-grown synthetic emeralds. *Journal of Gemmology*, 21(3), 145-64

- Schmetzer, K., 1989. Types of water in natural and synthetic emerald. *Neues Jahrbuch für Mineralogie Monatshefte*, 1983(1), 15-26
- Schmetzer, K., 1996. Growth method and growth-related properties of a new type of Russian hydrothermal synthetic emerald. *Gems & Gemology*, 32(1), 40-3
- Schmetzer, K., and Bernhardt, H.-J., 1994. Isomorphic replacement of Al and Si in tetrahedral Be and Si sites of beryl from Torrington, NSW, Australia. *Neues Jahrbuch für Mineralogie Monatshefte*, 1994(3), 121-9
- Schmetzer, K., and Kiefert, L., 1990. Water in beryl – a contribution to the separability of natural and synthetic emeralds by infrared spectroscopy. *Journal of Gemmology*, 22(4), 215-23
- Schmetzer, K., Kiefert, L., Bernhardt, H.-J., and Zhang, B.L., 1997. Characterisation of Chinese hydrothermal synthetic emerald. *Gems & Gemology*, 33(4), 276-91
- Schwarz, D., and Schmetzer, K., 2002. *The definition of emerald – the green variety of beryl colored by chromium and/or vanadium*. Emeralds of the World, extraLapis English, No. 2, 74-8
- Shatskiy, V.S., Lebedev, A.S., Pavlyuchenko, V.S., Kovaleva, L.T., Koz'menko, O.A., Yudin, A.N., and Belov, N.V., 1981. Conditions for entry of alkali cations into beryl. *Geochemistry International*, 18(2), 7-17
- Sherriff, B.L., Grundy, H.D., Hartman, J.S., Hawthorne, F.C., and ern, P., 1991. The incorporation of alkalis in beryl: Multi-nuclear MAS NMR and crystal-structure study. *Canadian Mineralogist*, 29, 271-85
- Solntsev, V.P., 1981a. Nature of color centers and EPR in beryl and chrysoberyl. *Trudy Instituta Geologii i Geofiziki (Novosibirsk)*, 499, 92-140 [in Russian]
- Solntsev, V.P., 1981b. Absorption spectra and EPR of trace impurities in beryllium-containing minerals and their relation to specimen color. *Issled. Fiz. Svoistv i Sostova Sintet. Mineralov i Monokristallov, Novosibirsk 1981*, 37-47 [in Russian]
- Solntsev, V.P., Lebedev, A.S., Pavlyuchenko, V.S., and Klyakhin, V.A., 1976. Copper centers in synthetic beryl. *Sov. Phys. Solid State*, 18(5), 805-6
- Vladimirova, M.V., Lebedev, A.S., and Gevork'yan, S.V., 1987. IR spectroscopic study of water in synthetic crystals of beryl. *Mineralogicheskii Zhurnal*, 9(6) 57-63 [in Russian]
- Wood, D.L., and Nassau, K., 1967. Infrared spectra of foreign molecules in beryl. *Journal of Chemical Physics*, 47(7), 2220-8
- Wood, D.L., and Nassau, K., 1968. The characterization of beryl and emerald by visible and infrared absorption spectroscopy. *American Mineralogist*, 53, 777-800

The identification value of the 2293 cm^{-1} infrared absorption band in natural and hydrothermal synthetic emeralds

J.M. Duroc-Danner

Geneva, Switzerland

Abstract: *Where ordinary gemmological tests fail to reveal the identity of a gemstone Fourier-Transform Infrared Spectroscopy (FTIR) can often provide the answer. Ways of distinguishing natural from synthetic emeralds of various types have been concentrated in the spectral region between 2240–2400 cm^{-1} , where many more- or less-strong absorptions are observed. Amongst these, the presence of a small absorption near 2293 cm^{-1} has been utilized by many authors to indicate a natural emerald since this absorption had not been found in synthetics.*

However, now a Russian Tairus hydrothermal synthetic emerald has been found which shows the 2293 cm^{-1} absorption, so this feature can no longer be used to prove a natural origin.

Keywords: *gem-testing, IR spectroscopy, synthetic emerald*

Introduction

Recently, the author was preparing a lecture on beryl and while dealing with emeralds, natural and synthetics, expected to describe a straightforward example of an FT-IR separation between a natural Gachalá (Colombia) emerald and a synthetic hydrothermal Tairus emerald. However, a synthetic Russian Tairus hydrothermal emerald of 2.01 ct (Figure 1) from my collection showed the 2293 cm^{-1} absorption not normally seen in hydrothermal synthetic emeralds (Stockton, 1987; Koivula *et al.*, 1996; Zecchini and Maitrallet, 1998).



Figure 1: *Hydrothermal synthetic emerald grown by Tairus in 1996. It is emerald cut, weighs 2.01 ct, shows apparent turbidity and has an infrared absorption band at 2293 cm^{-1} .*

Gemmological properties

The emerald-cut transparent synthetic Russian Tairus hydrothermal emerald, measured with a Mitutoyo micrometer, was 9.60 × 5.60 mm with a depth of 5.12 mm. The weight on a Mettler PL 300C carat scale was 2.01 ct.

The refractive index (RI) determinations were carried out using a Rayner Dialdex refractometer and monochromatic sodium light. The indices obtained from the table facet were $\omega = 1.582$, $\varepsilon = 1.575$, giving a birefringence of 0.007, with optic sign negative. The uniaxial interference figure, obtained using a glass sphere between crossed polars, indicated that the *c*-axis was nearly parallel to the table facet and slightly inclined to the short axis (width) of the table. These characteristics overlap those reported for natural emeralds (Anderson, 1980; Nassau, 1980; Sinkankas, 1981; Kane and Liddicoat, 1985; Webster, 1994).

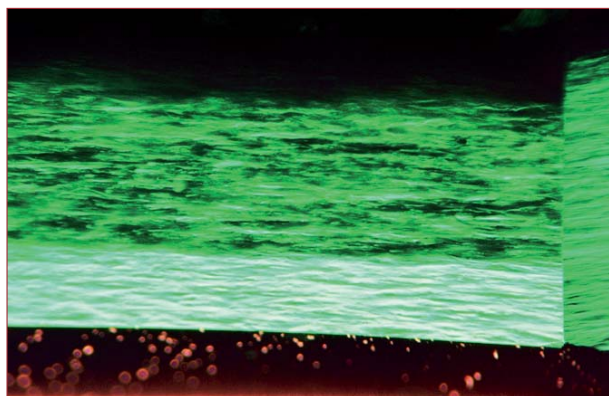


Figure 2: Turbidity is very apparent in hydrothermal emeralds, and particularly in a probable Russian sample, of 2.62 carats (dark-field illumination 15x).

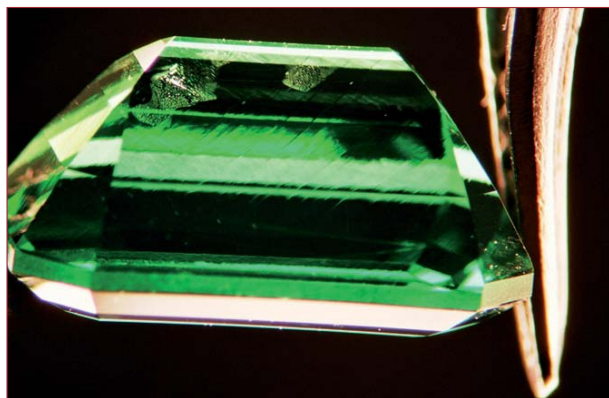


Figure 3: Strong parallel growth pattern was readily observed under the microscope in the 2.01 carat emerald cut hydrothermal Russian synthetic emerald. Also note the 'fingerprints' lying near the culet (dark-field illumination 10x).

Under a calcite dichroscope, with fibre optic illumination, a strong dichroism in yellowish green (ω ray) to bluish green (ε ray) was observed through the table facet. This is consistent with the behaviour of other natural and hydrothermal synthetic emeralds reported in the literature.

The absorption spectrum observed through the pavilion, in daylight conditions with a Beck spectroscopy, revealed a typical absorption spectrum for emerald (either natural or synthetic) with bands at 400-460, 580-600, 640, 670 and 680-700 nm.

The stone was examined with a Multispec combined LW/SW ultraviolet unit and as with many natural emeralds and other synthetic hydrothermal emeralds from other sources, remained inert to SW (254 nm) and LW (365 nm).

The specific gravity (SG) was obtained by hydrostatic weighing in distilled water using a Mettler PL 300C carat scale, and the stone was found to have a value of 2.70; this was



Figure 4: Characteristic chevron pattern is clearly visible in the 2.01 ct emerald cut hydrothermal Russian synthetic emerald (dark-field illumination 25x).



Figure 5: Very few 'fingerprints' consisting of tiny two-phase inclusions, were observed under the microscope in the 2.01 ct emerald cut hydrothermal Russian synthetic emerald (dark-field illumination 20x).

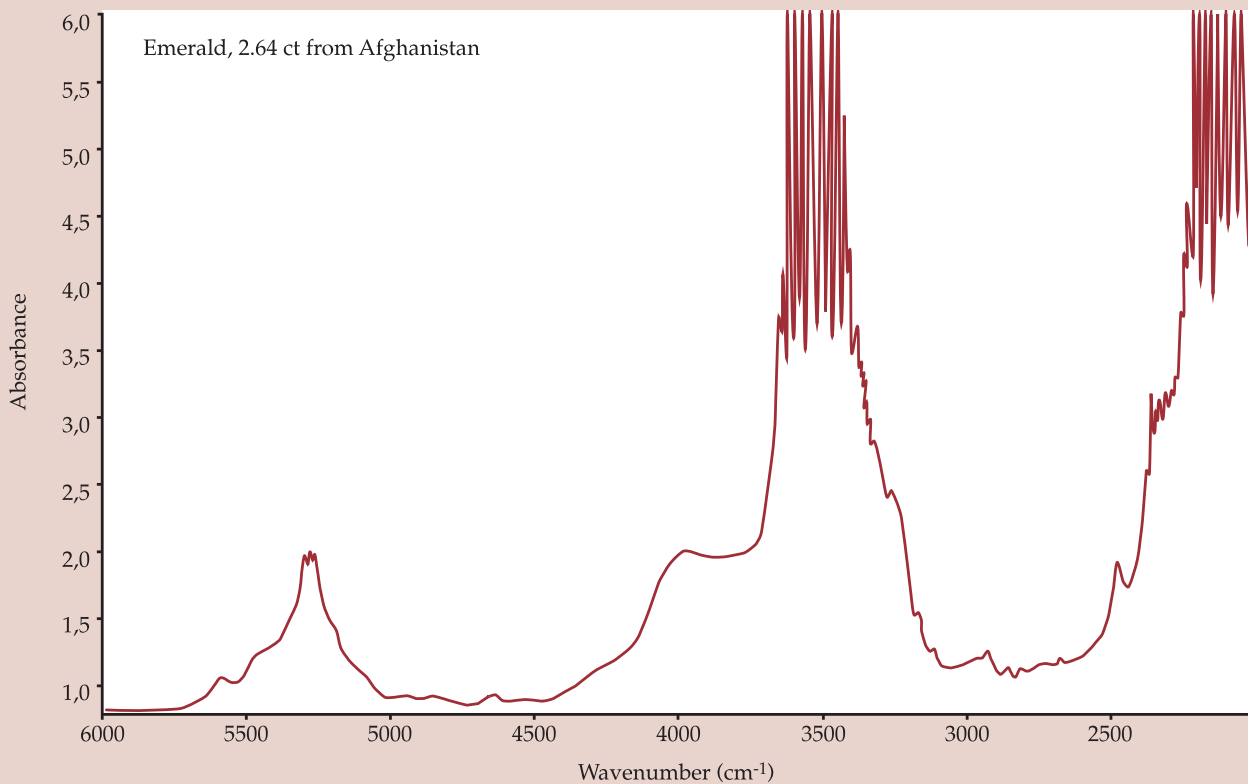


Figure 6a: Infrared spectrum characteristic for most natural emeralds, here recorded from a 2.64 ct emerald from Afghanistan.

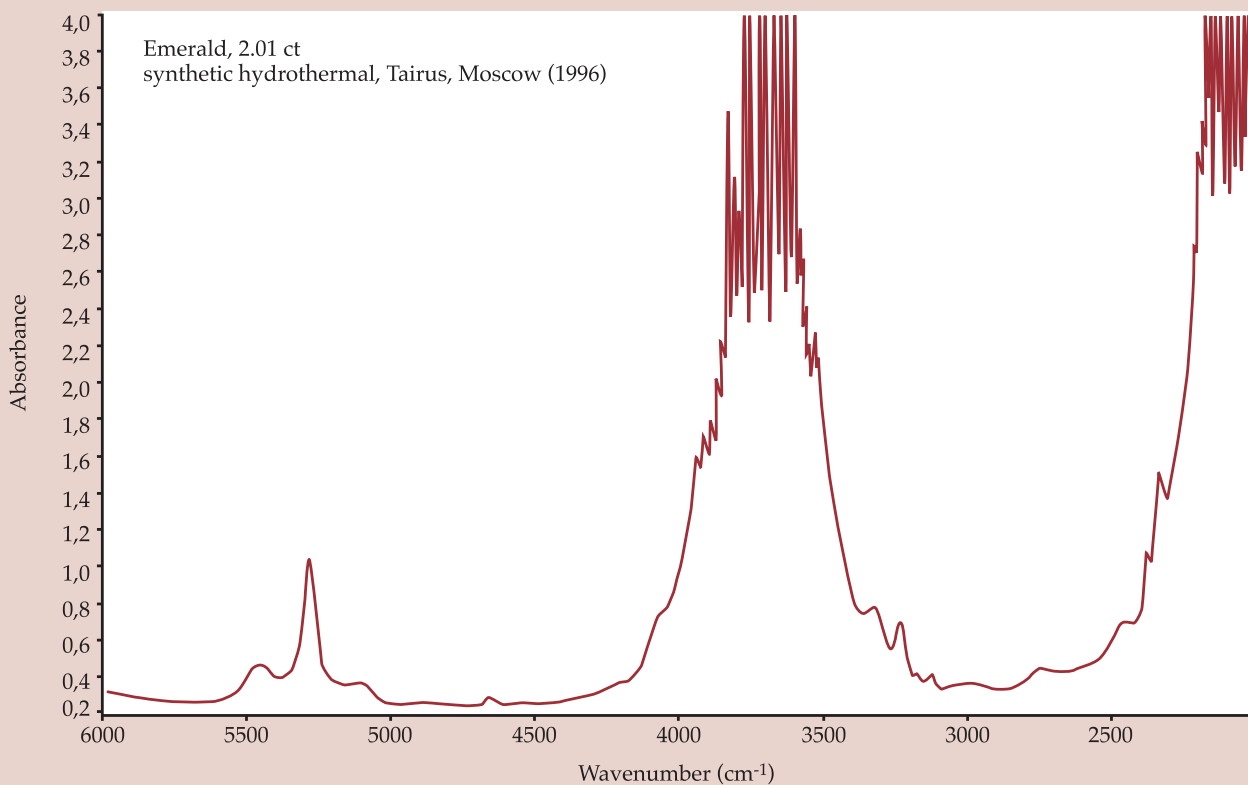


Figure 6b: Infrared spectrum typical of hydrothermal synthetic emeralds shown by a Tairus emerald of 1996.

confirmed when the stone sank slowly in the 2.67 heavy liquid. These values overlap those of natural emeralds and hydrothermal synthetic emeralds from other sources.

Under a Bausch & Lomb Mark V Gemolite binocular microscope using dark field illumination or overhead lighting as appropriate, no foreign inclusions were observed, but as in all the hydrothermal synthetic beryls (aquamarines and emeralds) examined by the author, the stone showed strong turbidity similar to that in another stone shown in *Figure 2*, with a distinct series of parallel growth planes (*Figure 3*), a characteristic chevron-like growth pattern (*Figure 4*) and some beautiful fingerprint-like patterns, one notably consisting of tiny two-phase inclusions resembling a dog's face (*Figure 5*) in the culet region of the stone. These characteristics are not found in natural emeralds, but are in line with those mentioned for hydrothermal Russian synthetic emeralds (Schmetzer, 1996; Koivula *et al.*, 1996; see also Schmetzer *et al.*, 1997).

Infrared spectroscopy

Infrared absorption spectra (FTIR) were obtained using a Fourier-Transform Nicolet Magna-IR ESP System 560 spectrometer.

Typical spectra for natural emeralds show strong absorptions around 2000-2300 cm^{-1} , a series of peaks between 2300-3300 cm^{-1} (their number and magnitude vary according to the crystallographic orientation of the stone tested), strong absorptions in the mid-infrared (due to their water content) around 3400-4000 cm^{-1} , series of peaks between 4100-5000 cm^{-1} , and intense absorption around 5000-5500 cm^{-1} , again due to water content.

This last absorption around 5000-5500 cm^{-1} often gives some clue as to whether the emerald is natural or hydrothermal synthetic. Indeed, independent of their geographical origin, the great majority of natural emeralds show a more or less triangular-shaped absorption band around 5000-5500 cm^{-1} (*Figures 6a* and *8*).

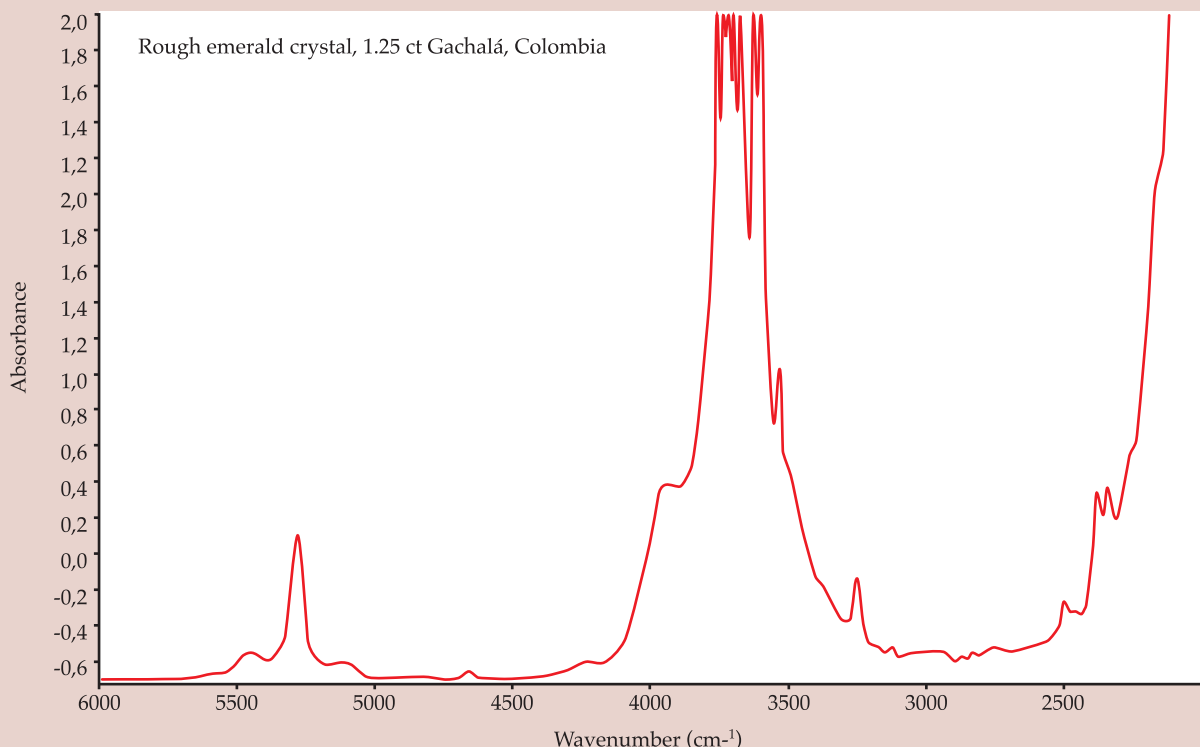


Figure 7: Very similar infrared spectrum to the one displayed by hydrothermal synthetic emeralds, here observed in a natural emerald from Gachalá (Colombia).

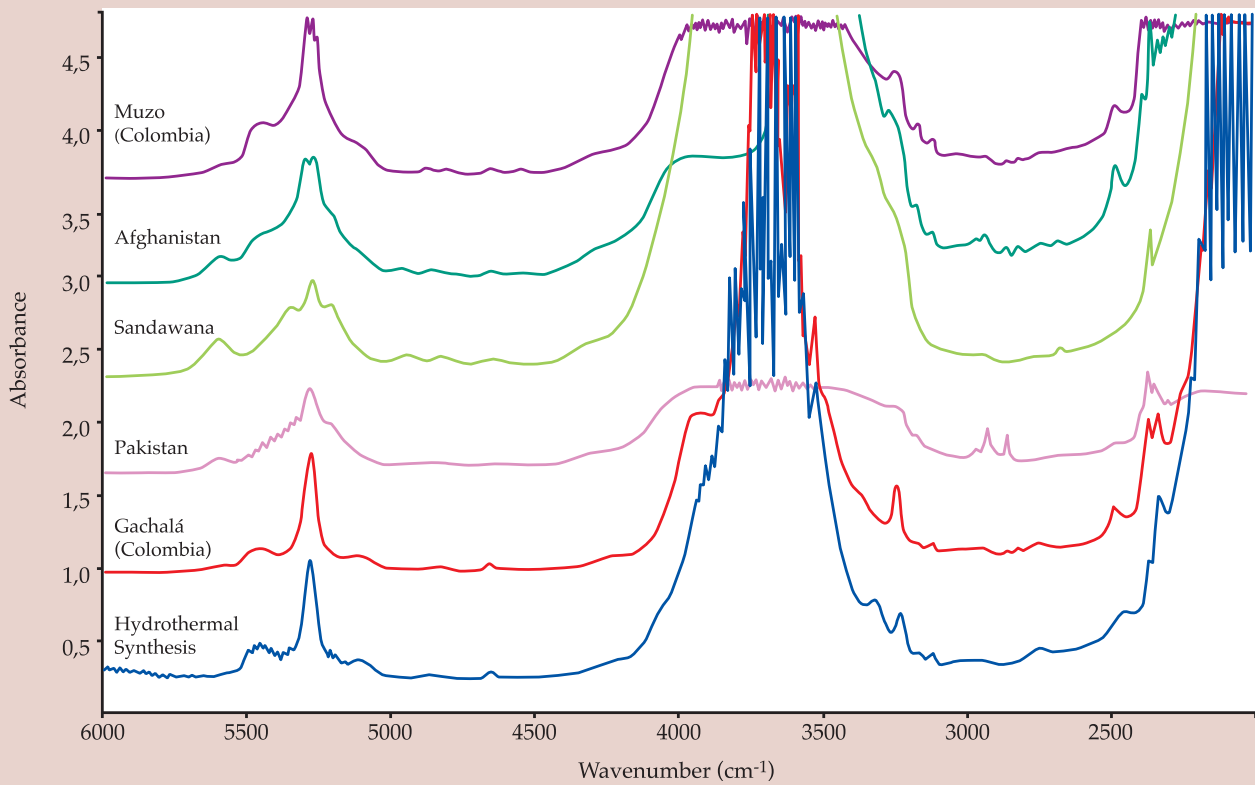


Figure 8: Typical infrared absorption bands in natural emeralds from different sources compared with the one shown by the Russian hydrothermal synthetic emerald of 2.01 ct. Note the similar aspect of the absorption band near 5000-5500 cm⁻¹ for both Gachalá (Colombia) emeralds and the hydrothermal synthetic emerald.

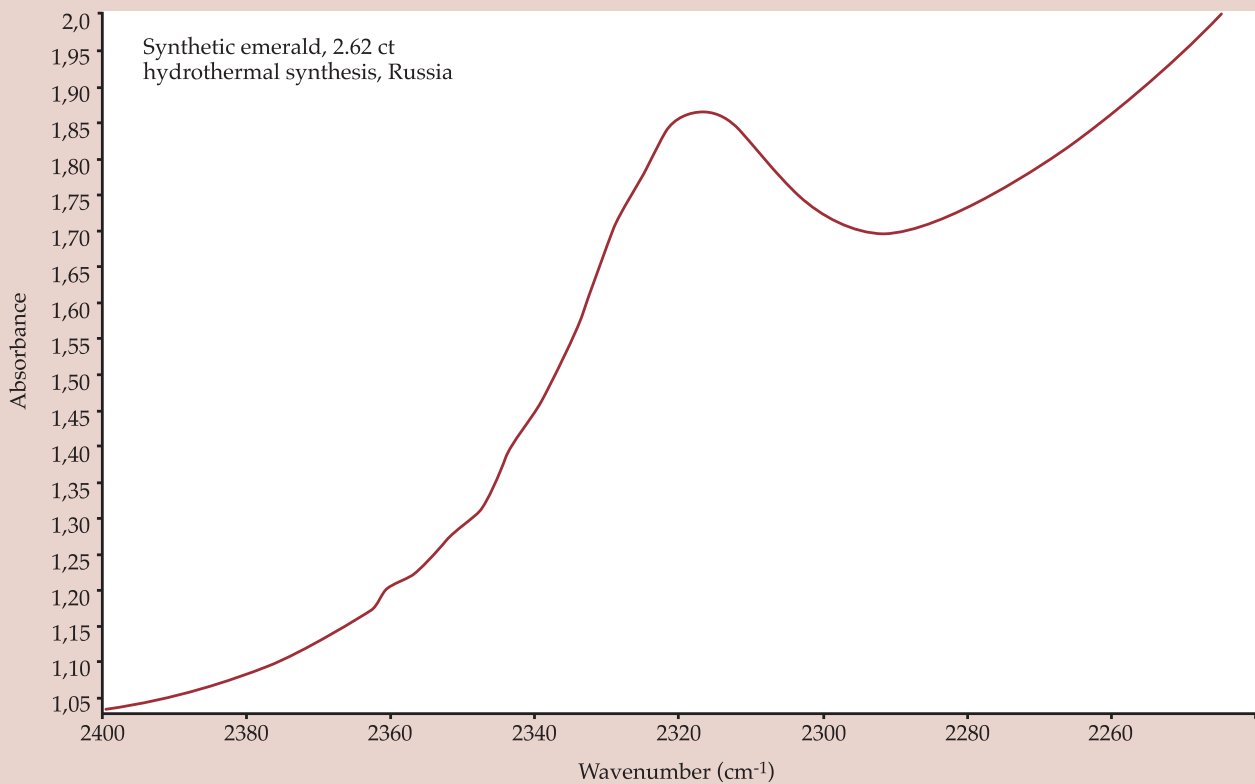


Figure 9: Many synthetic hydrothermal emeralds can be separated from Gachalá (Colombia) emeralds when they do not show the 2293 cm⁻¹ absorption band.

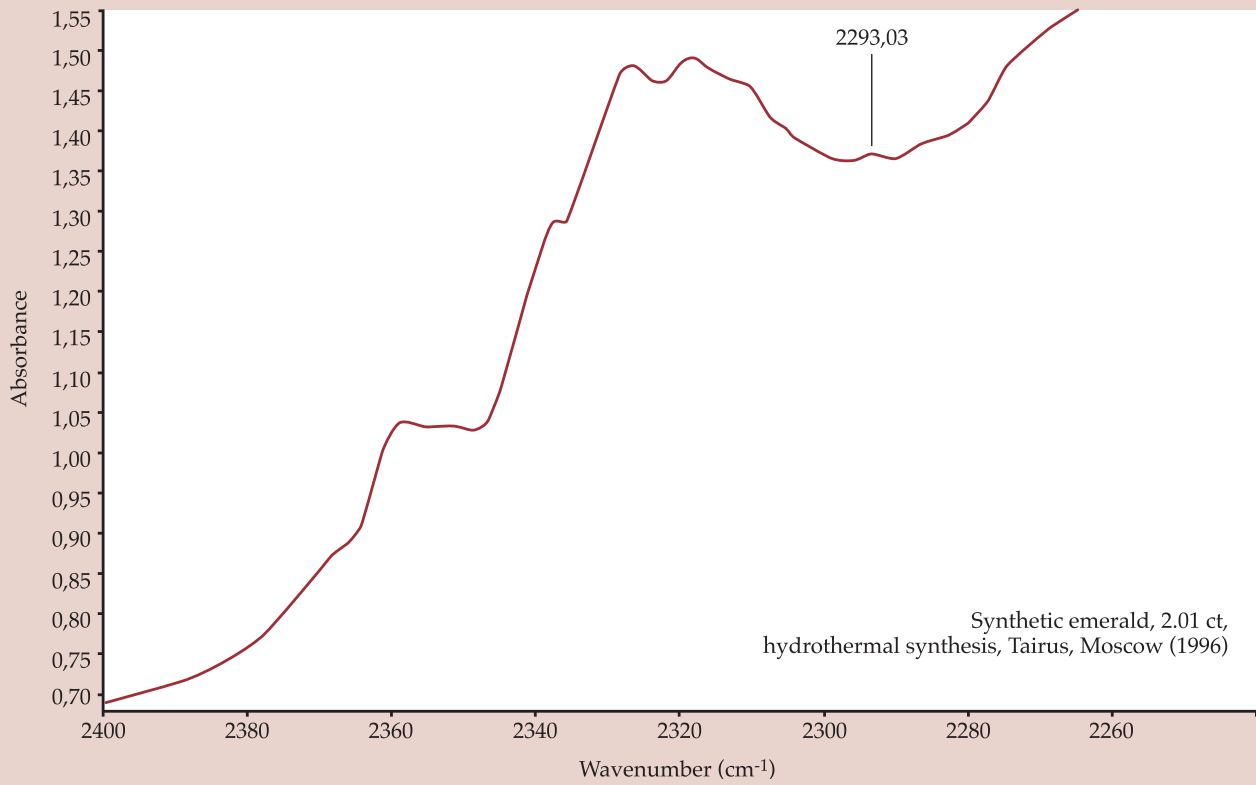


Figure 10a: The 2.01 ct synthetic Russian Tairus hydrothermal emerald exhibiting a 2293 cm⁻¹ absorption band which is also present in natural emeralds.

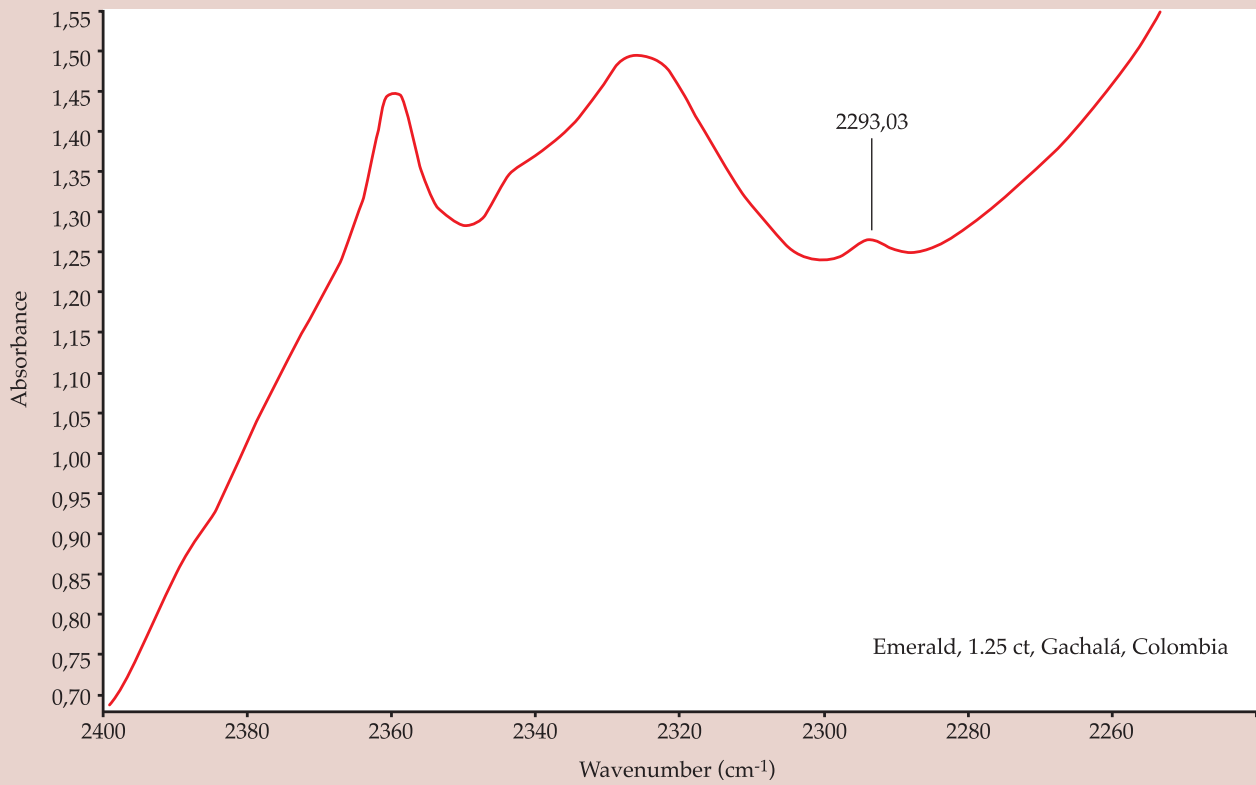


Figure 10b: Emeralds from Gachalá (Colombia) show the 2293 cm⁻¹ absorption band.

Hydrothermal synthetic emeralds often show similar absorption spectra to the one described for natural emeralds, but instead of a triangular-shaped absorption band around $5000\text{--}5500\text{ cm}^{-1}$, the main peak is found between two round absorptions (Figures 6b and 8).

Unfortunately, natural emeralds from Gachalá (Colombia) show very similar spectra (Figures 7 and 8), and therefore cannot be separated on this basis from their hydrothermal synthetic sisters.

Hitherto, hydrothermal synthetic emeralds have been indicated by the absence of a peak at 2293 cm^{-1} (Figure 9). So it was a surprise when the 2.01 ct synthetic Tairus hydrothermal emerald, like the natural emeralds, displayed the peak at 2293 cm^{-1} (Figure 10).

Finally, the presence of two minute peaks at 4052 cm^{-1} and 4375 cm^{-1} (Figure 11) indicate that this stone is synthetic as they have not been found in natural emeralds (Fritsch, *pers. comm.*, 2005).

Conclusion

On one hand, the standard gemmological properties, such as refractive index (RI), dichroism, absorption spectrum, UV fluorescence and specific gravity, confirm that the stone is emerald, but they are of no help in distinguishing natural from synthetic.

On the other hand, the strong turbidity, the characteristic chevron-like growth pattern, and the shapes of the 'fingerprint' inclusions, indicate a synthetic hydrothermal emerald.

So, although infrared spectroscopy was unnecessary to separate this synthetic hydrothermal emerald from its natural counterparts, it confirmed that the minute peaks at 4052 cm^{-1} and 4375 cm^{-1} were significant indicators of origin and cast doubt on using the presence or absence of the 2293 cm^{-1} peak to say that an emerald is natural or synthetic respectively.

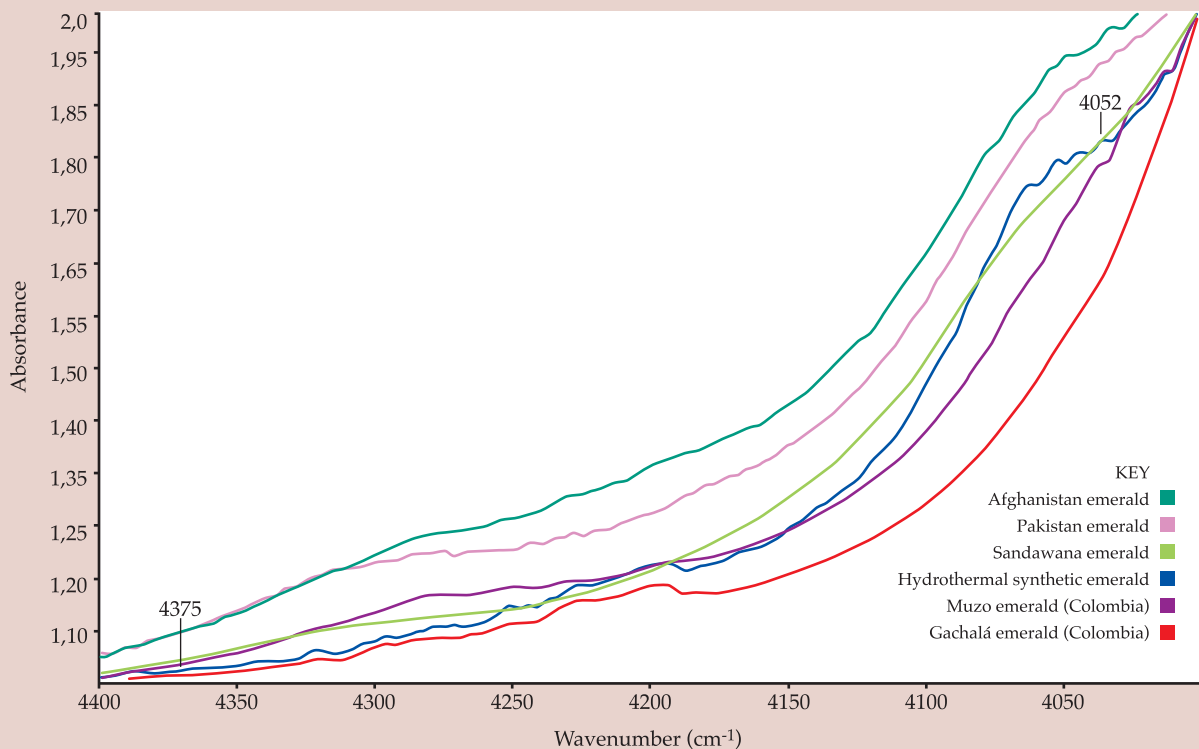


Figure 11: Natural emeralds can be distinguished from hydrothermal synthetics by the absence of the 4052 cm^{-1} and 4375 cm^{-1} absorption bands.

References

- Anderson B.W., 1980. *Gem Testing*. 9th edn. Butterworths & Co. Ltd, London, 126-36
- Kane R.E., and Liddicoat R.T. Jr, 1985. The Biron hydrothermal synthetic emerald. *Gems & Gemology*, 21(3), 156-70
- Koivula J.I., Kammerling R.C., DeGhionno D.G., Reinitz I., Fritsch E., and Johnson M.L., 1996. Gemological investigation of a new type of Russian hydrothermal synthetic emerald. *Gems & Gemology*, 32(1), 32-9
- Nassau K., 1980. *Gems made by man*. Chilton Book Co., Radnor, Pennsylvania, U.S.A., 155-6
- Schmetzer K., 1996. Growth method and growth-related properties of a new type of Russian hydrothermal synthetic emerald. *Gems & Gemology*, 32(1), 40-3
- Schmetzer K., Kiefert L., Bernhardt H.-J., Zhang Beili, 1997. Characterization of Chinese hydrothermal synthetic emerald. *Gems & Gemology*, 33(4), 276-91
- Sinkankas J., 1981. *Emerald and other beryls*. Chilton Book Co., Radnor, Pennsylvania, U.S.A., 313-23
- Stockton, C.M., 1987. The separation of natural from synthetic emeralds by infrared spectroscopy. *Gems & Gemology*, 23(2), 96-99
- Webster, R., 1994. *Gems: their sources, description and identification*. 5th edn, revised by P. G. Read, Butterworth-Heinemann Ltd., Oxford, 431-6
- Zecchini, P., and Maitrallet, P., 1998. *Que peut apporter la spectrographie infrarouge dans l'étude des émeraudes? In L'émeraude connaissances actuelles et prospectives*. D. Giard (Ed.). Association Française de Gemmologie, Paris, 81-96

Surface coating of gemstones, especially topaz – a review of recent patent literature

Dr Karl Schmetzer

Taubenweg 16, D-85238 Petershausen, Germany

Abstract: Different methods of surface coating of gem materials are reviewed with respect to various patent documents published recently. In addition to the longer known techniques of simple sputtering and dye-coating, two different types of coating processes are used: first, heat treatment of a faceted gem in contact with a transition metal-bearing powder, and secondly deposition of a coating on the facets of a sample and subsequent heat treatment of the coated stone. The reaction mechanisms, nomenclature and recognition of treated stones are discussed.

Introduction

Various types of surface-treated topaz have been seen in the gem market and described by different authors (see, for example, Millington, 2005). One major treatment process, producing pink, orange and red coloration, was characterized as a simple coating of the faceted stone with an easily removable dye layer. In contrast, a cobalt-bearing layer on another type of treated green, blue-green and blue topaz was more resistant to a simple scratching test (see, for example, Johnson and Koivula, 1998; Underwood and Hughes, 1999). Due to the lack of technical information describing the exact production processes, there was speculation about a possible 'diffusion' mechanism of this coloured layer into the surface of faceted colourless topaz samples (McClure and Smith, 2000). Schmetzer (2001) cited the first technical information from patent documents about the production process of green, blue-green, and blue surface-treated topaz as published in the

international patent application WO 98/48944 A1 and in the American patent US 5,888,918, both by R. Pollak (documents 3 and 4 in Table I). According to these descriptions, the faceted topaz samples are heat treated within a finely divided powder of cobalt metal or cobalt oxide.

Such or similar treated stones have even found their way not only onto the markets of gem consuming but also into the trade of gem producing countries such as Nigeria (see, for example, Krzemnicki, 2002; Figure 1) and, in the opinion of the present author, understanding the technical procedure of treatment mechanisms is essential for correct nomenclature of treated gems. In addition, detailed knowledge of treatment processes is one of the key features for the recognition of treated samples and for their distinction from untreated gem materials. Thus, the present review briefly summarises the contents of different patents related to surface treatment of gem materials, and especially of topaz.

Table 1: Patent documents describing surface treatment of gem materials, especially topaz*

Document/patent family**	No.	Issued	Inventor/applicant	First step of treatment	Coating/diffusion material	Colours (examples)	Remarks
WO 96/06961 A1	1	7.3.1996	Rogers/Deposition Sciences, CA, USA	Chemical vapour deposition or sputtering or others	Various oxides or plastics	Golden orange in transmission and blue in reflection or green in transmission and silvery pink in reflection	Alternating layers with high and low refractive indices creating an interference filter
US 6,197,428 B1	2	6.3.2001					
WO 98/48944 A1	3	5.11.1998	Pollak/Pollak, Encinitas, CA, USA	Contact heat treatment with powder	Cobalt metal or cobalt oxide, optional: additional metals or metal oxides	Blue, blue-green, green-blue, green	Additional heat treatment after coating is possible
US 5,888,918	4	30.3.1999					
US 6,376,031 B1	5	23.4.2002					
US 2002/0174682 A1	6	28.11.2002					
EP 1 017 504 B1	7	20.8.2003					
DE 698 17 380 T2	8	24.6.2004					
US 5,853,826	9	26.12.1998	Starcke <i>et al.</i> /Azotic Coating Technology, Rochester, Minn., USA	Sputtering or chemical vapour deposition or physical vapour deposition or others	Thin coating of the pavilion of a stone with one or several thin layers, especially Ti, TiO ₂ , Zr, ZrO ₂ , also other metals, metal oxides, nitrides, sulfides and carbon	Green to violet (at different angles)	Various reflection and interference phenomena are observed when viewed at different angles of observation
EP 0 888 730 A1	10	7.1.1999	Arends/Fitness Innovations & Technologies, Chester, N.J., USA	Adhering coloured ink to the surface, drying	Transparent ink including a dye	Red, blue, green, yellow	Removable coating
US 5,981,003	11	9.11.1999					
US 6,146,723	12	14.11.2000					
BR 2000-1034 A	13	27.11.2001	Soares Sabioni <i>et al.</i> /Soares Sabioni, Ouro Preto, Minas Gerais, Brazil	Contact heat treatment with powder	Mixtures of topaz powder and metal powder or metal oxide powder or metal salt powder	Blue (cobalt)	a. Preparation of mixture of powder b. heat treatment of mixture c. diffusion by contact heat treatment with powder; repeated treatment with different metals is possible

Document/patent family**	No.	Issued	Inventor/applicant	First step of treatment	Coating/diffusion material	Colours (examples)	Remarks
BR 2000-2321 A	14	30.4.2002	Soares Sabioni and Mendonça Ferreira/Soares Sabioni, Ouro Preto, Minas Gerais, Brazil	Vacuum sputtering	Transition metal	Yellow to reddish orange (iron)	a. deposition of transition metal coating to crown or pavilion b. heat treatment of coated stone
US 2002/0128145 A1 US 6,635,309 B2	15 16	12.9.2002 21.10.2003	Pollak/Pollak, Encinitas, CA, USA	Contact heat treatment with powder	Copper metal or copper oxide, optional: additional metals or metal oxides	Yellow to red	Iron can produce similar colours; additional heat treatment after coating is possible
US 2003/0008077 A1 EP 1 394 293 A1 US 6,872,422 B2	17 18 19	9.1.2003 3.3.2004 29.3.2005	Gupta and Goyal/Gupta and Goyal, Jaipur, Rajasthan, India	Chemical vapour deposition or physical vapour deposition or others	Metals, metal oxides, metallic compounds, alloys	Blue, green (cobalt); yellow, reddish yellow, orange, pinkish yellow (iron); green (chromium); blue (cobalt and chromium); blue to green (cobalt and nickel); imperial (iron and chromium and nickel)	a. deposition of coating to the faceted stone b. heat treatment of coated stone
DE 102 15 141 A1	20	16.10.2003	Anonymous/Meelis, Idar-Oberstein, Germany	Spraying	Iron oxide	Yellow-orange	a. deposition of coating to the faceted stone b. heat treatment of coated stone
RU 2 215 454 C1	21	10.11.2003	Balitsky <i>et al.</i> /Institute of Experimental Mineralogy RAS, Chernogolovka, Moscow district, Russia	Sputtering	Iron	Yellow to yellow-orange or orange	a. deposition of coating to the faceted stone b. heat treatment of coated stone
RU 2 215 455 C1	22	10.11.2003	Balitsky and Balitskaya/Institute of Experimental Mineralogy RAS, Chernogolovka, Moscow district, Russia	Contact heat treatment with powder	Cobalt oxides and zinc oxide	Dark blue	Cobalt of various valence states
US 2004/0083759 A1	23	6.5.2004	Starcke <i>et al.</i> , Rochester, Minn., USA	Sputtering or chemical vapour deposition or others	Any dielectric material, e.g. oxide, nitride, carbide, sulphide, with dopant	Yellow (titania and vanadium oxide), blue (silica and cobalt oxide)	Additional heat treatment after coating is possible or necessary

* patent documents are sorted in patent families (i.e., groups of patent documents with similar contents related to the same inventor or applicant, frequently based on the same priority application); patent families are presented chronologically according to the first member of a patent family published

** Abbreviations: BR Brazil; DE Germany; EP Europe; RU Russia; US United States of America; WO World Intellectual Property Organization



Figure 1: This surface-coated topaz is coloured by a thin iron-bearing layer on the pavilion of the stone; similar stones have been offered to gem dealers in Nigeria as natural topaz. The stone measures 10.1 × 8.0 mm, weight 2.95 ct. Photo by M. Krzemnicki, SSEF, Basel.

Review of the patent literature

A number of different patent documents have been published describing various techniques of surface enhancement of gem materials, which relate to the formation of surface coloration of natural and synthetic gemstones, especially topaz, quartz and sapphire. A general overview is given in Table I. The review covers documents published in the period 1996 to 2005.

Three patent documents describe simple coating technologies without specific heat treatment. In the US patent by Starcke *et al.* (document 9), a thin coating of a metal, metal oxide, nitride, sulphide or carbon is deposited on the pavilion of a faceted gem. Different colours are seen at different angles of observation, a feature which is caused by various reflection and interference phenomena. A more complex coating process is applied by Rogers (documents 1, 2). An optical interference coating is made of alternating layers of materials with relatively high refractive indices and relatively low refractive indices. The refractive indices and thickness of the alternating layers are chosen so that at least part of visible light incident on the gemstone is reflected. In this way, the coating creates an optical interference filter.

Different colours are observed in transmission and reflection as well as at different angles of observation. Stones with the features described in these patents (Figure 2) have been seen on the market with various trade names such as 'aqua aura' for surface-coated topaz and quartz or 'tavalite' for surface-coated cubic zirconia (Kammerling and Koivula, 1992; Johnson and Koivula, 1996 a,b).



Figure 2: These two 'fire topazes' are surface-coated with thin metallic layers deposited on the pavilion or the crown facets. Such stones may appear under different trade names. Various optical reflection, transmission and interference phenomena cause different coloration (from green to violet) when the samples are viewed at different angles. The stones are 9.2 × 7.0 mm, weights 2.27 and 2.21 ct. Photo by M. Glas.



Figure 3: The colour of this surface-coated pink topaz is due to an easily removable dye. The stone is 18.0 × 13.0 mm and weighs 15.17 ct. Photo by M. Glas.

A coating of transparent ink including a red, blue, green or yellow dye and which is removable has been described by Arends (documents 10-12). The permanent ink is made from n-propanol, n-butanol and



Figure 4 a, b: The colour of these surface-coated blue and green topazes is caused by cobalt-bearing layers with cobalt in different valence states. The stones are 16.2×12.0 mm (blue) and 20.2×15.2 mm, weights 10.57 and 21.84 ct. Photo by M. Glas.

diacetone alcohol and is adhered to the facets of the gemstone, for example cubic zirconia or white sapphire. The coating is easily removable in isopropyl alcohol. Nowadays, pink dye-coated topazes are not uncommon on the market (Figure 3).

Two major techniques are used for a more permanent surface coating of mostly colourless, natural and synthetic gem materials, especially for topaz, quartz and sapphire. The first technique is based on heat treatment of faceted gem materials in a transition metal-bearing powder (see documents 3-8, 13, 15, 16 and 22). The colour-causing transition metal may be present as metal or metal oxide. The transition metals used by Pollak are cobalt for blue, blue-green or green colours (Figure 4 a, b) and copper for yellow to red colours (documents 3-8, 15, 16). Using this technology, Pollak also mentioned that iron surface treatment produces colours comparable to copper (documents 15, 16). Furthermore, Pollak reported that various additional metals or metal oxides can be added to the cobalt- or copper-bearing powder used for treatment (documents 3-8, 15, 16). The colour of the material obtained by these processes can be changed by subsequent heat treatment of the coated gem material in different atmospheres without further contact with a metal- or metal oxide-bearing powder (documents 3-8, 15, 16). In this subsequent step of treatment, a shift of blue-green topaz colouration to a more

pure blue or the development of a red hue in yellow surface-treated topaz is achievable.

A special mixture of cobalt oxides and zinc oxide has been used by Balitsky and Balitskaya (document 22). For this type of contact heat treatment with powder, the powdered material used to surround the faceted gem during heat treatment can also contain fine grained material of the same gem mineral. In a Brazilian patent by Soares Sabioni *et al.* (document 13), the inventors used a mixture of powdered topaz with a powder of a metal or a metal oxide or a metal salt, which was heat treated in a first step before placing faceted topaz in this pre-heated powder for a second step of heat treatment. Repeated heat treatment is possible in powders containing various metals, in this way creating a succession of differently doped layers on the surface of the treated samples.

The second major technique requires two steps of treatment, (a) the deposition of a coating on the faceted stone and (b) heat treatment of the coated gem (documents 14, 17-19, 20, 21, 23). The coating of the gem may be carried out by vacuum sputtering, chemical vapour deposition, physical vapour deposition, spraying, or other techniques.

The coat may consist of metals, metal oxides, metallic compounds or alloys. As described by Gupta and Goyal (documents 17-19), a wide variety of colours is obtainable after subsequent heat treatment of the coated

material, such as blue to green (cobalt or cobalt and chromium or cobalt and nickel), green (chromium), yellow to orange (iron; see *Figure 1*). The appearance of 'Imperial' topaz is obtainable by a combination of iron, chromium and nickel. The colour of the sample can be controlled using different treatment conditions. For topaz with cobalt-bearing surface layers, heat treatment in air in a temperature range from 900 to 1000 C produces a green coloration, while under heat treatment in a temperature range of 950 to 1050 C a blue/green colour is obtained. Heat treatment in nitrogen or in a reducing environment, on the other hand, results in a blue coloration of the surface-coated topaz.

Another type of colour reaction within the surface layer is described by Starcke *et al.* (document 23). For topaz with a very light grey surface coating consisting of titania and vanadium oxide, a yellow body colour was obtained after heat treatment at 450 C. In another topaz with a colourless surface layer consisting of silica and cobalt oxide, a light blue colour was developed after heat treatment at 450 C.

Reaction mechanism

For both major techniques mentioned above, exact details of the chemical reactions are, in general, not disclosed. For both methods, 'diffusion into the outer surface' as well as 'chemical bonding to the surface' are claimed as reaction mechanisms (documents 3-8, 15, 16, 17-19). 'Diffusion into the outer surface' of a faceted gemstone indicates the production of a coloured zone or layer without a distinct interface, for example the diffusion of cobalt atoms into the crystal structure of topaz. 'Chemical bonding to the surface' of a faceted gemstone indicates the production of a coloured zone or layer with a distinct interface between the surface coating and the underlying gemstone.

According to the descriptions in the Brazilian patents of Soares Sabioni and co-authors (documents 13, 14), some transition metals such as cobalt are diffused into the surface of the treated topaz. Consequently, both techniques – i.e. contact heat treatment

with a metal-bearing powder and heat treatment of a surface deposited metal-bearing layer – result in a diffusion reaction between a cobalt-bearing layer or powder with the topaz crystal and the formation of a cobalt-bearing zone on the outer surface of the topaz crystal. Consequently, the treated sample might consist of an outer layer of a cobalt-bearing material deposited on to the surface and an inner layer in which cobalt is diffused into the topaz crystal structure. The exact composition and the crystalline and/or amorphous phases present within the surface layer or surface layers may vary according to treatment conditions and are unknown at present (see Underwood and Hughes, 1999). A detailed examination of the outer layers of variably treated gem materials, for example by a combination of X-ray powder diffraction with an electron microscope or with the electron microprobe, is necessary to clarify this point.

It is mentioned that other compounds than cobalt such as iron oxide diffuse less easily into the topaz crystal structure. For such compounds, contact heat-treatment with a metal-bearing powder is less effective and, consequently, iron-bearing layers are first deposited on the surface of topaz for subsequent heat treatment if, for example, a yellow to orange or reddish-orange coloration is desired (see documents 14, 17-19, 20, 21). After heat treatment, the iron-bearing layer is not easily removable from the topaz surface. As described in some documents cited, the iron-bearing layer or atoms of this layer are 'bonded' to the topaz surface. This description reflects the more or less stable formation of a topaz-iron oxide composite surface layer.

A special mechanism is claimed by Starcke *et al.* (document 23). These authors describe heat treatment of the surface-coated gemstone without any diffusion from the surface coating into the gemstone. This is due to heat treatment "at an elevated temperature below that at which there occurs substantial diffusion of material from the coating into the gemstone". The temperatures applied, however, are up to 1150 C and, consequently, in a temperature range in which other authors describe diffusion.



Figure 5: These two pink topazes are dye-coated on the pavilion facets of the samples. Different colour intensities are observed when viewed through the colourless crown and through the dyed pavilion. The stones are 18.0 × 13.0 mm and 15.8 × 12.0 mm, weights 15.17 and 10.59 ct. Photo by M. Glas.

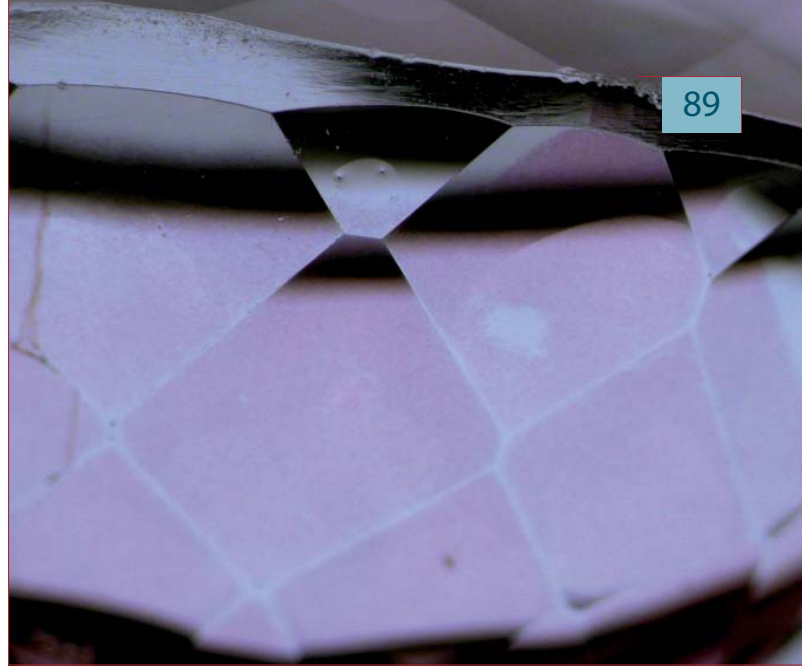


Figure 6: This dye-coated pink sapphire shows small colourless patches on pavilion facets. Magnification 30x. Photo by J.-P. Chalain, SSEF, Basel.

Detection of treatment

According to the various treatment techniques applied for surface coating of topaz and other gem materials, the criteria for the detection of treated material may vary (see also Millington, 2005). Thin metallic coatings causing interference and other optical effects (*Figure 2*) are not found on faceted examples of natural untreated stones. In coated stones different colours may be observed when the stones are viewed from different directions. For a number of samples such as some pink topazes examined recently (*Figure 3*), which are dye-coated on pavilion facets, the colour intensity observed through the colourless table will differ from that on the pavilion (*Figure 5*). Surface-coated samples of this type show colourless spots or small colourless patches on facets (*Figure 6*) or along facet junctions.

For a number of samples produced by contact heat treatment with powder or by heat treatment of a metal-bearing layer (*Figures 1, 4 a, b*), an irregular or somewhat spotty colour distribution on coated facets or facet junctions can also be observed. There are also frequent references in the literature to small colourless areas, also described as colourless chips within the coating (see, for example, Johnson and Koivula, 1998; Underwood and Hughes, 1999; McClure and Smith, 2000; Krzemnicki, 2002).

Nomenclature and conclusion

In summary, various mechanisms are described for different treatment techniques. The properties of the resulting type of coating are due to the actual process applied, but are also dependent on the main transition metal or group of transition metals, for example cobalt, iron or copper, used for coating. The different minerals such as quartz, topaz or corundum, subjected to a particular transition metal and treatment technique, may well show different reactions. Consequently, when naming a stone whose treatment history is not known, only a reference to the general technique applied should be made. All techniques described above are processes of surface-coating and, consequently, a description of a stone that has undergone any of these as 'surface-coated' reflects the applied treatment technique and distinguishes these gem materials from irradiated or simply heat-treated gemstones.

References

- Johnson, M.L., and Koivula, J.I. (Eds), 1996a. Gem News. "Tavalite," cubic zirconia colored by an optical coating. *Gems & Gemology*, 32(2), 139-40
- Johnson, M.L., and Koivula, J.I. (Eds), 1996b. Gem News. Coated quartz in "natural" colors. *Gems & Gemology*, 32(3), 220-1

- Johnson, M.L., and Koivula, J.I. (Eds), 1998. Gem News. Surface-treated topaz. *Gems & Gemology*, 34(2), 143-4
- Kammerling, R.C., and Koivula, J.I., 1992. An examination of 'Aqua Aura' enhanced fashioned gems. *Australian Gemmologist*, 23(2), 72-7
- Krzemnicki, M.S., 2002. Orange topaz with synthetic hematite coating. *Gems & Gemology*, 38(4), 364-6
- McClure, S.F., and Smith, C.P., 2000. Gemstone enhancement and detection in the 1990s. *Gems & Gemology*, 36(4), 336-59
- Millington, G., 2005. The things that turn up. *Gems & Jewellery*, 14(3), 58-9
- Schmetzer, K., 2001. Some light on the 'topaz-type diffusion process' of natural corundum. *Journal of Gemmology*, 27(6), 360-1
- Underwood, T., and Hughes, R.W., 1999. Surface-enhanced topaz. *Gems & Gemology*, 35(3), 154-5
10. Arends, R.W. (1999): *An enhanced gem stone, a jewellery enhancement kit and a method of simulating the appearance of an expensive gemstone*. EP 0 888 730 A1
11. Arends, R.W. (1999): *Gem stone having an enhanced appearance and method of making same*. US 5,981,003
12. Arends, R.W. (2000): *Enhanced gem stone and a method of simulating the appearance of an expensive gem stone*. US 6,146,723
13. Soares Sabioni, A.C., Mendonça Ferreira, C., Magela da Costa, G. (2001): *Processo de coloração e/ou modificação de cores de gemas lapidadas por dopagem em etapas múltiplas*. BR 2000-1034 A
14. Soares Sabioni, A.C., Mendonça Ferreira, C. (2002) *Processo de coloração de gemas lapidadas por dopagem ou recobrimento químico de seu pavilhão ou coroa*. BR 2000-2321 A
15. Pollak, R. (2002): *Process for the color enhancement of gemstones*. US 2002/0128145 A1
16. Pollak, R. (2003): *Process for the color enhancement of gemstones*. US 6,635,309 B2
17. Gupta, S., Goyal, M. (2003): *Process for imparting and enhancement of colours in gemstone minerals and gemstone minerals obtained thereby*. US 2003/0008077 A1
18. Gupta, S., Goyal, M. (2004): *Process for imparting and enhancement of colours in gemstone minerals and gemstone minerals obtained thereby*. EP 1 394 293 A1
19. Gupta, S., Goyal, M. (2005): *Process for imparting and enhancement of colours in gemstone minerals and gemstone minerals obtained thereby*. US 6,872,422 B2
20. Anonymous (2003): *Verfahren zur Behandlung von Edelsteinen*. DE 102 15 141 A1
21. Balitsky, V.S., Balitskaya, L.V., Volkov, V.T. (2003): *Method for coloring of natural and artificial jewelry stones*. RU 2 215 454 C1 [in Russian]
22. Balitsky, V.S., Balitskaya, L.V. (2003): *Method for coloring of natural and artificial jewelry stones*. RU 2 215 455 C1 [in Russian]
23. Starcke, S.F., Kearnes, R.H., Bennet, K.E. (2004): *Coatings for gemstones and other decorative objects*. US 2004/0083759 A1

Patent documents

1. Rogers, D.Z. (1996): *Novel gemstones and decorative objects comprising a substrate and an optical interference film*. WO 96/06961 A1
2. Rogers, D.Z. (2001): *Gemstones and decorative objects comprising a substrate and an optical interference film*. US 6,197,428 B1
3. Pollak, R. (1998): *Method for enhancing the color of minerals useful as gemstones*. WO 98/48944 A1
4. Pollak, R. (1999): *Method for enhancing the color of minerals useful as gemstones*. US 5,888,918
5. Pollak, R. (2002): *Method for enhancing the color of minerals useful as gemstones*. US 6,376,031 B1
6. Pollak, R. (2002): *Method for enhancing the color of minerals useful as gemstones*. US 2002/0174682 A1
7. Pollak, R. (2003): *Method for enhancing the color of minerals useful as gemstones*. EP 1 017 504 B1
8. Pollak, R. (2004): *Verfahren zur Verstärkung der Farben von Mineralen, die als Edelsteine benutzt werden*. DE 698 17 380 T2
9. Starcke, S.F., Kearnes, R.H., Bennet, K.E., Edmonson, D.A. (1998): *Method of improving the color of transparent materials*. US 5,853,826

Gem minerals from the Saranovskoye chromite deposit, western Urals

Ernst M. Spiridonov¹, Maria S. Alferova¹,
Talgat G. Fattykhov²

1. Geology Department, Moscow State University, Moscow, Russia,
Email alferova@geol.msu.ru
2. Saranovky Mine, Sarany, Russia

Abstract: Gem-quality minerals, including uvarovite, Cr-grossular and Cr-titanite, associated with the Saranovskoye chromite deposit, northern Urals, are described. The geology and mineralogy of the deposit indicates its formation following a well-known cycle of low-grade metamorphic processes and hydrothermal activity.

Keywords: 'alexandrite' effect, Cr-amesite, Cr-grossular, Cr-titanite, low grade metamorphism cycle, uvarovite



Introduction

Many gem-quality minerals and ornamental stones are formed in rocks which have undergone low grades of metamorphism. These include agates, datolite, natrolite and prehnite in the zeolite facies of metamorphism; powellite, jasper, xonotlite, grossular and hydrogrossular (including Transvaal 'jade'), andradite, diopside, vesuvianite (including californite), amethyst, titanite (sphene) in the prehnite-pumpellyite facies of metamorphism; and demantoid in the pumpellyite-actinolite facies (Spiridonov, 1998). The temperatures and pressures of formation of the different

facies are: zeolite facies 150-290°C, 0.5-4kb; and prehnite-pumpellyite facies 250-330°C, 1.5-7kb (Coombs *et al.*, 1959; Cho *et al.*, 1986; Philpotts, 1990; Frey and Robinson, 1999; Spiridonov *et al.*, 2000). Due to the fluid-dominant character of the low-grade metamorphism (Fyfe *et al.*, 1981), the rocks at the Saranovskoye chromite deposit contain alpine-type veins (Vertushkov and Kobyashev, 1975) with emerald-green uvarovite crystals (Hess, 1832; Ivanov, 1997), Cr-titanite (Ivanov, 1979), violet Cr-amesite (Zimin, 1939) and ruby-red Cr-diaspore – 'saranite' (Fersman, 1954).

Materials and methods

All of the samples in this study were collected from the mine by T.G. Fattykhov over a 30 year period and, over the last 10 years, by E.M. Spiridonov. This systematic collection is representative of the full range of levels at the deposit, from the lower horizons at a depth of 300 m to the surface.

Optical and electron microscopy methods were used to investigate and distinguish minerals and document their optical and internal features. More than 200 samples were analysed using electron microprobe analysis (EMPA) and scanning electron microscope with energy-dispersive X-ray spectrometer (SEM-EDS). Analyses were performed on different colour zones, mineral assemblages and mineral inclusions. X-ray diffraction (XRD) was used to determine mixed-layered minerals and pumpellyite group minerals. For gem-quality minerals, standard gemmological instrumentation was used to record optical character, pleochroism, colour (using standards in GemSet based on Munsell colour theory), optical transmission spectra and reaction to ultraviolet radiation (365 nm long-wave, 254 nm short-wave). Specific gravity was determined by hydrostatic weighing. The description of OH-bearing garnets is based on the nomenclature of Passaglia and Rinaldi (1983) and chlorite group minerals are named after Strunz (2002) and, where refinements were needed, after Hey (1954).

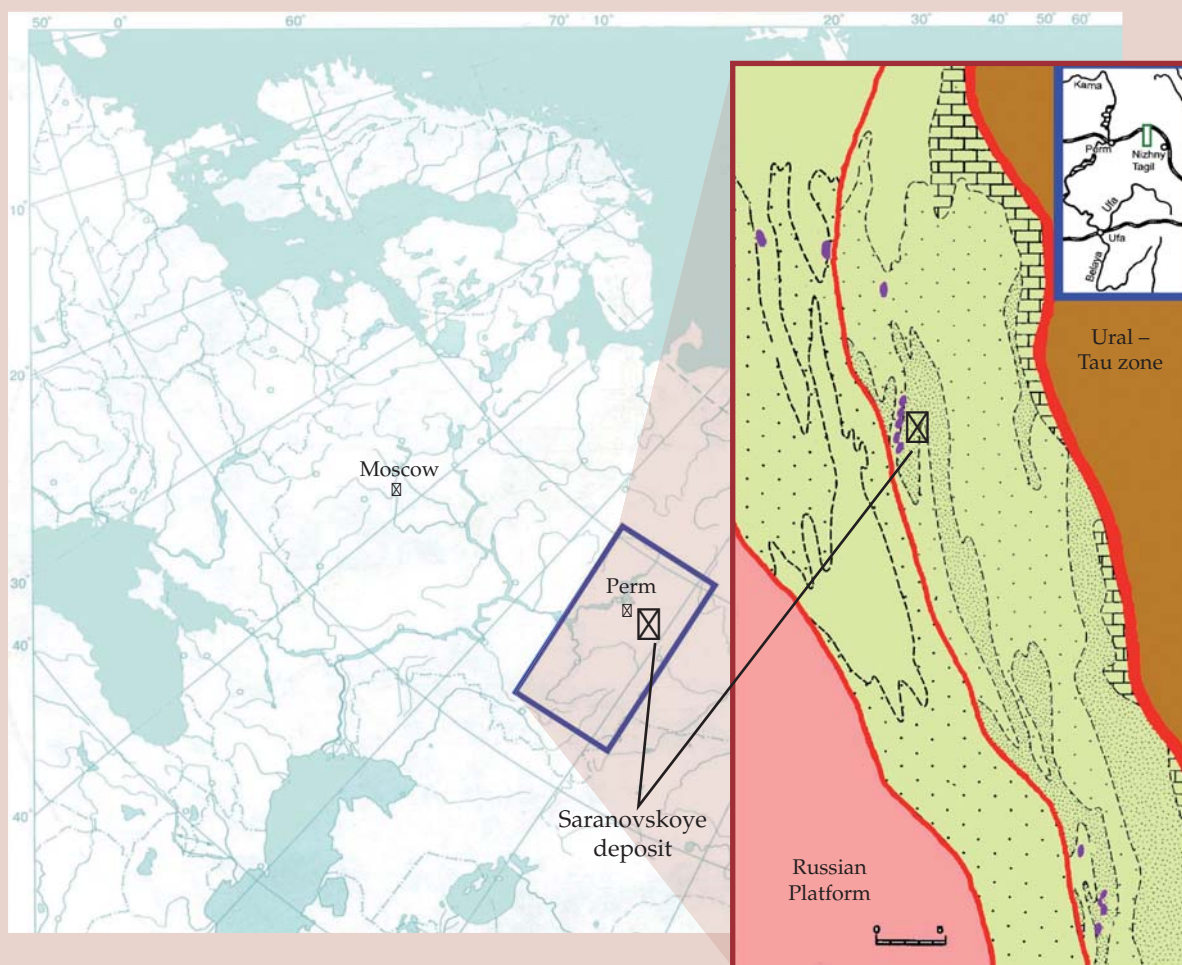


Figure 1: Geographical and geological position of the Saranovskoye chromitiferous belt.

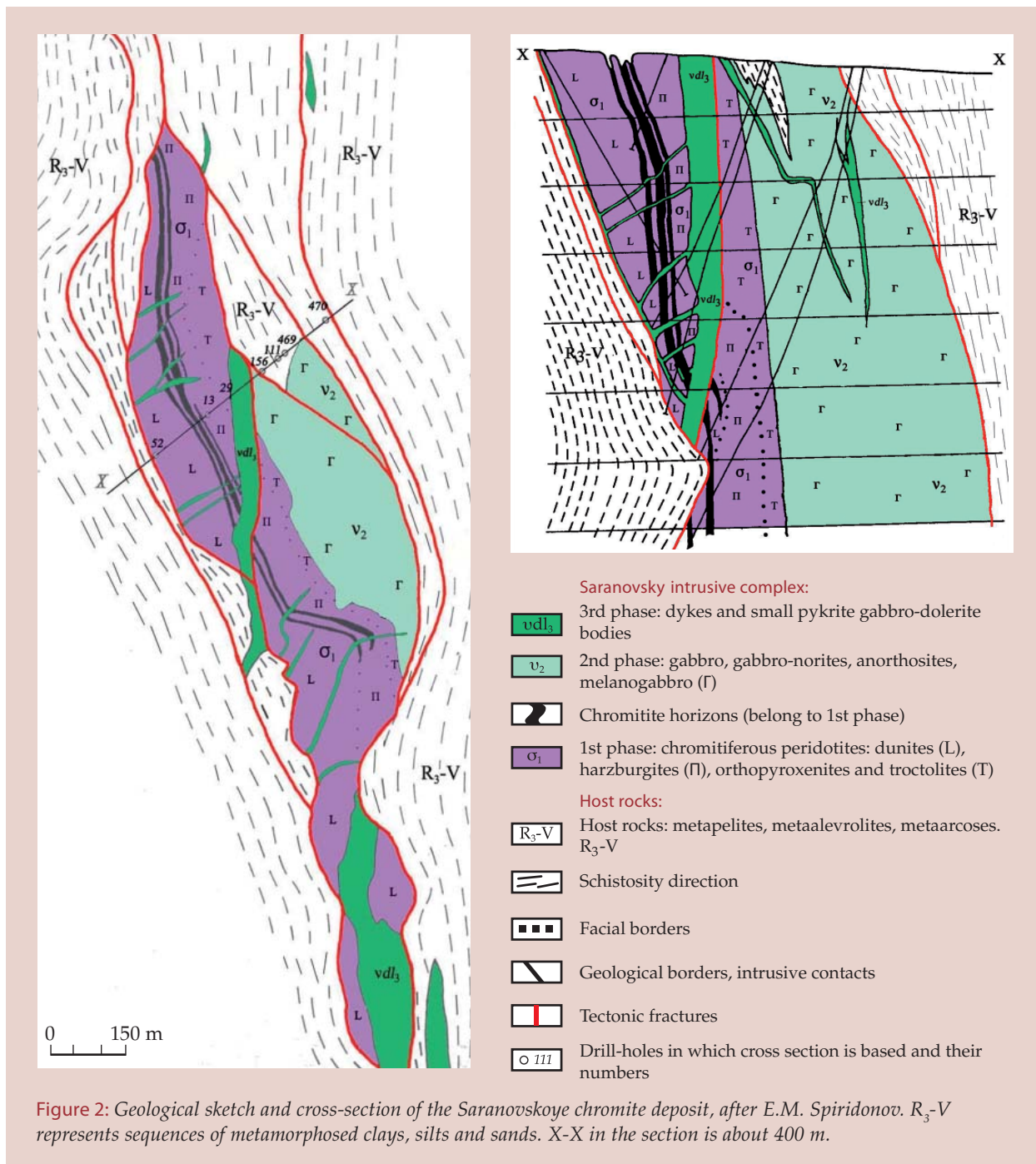
Geology

The Saranovskoye chromite mine is located in the Perm' region, 98 miles NW from Perm' city, on the north-western slopes of the Urals (Figure 1), and at the time of writing (2005) is the only industrial chromite mine in Russia. From its opening in 1889, it was mined open-cast, but now extraction is mainly from underground.

The ore is recovered from up to 30 chromitite horizons, 0.5-14 m thick, located in Precambrian dunites and harzburgites

(olivine-pyroxene rocks) of the Saranovsky massif. These ultrabasic rocks are crossed by gabbro and gabbro-dolerite bodies and a number of dolerite and picrite dykes (Figure 2) (Ivanov, 1997). The gabbro-dolerites contain stratified sulphide blebs and measurement of the details of their stratification allowed reconstruction of the original flat bedding of the chromitiferous dunite-harzburgite massif.

Since their formation, the ultrabasic rocks have, together with siliceous and carbonate rocks, been folded and metamorphosed in



Paleozoic time and many units are near-vertical. They have also been overthrust by crystal blocks of considerable thickness which caused local high pressure-low temperature metamorphism. This mixture comprises the Saranovsky massif and lies on the western slopes of the Ural Mountains. Surrounding the massif, at the edge of the Russian platform, are many varieties of siliceous schists, some of which contain pyrite.

The low grade metamorphism

Minerals of the pumpellyite group and diaspore are widely developed in all the rocks associated with the Saranovskoye chromite deposit and it may be concluded that the grade of metamorphism did not exceed that of the prehnite-pumpellyite facies. The following stages of the low-grade metamorphism have been established:

- First stage – zeolite facies to prehnite-pumpellyite facies of moderate pressure;
- Second stage – prehnite-pumpellyite facies of high pressure (330-340°C and 6-6.5 kb, based on the epidote-

pumpellyite thermobarometer of T.Arai (Tiriumi and Arai, 1989);

- Third stage – prehnite-pumpellyite facies of higher pressure;
- Fourth stage – prehnite-pumpellyite facies of moderate pressure (~3 kb);
- Fifth stage – zeolite facies.

In general, this trend corresponds to the standard 'Perchuk's loop' (Perchuk, 1983).

The intensity of this low grade metamorphism is extremely uneven.

Magnesiochromite in the original ultrabasic rocks was first locally replaced by chromite and then by ferrian chromite and chromian magnetite, which were later replaced by Cr-containing gem minerals (*Figure 3*). Cr-containing gem minerals form crusts on the sides of carbonate alpine-type veins.

Uvarovite and Cr-grossular were formed as a result of the second stage of metamorphism; at the third stage, Cr-amesite and Cr-diaspore (both with an alexandrite effect) were formed and gem-quality Cr-titanite formed at both the third and fourth stages. Cr-grossular, Cr-amesite, Cr-diaspore and Cr-titanite usually occur near the metachromitite-metabasic rock contact.

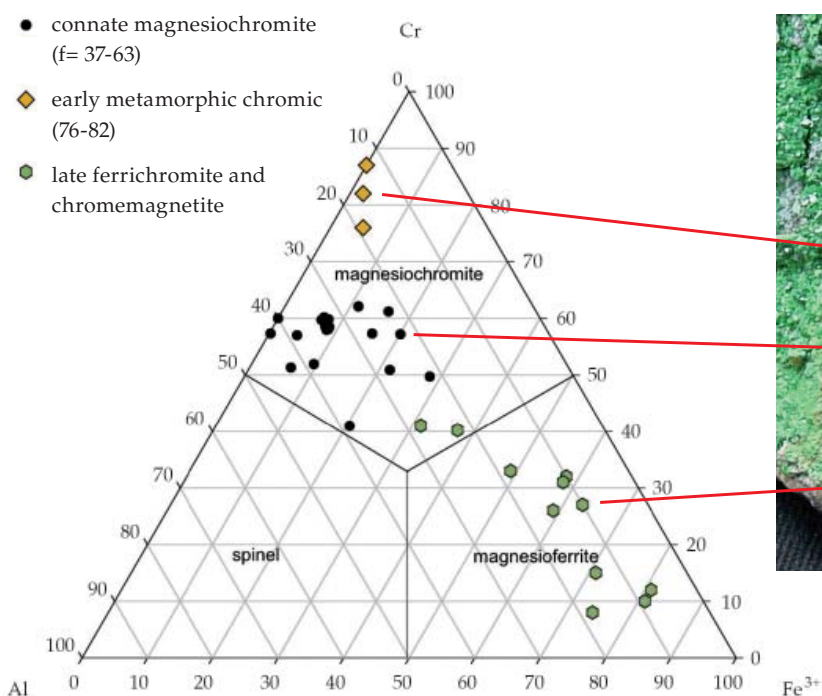


Figure 3: Successive replacement of magnesiochromite by chromite and uvarovite is indicated by the crust of green uvarovite crystals and the analyses of opaque minerals in the grey ultrabasic rock. Image size 8 cm. Photo by M.S. Alferova.

First stage

Lizardite is widespread in meta-ultrabasic rocks of the first stage. It may also be found as separate relic nests among brucite-antigorite serpentinites of the second stage.

Second stage – the main, ‘green’ stage

Here brucite-antigorite and antigorite serpentinites, metachromitites, metagabbro, metasediments, including rodingites are widespread. Among these there are many alpine-type veins which contain parallel-columnar aggregates of crystals, among which are the following associations:

- quartz (opaque crystals or clear rock crystal up to 13 cm long) ± albite ± ankerite ± calcite ± stilpnomelane (enriched in Ba) ± fengite (among metasediments);
- carbonate + epidote-clinozoisite ± ferroan chlorite (‘corundophilite’ and ‘ripidolite’ according to Hey (1954)) ± albite ± magnetite ± titanite (or rutile) ± Fe-Cu sulphides (among metabasic rocks);
- antigorite ± carbonate + brucite ± magnetite (among metaultrabasic rocks);
- calcite or dolomite + green clinocllore (‘corundophilite’ of Hey (1954)), including 3-11 wt.% Cr_2O_3 , + titanite ± Cr-containing garnet (grossular, hydrogrossular, uvarovite) ± Cr-pumpellyite (up to shuiskite – Ivanov *et al.*, 1981), and among metachromitites, calcite + Cr-chlorite + Cr-fengite (fuchsite).

Chromium-containing derivatives from metabasic rocks

Fine-grained aggregates of optically anisotropic Cr-garnet have almost completely replaced metachromitites near contacts of chromitites and basic dykes in some zones of crushing and mylonitisation and along glide planes (Figures 4, 5). They form continuous crusts, groups of crystals on metachromitites, commonly with chromian clinocllore (‘corundophilite’ of Hey (1954)), opaque Cr-titanite (Figure 6), shuiskite, Cr-pumpellyite and apatite. Gem-quality uvarovite and Cr-grossular of a deep emerald-green colour



Figure 4: Tectonic glide plane in metachromitite (a), and uvarovite overgrown by late calcite crystals (b). Sample sizes: left – 15 cm, right – 7 cm. Photos by M.S. Alferova.

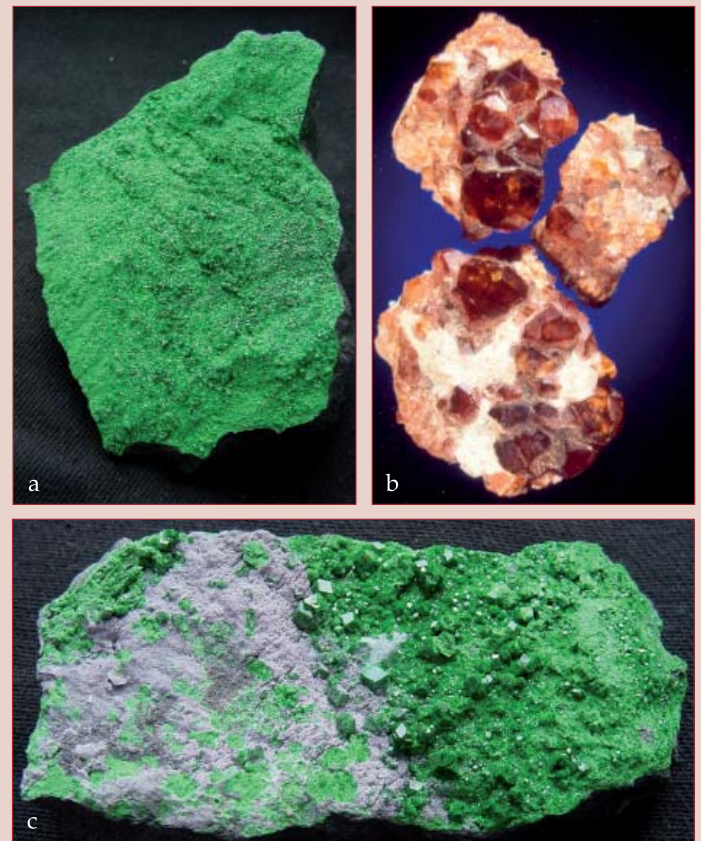


Figure 5: Continuous uvarovite aggregate (20 cm) (a); red grossular crystals (largest crystal 25 mm) with albite (b); uvarovite crystals up to 7 mm across (c). Photos by M.S. Alferova.

are minerals which developed relatively late in the second stage. They form transparent rhombic dodecahedra up to 12 mm across. The green garnets lie in the composition range covered by the end-members grossular,

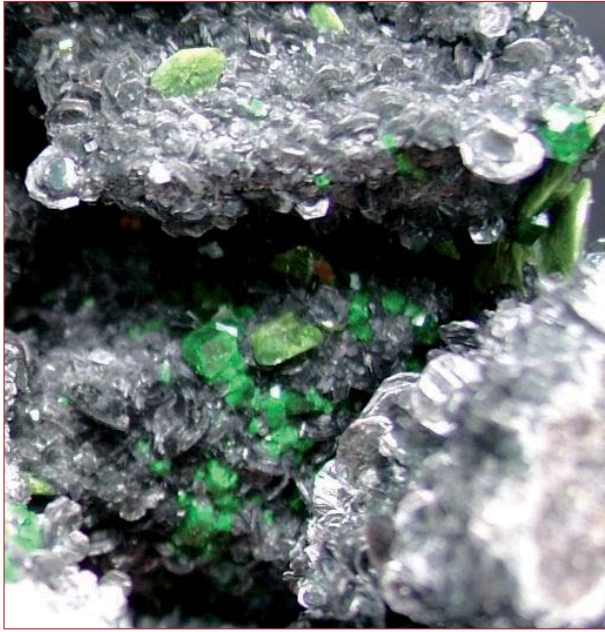


Figure 6: Transparent uvarovite (green) associated with opaque Cr-titanite (pale-green) and Cr-clinochlore ('corundophilite') (silver-grey). Specimen 6 cm across. Photo by M.S. Alferova.

andradite and uvarovite and representative analyses are shown in Table I. They contain 17-92% of uvarovite end-member, up to 2 wt.% TiO₂, ~0.5 wt.% Fe₂O₃ and traces of Zn, Ni, V, Cu, Mg and Mn. In the marginal

parts of the Saranovsky massif uvarovite is often associated with quartz which forms overgrowths on the rhombic-dodecahedral crystal edges. At that time the Saranovsky massif was probably an 'open' system with Si available from hydrothermal fluids. Uvarovite and Cr-grossular show fine oscillatory zoning similar to that described in Cr-garnets from rodingites by Mogessie and Rammlmair (1994).

Cr-titanite of this second stage occurs in euhedral opaque pale-green crystals and contains 0.3-1 wt. % Cr₂O₃ and up to 0.5% Al; heterovalent isomorphism Ti + O ↔ Al, Cr + OH is typical as noted by Hammer *et al.* (1996).

Chrome-free derivatives from metabasic rocks and metasediments

Some fracture zones through the rodingites contain grossular (hessonite) in cherry-red to orange crystals up to 35 mm across (Figure 5). The grossular contains iron with 4-17% of the andradite end-member, up to 3 wt.% TiO₂ and up to 0.1 wt.% Cr₂O₃. Transparent crystals of quartz (up to 15 cm) and albite (up to 3 cm) commonly occur in the metasediments.

At the end of the second stage CO₂ fugacity

Table I: Chemical compositions of uvarovite (1-3), Al-uvarovite (4-5), Cr-grossular (6), Fe-grossular (7-9) from the Saranovskoye chromite deposit

wt. %	1	2	3	4	5	6	7	8	9
SiO ₂	34.13	35.69	36.46	36.22	36.56	36.37	39.22	39.27	39.30
TiO ₂	1.53	0.69	0.77	0.22	0.36	0.72	0.22	0.14	0.19
Al ₂ O ₃	1.13	3.47	5.07	7.55	7.94	10.09	19.41	18.26	18.31
Fe ₂ O ₃	0.58	0.29	b.d.	1.23	0.29	2.01	3.37	4.70	4.69
V ₂ O ₅	0.35	b.d.	0.13	b.d.	b.d.	0.45	b.d.	b.d.	b.d.
Cr ₂ O ₃	26.13	24.03	22.57	18.87	18.49	13.92	0.07	0.20	b.d.
FeO	n.d.	n.d.	0.56	n.d.	n.d.	n.d.	2.87	1.87	2.62
MnO	b.d.	b.d.	b.d.	0.05	0.10	0.31	2.56	2.82	2.08
MgO	0.08	0.03	0.05	0.06	b.d.	0.15	0.10	0.11	traces
CaO	33.46	33.18	33.97	33.79	34.22	33.62	32.26	32.70	32.87
ZnO	n.d.	n.d.	n.d.	n.d.	n.d.	0.35	0.15	b.d.	0.35
NiO	b.d.	b.d.	b.d.	b.d.	b.d.	b.d.	traces	0.24	b.d.
Total	97.39	97.38	99.58	97.99	97.96	97.99	100.23	100.31	100.41

Analyst I.M. Kulikova, using a Camebax SX50 electron microprobe

b.d. = below detection

n.d. = not determined

increased, as titanite became unstable and was replaced by rutile (Philpotts, 1990). Rutile forms prismatic crystals up to 40 x 6 x 6 mm and needle-like crystals up to 120 x 0.5 x 0.5 mm; it also occurs as felt-like aggregates.

Third stage – ‘violet’ stage

Mineralization was predated by another phase of movement and crushing. Typical of the third stage are silica-deficient minerals such as amesite, perovskite, diaspore, Cr-hydrogarnet and brucite. Thus, at this stage the Saranovsky massif appears to have been a relatively closed system, not open to Si-bearing fluids.

The main mineral of that stage is violet-lilac Cr-bearing (1-4 wt.% Cr₂O₃) amesite showing a pearly lustre and a strong alexandrite effect (Figure 7; see Table II, 1-2). Cr-amesite is developed in metamorphic-hydrothermal calcite veins in contact with metachromitites. Many of the Cr-amesite crystals are polychromatic, the bases of the

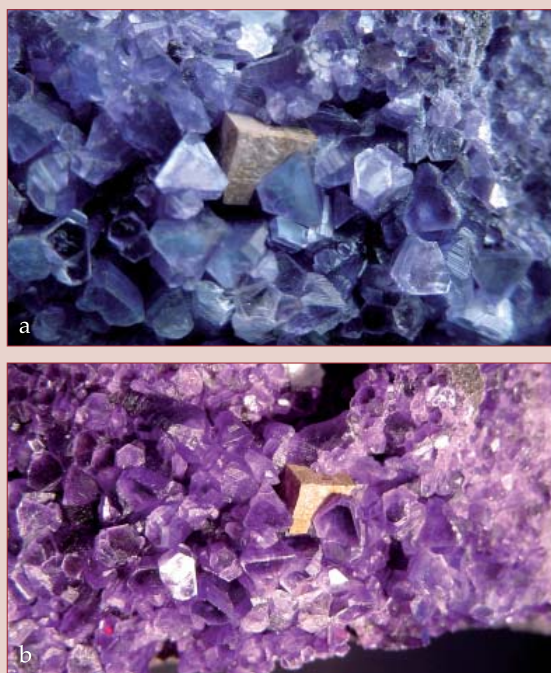


Figure 7: Cr-amesite showing a strong ‘alexandrite’ effect. (a) in daylight, (b) in electric (tungsten) light. Perovskite cubic crystal edge size 5 mm. Photo by M.S. Alferova.

Table II: Chemical compositions of Cr-amesite (1-2), Cr-diaspore (3-5), titanite (6-7) and Cr-clinochlore (‘kammererite’) (8-9)

wt.%	1	2	3	4	5	6	7	8	9
SiO ₂	20.00	21.37	n.d.	n.d.	n.d.	30.41	30.50	30.13	33.58
Nb ₂ O ₅	n.d.	n.d.	n.d.	n.d.	n.d.	0.14	0.19	n.d.	n.d.
TiO ₂	b.d.	b.d.	0.35	0.19	0.33	38.56	38.96	b.d.	b.d.
Al ₂ O ₃	33.88	34.81	78.69	77.95	77.28	0.02	0.28	14.15	11.61
Cr ₂ O ₃	0.87	1.88	3.71	4.42	5.49	0.98	0.86	8.97	4.66
Fe ₂ O ₃	n.d.	n.d.	0.11	0.15	0.13	n.d.	n.d.	n.d.	n.d.
V ₂ O ₃	0.03	b.d.	0.52	0.18	0.19	0.54	0.45	0.13	0.11
FeO	0.70	0.89	b.d.	b.d.	b.d.	0.40	0.12	0.87	2.39
MnO	0.01	b.d.	n.d.	n.d.	n.d.	0.05	0.06	0.12	traces
MgO	26.34	27.52	n.d.	n.d.	n.d.	b.d.	0.01	33.15	35.02
CaO	n.d.	n.d.	n.d.	n.d.	n.d.	28.06	28.30	n.d.	n.d.
NiO	0.31	0.79	n.d.	n.d.	n.d.	b.d.	b.d.	b.d.	b.d.
F	0.07	b.d.	n.d.	n.d.	n.d.	0.25	0.21	n.d.	n.d.
Cl	n.d.	n.d.	n.d.	n.d.	n.d.	traces	b.d.	n.d.	n.d.
H ₂ O*	n.d.	n.d.	n.d.	n.d.	n.d.	0.09	0.06	n.d.	n.d.
Total	82.21	87.26	83.38	82.89	83.42	99.50	100.00	87.52	87.37

Analyst N.N. Kononkova, using a Camebax SX50 electron microprobe; H₂O* – calculated
 b.d. = below detection
 n.d. = not determined



Figure 8: Cr-diaspore of lavender and lilac colours together with Cr-amesite (greyish-violet) and hydrogrossular (pale-green). Specimen 8 cm across. Photo by M.S. Alferova.



Figure 9: Gem-quality Cr-titanite crystal (green) associated with Cr-amesite (grey) and calcite (white). Titanite is 9 mm across. Photo by M.S. Alferova.

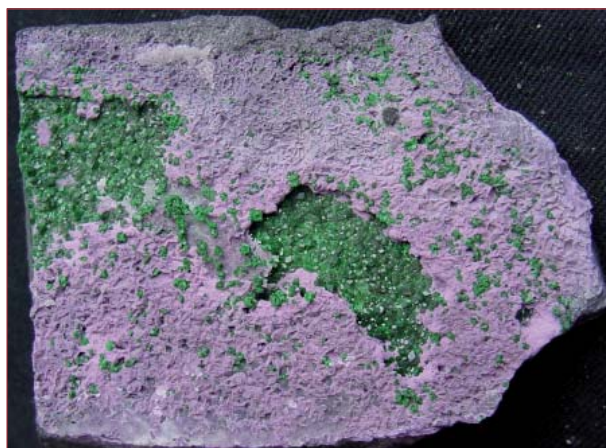


Figure 10: Lilac chromian clinochlore ('kammererite') with uvarovite. Specimen size 17 cm. Photo by M.S. Alferova.

pillar-like crystals being enriched in Cr and of a deep lilac colour, but upwards towards the carbonates the colour pales as the Cr content decreases, eventually becoming colourless. Amesite crystals with low Cr content are typically split vermicular crystals.

In the contact zones of metachromitites and metabasites, plates of lavender, lilac or red Cr-diaspore (Figure 8) together with Cr-amesite and Cr-hibschite are commonly developed. The plate sizes are up to 8 cm across. Diaspore contains up to 5 wt.% Cr₂O₃ (see Table II, 3-5), and shows an alexandrite effect.

Cr-titanite is the latest gem-quality mineral of this stage (Figure 9). It forms as pseudomorphs after perovskite, overgrowths on columnar Cr-amesite crystals or on chromitites along calcite vein contacts. In these veins Cr-titanite forms translucent deep-green tabular crystals of up to 35–22

14 mm in size. In cavities of dissolution it forms intergrowths with tabular Cr-amesite crystals and also forms transparent crystals which may be almost isometric, tabular or variously twinned. Sizes are up to 45–25–3 mm exhibiting superb emerald-greens of varying intensity to light-green, often with a golden tint. Cr-titanite is biaxial and shows strong pleochroism from apple-green (across {100}) to olive-green (along {100}). Gem-quality crystals contain 0.7-1.0 wt.% Cr₂O₃ and up to 0.25 wt.% F, with traces of Al, Fe, Mg, V, Zn, Ni, Cu and Cl (see Table II, 6-7); a typical formula is (Mg_{0.01}Fe_{0.02}Ca_{0.97})_{1.00}(Ti_{0.90}Al_{0.04}Cr_{0.02})_{0.96}[Si_{1.02}O₄][O_{0.88}(OH)_{0.12}]_{1.00}.

Fourth stage – 'pink' stage

This is a stage of lower temperatures and pressures, characterised by yellowish-green lizardite which occur as pockets, bands or blocks, replacing antigorite serpentinites. In peridotites and chromitites aluminian magnesiochromite is extensively replaced by chromian magnetite, which in turn is replaced by brightly coloured red and pink-lilac chromian clinochlore ('kammererite' of Hey (1954)) (Figure 10). In the clinochlore structure Cr fills both octahedral and

tetrahedral positions giving rise to its colour (Lapham, 1958). Chemically, chromian clinocllore from the Saranovsky massif contains between 6 and 14 wt.% Cr_2O_3 (see Table II, 8-9). Areas of chromian clinocllore crusts on metachromitites may be up to several square metres, and not infrequently there are overgrowths of calcite, small plates of apatite and Cr-titanite crystals.

The most significant products of the fourth stage are perfect Cr-titanite twins (Figure 11). They are emerald green and are of various habits from blade-like (1-3 mm thick) to plate-like (in fractions of a millimetre). The crystals and twins are found in cavities of dissolution and late calcite veins.

Later fourth stage minerals include ilmenite and redledgeite; these are products of titanite replacement. Ilmenite forms flattened crystals up to 7 mm across, but is not pure – rather it is an almost equal mixture of the Mg, Mn and Fe end-members geikielite, pyrophanite and ilmenite. The most interesting mineral in alpine-type veins is redledgeite ($\text{BaCr}_2\text{Ti}_6\text{O}_6 \cdot \text{H}_2\text{O}$), which derives its Cr, Ti and Ba from metachromitites, metabasites and metasediments respectively.

At the end of the fourth stage CO_2 fugacity increased and titanite was replaced further by polycrystalline aggregates of quartz, calcite and anatase ($\text{CaTiSiO}_5 + \text{CO}_2 \rightarrow \text{CaCO}_3 + \text{SiO}_2 + \text{TiO}_2$) which kept the habit of the titanite and formed pseudomorphs. Polycrystalline pseudomorphs of kassite $\text{CaTi}_2\text{O}_4(\text{OH})_2$ were also formed. Ilmenite is replaced by needle-like intergrowths of rutile or polycrystalline aggregates of anatase. Where titanite and ilmenite have been completely replaced, the result is commonly a Cr-clinocllore crust with many small flattened light-brown anatase crystals.

Fifth stage

The lowest-temperature products of low-grade metamorphism are developed in separate blocks, strips and pockets among earlier rocks and minerals, extensively replacing them. Antigorite and lizardite in



Figure 11: Perfect Cr-titanite twins (up to 14 mm across) (green) and calcite crystals (white) on a matrix of Cr-clinocllore (pale-grey). Photo by M.S. Alferova.

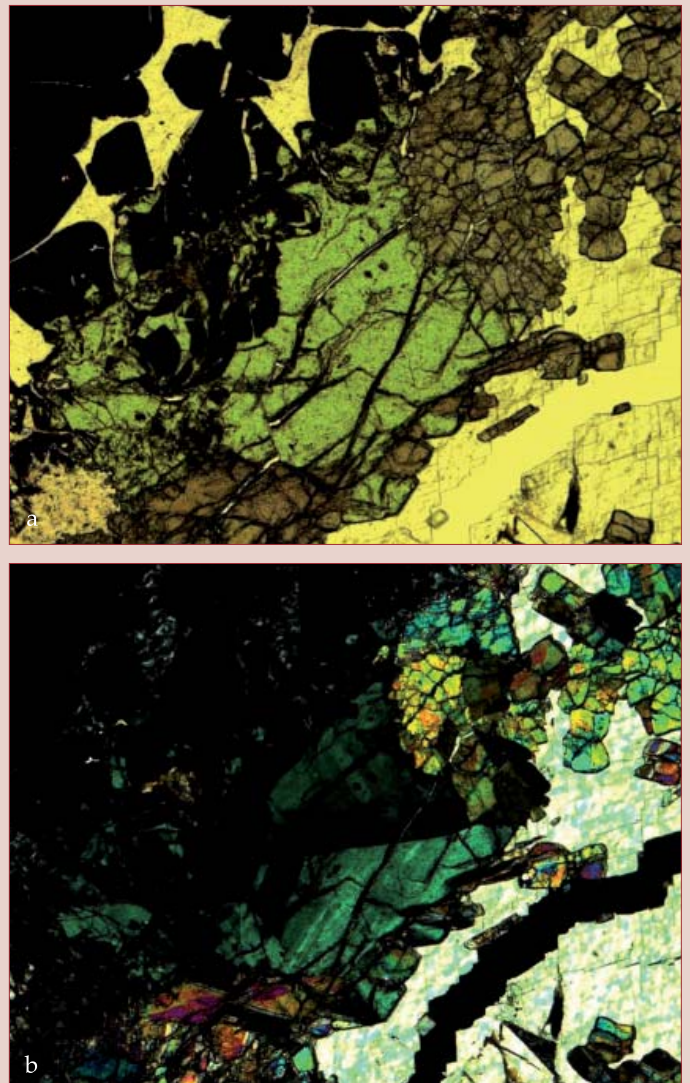


Figure 12: (a) Thin section of uvarovite (green) and shuiskite (brown) in plane-polarized light. (b) In cross-polarized light, the garnet shows transmission in the lower part indicating anisotropy. Thin section 9 mm across.

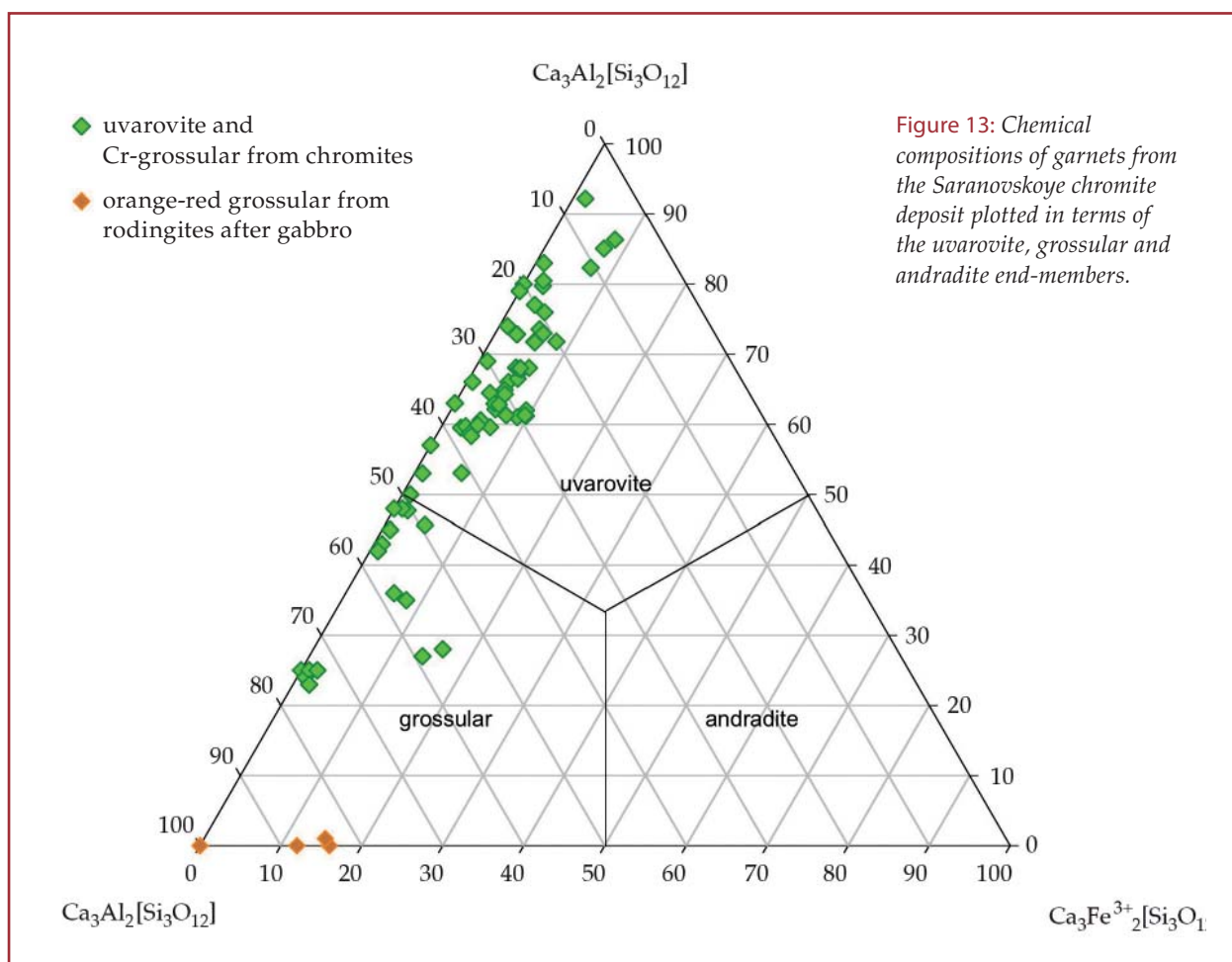


Figure 13: Chemical compositions of garnets from the Saranovskoye chromite deposit plotted in terms of the uvarovite, grossular and andradite end-members.

serpentinites are replaced by fine-grained hydrotalcite, and chromite may be replaced by pink and pink-violet stichtite. Granular calcite aggregates may be dissolved and replaced by calcite crystals up to 40 cm long either singly or in groups and associated with the calcite in places are sulphides, clay minerals and pale-green titanite.

Gem minerals

Uvarovite and Cr-grossular. The rough crystals are predominantly rhombic dodecahedra, up to 8-12 mm across, show no evidence of dissolution on their surfaces and commonly form crusts of intergrown crystals on chromite surfaces. Many garnet crystals are transparent and range from a 'pure' green uvarovite (G6/4, G7/4, G5/5 using the Munsell notation) to pale-green Cr-grossular (G5/3). Some show strong oscillatory colour and optical zoning in thin section and others display optical anisotropy (Figure 12); this is due to ordering of Al and Cr in the structure

(Ivanova *et al.*, 1998). Representative analyses of garnets from the Saranovskoye deposit are given in Table I, and more are plotted in Figure 13 to indicate the range for green garnets which may contain from 17% up to 92% of the uvarovite end-member. These Urals garnets have refractive indices of 1.740-1.870 (Anderson, 1996), birefringence up to 0.008, (measured using Michel-Levy interference colour chart for thin sections), a specific gravity range of 3.41-3.65 and show no reaction to ultraviolet radiation. Normally transparent uvarovite crystals do not contain inclusions but many semi-transparent crystals contain relic chromite, fluid inclusions and cracks. Uvarovite is generally too small for cutting as individual stones, but small sparkling mats of uncut crystal aggregates on matrix are often set in jewellery. Larger pieces grace the collections of many museums.

Fe-grossular (hessonite) forms tetragon-trioctahedral (trapezohedral) crystals up to 35 mm across. Crystals are transparent, from



Figure 14: Gem Cr-titanite flat twin. Photo by M.S. Alferova.

cherry-red (O5/3, yO4/5) to orange (oY5/5, Y5/5, Oy4/5) (Figure 5b) and, although rare, are readily used for cutting. Table I, columns 7-9, contain representative compositions.

Cr-titanite is the gem symbol of the Saranovskoye deposit (Figure 14). Typical habits show {100}, {001}, {111}, {102} and {110} faces, with twinning on (100). Gem-quality

crystals and many twins are transparent, variously green (slyG8/3 to slyG6/3), and with strong pleochroism (Figure 15). Typical compositions are given in Table II, columns 6-7, and no zoning was found. The green colour is due to the chromium content of up to 0.98 wt.%; vanadium (up to 0.54 wt.%) probably contributes a bluish tint to the green colour. The chromophore pair $\text{Fe}^{2+}\text{-Fe}^{3+}$ is absent. Gem-quality Cr-titanite contains fluorine up to 0.25 wt.% in contrast to earlier Cr-titanite which is opaque and fluorine-free. Refractive indices of gem Cr-titanite exceed 1.8 and range from 1.900 to 2.034, dispersion 0.022-0.035 (Anderson, 1996), specific gravity 3.52 ± 0.02 ; no reaction to ultraviolet radiation was seen. Inclusions are represented by amesite, chlorite, clinocllore and fluid inclusions. Due to its relatively low hardness (5-5.5 on the Mohs scale) Cr-titanite is seldom used in jewellery, but its brilliance is comparable with the best demantoid.

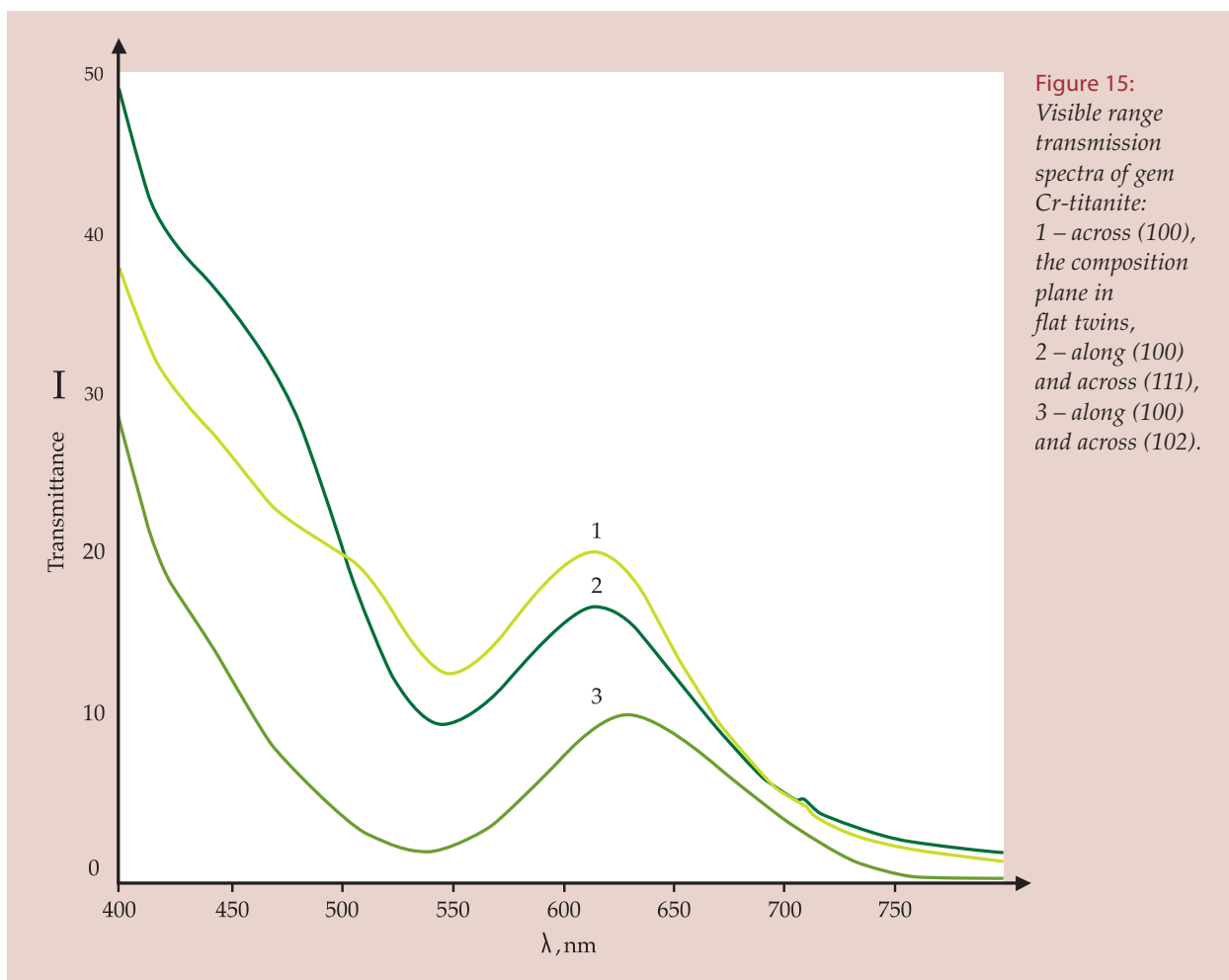


Figure 15: Visible range transmission spectra of gem Cr-titanite: 1 – across (100), the composition plane in flat twins, 2 – along (100) and across (111), 3 – along (100) and across (102).

Conclusion

In the Saranovskoye chromite deposit there is a wide range of Cr-rich minerals, many of which have potential as gems and ornamental stones. Such diversity was generated by a low-grade metamorphism cycle which caused the chromium to become mobile and enter such minerals as uvarovite, Cr-titanite, shuiskite, amesite and diaspore. Some areas in and around the massif contain no chromium but nevertheless yield cherry grossular, rock crystal and jewellery-grade albite.

Acknowledgements

Oleg K. Ivanov is gratefully thanked for assistance, I.M. Kulikova and N.N. Kononkova for providing microprobe analyses, and A.V. Vasil'ev for providing optical spectra. We thank B. Jackson for revision of the translated text. The study was supported by RFBR grant (04-05-64152).

References

- Anderson B.W., 1996. *Gem testing*. World of Stone, Moscow, p. 455 (in Russian)
- Cho, M., Liou, J.G., and Maruyama, S., 1986. Transition from the zeolite to prehnite-pumpellyite facies in the Karmutsen metabasites, Vancouver Island, British Columbia. *J. Petrol.*, 27, 467-94
- Coombs, D.S., Ellis, A.D., Fyfe, W.S., and Taylor, A.M., 1959. The zeolite facies, with comments on the interpretation of hydrothermal syntheses. *Geochim. Cosmochim. Acta*, 17, 53-107
- Fersman, A.E., 1954. *History of stone*. AN SSSR, Moscow, 1. 371pp (in Russian)
- Frey, M., and Robinson, D. (eds), 1999. *Low Grade Metamorphism*. Blackwells Science, Oxford, 313 pp
- Fyfe, W.S., Price, N., and Thompson, A.B., 1981. *Fluids in Earth crust*. Mir., Moscow, 436 pp (in Russian)
- Hammer, V.M.F., Beran, A., Endisch, D., and Rauch, F., 1996. OH concentrations in natural titanites determined by FTIR spectroscopy and nuclear reaction analysis. *Eur. J. Mineral.*, 8(2), 281-8
- Hess, H., 1832. Über der Uwarowit, ein neue Mineralspecies. *Pogg. Ann. Phys. Chem.*, 24, 338-9
- Hey, M.H., 1954. A new review of the chlorites. *Mineral. Mag.*, 30, 277-92
- Ivanov, O.K., 1979. About chrome-containing sphene. *Zap. VMO*, 108, 600-1 (in Russian)
- Ivanov, O.K., 1997. *Mineral associations of Saranovskoye chromite deposit*. Yekaterinburg: UGGGA. 123pp (in Russian)
- Ivanov, O.K., Arkhangel'skaya V.A., and Miroshnikova L.D., 1981. Shuiskite – chrome analogue of pumpellyite from Bisersky deposit, Urals. *Zap. VMO*, 110, 508-12 (in Russian)
- Ivanova, T.I., Shtukenberg, A.G., Punin, Yu.O., Frank-Kamenetskaya, O.V. and Sokolov, P.B., 1998. On the complex zonality in grandite garnets and implications. *Mineral. Mag.*, 62(6), 857-68
- Lapham, D., 1958. Structural and chemical variation of chromian chlorites. *Amer. Mineral.*, 43, 921-56
- Mogessie, A., and Rammlmair, D., 1994. Occurrence of zoned uvarovite-grossular garnet in a rodingite from the Vumba Schist Belt, Botswana, Africa: implications for the origin of rodingites. *Mineral. Mag.*, 58(3), 375-86
- Passaglia, E., and Rinaldi, R., 1983. Katoite, a new mineral of the $\text{Ca}_3\text{Al}_2[\text{SiO}_4]_3$ - $\text{Ca}_3\text{Al}_2[(\text{OH})_4]_3$ series and new nomenclature for the hydrogrossular group minerals. *Bull. Mineral.*, 104, 605- 18
- Perchuk, L.L., 1983. Thermodynamic aspect of polymetamorphism. In: *Metamorphic zonality and metamorphic complexes*. Ed.: Zarikov, V.A., Nauka, Moscow, p. 21-37 (in Russian)
- Philpotts, A.R., 1990. *Principles of igneous and metamorphic petrology*. Prentice Hall, New Jersey, p. 498
- Spiridonov, E.M., 1998. Gemstone deposits of the former Soviet Union. *J. Gemmol.*, 26(2), 111-25
- Spiridonov, E.M., Ladygin, V.M., and Stepanov, V.K., 2000. *Metavolcanites of prehnite-pumpellyite and zeolite facies of trapp formation at Noril'sk region, Siberian platform*. MSU, Moscow, 212 pp (in Russian)
- Strunz, H., and Nickel, E.H., 2001. *Strunz Mineralogical Tables*. 9th edn. E. Schweizerbart'sche Verlagsbuchhandlung, Berlin and Stuttgart, 870 pp
- Tiriumi, M., and Arai, T., 1989. Metamorphism of the Izu-Tanzawa collision zone. *Tectonophysics*, 160, 293-303
- Vertushkov, G.N., and Kobyashev, Yu.L., 1975. Minerals of alpine-type veins from Magnitigorskoye and Saranovskoye deposits, Urals. *Transactions of Sverdlov. Mining Inst.*, 106, 135-7 (in Russian)
- Zimin, I.A., 1939. Chromeamesite from Saranovskoye chromite deposit. *Zap. VMO*, 2, 192-8 (in Russian)

Letters to the Editor

Iridescent colours of the abalone shell

The recent paper by T.L. Tan, D. Wong and P. Lee (*The Journal of Gemmology*, 29(7/8), 395-9) addresses the long-standing question of whether the iridescence of abalone and other shells may be due to diffraction from any evenly grooved two-dimensional, surface structure, a compact disk being a common example, or related to the well known multi-layered aragonite/conchiolin, three-dimensional, microstructure below the surface. Iridescence due to repeating internal structures is exemplified by polysynthetically twinned labradorite or precious opal, familiar to all gemmologists.

The research of Tan, Wong and Lee clearly demonstrates that a grating structure is present on the surface of the abalone they studied, as shown both by the diffraction given by the lasers and by the SEM illustrations. They then conclude that the iridescence is due to this grating structure. They certainly provide sufficient evidence that the iridescence may be due to diffraction from the surface structure. However, we do not believe that they provided conclusive evidence for diffraction as a cause of the abalone iridescence.

Consider the layered nature of the shell, alternating regularly between the harder aragonite tiles and the softer conchiolin. When the shell is polished we would expect that the conchiolin would undercut forming a rippled surface much as jade develops an 'orange peel' surface, and some banded agates reveal their bands by small undulations in the polished surface. Thus, it is not surprising to see the surface of the layered shell develop a grating-like structure when cut and polished. This appears to be what Tan, Wong and Lee have shown. With the presence of both a

layered microstructure below the surface and a grating structure at the surface, it remains to be demonstrated to what extent each of the optical structures may contribute to the observed iridescence.

Nassau (2001) in his discussion of biological coloration notes that the identification of structural colours can be difficult. He also states (p. 318): "*Many of the imputed biological diffraction grating colours have been shown on detailed study to originate in thin film interference; observation of a periodic grating structure is quite insufficient as evidence*" (emphasis ours). Yet this is the only evidence presented by Tan, Wong and Lee. Nassau (2001, p. 318) cites an example of butterfly wings where a grating can be observed under the microscope, but the naked eye only sees the iridescence due to thin-film interference. He also gives various ways to distinguish between colours based on interference or diffraction and most readers can easily test any shell material they may have by some of his criteria. The simplest is to observe the iridescent colours going between a direct light source such as an incandescent bulb indoors, to a very diffuse light source, such as outdoors on an overcast day. Your readers can compare a compact disk, a labradorite and opal cabochon, and a shell sample; in diffuse light iridescence due to a surface grating becomes very weak, while that due to internal layered structures remains strong. When we perform this test on a variety of shells the iridescence remains strong in diffuse light. Such observations lead us to conclude that internal layering as opposed to surface diffraction is the primary, but not necessarily the only, cause of iridescence in many shells.

Snow and Pring (2005) in their study of abalone attribute the colour to Bragg diffraction in the layered structure of the nacre. Additionally, they show by sputter coating the abalone surface with gold, which would preserve a surface grating, that the iridescence was mostly lost. Clearly showing that surface effects didn't contribute to the colour. Similar methods should be done on the abalone studied by Tan, Wong and Lee.

D.B. Hoover FGA
Springfield, MO, U.S.A.

Bear Williams CG
Jefferson City, MO, U.S.A.

Response from Dr T.L. Tan

The valuable comments and suggestions of D. B. Hoover and B. Williams are truly appreciated, and have prompted me and my co-authors to carry out further studies on the iridescent colours on the shell. These are discussed below.

Internal microscopic structure of the abalone shell by SEM

The structure of the abalone shell below its surface is examined at 3000x magnification using a scanning electron microscope (SEM). The micrograph of a cross-section of the shell reveals a regularly layered microstructure composed of nacreous aragonite platelets, separated by a thin layer of conchiolin. The thin conchiolin layers are not as obvious as the thicker aragonite layers. Preliminary measurements of the aragonite layers at various cross-sections of the shell give the thickness of the layer to be about 1.0 μm . Further measurements of the thickness of the layers will be accurately made and analysed.

Iridescent colours caused by Bragg diffraction in the layered structure

Due to the layered structure of the aragonite nacre, multilayer interference has been considered to be a possible cause of iridescence (Nassau, 2001). Furthermore, the stacks of identical layers can form a three-dimensional diffraction grating which can cause iridescent colours, in accordance with

Bragg's law (Nassau, 2001). As mentioned by Hoover and Williams, Snow and Pring (2005) had explained the blue-green iridescent colours in the abalone (*Haliotis iris*) shell using Bragg diffraction. In this abalone species, the thickness of the aragonite layer is 0.25 to 0.39 μm . They also studied two other species of abalone. The Bragg equation $n\lambda = 2d\sin\theta$ was used. We will attempt to explain the iridescent colours of the abalone (*Haliotis glabra*) shell of this work using the Bragg equation. Further experimental studies on the colours of the shell at various diffraction angles will be needed to better understand the mechanism of Bragg diffraction in the layered structure of the shell of this abalone species.

Contribution to iridescent colours by diffraction from surface grating structure

To understand the possibility of iridescent colours arising by surface diffraction from the grating structure of the shell, we will be coating a thin layer of gold using the sputtering method as done by Snow and Pring (2005), and as suggested by Hoover and Williams. The opaque gold layer would preserve the surface grating structure and prevent transmission of colours from the layered structure below the surface. However, gold has a strong yellow tint which may mask the iridescent colours. We will explore the use of platinum as a coating material.

Discussion

Hoover and Williams suggested that we look at the intensity of iridescent colours on the shell as it is moved from direct light to diffused light, and this experiment was conducted on a few abalone shell samples. We found that the iridescent colours remain unchanged under both types of light in agreement with that observed by Hoover and Williams. This shows that the internal layered structure contributes partly or significantly to the iridescent colours on this shell. In a study on abalone shell, Snow and Pring (2005) attributed the colours primarily to Bragg diffraction in the layered structure of the nacre. On the other hand, Liu, Shigley and Hurwit (1999) investigated the colours on the shell of the black-lipped

oyster and concluded that strong iridescent colours on the shell were caused mainly by surface diffraction from the regular reflection grating structure of the shell. It is obvious that the surface grating structure was the result of fine polishing of the shell which has an internal layered structure. Therefore the question of whether the iridescence shown by abalone shell or other shells may be caused by surface diffraction and/or multilayered Bragg diffraction or interference remains to be investigated.

We fully agree with the suggestion of Hoover and Williams to further investigate the contribution of diffraction and/or interference due to the internal layered structure to the iridescent colours of abalone shell. We will be working on this and will report the results of investigations in the near future.

Dr T.L. Tan
Natural Sciences and Science Education
National Institute of Education, Nanyang
Technological University
Singapore

References

- Liu, Y., Shigley, J.E., and Hurwit, K.N., 1999. Iridescence color of a shell of the mollusc *Pinctada margaritifera* caused by diffraction. *Optics Express*, 4, 177-82
- Nassau, K., 2001. *The physics and chemistry of color*. J Wiley & Sons, New York, 247-77
- Snow, M.R., and Pring, A., 2005. The mineralogical microstructure of shells: Part 2. The iridescent colors of abalone shells. *American Mineralogist*, 90(11/12), 1705-11

Abstracts

Diamonds

[The mutual relation between the angle and direction of the incident ray on the crown main facet and of the radiation ray from the facing crown main facet.]

M. KATO. *Journal of Gemmological Society of Japan*, 23(1-4), 2002, 22-5, 3 figs (in Japanese with English abstract).

This is the fifth paper concerning mathematical analyses of optical paths through a cut stone. In this paper, the mutual relation of the facing crown main facets are developed from the analyses given in previous papers. First, relating to the optical path inside a stone, a fancy crown angle is estimated from incident orientation, crown angle and radiant side. Then the incident ray and emerging ray are drawn from several refraction angles. Two figures are presented to show the radiant angle calculated factors against incident orientation.

I.S.

Characterization and grading of natural-color yellow diamonds.

J.M. KING, J.E. SHIGLEY, T.H. GELB, S.S. GUHIN, M. HALL AND W. WANG. *Gems & Gemology*, 41(2), 2005, 88-115.

The analysis of data collected over a five-year period on more than 24,000 natural-colour yellow diamonds is reported, including colour-grade, type of cut, clarity grade, weight, UV fluorescence and UV-visible and IR spectra. Among natural-colour diamonds, those with a yellow hue are some of the most abundant, although they are much less common than the colourless to light yellow diamonds associated with the GIA's D-to-Z colour grading scale. Since the yellow colour is a continuation of the gradation of colour associated with this scale, there can be misconceptions about the colour grading which involves

appearance, as well as other characteristics of yellow diamonds. The grading and appearance aspects are discussed to clarify these differences. Five sub-groups of type I yellow diamonds are also identified, which (with some overlap) are characterized by representative spectra and colour appearances.

R.A.H.

Lab Notes.

T.M. MOSES AND S.F. McCLURE (Eds). *Gems & Gemology*, 41(2), 2005, 16475.

Notes are given on a natural fancy dark pink-brown type Ib diamond with an unusually high nitrogen content.

R.A.H.

Lab notes.

T.M. MOSES AND S.F. McCLURE (Eds). *Gems & Gemology*, 41(3), 2005, 256-63.

Notes are included on dyed rough diamond crystals, two strongly coloured natural type IIb blue cut diamonds which showed strong red phosphorescence after exposure to short-wave UV radiation in DiamondView, and a greenish-blue 19.66 ct cut stone of yttrium zirconium oxide resembling a high-quality zircon.

R.A.H.

Diamonds from the Udachnaya pipe, Yakutia.

V. ROLANDI, A. BRAJKOVIC, I. ADAMO AND M. LANDONIO. *Australian Gemmologist*, 22(9), 2006, 387-97, 15 illus, 1 map.

This study of ten rough diamonds from the Udachnaya mine in the Sakha Republic of Yakutia includes descriptions of their morphology, surface and internal features, FTIR absorption spectra and CL topography. The diamond specimens ranged in weight from 0.066 to 0.622 ct and were greyish-yellow to brownish orange-yellow in colour. The paper contains a description of the geological setting of the Siberian platform and details the exploration of Siberian diamond deposits initiated by Professor V. Sobolev. In 1937

Sobolev predicted that diamonds might be found in the Siberian cratonic area after comparing the Siberian geological conditions to those of the Karoo formation in South Africa.

P.G.R.

Diamants cubiques ou presque cubiques: définitions utiles sur la morphologie.

B. RONDEAU, E. FRITSCH, M. MOORE AND J.F. SIRAKIAN. *Revue de Gemmologie AFG*, 153, 2005, 13-16.

Review of cubic or near-cubic diamond crystals with observations on their morphology.

M.O'D.

A review of political and economic forces shaping today's diamond industry.

L. SHOR. *Gems & Gemology*, 41(3), 2005, 202-33.

During the past 15 years, political and economic forces have converged to transform radically the structure of the diamond industry worldwide. Upheavals in the former Soviet Union and several African nations – as well as the development of new sources such as in Australia and Canada – led to restructuring of the rough diamond market. This in turn created new competitive pressure at the wholesale and retail levels, including a movement to establish new diamond cuts and diamonds as branded items. At the same time, technological advances enabled the faster, more efficient manufacturing of rough diamonds, created new treatments and fostered the introduction of economically viable gem-quality synthetic stones. While demand for diamond jewellery remains strong in the United States, which accounts for nearly 50% of world consumption, new markets such as India and China are likely to spearhead continued growth. New social and governmental initiatives have affected how the entire industry conducts business.

R.A.H.

Gems and Minerals



Amber-like fossil resin from North Queensland, Australia.

D.M. COLCHESTER, G. WEBB AND P. EMSEIS. *Australian Gemmologist*, 22(9), 2006, 378-85, 8 illus, 1 table.

Although Australia is practically devoid of fossil resin occurrences, recently pieces of amber-like fossil resin have been found on remote beaches near Cape Weymouth on the east coast of Cape York Peninsula in north Queensland. The Cape Weymouth specimens, which range in colour from clear pale yellow to almost opaque dark brown, were examined for their appearance and inclusions. They were then subjected to standard gemmological tests to discriminate between amber and copal resin. The fossil resins were found to be stable to semi-stable and therefore suitable for gemmological purposes, while the insect inclusions were considered to be of scientific importance. The specimens were also checked using FTIR spectroscopy and their spectra were found to be broadly similar to that of kauri gum (a copal resin) and to Baltic amber but were sufficiently different in the finer detail to have their own distinctive signature. The paper includes a classification of names applied to fossil resins and Anderson and Crelling's fossil resin classification.

P.G.R.

The Devonshire mineral collection at Chatsworth House.

M.P. COOPER. *Mineralogical record*, 36, 2005, 239-72.

Specimens of gem and ornamental quality minerals form part of the Devonshire collection at Chatsworth House, Derbyshire, England. The paper describes the progress and successful completion of a cataloguing and conservation programme.

M.O'D.

Gemmologisch-lagerstättenkundliche Untersuchungen an Türkisen aus magmatischen und sedimentären

Kupfererzorkommen.

H.G. DILL AND U. HENN. *Gemmologie. Z. Dt. Gemmol. Ges.*, 54, 2005, 85-96, 20 photographs, bibl.

Turquoise is a copper aluminium phosphate with a wide range of other elements, either in the unit cell, or as inclusions. Cu-Al phosphates are found in either the top layer of phosphate bearing sedimentary rocks or in Cu bearing metal deposits of magmatic origin. The present investigations did not discover any significant differences among the trace elements and minor inclusions which could be related to their parent rock. High resolution techniques have shown that the separation of elements of turquoise from its trace elements may have occurred when late stage fluids percolated through the matrix mineral.

E.S.

Emeralds from the Panjshir Valley (Afghanistan).

J. FIJAL, W. HEFLIK, L. NATKANIEC-NOWAK AND A. SZCZEPANIAK. *Gemmologie. Z. Dt. Gemmol. Ges.*, 53(4), 2004, 127-42, 8 photographs, 5 diagrams, 3 tables, bibl.

The emerald crystals examined came from the Panjshir valley in Afghanistan, probably from the southern mines. The mines are situated at 3-4000 m above sea level and are the highest emerald mines in the world. They are accessible by dirt tracks. The mining is intermittent, unsystematic and of limited range. The mines consist of systems of tunnels and small shafts opened in hard marbles using explosives. Afghan emeralds vary from dark to light green, the latter with various tints from yellow to blue. They were examined by microscopy and by chemical, X-ray and infrared spectroscopic analyses. The authors concluded that the emeralds from Panjshir valley were most probably the result of metasomatic alterations associated with regional metamorphism initiated by tectonic changes.

E.S.

Prächtige Bilder jaspise von der Morrison Ranch in Oregon.

H. GAMMA. *Mineralien Welt*, 16(6), 2005, 66-72.

Ornamental quality jasper is described from the Morrison Ranch in the Owyhee River Canyon, Oregon, U.S.A.

M.O'D.

Gemmologische Kurzinformationen.

Tansania- Mondstein: Albit (Peristerit) mit blauem Flächenschimmer.

U. HENN. *Gemmologie. Z. Dt. Gemmol. Ges.*, 54(2/3), 2005, 114-7, 4 photographs, 1 table, bibl.

Since mid 2004 transparent adularic feldspars from Tanzania have been offered on the market. Physical and chemical properties are given. The blue adularic is due to Tyndall scattering. Under the microscope the moonstones show white, parallel needle-like inclusions.

E.S.

Gemmologische Kurzinformationen.

Gemmologische Untersuchungen an Korunden aus Pakistan.

U. HENN AND C.C. MILISENDA. *Gemmologie. Z. Dt. Gemmol. Ges.*, 54(2/3), 2005, 111-4, 8 photographs, bibl.

The article describes properties of pink to pink-red and pink-blue bi-coloured corundum from recent finds in Kohistan and the Neelum valley in Pakistan. The pinks show a Cr spectrum, while the blue parts show the Fe³ and Fe² Ti⁴ spectrum. RI, birefringence and SG are in the normal corundum range. Healing cracks and lamellar twinning are typical internal features. Additionally there are rutile needles arranged in the form of star shapes.

E.S.

Türkis – Eigenschaften und Vorkommen, Imitationen und künstliche Eigenschaftsveränderungen.

U. HENN AND C.C. MILISENDA. *Gemmologie. Z. Dt. Gemmol. Ges.*, 54(2/3), 2005, 97-110, 11 photographs, 1 table, 6 graphs, bibl.

Turquoise is one of the oldest known gemstones. It has been known by this name since about 1550 because it was mainly traded via Turkey. It is mostly found in porous aggregates. Chemical and physical properties are given. The oldest occurrence was Egypt, where it was known 5000 years ago. 2000 years ago it was found in Iran, other finds are in South West U.S.A., Mexico, Hubei province in China, Uzbekistan, Kazakstan and the Umba valley in Tanzania.

Because of its high porosity it is often impregnated with various organic substances, enhancing the colour and allowing a better polish. Reconstructed turquoise is constructed from small pieces which are powdered and pressed into blocks with or without matrix. It is imitated by a number of different minerals such as ceruleite, or by dyed minerals. Identification of opaque gemstones is difficult, infrared spectroscopy is a useful tool. E.S.

The identification of impregnated nephrite.

L. JIANJUN. *Australian Gemmologist*, 22(7), 2005, 310-17, 9 illus., 2 maps, 2 tables.

Among all the jades revered by the Chinese, white nephrite from the Hetian County in China's Xinjiang province is considered to be the top grade and the most popular. Unfortunately this white Hetian nephrite is becoming worked out and is being replaced with less costly white nephrite from Russia and the Qinghai province in China. Recently this alternative material, bleached (to remove iron oxide stains) and impregnated (with epoxy resin) to imitate the Hetian white nephrite, has appeared on the market. Research by the author has suggested that the best way that these treated nephrites can be positively identified is by the use of the infrared spectrometer; the paper describes this method. P.G.R.

The adverse impact of scatter on the tone of Shandong sapphire.

L. JIANJUN. *Australian Gemmologist*, 22(9), 2006, 408-11, 3 illus.

Theoretical analysis of the results from the photometry and colorimetry of sapphires from Shandong in the Peoples Republic of China has shown that the large number of micro-inclusions present in these gems have a scattering effect on any light incident on the stones. Attempts to enhance the colour of the Shandong sapphires by heat treatment is only effective in 10% of the material as the heating creates additional stress fractures and increases the scattering effect. P.G.R.

A gemological pioneer: Dr Edward J. Gübelin.

R.E. KANE (finegemsintl@msn.com), E.W. BOEHM, S.D. OVERLIN, D.M. DIRLAM, J.I. KOIVULA AND C.P. SMITH.

Gems & Gemology, 41(4), 2005, 298-327.

This paper gives a detailed account of the work of the late Dr Gübelin (1913-2005) of Switzerland who, during a career that spanned more than 65 years, built a monumental reputation as a gemmologist. He wrote extensively on nearly all aspects of gemmology and produced more than 250 articles and 13 major books. He established the first systematic classification of inclusions in natural gem materials and demonstrated the importance of these internal features in determining not only the identity of the gemstone but also its country of origin. This account is accompanied by 29 photographs (including one with Basil Anderson) reflecting various aspects of his work. R.A.H.

[Natural amethysts from Caxarai mine, exhibiting infra-red absorption at 3543 cm⁻¹.]

H. KITAWAKI. *Journal of Gemmological Society of Japan*, 23(1-4), 2002, 16-21, 10 figs (in Japanese with English abstract).

The IR peak at 3543 cm⁻¹ has been used as a diagnostic peak to discriminate synthetic from natural amethysts with synthetic amethyst showing the peak, whereas the natural stones do not. This paper reports the occurrence of natural amethyst which shows this peak. The amethysts occur possibly in a pegmatite at Caxarai mine, Rondonia State, Brazil, 130 km north of Porto Velho, the state capital. The amethysts show characteristically different features from those occurring in geodes in basalt lava flows. Their z {0111} growth sectors show a deeper amethyst colour and sharper growth zoning than r {1011} growth sectors. This is opposite to the ordinarily observed characteristics in natural amethysts from hitherto known localities. The amethysts sometimes show strongly bluish pleochroism. Brazil twinning associated with Dauphine twinning and showing conical forms, often encountered in synthetic amethyst, is a pattern also present in some Caxarai specimens. I.S.

[Light interference phenomena observed in pearls with pale and

dark colour and the measurement.]

H. KOMATSU, C. SUSUKI, AND S. OGURA. *Journal of Gemmological Society of Japan*, 23(1-4), 2002, 5-15, 28 figs (in Japanese with English abstract).

The beauty of pearls comes from 'teri', a Japanese term to express the combined effect of lustre and interference colours seen in pearls. 'Teri' is not a simple equivalent to lustre, but appears due to light interference from the textures of pearls. Thus, pearls of different colours exhibit different 'teri'. 'Teri' exhibited by pale pearls such as Akoya pearls, appears phenomenologically opposite to that exhibited by dark pearls such as kurocho. Based on theoretical analysis of 'teri', optical methods combined with computer evaluation are designed to quantitatively evaluate the 'teri' of pearls in the series of dark and pale coloured pearls. I.S.

[A note on the relationship between the origin of "teri" and nacreous layer structure.]

H. KOMATSU, AND J. YAZAKI. *Journal of Gemmological Society of Japan*, 24, 2004, 24-8, 12 figs (in Japanese with English abstract).

The thickness of single aragonite layers and regularity in their stacking in both dark and pale coloured pearls have been measured by SEM observations and the results are correlated with the brightness of 'teri', the surface interference seen when a pearl is radiated by direct light from above. It was shown that the colour relates to the thickness and the brightness to the regularity of the aragonite layers. It was also shown that organic mechanisms in the environment surrounding the pearl sac control the thickness and regularity of these layers. I.S.

[Interference of light in upper and lower hemisphere of a pearl. An "Aurora" effect.]

H. KOMATSU AND C. SUZUKI. *Journal of Gemmological Society of Japan*, 24(1-4), 2004, 29-37, 27 figs (in Japanese with English abstract).

The origin and mechanism of the 'Aurora' effect, an interference

colour appearing on the lower half of a pearl sphere when it is irradiated by diffused light from below, is analysed and related to 'teri', an interference phenomenon appearing on the upper surface when it is illuminated from above. An apparatus called an Aurora Viewer was constructed, and the interference colour is quantitatively measured from the centre to the periphery of a sphere for dark and pale coloured pearls. It was shown that there is a qualitative correlation between the 'Aurora effect' and 'teri'. I.S.

The pegmatic gem deposits of Molo (Momeik) and Sakhan-gyi (Mogok).

U.H. KYI, T. THEMELIS AND U.K. THU. *Australian Gemmologist*, 22(7), 2005, 303-9, 11 illus., 2 maps, 5 tables.

Molo is situated in a remote area 51 km north-east of Momeik in Myanmar's Shan State. Its alluvial sediments are a new source of many rare gemstones and minerals (such as phenakite, petalite, hambergite, Cs-rich morganite and pollucite) as are the pegmatite dykes that are intruded into the peridotite country rock. The pegmatite deposit at Sakhan-gyi is located 16 km west of Mogok (in Mandalay Division) and for more than 100 years has been the main source in Myanmar of aquamarine, goshenite, topaz, quartz and danburite. The paper discusses these two pegmatite deposits and concludes that by their intrusive nature and mineral assemblages they are not contemporary. P.G.R.

A new deposit of jeremejevite from the Mogok stone tract, Myanmar.

U.H. KYI AND U.K. THU. *Australian Gemmologist*, 22(9), 2006, 402-405, 6 illus., 3 tables.

Although purchased by the authors in Mogok as quartz and beryl specimens, these colourless and light yellow terminated prismatic crystals were found to be jeremejevite, one of the world's rarest gemstones. The paper lists the constants of jeremejevite and provides the confirmatory XRD and EDX-RF identification data for this material. It is possible that further discoveries of gem quality jeremejevite in the Mogok stone tract could make it a gemstone of interest to gemmologists and gem collectors. P.G.R.

Gem news international.

B.M. LAURS (ED.) (blaurs@gia.edu). *Gems & Gemology*, 41(2), 2005, 176-87.

Items mentioned include pyrope-almandine from Ethiopia, inclusions of orange spessartine in Bolivian obsidian, a brownish-yellow synthetic sapphire from Jaipur, and a natural 8.01 ct faceted ruby with lead glass-filled fractures and other glass-filled rubies making their appearance from laboratories in the Middle East. R.A.H.

Gem news international.

B.M. LAURS (ED.) (blaurs@gia.edu). *Gems & Gemology*, 41(3), 2005, 264-79.

Items mentioned include a fuchsite-corundum-alkali feldspar rock from near Serra de Jacobina in northern Bahia, Brazil; pinkish-orange to purple sapphires from a new locality in the Kurur area of Tamil Nadu, India; a tenebrescent scapolite from Afghanistan, changing from colourless to blue on exposure to UV radiation; a quartz cabochon from Paraiba, Brazil, containing blue clusters of gilarite fibres; and a fibrolite (sillimanite) dyed and impregnated to imitate ruby. R.A.H.

Gem news international.

B.M. LAURS (ED.) (blaurs@gia.edu). *Gems & Gemology*, 41(4), 2005, 350-69.

Details are given of a blueschist (blue glaucophane, green omphacite and red garnet) from the lower Aosta Valley of the Western Italian Alps which takes a good polish and is sold as an ornamental material and cut into cabochons. Other items include a 68.55 ct bright greenish-yellow grossular from East Africa, green orthoclase from Vietnam, a nearly transparent bright green feldspar from Mogok and bright orange-red cut stones of plagioclase from Tibet. A new discovery of the rare mineral painite in situ at Thurein-taung and at the Wetloo mine near Mogok is reported, which has yielded more than 167 faceted stones (0.05-0.30 and rarely to 2 ct). R.A.H.

Jaspisvarietäten aus dem Eibenstocker Granit, Sachsen.

U. LEHMANN. *Lapis*, 30(11), 2005, 34-40.

Ornamental deep red jasper is described from granite at Eibenstock, Saxony, Germany. M.O'D.

Chinese cinnabar.

G. LIU. *The Mineralogical record*, 36, 2005, 69-80.

Cinnabar is more likely to turn up in the mineral cabinet than as an ornament despite its magnificent red colour and its translucency, but fashioned specimens are known. The main mining districts are identified and described. M.O'D.

Le traitement des corindons du béryllium: une mise au point.

S.F. McCCLURE. *Revue de gemmologie AFG*, 153, 2005, 4-7.

Summary in French, with adaptations and additional photographs, of a paper first published in *Gems & Gemology*, 38(3), 2002, 255-6. M.O'D.

Gemmologie Aktuell.

C.C. MILISENDA. *Gemmologie. Z. Dt. Gemmol. Ges.*, 53(4), 2004, 123-6.

The author describes briefly a transparent, yellowish-green tremolite-actinolite from Pakistan and some pink to red spinels from Tanzania weighing approx. 0.3 g each. There is also a description of a colour-change (blue to purple-violet) sapphire from the Luc Yen region of Vietnam weighing 2.21 ct and a 27.60 ct star sapphire from Laos; the asterism was caused by healing cracks and orientated dust-like mineral inclusions. From Tanzania a glass was offered as tanzanite. Another glass with an RI of 1.81 was offered as peridot. E.S.

"Paraiba-Tourmaline" aus

Quintos de Baixo, Rio

Grande do Norte, Brasilien.

C.C. MILISENDA. *Gemmologie. Z. Dt. Gemmol. Ges.*, 54(2/3), 1005, 73-84. 1 map, 9 photographs, 2 tables, 1 graph, bibl.,

Paraiba tourmalines occur in pegmatites near the village of Soa in the Paraiba state and in two other sites in the neighbouring Rio Grande do Norte state. One of those is the Quintos de Baixo mine, about 45 km northeast of Sao Jose de Batalha. Originally this produced commercial beryls and they were joined by tourmalines in 1996. Twelve samples were analysed by electron microprobe. They showed typical elbaite composition with the copper and manganese being the most

important trace elements responsible for the bright blue to green colours.

E.S.

Gemmologie Aktuell.

C.C. MILISENDA. *Gemmologie. Z.Dt. Gemmol. Ges.*, 54(2/3), 2005, 63-72, 16 photographs.

A new source of cuprian tourmalines has been discovered near Alto Ligonha in Mozambique. The stones weighed between 1 and 6 ct each and showed the characteristic absorption bands for copper and manganese. A translucent brownish-yellow chrysoberyl cat's-eye from Sri Lanka weighing 8.65 ct yielded SG 3.772 and RI 1.75. It showed parallel orientated tubes as well as short, needle-like inclusions orientated in a second direction. Both these inclusions are responsible for the asterism. Nine red, violet and purple stones from Rakwana in Sri Lanka were examined. They are star spinels and weighed between 1.91 and 4.95 ct. Eight showed a six-rayed star, while one exhibited a four-rayed star. A faceted, cushion-shaped sapphire from Madagascar weighing 2.19 ct showed all the usual properties, but was found to be colour-changing from green in daylight to reddish-brown in incandescent light. Under the microscope the stone showed numerous small zircon crystals. The absorption spectrum showed iron, chromium and vanadium. Other stones reported on included colour-change garnets from Madagascar. The stones changed from bluish-green in daylight to reddish-violet in incandescent light. RI 1.765, SG 3.9. Amethyst-coloured and colourless quartz from an occurrence near Karoor in southern India contained numerous hematite inclusions. Olive to brownish-green kornerupine cat's-eyes from Sri Lanka were examined as were some translucent blue rough anhydrite from Peru, RI 1.575, SG 2.93, hardness 3.5. There is also a report on a new find of aquamarines from Sao Jose de Safira in Valadares, Minas Gerais, Brazil. Spodumene from Pakistan has been offered in the trade. One of the hiddenites weighing 9.19 ct showed an intense green colour which was shown to have been produced by irradiation; the colour, however, faded on exposure to light, becoming pale pink. If kept in the dark the colour seemed

more constant. A lot of faceted red stones which had been purchased in Afghanistan as rubies were identified as dyed sillimanite (fibrolite). The red colour was concentrated in cracks and pores between individual fibres. E.S.

Hydrophanopal aus Indonesien.

C.C. MILISENDA AND M. WILD. *Gemmologie. Z. Dt. Gemmol. Ges.*, 53(4), 2004, 169-72, 5 photographs, bibl.

Hydrophane opals are porous and with increased absorption of liquids show increased diaphaneity and colour play. The examined samples came from Java and weighed between 0.96 and 12.05 ct. They were black, greyish-brown, brown to orange, some showing attractive play of colours. When immersed in water, they increased between 2 and 25% in weight. One opaque to translucent specimen weighing 0.96 ct, brownish-orange, showed a vivid play of colour; immersion in water caused the play of colour to disappear and the weight to increase to 1.24 ct. When taken out of water the colours disappeared and the stone became opaque, however after a few minutes, the play of colours returned; the stone then weighed 1.15 ct, eventually reducing to 1.00 ct with attractive colour play. E.S.

Inclusions in transparent gem rhodonite from Broken Hill, New South Wales, Australia.

P.W. MILLSTEED, T.P. MERNAGH, V. OTIENO-ALIEGO AND D.C. CREAGH. *Gems & Gemology*, 41(3), 2005, 246-54.

Solid, vapour and fluid inclusions in transparent rhodonite crystals from Broken Hill have been identified by Raman spectroscopy and gemmological/petrographic techniques. Among the solid inclusions are sphalerite, galena, quartz and fluorite. The rhodonite also contains hollow needle-like tubes and negative rhodonite crystals. Three-phase inclusions were found to contain a saline liquid, a gaseous mixture of N₂ and CH₄, and ilmenite crystals. R.A.H.

What's new in minerals.

T.P. MOORE. *Mineralogical Record*, 36, 2005, 285-301.

Among unusual and potentially gem-quality specimens reported from mineral shows are a crystal of väyrynenite, red-orange, near transparent, from Shengus, Gilgit District, Northern Areas, Pakistan, and red-orange transparent to translucent triplite, 1 cm, from Alchuri, Shigar Valley, Baltistan, Pakistan. A chrome-green hiddenite crystal of 6.7 cm is described and illustrated from Hiddenite, NC, U.S.A. Other ornamental gem-quality crystals from the United States include aquamarine crystals from Mount Antero, Chaffee County, Colorado. M.O'D.

Lab Notes.

T.M. MOSES AND S.F. MCCCLURE (EDS). *Gems & Gemology*, 41(2), 2005, 16475.

Notes are given on a yellowish-orange magnesioaxinite from Tanzania and Cu-bearing (CuO up to 0.09 wt %) colour-change tourmaline from Mozambique. R.A.H.

Lab notes.

T.M. MOSES AND S.F. MCCCLURE (EDS). *Gems & Gemology*, 41(4), 2005, 340-8.

Notes given included a diaspore 'vein' in a 3.96 ct natural sapphire. R.A.H.

Chinese fluorite.

B. OTTENS. *The Mineralogical Record*, 2005, 36, 59-68.

Fine ornamental and gem-quality Chinese fluorite has been known for many years. Locations and examples are described; most specimens are reported to be oiled. M.O'D.

Tongbei.

B. OTTENS. *The Mineralogical record*, 2005, 36, 35-43.

Fine crystals of spessartine and smoky quartz are described from granite outcrops in Fujian Province, China. Tongbei is the local centre. M.O'D.

Xueboading.

B. OTTENS. *The Mineralogical record*, 2005, 36, 45-57.

Fine orange scheelite and aquamarine are among minerals found in the Mount Xueboading area of Sichuan Province, China. M.O'D.

Mining in China.

B. OTTENS. *The Mineralogical record*, 2005, 36, 4-11.

Brief account of discoveries and personalities concerned with mining in China during the past 300 years. M.O'D.

Gemstone resources in China.

C.M. OU YANG. *Australian Gemmologist*, 22(8), 2005, 349-59, 18 illus., 6 maps, 2 tables.

The People's Republic of China is a large country that has a very complex geological structure. Its ancient land mass is host to vast, largely untapped, reserves of gemstones. The author describes and illustrates the occurrences and localities of a range of gemstones which are relatively common in China. These include diamond, sapphire, ruby, emerald, aquamarine, tourmaline, quartz, garnet, peridot, nephrite and bowenite. P.G.R.

Use of IR-spectroscopy and diffraction to discriminate between natural, synthetic and treated turquoise, and its imitations.

A. PAVESE, L. PROSPERI AND M. DAPIAGGI. *Australian Gemmologist*, 22(8), 2005, 366-71, 3 illus., 4 tables.

A total of 94 samples of natural, synthetic, treated and imitation turquoise samples were analysed by infrared spectroscopy in the non-destructive reflectance mode. Treated turquoise specimens were also studied in the IR transmission mode. With some of the imitations it was necessary to resolve ambiguities by the use of non-destructive X-ray diffraction. P.G.R.

Un nouvel outil géochimique de reconnaissance des saphirs bleus basaltiques et métamorphiques: le rapport Ga/Mg.

J.-J. PEUCAT, P. RUFFAULT, E. FRITSCH, C. SIMONET, M. BOUHNIC-LE-COZ AND B. LASNIER. *Revue de gemmologie AFG*, 153, 2005, 9-12.

Basaltic blue sapphires may be distinguished from their metamorphic counterparts by a study of their respective Ga/Mg ratio. Two types of sapphire are distinguished; specimens from syenites and alkali basalts, with a Ga/Mg ratio and sapphires from metamorphic hosts or plumasites where the ratio is lower. M.O'D.

New finds of sapphire placer deposits on Nosy-Be, Madagascar.

R. RAMDOHR AND C.C. MILISENDA. *Gemmologie. Z. Dt. Gemmol. Ges.*, 53(4), 2004, 143-58, 14 photographs, 1 map, 4 diagrams, bibl.

There are many corundum occurrences in northern Madagascar. Late Mesozoic basaltic extrusions have transported many xenocrysts, now to be found in various placer deposits. A new deposit is Nosy-Be and this is compared with occurrences on the Ambato peninsula and at Ambilobe, both north-east Madagascar. Sapphires are mainly found in the alluvium of small creeks. Searching and exploitation is largely by local villagers, who mine selected creek beds. The size of the deposits does not warrant large scale mining. The bulk of the material found is opaque corundum, some of which can be enhanced by heat treatment. E.S.

Gem corals – classification and spectroscopic features.

V. ROLANDI, A. BRAJKOVIC, I. ADAMO, R. BOCCHIO AND M. LANDONIO. *Australian Gemmologist*, 22(7), 2005, 285-97, 12 illus., 2 tables.

Until the beginning of the eighteenth century the origin of coral was unknown, and it was not until 1723 that G.A. Peyssonel demonstrated that corals are formed from the skeletons of marine animals. This paper analyses several gem corals belonging to the classes Hydrozoa and Anthozoa of the phylum Cnidaria. Identification of gem-quality corals requires a sequence of scientific investigations including the study of surface structures, the distribution of colour and the determination of physical data. Both FTIR- and Raman-spectroscopy have been shown to be useful tools for analyzing the mineral phases (calcite or aragonite) and the chromophore composition of each coral. With the use of both methods the characterization of genera and species of Cnidaria that have gem potential have been shown to be possible. P.G.R.

Kosmochlor and chromian jadeite aggregates from the Myanmar jadeite area.

G.H. SHI (shiguanghai@263.net.cn),

B. STÖCKHERT AND W.Y. CUI. *Mineralogical Magazine*, 69(6), 2005, 1059-75.

Four distinct textures and related compositions of kosmochlor and chromian jadeite are described from rocks in the Myanmar jadeite area. One of these four textures involves recrystallized fine-grained aggregates in deformed jadeite. The concomitant redistribution of chromium from chromite into kosmochlor, chromian jadeite and finally jadeite with < 1 wt % Cr₂O₃, together with the high transparency related to the fine-grained microstructure, produces the gemmologically important green jadeite. R.A.H.

[Investigation of corundum heat treated by a new technique.]

J. SHIDA, H. KITAWAKI AND A. AHMADJAN. *Journal of Gemmological Society of Japan*, 24(1-4), 2004, 13-23, 12 figs, 3 tables (in Japanese with English abstract).

To clarify what sort of treatment is applied to produce sapphire showing intense orange-pink hue, which has recently appeared in the gem market, various characterization techniques are applied to suspect stones. In addition to ordinary gem testing methods, internal and surface features were investigated by laser tomography and SEM, element distributions in stones were determined by EDXRF, SIMS, LA ICP, XPS, etc. In the new technique, only those sapphires coloured pink by initial heat treatment are subjected to a second heat treatment together with chrysoberyl in aluminium crucibles. It was confirmed that the main cause of the observed colour change is diffusion of Be inwards from the surface. I.S.

Mt. Mica: a renaissance in Maine's gem tourmaline production.

W.B. SIMMONS, B.M. LAURS, A.U. FALSTER, J.I. KOIVULA AND K. L. WEBBER. *Gems & Gemology*, 41(2), 2005, 150-63.

The Mt. Mica area in south-western Maine has been mined for tourmaline and other pegmatite gems since the 1820s, with most of the tourmaline production occurring during the late 1880s to the 1910s, with only occasional finds made from

the 1960s to the 1990s. Since May 2004, however, a new mining venture has produced gem- and specimen-quality tourmaline in a variety of colours. The faceted stones typically are yellowish green to greenish blue, although pink and bi- or tri-coloured stones have been cut. Their gemmological properties are typical for gem tourmaline. Microprobe analyses show that the tourmaline mined from pockets at Mt. Mica predominantly fell in the elbaite field, but minor amounts of schorl, foitite and rossmanite also occur. R.A.H.

Klare Bergkristalle aus dem Norden Islands.

H. STEEN. *Lapis*, 30(11), 2005, 30-34.

Well-formed clear quartz crystals and accompanying minerals are described from deposits in northern Iceland. M.O'D.

From the laboratory.

TAY THYE SUN. *Australian Gemmologist*, 22(9), 2006, 406/7, 6 illus.

The author reports on two unusual items of gemmological interest that were submitted for testing to his Far East Gemological Laboratory in Singapore. The first of these consisted of two octahedral 'diamond' crystals purchased by a client in Madagascar. Standard gemmological tests proved that one of these crystals was topaz and the other was colourless cubic zirconium oxide. The CZ diamond imitation was the more convincing but lacked trigons on its octahedral faces. The second item was a 3.76 ct Burmese ruby whose surface-reaching fractures and cavities were filled with a waxy substance. FTIR spectroscopy identified wax peaks at 2923 and 2855 cm^{-1} . Subsequently the author examined a 14 ct natural ruby which was also wax-filled in a similar way. P.G.R.

Glass filled rubies: clarity-enhanced rubies with glass-forming additives.

T. THEMELIS. *Australian Gemmologist*, 22(8), 2005, 360-5, 10 illus., 1 table.

The successful filling of surface-reaching fractures in diamonds was first reported in 1982 by Israeli diamond cutter Zvi Yehuda. At the time the exact nature of the filler was unknown and the process was often used following laser drilling. By 1990

several firms had started providing this service to the diamond industry. In 2004 a series of experiments were performed at the author's gem treatment laboratory in Bangkok using rubies at relatively low to mid range temperatures of 900-1300 C. Details of the process used are given including the selection of the starting material, the preparation of the rubies prior to treatment, selection of additives and the selection of heating parameters. Characteristic identifying features are given and the paper concludes with some cautionary words on the process, a warning on potential health hazards and a note on the need for disclosure at every level of gem merchandising. P.G.R.

Unverhofft kommt oft: Amethyst aus dem mättital, Wallis.

P. WINKLER. *Lapis*, 30(10), 2005, 69.

Crystals of amethyst are described from the Mättital, Valais, Switzerland. M.O'D.

Emeralds from the Kafubu area, Zambia.

J.C. ZWAAN, A.V. SEIFERT, S. VRANA, B.M. LAURS, B. ANCKAR, W.B. SIMMONS, A.U. FALSTER, W.J. LUSTENHOUWER, S. MUHLMEISTER, J.I. KOIVULA AND H. GARCIA-GUILLERMINET. *Gems & Gemology*, 41(2), 2005, 116-48.

After Colombia, Zambia is considered as the world's second most important source of emeralds (by value). Most of the emeralds are being mined from large open pit operations in the Kagern, Grizzly and Chantete concessions, near the Kafubu River in the Ndola Rural Restricted Area. The economic emerald mineralization is confined almost entirely to phlogopite reaction zones adjacent to Be-bearing quartz-tourmaline veins that have metasomatically altered Cr-bearing metabasite host rocks. The Zambian emeralds have relatively high refractive indices (n_o 1.591, n_e 1.599), high birefringence (0.006–0.009) and specific gravity (2.71–2.78), with inclusions typically consisting of partially healed fissures, as well as actinolite, phlogopite, dravite, fluorapatite, magnetite and hematite. Electron microprobe analyses indicate moderate amounts of Cr, Mg and Na, moderate-to-high Fe and relatively high Cs and Li. Their physical

properties, microscopic characteristics and chemical compositions should in many cases allow the Zambian emeralds to be distinguished from those from other commercially important localities. R.A.H.

Instruments and Techniques



Practical application for measuring gemstone dispersion on the refractometer.

T. LINTON. *Australian Gemmologist*, 22(8), 2005, 330-44, 4 illus., 3 tables.

Two previous papers by D.B. Hoover and T. Linton were published on this subject in the *Australian Gemmologist*, 20(12), 2000, and 21(4), 2001). These earlier papers are summarized and then the author describes the use of a refractometer employing a hemisphere or hemicylinder prism (such as the Eickhorst SR/XS) in order to achieve the necessary accuracy of readings. Because the gemmological standard reference wavelengths chosen to measure dispersion (Fraunhofer lines B at 686.7 nm and G at 430.8 nm) are close to the limits of human vision, it is recommended that the narrower range of C (656.3 nm) to F (486.1 nm) is used and the results extrapolated out to the B and G lines. However as the relationship between refractive index and wavelength is non-linear and produces a curve when plotted, this curve must first be linearized (i.e. converted into a straight line). Although measurement, linearization and extrapolation of refractive index data can be accomplished by the gemmologist using the methods described in the paper, the author proposes that the process is simplified by accepting the C-F interval as the standard for gemmology as it is in other scientific disciplines. This short cut eliminates the need for linearization and only involves the determination of three or four refractive indices at appropriate wavelengths.

Dispersion is not presently considered as a viable and accurate identification criterion and extrapolation of apparent C-

F dispersion readings to the B-G wavelengths is a complex and time consuming process. In addition, a single number cannot fully represent the dispersion of a birefringent gemstone. The author suggests that the data contained in the paper's final table be considered as a basis for the future use of C-F dispersion figures as an aid to gemstone identification. P.G.R.

Krüss PO11 proportion ocular and stone holder.

T. LINTON, R. BEATTIE AND K. HUGHES, *Australian Gemmologist*, 22(9), 2006, 398-401, 9 illus.

This well-illustrated report by the GAA Instrument Evaluation Committee examines the Krüss PO11 device for measuring a diamond's proportions and facet angles when used in conjunction with a standard zoom microscope fitted with sub-stage illumination. The 30 mm proportion-measuring ocular is fitted into the microscope's eyepiece tube, and a spring-loaded stone holder enables the diamond to be manipulated over the projected image of the ocular. The ocular contains a calibrated profile of a Tolkowsky brilliant cut diamond which allows the measurement and comparison of cut proportions for total height, crown height, pavilion depth, table size, girdle thickness, and eccentricity of culet, table and girdle shape to be accurately determined. P.G.R.

Synthetics and Simulants

Characterization of the new Malossi hydrothermal synthetic emerald.

I. ADAMO (ilaria.adamo@unimi.it), A. PAVESE, L. PROSPERI, V. DIELLA, M. MERLINI, M. GEMMI AND D. AJ. *Gems & Gemology*, 41(4), 2005, 328-38.

A report is presented of a new production of hydrothermal synthetic emeralds, grown in the Czech Republic with Italian technology, and marketed with

the trade name Malossi synthetic emerald. Details of an investigation of several crystals (1-141 ct) by microprobe and UV-Vis-NIR and IR spectroscopy are given, together with a comparison of this material with natural and synthetic emeralds (the latter grown by the flux and hydrothermal techniques). These studies reveal that Malossi hydrothermal synthetic emerald can be identified on the basis of microscopic features and chemical composition, along with the mid-infrared spectrum. Chromium was the only chromophore found in the Malossi samples. R.A.H.

Prospects for large single crystal CVD diamonds.

S. S. HO, C. S. VAN, Z. LIU, H. K. MAO AND R. J. HEMLEY. *Industrial Diamond Review*, 1/2006, 28-32.

A description is given of chemical vapour deposition (CVD) techniques for fabricating large single-crystal diamond at very high growth rates (up to > 100 J-lm/h). Single crystals more than 1 cm in thickness and weighing more than 10 ct can now be produced with a range of optical and mechanical properties for different applications. This diamond can be tailored to possess high fracture toughness, and high-pressure/high-temperature annealing can increase its hardness significantly. The size of the diamonds can be further enlarged by successive growth on different faces. The process has been optimized to produce diamond with improved optical properties in the ultraviolet to infrared range, opening prospects for new technological and scientific applications. Illustrations are given of a 5 ct single-crystal CVD diamond (without seed), 12 mm high and 6.7 mm diameter, cut from a 10 ct block using a computer-controlled YAG laser system, and of a 0.2 ct brilliant cut diamond produced from a 1 ct block. R.A.H.

Lab notes.

T.M. MOSES AND S.F. MCCLURE (EDS). *Gems & Gemology*, 41(4), 2005, 340-8.

Notes are given for yellow cut

stones of cubic zirconia imitating irradiated and annealed Cape diamonds, and small (0.11-0.16 ct) bright orange-yellow synthetic diamonds presenting a challenge for their identification with standard gemmological techniques alone. R.A.H.

Crystallographic and spectroscopic analyses of synthetic moissanite.

C. RINAUDO. *Gemmologie. Z. Dt. Gemmol. Ges.*, 53(4), 2004, 159-68, 8 photographs, 9 diagrams, 1 table, bibl.

Synthetic moissanite (SiC) varying in colour from near colourless to almost black were examined under microscope, by Raman spectroscopy and X-ray transmission topography with synchrotron radiation. All near-colourless samples proved to be single crystals, while the dark samples were composed of at least two polytypes. E.S.

Experimental CVD synthetic diamonds from LIMHP-CNRS, France.

W. WANG, A. TALLAIRE, M.S. HALL, T.M. MOSES, J. ARCHARD, R.S. SUSSMANN AND A. GICQUEL. *Gems & Gemology*, 41(3), 2005, 234-44.

The gemmological and spectroscopic features of six synthetic type IIa diamonds grown in the Laboratoire d'Ingénierie des Matériaux et des Hautes Pressions (LIMHP) at the Centre National de la Recherche Scientifique in Paris are reported, and their diagnostic features are compared to those of diamonds produced by chemical vapour deposition (CVD). Three of the six samples were nitrogen doped, whereas the other three were classified as high purity. A number of characteristics diagnostic of CVD synthetic diamonds were present in the nitrogen-doped crystals, despite an absence of defect-related absorption features in the infrared region. The identification of the high-purity samples was more complicated, but it was still possible based on features in their photoluminescence spectra, their distinctive birefringence and characteristic luminescence images. R.A.H.

Abstractors

R.A. Howie R.A.H. M. O'Donoghue M.O'D. P.G. Read P.G.R. E. Stern E.S. I. Sunagawa I.S.

Book Reviews

Photoatlas of Inclusions in Gemstones. Volume 2.

E.J. GÜBELIN AND J. I. KOIVULA, 2005. Opinio Verlag, Basel. 829 pp, over 2200 colour plates. Hardcover. ISBN 3-03999-029-2. £160.00.

This rigorous volume builds on the original *Photoatlas of Inclusions in Gemstones*, enhances its usefulness and extends the original work by incorporating new information and developments that have occurred in the field of micro gemmology since 1986.

The first thing that strikes you about this book is its size. It has a whopping 829 pages (containing 2167 inclusion images) compared with the 532 pages in Volume 1 that has become the standard reference book in the field of inclusions and micro features in gemstones. The price (\$260 plus tax where appropriate) may seem steep but you get a huge amount for your money. The quality of production is excellent and the images, virtually all of which have not previously been published, are often of exceptional beauty. Anyone who has attempted photomicroscopy will feel humbled by the outstanding quality of the images which are a testament to the skill, knowledge and patience of the authors.

The basic premise of the study of microscopic features in gemstones is that similar processes will result in a range of similar features in gems of the same species. So whether these processes are geological, treatment or synthesis, significant information is stored within the gems that aid in their identification and separation.

Although the volume is portrayed as a voyage of discovery and exploration into the world of inclusions in natural gemstones, their treatments, imitations and synthetics it keeps a firm hold on the importance of the basic premise and does not lose sight of the fact that this is primarily an image reference library albeit aesthetically pleasing for all that.

The *Introductory Section* contains useful abbreviations and definitions of the types of inclusions. Whilst illumination and magnification abbreviations accompany each image, regrettably, but understandably because of the inherent difficulty in unequivocally assigning a type to inclusions, little information on this latter aspect accompanies the images. This latter aspect is more than compensated for by expansive descriptive captions on the nature of the inclusions that facilitate 'typing' of inclusions by the reader.

Section two, the *Thematic Section*, has a clear and instructive piece on photomicroscopy methods. It is accompanied by examples of the results achieved by the various techniques. Particularly revealing are images of the same field of view photographed using different techniques, lending truth to the saying that a picture can be worth a thousand words. Inclusion analysis with accompanying photomicrographs is also included in this section. Whilst this is especially useful for those with access to specialist analytical instruments it is nevertheless helpful in painting the picture of the gamut of analytical options available and the results they produce. Inclusions within inclusions (with accompanying photomicrographs) complete this section and serve to remind us of the complex geological history of many gemstones. It is an area of investigation that is largely untapped due to present technology limitations.

Section three, *Characteristics of Inclusions*, devotes 172 pages to the diagnostic features of inclusions, colours, morphology, fluid inclusions and their geological correlation. Having these in a separate section serves to focus on the salient features used in characterisation and the degree to which they are diagnostic. This new method of presentation may initially be undervalued until readers learn to familiarise themselves with

its benefits before diving into the gem specific section.

The 'meat' of Volume 2 is in section four; *Inclusions in Gems of Commercial Importance*. There are 526 pages containing 1597 images; almost the same number of pages as in the whole of Volume 1: The species and varieties covered are amber, beryl, chalcedony, chrysoberyl, feldspar, garnet, opal, peridot, quartz, spinel, topaz, tourmaline, zircon and zoisite. Each is preceded by a few pages of supporting text that addresses to a greater or lesser degree as befits the gemstone the petrogenesis, mineral genesis and paragenesis, treatments, colour, structures, synthetic versions and simulants, locality sources, and not least the nature of the inclusions. The gem specific sections are subdivided. Natural gems come first and a printed subheading indicates the beginning of treated and/or synthetic gems. This is not consistent for all gem specific sections but as the latter comes at the end of each section this aids navigation. Considerably more images of lab grown, manufactured and treated stones are included compared with the same gemstone in Volume 1. This attests to the extensive developments and improvements in these fields. Additional reading references are also given. If the reader is wondering what has happened to new information on diamond, emerald, ruby and sapphire these are covered in the as yet unpublished Volume 3.

The conclusion serves to re-emphasize the power, versatility, usefulness and cost effectiveness of microscopy in gemmology and urges gemmologists to re-establish their microscopy skills and consequently keep their gemmological knowledge alive. Microscopy, they argue, stimulates the thought process more so than relying on 'black box' generated answers provided by modern analytical equipment.

Indexes are important. The reader needs to find things quickly. Lack

of an index was a major weakness of the *Internal World of Gemstones*. A purposeful sampling of the index found it to be accurate and with breadth. There were some very minor terminology differences arising from nationality differences in the use of descriptive terms for example *zebra stripes* in amethyst when the term *tiger stripes* is used in the UK but these were readily overcome.

Truly this superb volume is the consummate companion to a properly equipped gemmological microscope and every gemmologist should have both. B.J.

Artificial Gemstones.

M. O'DONOGHUE, 2005. NAG PRESS, LONDON. pp 294, illus. in colour. Hardcover. ISBN 0 7198 0311 X. £30.00.

After a brief introduction, the book's opening chapter, entitled 'The structure and development of crystals', takes the reader through basic crystallography to the fascinating world of crystal growth, a subject which over the years has become the author's speciality. The main production techniques of flame-fusion, flux growth and hydrothermal methods of gemstones synthesis are then outlined and typical examples grown by these methods are described.

The following chapter covers enhancement treatments and includes dyeing, bleaching, coating, impregnation, heating, diffusion, irradiation and even sputtering. Detection of many of these processes is by the use of the microscope to examine both the surface and interior of the treated gem. Gem testing instruments are briefly covered in the next chapter and this is followed by one containing advice on the photographing of inclusions.

The bulk of the book contains information-packed chapters on synthetic versions and simulants of each of the major gem species, beginning with diamond and including corundum, beryl, opal, quartz, chrysoberyl and spinel. A valuable addition to several of these chapters is 'Notes from the literature' which provides up-to-date information on recent or significant developments abstracted from current reports.

'Artificial gemstones' is profusely illustrated with 75 half-page size

colour microphotographs illustrating typical inclusions. Many of these photographs, complete with their captions, come from the collection of the late Professor Dr Eduard Gübelin. A useful list of all the illustrations, with their captions and page numbers appears at the front of the book and enables them to be linked to the appropriate text when using the presence of inclusions to distinguish between artificial and natural materials.

The book concludes with a useful bibliography as an aid to further research into the principles and practice of crystal growth. P.G.R.

Comparative study of gem minerals, beryl and corundum, from various Indian occurrences.

J. PANJIKAR, 2004. Pangem Publishers, Pune, India. pp xii, 119, illustrated in colour. Hardcover. ISBN 81 901 22208. Price on application.

The literature of Indian gem materials is far from profuse and this opportune book, developed from a PhD thesis submitted by the author to the University of Bombay [Mumbai] is one of the few recent accounts of features by which Indian corundum and beryl may be recognized. Beryl varieties covered are emerald and blue beryl, corundum varieties are ruby and blue sapphire. The two minerals and their varieties are described by state; thus beryl is described from locations in Jammu and Kashmir, Rajasthan, Orissa, Andhra Pradesh and Gujarat, and corundum from Jammu and Kashmir, Orissa, Andhra Pradesh, Karnataka, Tamil Nadu and Kerala.

In each case the geology of the deposits is briefly described with notes on physical and optical properties. Inclusions are examined and analysed where possible by the electron microprobe. Many inclusion features are illustrated in colour and the quality of the photographs is good (use of the red compensator was found useful; magnifications are most commonly 50 and 100).

The whole book is a fine example of mineralogical research and its already high quality is enhanced by a ten-page bibliography in which only serious studies are cited. Tables are plentiful

and there are maps of the states in which deposits of corundum and beryl are reported. M.O'D.

Pearls.

E. STRACK, 2006. Ruehle-Diebener Verlag, Stuttgart, Germany. pp 707, 658 illustrations, mainly photographs and maps. Hardcover and dust cover. £75.00.

This is the English translation of the German edition published in 2001. It is beautifully produced with many photographs and explanatory maps. The book is divided into two parts, one dealing with natural pearls, the other with cultured pearls. Each of the many chapters is accompanied by an extensive bibliography.

In the natural pearl section, the process of pearl formation is explained in detail and the geographic occurrences and characteristics, molluscs, *pinctada*, freshwater and various other sources described. There is also an interesting chapter on large and famous pearls and pearl objects. An introduction to the natural pearl market and the evaluation of pearls is given. The historical chapter on natural pearls covers the role of pearls in antiquity to the present time.

The part of the book dealing with cultured pearls starts with an historical overview and has detailed chapters on pearls from Japan, Korea and China. The freshwater cultured pearls from Japan, Lake Biwa and Lake Kasumigaura and the freshwater cultured pearls from China are described, as well as those from North America and the South Seas. White South Sea pearls are compared with black South Sea pearls (Tahitian) and the varied sources described. Mabe pearls are produced in many countries as are cultured pearls from gastropods.

Amongst the most useful chapters are those dealing with fakes and imitations, testing methods, artificial coloration, and care and maintenance.

There are a number of indices to facilitate finding specific subjects. It is a most comprehensive reference book, the photographs are well chosen and readers will find much to interest them. The book will make a most useful and attractive addition to any library, especially one belonging to a gemmologist, gem laboratory or pearl enthusiast. E.S.

Proceedings of the Gemmological Association and Gem Testing Laboratory of Great Britain and Notices

Presentation of Awards

The Presentation of Awards gained in the 2005 examinations was held at Goldsmiths' Hall in the City of London on Monday 31 October. Alan Jobbins, President of the Association, presided and welcomed those present, particularly successful candidates attending from as far away as Australia, Canada, Hong Kong, India, Korea, Madagascar, New Zealand and the U.S.A., as well as Denmark, France, Greece, the Netherlands, Sweden and Switzerland.

The President introduced John I. Koivula, Chief Gemmologist at the American Gem Trade Association's Gemological Testing Center (AGTA-GTC) in Carlsbad, California, who presented the Diplomas and prizes. Following the presentations, John Koivula

gave his address. John encouraged the students to continue their education: "This is just the starting point for those receiving their diplomas today" he said. "I hope that everyone finds something in gemmology that excites them, as I did with inclusions." He stressed the need to protect the word 'natural', and emphasized that great care should be taken to identify treated stones. John said: "You are gemmologists now and you have your reputation as gemmologists to uphold."

A vote of thanks to John Koivula was given by Dr Jack Ogden, Chief Executive of the Gemmological Association.

A reception attended by over 200 members, students and their guests, was held following the ceremony.



The 2005 prize winners (from left): Nicola Sherriff from Verdun, Quebec, Canada, winner of the Anderson Medal and the Hirsh Foundation Award; Sheila Smithie from Boston, Massachusetts, U.S.A. winner of the Christie's Prize for Gemmology; Chaman Golecha from Chennai, India, winner of the Anderson Bank Prize; and Torbjorn Lindwall from Lannavaara, Sweden, winner of the Deeks Diamond Prize.



Guest speaker John Koivula gives his address. Photo: Lewis Photos Ltd.

Gem-A Awards

Gem-A examinations were held worldwide in January 2006. In the Examinations in Gemmology, 137 candidates sat the Diploma Examination of whom 61 qualified including one with Distinction and 12 with Merit, and 204 sat for the Foundation Examination, of whom 150 qualified. In the Gem Diamond Examination 91 candidates sat of whom 42 qualified, including four with Distinction and six with Merit.

The names of the successful candidates are listed below:

EXAMINATIONS IN GEMMOLOGY

Gemmology Diploma

Qualified with Distinction

Zhu Hanli, Shanghai, P.R. China

Qualified with Merit

Cen Qicong, Guilin, Guangxi, P.R. China
 Challani, D. Mohit, Chennai, India
 Chandhok, Simran Kaur, New Delhi, India
 Emond, Jacinthe, Laval, Quebec, Canada
 Hu Yuan, Guilin, Guangxi, P.R. China
 Jensen, Annalisa Tintern, Esher, Surrey
 Lai Suk Kwan, Eleanor, Kowloon,
 Hong Kong
 Lam Kwok Man, May, West Smithfield,
 London
 Lam Kwok Yee, Monica, West Smithfield,
 London
 Sun Xiaolei, Beijing, P.R. China
 Xu Hui, Shanghai, P.R. China
 Zhang Xiaopu, Wuhan, Hubei, P.R. China

Qualified

Al-Hadad, Raed Mustafa, Montreal Quebec,
 Canada
 Badrov, Irena, London
 Chan Mei Fong, Frances, Kowloon, Hong
 Kong
 Chaudry, Mohamed Ashraf, Wardle,
 Rochdale, Lancashire
 Chen Cheng Tang, Taipei, Taiwan,
 R.O. China
 Chen Xinxing, Guilin, Guangxi, P.R. China
 Chitou, Aurelie Gisele, Antananarivo,
 Madagascar
 Chu Hon Chung, New Territories,
 Hong Kong
 Costin, Charlotte, Horsham, West Sussex
 Darell, Rikard, Uppsala, Sweden

Eastwood-Barzdo, Elizabeth, Dully,
 Switzerland
 Edwards, Catherine, Salisbury, Wiltshire
 Fan Jing, Beijing, P.R. China
 Flower, Caro, Brinton, Melton Constable,
 Norfolk
 Goncalves Coelho, Ana Cristina,
 Antananarivo, Madagascar
 Guo Yu, Wuhan, Hubei, P.R. China
 Huang Mingcai, Guilin, Guangxi, P.R. China
 Jang Wei-Jen, Taipei, Taiwan, R.O. China
 Jiang Lihua, Wuhan, P.R. China
 Kwok Men Yee, New Territories,
 Hong Kong
 Leung Ka Lok, Kowloon, Hong Kong
 Leung Kam Ping, Sai Kung, Hong Kong
 Li Mengjie, Guilin, Guangxi, P.R. China
 Lin Lang-Dong, Taipei, Taiwan, R.O. China
 Liu Xi, Guilin, Guangxi, P.R. China
 Liu Zuodong, Guilin, Guangxi, P.R. China
 Luo Yueping, Beijing, P.R. China
 Ma Jun, Guilin, Guangxi, P.R. China
 Meyer, Constance Marie, Paris, France
 Michaels, Sarah A., Virginia Beach,
 Virginia, U.S.A.
 Ong Chin Siang, Gary, Singapore
 Peers, Sofia L. R., London
 Qin Ting, Guilin, Guangxi, P.R. China
 Rana, Ashka Sureshkumar, A'bad, Gujarat,
 India
 Ranjatoelina, Domoina, Antananarivo,
 Madagascar
 Scott, Craig John, West Meon, Petersfield,
 Hampshire
 Shen Bin, Wuhan, Hubei, P.R.China
 Shen Mengxi, Guilin, Guangxi, P.R. China
 Soderholm, Kathryn Ashe, Dulles,
 Virginia, U.S.A

Gem-A Awards

Tessari, Claudio, Ora, Italy
 Tsang Kwai Ying, Yau Yat Tsuen, Hong Kong
 Tu Yu-Chieh, Taipei, Taiwan, R.O. China
 Wang Ying, Wuhan, Hubei, P.R. China
 Xu Ning, Beijing, P.R. China
 Ye Xiaohong, Beijing, P.R. China
 Yee Yee Mon, Yangon, Myanmar
 Zeng Linghan, Guilin, Guangxi, P.R. China
 Zhuang Lingyan, Guilin, Guangxi, P.R. China

Gemmology Foundation Certificate

Qualified

Adler, Stevan, New York, U.S.A.
 Al-Hadad, Raed Mustafa, Montreal, Quebec, Canada
 Andriambelo, Andry Rainier, Antananarivo, Madagascar
 Andrianamoizana, Claudia, Antananarivo, Madagascar
 Andriasamy, Francine Gisele, Antananarivo, Madagascar
 Asvine Tsakou, Kawindre, Antananarivo, Madagascar
 Ayeb, Kaled, Montpellier, France
 Bae Hong Ryul, Seoul, R.O. Korea
 Barbour, Alexandra, Dorchester, Dorset
 Bieri, Willy, Escoltzmatt, Switzerland
 Brooks, Candy, Catcott, Bridgwater, Somerset
 Chan Wai See, Lavinia, Guangzhou, P.R. China
 Chan Po Ling, Kowloon, Hong Kong
 Chan Wing Sze, Herleva, Kowloon, Hong Kong
 Chandhok, Simran Kaur, New Delhi, India
 Chang Mei-Yen, Karen, Taipei, Taiwan, P.R. China
 Chau Shan Yuen, Wan Chai, Hong Kong
 Chen Ying-Chen, Taipei, Taiwan, R.O. China
 Chen Hsiuchuan, Taipei, Taiwan, R.O. China
 Chen Shioulin, Taipei, Taiwan, R.O. China
 Chen Hsiang Ling, Taichung, Taiwan, R.O. China

Chen Li, Guilin, Guangxi, P.R. China
 Chester, Mel, St. Denys, Southampton, Hampshire
 Cheung Hoi Man, Shau Kei Wan, Hong Kong
 Chok, Georges, Paris, France
 Chow Man Yee, Tai Hang, Hong Kong
 Chu Man Tsz, Sylvia, Chai Wan, Hong Kong
 Coppin, Daisy, Corsham, Wiltshire
 De La Tullaye, Remi, Fublaines, France
 Faugeroux, Valerie, La Gardelle, France
 Flower, Caro, Brinton, Melton Constable, Norfolk
 Forsberg, Erika, Lannavaara, Sweden
 Frei, Thomas, Pratteln, Switzerland
 Garbis, Angela, Koukaki, Athens, Greece
 Green, Anthony, Westcliff-on-Sea, Essex
 Grimal, Marie, Marseille, France
 Haaja, Pasi Janne, Helsinki, Finland
 Han Fen, Shanghai, P.R. China
 Hartley, Daisy, Ilkley, West Yorkshire
 Higginson, Matthew J., Cassington, Oxfordshire
 Hilde Lam Nga Sheung, North Point, Hong Kong
 Hnin Lwin Aye, Yangon, Myanmar
 Ho Tak Kwong, Kowloon, Hong Kong
 Hon Wai Ching, Kowloon, Hong Kong
 Hossenlopp, Patricia, Chene – Bougeries, Switzerland
 Huang Hui Wen, Taichung, Taiwan, R.O. China
 Hui Ngai Yin, North Point, Hong Kong
 Hwang, Sang Un, Goryung, R.O. Korea
 labrazzo, Richard, Cannes, France
 Jiang Jingxia, Shanghai, P.R. China
 Kallioniemi, Mari, Helsinki, Finland
 Kao, Chen, Taipei, Taiwan, R.O. China
 Kasumu, Maambwa S., Finchley, London
 Kearney, Sonny Michael, Kimberley, Nottingham
 Kim Hyo Sook, Gyoungbuk-Do, R.O. Korea
 Kim, Ji A, Daegu, R.O. Korea
 Kim, Mi Hyun, Seoul, R.O. Korea
 Ko, Cheuk Wah, Quarry Bay, Hong Kong
 Krska, Gemma, Durban, South Africa

Gem-A Awards

Kuhn, Barbara, Duebendorf, Switzerland
 Kweon Ji Eun, Daegu, R.O. Korea
 Kwok Sau Ying, Tuen Mun, Hong Kong
 Kwon Sae Ra, Seoul, R.O. Korea
 Kyaw Kyaw, Yangon, Myanmar
 Lam Wai Han, Kowloon, Hong Kong
 Larsson, Jacqueline, Hammersmith, London
 Larsson, Niclas, Lannavaara, Sweden
 Lee Hui Min, Taipei, Taiwan, R.O. China
 Lee Kit Kau, Fanling, Hong Kong
 Leung Hang Fai, Henry, Kowloon,
 Hong Kong
 Li Liu Fen, Guangzhou, P.R. China
 Li Mei, Guilin, Guangxi, P.R. China
 Lin Jui-Yi, Taipei, Taiwan, R.O. China
 Lin Chia Hui, Taipei, Taiwan, R.O. China
 Lo Pui Yin, Shirley, Tai Po, Hong Kong
 Lorentzen, Roy Roger, Tromsø, Norway
 Manassero, Robert, Simiane, France
 Meninno, Marco, London
 Naartjarvi, Eva, Kiruna, Sweden
 Nam Yong Ju, Seoul, R.O. Korea
 Netsah, Maayane, Finsbury Park, London
 Ng Ka Kit, New Territories, Hong Kong
 Ng Kim Ling, Kowloon, Hong Kong
 Ni Ziqian, Guilin, Guangxi, P.R. China
 Or Wing Chee, Stella, Kowloon,
 Hong Kong
 Ovaskainen, Sami, Helsinki, Finland
 Pan Pai, Guilin, Guangxi, P.R. China
 Pang Yufei, Guilin, Guangxi, P.R. China
 Park Mi Young, Seoul, R.O. Korea
 Piha, Saara, Espoo, Finland
 Piirto, Irmeli, Espoo, Finland
 Poon Mei Ling, Hong Kong
 Pyrro, Riku, Kirkkonummi, Finland
 Quint, Camilla, London
 Rakotobe, Alice Hortense, Antananarivo,
 Madagascar
 Rakotomanantsoa, Miguel, Antananarivo,
 Madagascar
 Ranaivoson, Hantaranoro, Antananarivo,
 Madagascar
 Randrianantoandro, Minoarisoa Michelle,
 Antananarivo, Madagascar
 Rasatranabo Razakarivony, Aina Anthony,
 Antananarivo, Madagascar
 Razafimahafaly, Fanjamalala Blandine,
 Antananarivo, Madagascar
 Razafimahatratra, Tojoniaina Harintsoa,
 Antananarivo, Madagascar
 Razafindrasolo, Toky Ny Aina,
 Antananarivo, Madagascar
 Retsin d' Ambroise, Laura, Paris,
 France
 Rodman, Anna, Lund, Sweden
 Rudomino-Dusiacki, Patrick, London
 Shan Luk, Kowloon, Hong Kong
 Shi Huayan, Shanghai, P.R. China
 Shukla, Satyendra Kumar, Gujarat, India
 Sourendre Shah, Rupal, Antananarivo,
 Madagascar
 Spagnoletti Zeuli, Lavinia, London
 Stidwill, Thuong, Upper Tooting, London
 Stockwell, Hilary, Brussels, Belgium
 Sun Yuan, Guilin, Guangxi, P.R. China
 Sundell, Andreas, Lannavaara, Sweden
 Suokko, Teija, Tampere, Finland
 Tam Shuk Man, Tai Po, Hong Kong
 Tang Kit Yee, Tsing Yi, Hong Kong
 Teh Hong Kee, Penang, Malaysia
 Thanadtamakul, Pakamon, Nonthaburi,
 Thailand
 Thomas, Estelle Melissa, Surbiton, Surrey
 Tikkunen, Anni, Lahti, Finland
 Tsui Wan Kam, Barbara, Hong Kong
 Vasquez, Alejandra, London
 Villeneuve, Jeanne, Paris, France
 Wang Ling, Guilin, Guangxi, P.R. China
 Wang Wei, Guilin, Guangxi, P.R. China
 Wat Wing Suet, Tsim Sha Tsui, Hong Kong
 Wen Chia-Ling, Taipei, Taiwan, R.O. China
 Withey, Alison, Encinitas, California, U.S.A.
 Wong Man Yat, Kowloon, Hong Kong
 Wong Kit Man, Angela, Tin Shui Wai, Hong
 Kong
 Wong Man Yuen, Daniel, Hong Kong
 Wong Tung Wing, Hong Kong
 Woo Jung, Daegu, R.O. Korea
 Wu Chung-Kang, Taipei, Taiwan, R.O.
 China
 Wu Shih-Han, Taipei, Taiwan, R.O. China

Gem-A Awards

Yang Hsu-Chiao, Taipei, Taiwan, R.O. China
 Yang Tak Him, Tsuen Wan, Hong Kong
 Ye Mengqian, Guilin, Guangxi, P.R. China
 Yoon Jung Mi, Daegu, R.O. Korea
 Yu Heyu, Guilin, Guangxi, P.R. China
 Yun Soo Min, Gimhae, R.O. Korea
 Yung Pan, Kowloon, Hong Kong

Zhang Chao, Guilin, Guangxi, P.R. China
 Zhang Wei, Shanghai, R.O. China
 Zhou Huijuan, Guilin, Guangxi, P.R. China
 Zhou Ye, Guilin, Guangxi, P.R. China
 Zhu Hanli, Shanghai, P.R. China
 Zhu Cheng, Guilin, Guangxi, P.R. China
 Zou Jin, Guilin, Guangxi, P.R. China

GEM DIAMOND EXAMINATION

Qualified with Distinction

Huck. Perry, London
 Lau Man Yu, Kowloon, Hong Kong
 Michaels, Sarah A., Virginia Beach,
 Virginia, U.S.A
 Wong Man Yee, Kowloon, Hong Kong

Qualified with Merit

Cai Yitao, Wuhan, Hubei, P.R. China
 Ho Ching Yee, New Territories,
 Hong Kong
 Lai Siu Kwong, New Territories,
 Hong Kong
 Lam Kwok Yee, Monica, West Smithfield,
 London
 Lo Wing See, Kowloon, Hong Kong
 Ng Ka Kit, New Territories,
 Hong Kong

Qualified

Chan Hing Yip, Kowloon, Hong Kong
 Chen Chih-Wei, Taichung City, Taiwan,
 R.O. China
 Chen Jianhua, Kowloon, Hong Kong
 Chow Po Ling, Sai Ying Pun,
 Hong Kong
 Chu Kong Ting, New Territories,
 Hong Kong
 Chuk Yim Ming, Kowloon,
 Hong Kong
 Chung Tsz Bun, Kowloon, Hong Kong
 Freeman, Derek, Hove, East Sussex
 Gits, Hugo, Knokke, Belgium
 Howells, Robert, Abergavenny,
 Monmouthshire

Jiang Huan, Wuhan, Hubei, P.R. China
 Jiang Yi, Beijing, P.R. China
 Kapos, Thomas, Voula, Athens,
 Greece
 Kong, Jason, Kowloon, Hong Kong
 Kuchard, Monika, London
 Lai Sau Han, Winnie, Hong Kong
 Lam Kwok Man, May, West Smithfield,
 London
 Lam Lai Wah, Tsuen Wan,
 Hong Kong
 Lau Ho, Kowloon, Hong Kong
 Leung Man Yee, New Territories,
 Hong Kong
 Ma Yaw Lan Hsiung, Ruth, Hong Kong
 McHugh, Trudi, Eastleigh, Hampshire
 Mo Ying Lin, Marilyn, Kowloon,
 Hong Kong
 Pang Shing Kwan, New Territories,
 Hong Kong
 Papapavlou, Despina-Maria, Christoforos,
 Rhodes, Greece
 Parsonson, Chloe Celine, London
 Rahn, Adelle, Pewsham, Chippenham,
 Wiltshire
 Tsang Wa, New Territories, Hong Kong
 Wallbank, Julie Samantha, Lichfield,
 Staffordshire
 Webster, Eric T., West Chiltonington,
 West Sussex
 Wong Kin Ching, New Territories,
 Hong Kong
 Wong Yu Lap, Hong Kong
 Zhang Niaoniao, Wuhan, Hubei,
 P.R. China

Members' Meetings

Gem Discovery Club

Specialist Evenings

Once a month Club members have the opportunity to examine items from the collections of gem and minerals specialists.

The November guest was Gem-A Conference keynote speaker John Koivula, who divulged some of his latest research on the inclusions in gemstones, particularly that on the detection of heat-treated corundum. In December David Hargreaves, owner and operator of the Chimwadzulu ruby mine in Malawi, spoke to Club members about the formation and mining of rubies and sapphires, the treatment of the stones, current production issues affecting the market today and price trends. Members had the opportunity to examine the many samples that David had brought along. Maria Alferova of the Moscow State University was the February specialist, when she gave an illustrated talk on her recent gem fieldtrip to Transbaikalia. 'Nature v. jewellers' was the title of Harry Levy's presentation to Club members in March, when he discussed what jewellers could and could not do with gemstones.

Annual General Meeting

The 2005 Annual General Meeting was held on 11 October at 27 Greville Street, London EC1N 8TN (see report p. 122). The AGM was followed by an illustrated talk by Vivian Watson entitled 'A walk in the garden', when Vivian took a stroll through the history of the jewellery trade in Hatton Garden. After the talk, members attended an informal dinner at the Abbaye Belgian Restaurant, Charterhouse Street, celebrating the 80th anniversary of the founding of the Gem Testing Laboratory.

Gem-A Conference

The 2005 Gem-A Conference, a celebration of the life and work of the late Professor Dr Edward Gübelin, was held on Sunday 30 October at the Renaissance London Heathrow Hotel. The theme, 'The Inside Story: the inclusions in gemstones', recognized

Professors Gübelin's lifetime study of inclusions in gemstones. The speakers at the event were John I. Koivula (keynote), Edward Boehm, Professor Henry Hänni, Dr Daniel Nyfeler, Stephen Kennedy and Professor Andy Rankin.

A programme of events arranged to coincide with the Conference included a Private Viewing of the Crown Jewels with Crown Jeweller David Thomas and a guided tour of the Diamonds exhibition at the Natural History Museum.

A full report of the Conference was published in the December 2005 issue of *Gems & Jewellery*.

Midlands Branch

At the Branch AGM held at the Earth Sciences Building, University of Birmingham, Edgbaston, on 27 January, Gwyn Green retired as Chairman. Branch President David Larcher thanked Gwyn for her enthusiasm and hard work during the ten years she had held the office. Elizabeth Gosling and Stephen Alabaster were re-elected Secretary and Treasurer respectively. Paul Phillips was later elected as Chairman of the Branch. The AGM was followed by a Bring and Buy Sale and Team Quiz. Other Branch meetings held at the Earth Sciences Building included a demonstration on the identification of gem materials using a microscope by Gwyn Green on 28 October, 'A history of buttons' by Jenny Swindells on 25 November, 'Horological Jewelling' by John Moorhouse on 24 February, and 'Chasing rainbows by observing gemstone spectra' by John Harris on 31 March.

The 53rd Anniversary Branch Dinner, held at Barnt Green, again proved to be a very popular and successful event. On 19 March a one-day Loupe and Lamp event was held at Barnt Green. Working in pairs, participants had to identify 60 stones using only a 10x lens and a hand torch or lamp. This was followed by a presentation by Gwyn Green pointing out the relevant identifying features for each stone.

North East Branch

In September 2005 Neil Rose retired as Branch Chairman and Mark Houghton and

Sara North were appointed jointly to the position.

Branch meetings held at the Ramada Jarvis Hotel, Wetherby, included 'Cartier, the King of Jewellers' by Terry Davidson on 3 November, and 'Spectroscopy for Gemmology Students', a hands-on event with Colin Winter on 22 March.

North West Branch

On 19 October Maggie Campbell Pedersen gave a talk on organic gemstones entitled 'Gems of Life'. The Branch AGM was held on Wednesday 16 November when Deanna Brady, Ray Rimmer and Eileen Franks were re-elected Chairman, Secretary and Treasurer respectively. These meetings were held at YHA Liverpool International, Wapping, Liverpool 1.

A special event was held on 15 February to celebrate the 30th anniversary of the Branch, held at Liverpool Cathedral. Following a reception, Maria Alferova of the Moscow State University gave a presentation on the Gems of Russia.

Scottish Branch

Regular meetings have been held at the British Geological Survey, Murchison House, West Mains Road, Edinburgh. Dr Bruce Cairncross spoke on the gem deposits of southern Africa on 24 August. On 27 September Maggie Campbell Pedersen gave a talk entitled 'Gems of Life', describing organic gems and how imitation and treated specimens may be identified. Terry Davidson gave a presentation entitled 'Cartier: the 20th century' on 24 October. On 7 November Basil Dunlop spoke about the cultural history as well as the natural history of Cairngorm gemstones.

A buffet, followed by a Bring and Buy Sale and a Quiz, were held at the Bruntsfield Hotel, Edinburgh, on 18 January.

On 21 February at the British Geological Survey Roger Key gave an illustrated talk on the hunt for diamonds in Mozambique, where he had been working to assess the gemstones deposits, and also showed slides

from his exploratory mapping visit to Madagascar. Alan Jobbins gave a talk entitled 'A gemmological journey from the Alps to Vesuvius' on 14 March.

South East Branch

The Branch AGM was held on 18 December at the Gem-A headquarters in Greville Street, London EC1, followed by a talk by Dr Frances Wall entitled 'Diamonds and the deep carbon cycle'.

Annual General Meeting

The 2005 Annual General Meeting was held at the Gem-A headquarters at 27 Greville Street, London EC1N, on 11 October. Professor Alan Collins chaired the meeting and welcomed those present. The Annual Report and Accounts were approved.

Terry Davidson and Evelyne Stern were re-elected and Marcus McCallum elected to the Council. Lawrence Hudson retired in rotation from the Council and was not seeking re-election. The Chairman reported that Dr Roger Harding and Ian Mercer had resigned from the Council in November 2004, and Jeffrey Monnickendam and Vivian Watson had resigned in June and May 2005 respectively.

Peter Dwyer-Hickey and John Greatwood were re-elected and Jim Collingridge, Gwyn Green and David Lancaster elected to the Members' Audit Committee. The Chairman reported that Lawrence Music and Dr Jamie Nelson had resigned from the Members' Audit Committee in April 2005. Hazlems Fenton were re-appointed auditors.

Membership

Between 1 October 2005 and 31 March 2006 the Council approved the election to membership of the following:

Fellowship and Diamond Membership (FGA DGA)

Lee Fung Mei, Kowloon, Hong Kong, 2004/05
Leondaraki, Marialena, Athens, 2005
Taylor, Daniel, Leeds, West Yorkshire, 2004/05

Donations

The Council of the Association is most grateful to the following for their donations. Donation levels are Circle of Benefactors (£5000 and above), Diamond (£1000 to £4999), Ruby (£500 to £999), Emerald (£250 to £499), Sapphire (£100 to £249) and Pearl (£25 to £99).

Emerald Donation:

Terry Davidson, FGA, Coln St Aldwyn,
Gloucestershire

Sapphire Donations

Dr Genevieve Davies, London
Torbjorn Lindwall FGA DGA, Lannavaara,
Sweden
Robert L. Rosenblatt FGA, Salt Lake City,
Utah, U.S.A.
Elaine Rowley FGA, London

Pearl Donations

Burton A. Burnstein, Los Angeles,
California, U.S.A.
Dennis Durham, Kingston upon Hull,
East Yorkshire
Victoria Forbes FGA DGA, Portadown,
Northern Ireland
Gwyn Green FGA DGA, Barnt Green,
Hereford and Worcester
Yvonne Holton FGA DGA, Edinburgh,
Scotland

Bede Johnson, Lewes, East Sussex
Marcia Lanyon FGA, London
Sandra Lear FGA, Rothbury, Morpeth,
Northumberland
Masao Kaneko FGA, Tokyo, Japan
Paul R. Milton FGA, Liverpool
Ernest R. Mindry FGA, Chesham,
Buckinghamshire
Sara Naudi FGA, London
Gabriella Parkes DGA, London
David J. Sayer FGA DGA, Wells, Somerset
Moe Moe Shwe FGA, Singapore
Karen Tulo FGA, Ludwigshafen, Germany
Anne Van der Meulen FGA DGA, Chicago,
Illinois, U.S.A.
Nancy Warshow FGA DGA, Nairobi, Kenya
Keith P. Whitehouse BSc(Hons) FGA DGA,
Stafford

Wong Ching Man, Happy Valley, Hong Kong,
2004

Zebrak, Tracy, London, 1981/82

Fellowship (FGA)

Chaiyawat, Yuanchan, Bangkok, Thailand,
2005

Chan Pak Lin, Tsuen Wan, Hong Kong, 2005

Chan Pik Kwan, Cecilia, New Territories,
Hong Kong, 1982

Chan Wai Fong, Wah Fu Estate, Hong Kong,
2005

Cheung Ching Chung, Aberdeen, Hong Kong,
2005

Davidge, Elizabeth Anne, Eastbourne,
West Sussex, 1998

Davis, Shelley, Toronto, Ontario, Canada, 2005

Dupuis, Ronald J.R., Toronto, Ontario, Canada,
1979

Eguchi, Yumi, Fukuoka-City, Fukuoka-Pref.,
Japan, 2003

Fellows, Andrew Simon, Aldridge, West
Midlands, 2005

Fossurier, Anne, Montreal, Quebec, Canada,
2005

Gillman, Scott, Sudbury, Massachusetts,
U.S.A., 2005

Glass, Krista-Leigh, Stratford, Ontario,
Canada, 2005

Golecha, Chaman, Chennai, India, 2005

Hoso, Sadayuki, Fukuoka-City, Fukuoka Pref.,
Japan, 1992

Ip Wai Yin, Renée, Toronto, Ontario, Canada,
2005

- Janssen, Marjo, Voorschoten, The Netherlands, 2005
- Kandalepa, Theophano, Patissia, Greece, 2005
- Kwan, Kai Lion, Tananarive, Madagascar, 2005
- Kwok Mei Yee, Sindy, Ap Lei Chau, Hong Kong, 2005
- Lawton, Sarah, Enderby, Leicestershire, 2005
- Lee Lai Ha, New Territories, Hong Kong, 2005
- Lee Tin Wan, Shatin, Hong Kong, 2005
- Leung Chi Fai, Hong Kong, 2005
- Li Chi Man, Tin Hau, Hong Kong, 1992
- Li Po Man, North Point, Hong Kong, 2005
- McKercher, Jennifer, Toronto, Ontario, Canada, 2005
- Pang Shing Kwan, New Territories, Hong Kong, 2004
- Qingfeng, Ruan, Guilin, Guangxi, China, 2005
- Rakotoson, Eric, Antanimora, Madagascar, 2005
- Raelison, Ivan Ludovic, Antanimora, Madagascar, 2005
- Rasoanaivo, Annick Sylvie, Antananarivo, Madagascar, 2005
- Ryu, Keiko, Hamamatsu-City, Japan, 1974
- Salmi, Tarja, Sodankylä, Finland, 1991
- Sanders, Jacqueline, Towcester, Northamptonshire, 2005
- Shapshak, Leon, Highlands North, South Africa, 1952
- Susawee, Namrawee, Bangkok, Thailand, 2005
- Tammilehto, Eero Juhani, Helsinki, Finland, 2005
- Thawornmongkolkij, Monruedee, Bangkok, Thailand, 2005
- Wong Cheng Shin Wan, Lina, Tai Po Kau, Hong Kong, 2005
- Wong Ching-Man, Ruby, New Territories, Hong Kong, 2005
- Yokote, Hideki, Maubaru-City, Fukuoka-Pref., Japan, 1993
- Yoshimoto, Misako, Fukutu-City, Fukuoka-Pref., Japan, 1988
- Zee Gar Bo, Michelle, Kowloon, Hong Kong, 2005
- Zoeter, Johannes Simon, Bergen op Zoom, The Netherlands, 1990
- Fong Yan, William, Tai Po, Hong Kong, 2005
- Head, Jemima Elizabeth, Bingley, West Yorkshire, 2005
- Kathris, Ioannis, Holargos, Greece, 2005
- Ko Cheuk Wah, Quarry Bay, Hong Kong, 2005
- Kwan Ka Lun, Karen, Wanchai, Hong Kong, 2004
- Lee Ka Wai, Shatin, Hong Kong, 2005
- Lee Oi-Yan, Christine, Tai Po, Hong Kong, 2005
- Powar, Krishna, Smethwick, Birmingham, West Midlands, 2005
- Terry, Dennis, Petts Wood, Kent, 2005
- Tsang Yuen King, New Territories, Hong Kong, 2005
- Warner, Simon, Tring, Hertfordshire, 2005
- Wong Wai-Lok, Calvin, Kowloon, Hong Kong, 2005
- Yamout, Sabah, Leeds, West Yorkshire, 2005
- Yeung Tsz Ming, New Territories, Hong Kong, 2005

Associate Membership

- Akaishi, Hitomi, Hannou City, Saitama Pref, Japan
- Akiyama, Claire Nozomi, Woodbury Down Estate, London
- Al-Othaim, Abrar, Acton, London
- Annetts, Deborah, London
- Aung Than, Hay Mar, London
- Azzopardi, Malcolm, St Julians, Malta
- Bhartiya, Saurabh, Hendon, London
- Brimming, Julie Anne, Bristol, Avon
- Bundu, Bukl'elo, London
- Buttle, Nicholas James, Bexhill-On-Sea, Sussex
- Cahalon, Maureen, Ballinasloe, County Galway, Ireland
- Chau Kit Ying, Lily, Hong Kong
- Chen Chih-Wei, London
- Cho, Jungmin, London
- Craig, Roselind, London
- Craig, Veronica, Hindhead, Surrey
- Dhillon, Mandeep, Smethwick, West Midlands
- Diallo, Abdoulaye, London
- Edwards, Catherine, Salisbury, Wiltshire
- El-Kassir, Mariam, Acton, London
- Flower, Caro, Melton Constable, Norfolk
- Frost, Richard Henry John, Rochester, Kent
- Fukuoka, Shinobu, Osaka City, Osaka, Japan
- Fukuoka, Y., Toyonaka City, Osaka, Japan
- Hassey, Lauren, Putney, London

Diamond Membership (DGA)

- Baker, David Mark, Bath, Somerset, 2005
- Chan Chi Wai, Hong Kong, 2005
- Clarkson, Mia Helen, London, 2005
- Davis, Samantha Angela, Bearwood, Warley, West Midlands, 2005

Gifts

The Association is most grateful to the following for their gifts for research and teaching purposes:

Marino and Beatriz Aragon, San Pedro, California, U.S.A., for rough and polished Colombian copal specimens.

Luella Woods Dykhuis FGA DGA, Tucson, Arizona, U.S.A., for parcels of tumbled peridot beads from Mahana Bay, Hawaii, and faceted amethysts, samples of opal in matrix from Spencer, Idaho, U.S.A., and Mount St. Helens glass (made from the ash from St Helens), a ruby in matrix from India, a brass bead decorated with blue bird feathers, a Tahiti pearl, a rough pink smithsonite and a fibrous serpentine cabochon.

Gwyn Green FGA DGA, Barnt Green, Hereford and Worcester, for 400 faceted quartzes.

John Hay Mo Ho FGA, Hong Kong, for two painite crystals.

Dr Donald B. Hoover FGA, Springfield, Missouri, U.S.A., for topaz crystals.

Padam Jain, RMC Gems HK Co., Kowloon, Hong Kong, for two faceted glass stones displaying colour change.

Dr Joachim Lindblom PhD FGA, Turku, Finland, for a copy of his book Mineralogical studies on luminescence in diamond, quartz and corundum.

Jonathan Mehdi, London, for a cushion-shape faceted quartz with a purple-blue fluorite inclusion.

Ngwe Lin Htun, Gemmological Science Centre, Yangon, Myanmar, for two painite crystals.

Christien Oldbury, Salisbury, Wiltshire, for a tagua nut.

Eric Van Valkenburg, Tucson, Arizona, U.S.A., for a painite crystal.

Jason Williams FGA DGA, G.F. Williams & Co. Ltd., London, for a selection of gemstones.

Hiroko Wilson, Hong Kong, for a collection of gemmological instruments

Huen Lai-Kei, Sheree, Richmond, British Columbia, Canada
 Jamieson, Katie Jane, London
 Jatia, Vijaykumar, Mumbai, India
 Kaneda, Mitaka, Minato-ku, Tokyo, Japan
 Kasumu, Maambwa, Whitechapel, London
 Khan, Amjad, Harrow, London
 Knowles-Cutler, Laura, Westerham, Kent
 Kobayashi, Taisuke, Arakawa-ku, Tokyo, Japan
 Komachi, Ryusuke, Kyoto City, Kyoto, Japan
 Kuchard, Monika, London
 Lam Kwok-Yee, Monica, West Smithfield, London
 Lam Kwok-Man, May, West Smithfield, London
 Latham, Elizabeth, Wallingford, Oxfordshire
 Lau, Tim, London
 Mathurata, Kaneel, London
 Matsuura, Miho, Yokohama City, Kanagawa Pref., Japan

Michaels, Sarah, London
 Mistry, Mahesh, Leicester
 Miyamoto, Kazuhiko, Osaka City, Osaka, Japan
 Moroz, Magdalena, Richmond, Surrey
 Naito, Ayako, Taito-ku, Tokyo, Japan
 Nagao, Saeko, Kooriyama City, Fukushima Pref, Japan
 Nakagawa, Yumi, Kitakatsuragi-gun, Nara Pref, Japan
 Nakamura, Takatsugu, Osaka City, Osaka, Japan
 Nakanishi, Nobuo, Ikeda City, Osaka, Japan
 Nishizawa, Kazumi, Ibaraki City, Osaka, Japan
 Obayashi, Koko, Setagaya-ku, Tokyo, Japan
 O'Doherty, Brigid Isobel, Belfast, Northern Ireland

Okabe, Yuichi, Kawasaki City, Kanagawa Pref., Japan
 Parkinson, David, Hackney, London
 Preston, Paula, Blackheath, London
 Reeves, Victor, Leicester
 Ringhiser, Barbara, Lake Worth, Florida, U.S.A.
 Ross, Lynne, Harrow, Middlesex
 Russell, Elaine, Dundee, Scotland
 Saito, Rieko, Numazu City, Shizuoka Pref., Japan
 Sarginson, Jane, London
 Sawamura, Tsukasa, Toshima-ku, Tokyo, Japan
 Schonboschler, Christiané, London
 Scott, Craig John, West Meon, Hampshire
 Shimizu, Maki, Oyama City, Tochigi Pref., Japan
 Shpartova, Irina, London
 Soderholm, Kathryn Ashe, London
 Swaenen, Marcel, Brasschaat, Belgium
 Tai, Wai, London
 Tanaka, Makiko, Tokorozawa City, Saitama Pref., Japan
 Tanikawa, Masatoshi, Hino City, Tokyo, Japan
 Thiebaut, Ivane, London
 Uchiyama, Mio, Ichikawa City, Chiba Pref., Japan
 Ueda, Miwa, Matsue City, Shimane Pref., Japan
 Ushioda, Motofusa, Suginami-ku, Tokyo, Japan
 Usujima, Chika, Machida City, Tokyo, Japan
 Vafaei, Khatereh, North York, Ontario, Canada
 Warren, Cherry Elizabeth, Stokenchurch, Buckinghamshire
 Wenbo, Han, Ji Nan, Shandong, P.R. China
 Yamada, Masashi, Toshima-ku, Tokyo, Japan

Laboratory Membership

Gem Road Ltd, London, W14 0RT

Transfers

Diamond Membership (DGA) to Fellowship and Diamond Membership (FGA DGA)

Chawla, Jaspreet Kaur, London, 2005
 Godfrey, Kay, Halstead, Essex, 2005
 Kiamos, George K., Maroussi, Athens, Greece, 2005
 Konstantopoulos, Konstantinos, Athens, Greece, 2005

O'Dwyer, Michael, Johnswell Road, Kilkenny, Ireland, 2005
 Pearson, Heather, Belper, Derbyshire, 2005

Fellowship (FGA) to Fellowship and Diamond Membership (FGA DGA)

Klimek, Karina S., Truro, Cornwall, 2005
 Lancaster, David, Hemel Hempstead, Hertfordshire, 2005
 Lovelock, Justina E., London, 2005
 Scragg, Claire P., Little Kingshill, Buckinghamshire, 2005
 Van der Molen, Wouter N., Zwolle, The Netherlands, 2005

Associate Membership to Fellowship (FGA)

Ahren, Anna Ekstrom, Tyreso, Sweden, 2005
 Anderson, Judith S., Manchester, New Hampshire, U.S.A., 2005
 Bardehle, Petra, Munich, Germany, 2005
 Bayoumi-Stefanovic, Nevin, London, 2005
 Gillman, Scott, Sudbury, Massachusetts, U.S.A., 2005
 Kim, Yoonjin, Bucheon City, South Korea, 2005
 Leondaraki, Marialena, Syntagma, Athens, Greece, 2005
 Li, Kehan, Enfield, Middlesex, 2005
 Lu, Shan, Nerima-ku, Tokyo, Japan, 2005
 Miyazaki, Satoshi, Toyonaka City, Osaka, Japan, 2005
 Natsuka, Masaki, Toyonaka City, Osaka, Japan, 2005
 Omotedani, Hiroki, Matsudo City, Chiba, Japan, 2005

Associate Membership to Diamond Membership (DGA)

Lampson, Ming, London, 2005
 Ota, Shinya, Yamanashiken, Japan, 2005
 Palmares, Richard P., Sale, Cheshire, 2005
 Yamout, Sabah Ibrahim, Leeds, West Yorkshire, 2005
 Yeung Tsz Ming, New Territories, Hong Kong, 2005

Obituary

Leslie Fitzgerald

We announce with deep regret the death of Leslie Fitzgerald FGA (D.1983), Woking, Surrey, at the age of 83. Leslie first came to the jewellery trade in 1947 working in both the manufacturing and retail sections of the industry. In 1979 he joined the Gemmological Association and National Association of Goldsmiths as Education Secretary, responsible for the administration of courses and examinations until his retirement in 1990. He lectured at the College for the Distributive Trades and also taught gemmology in Harrow. NAG tutor, Eddie Stanley, who worked closely with Leslie for many years, writes: "Leslie was a practising Christian and indeed one of the first joining members of the Christian Jewellers Association. His quiet belief system directly affected how he treated all who came into contact with him, his judgement was sound. His tutoring was carried out from a dedication to serve the trade by passing on his knowledge and understanding of trade matters. There are many in the jewellery trade today who have good reason to be thankful for the life and input from Leslie."

It is with deep regret that we announce the death on 7 April of R. Keith Mitchell FGA (Tully Medallist 1934), a Vice President of the Association.

A full obituary will be published in the next issue of *The Journal*.

Anita Axell FGA (D.1988), Stockholm, Sweden, died recently.

Reginald Bridges FGA DGA (D.1951), Chigwell, Essex, died in June 2005.

Deborah J. Cloke FGA (D.1983), Sevenoaks, Kent, died suddenly on 5 May 2005.

Matthew C.M. Faulds BSc, FGA (D.1972), Keswick, Cumbria, died in 2005.

George A. McNair FGA (D.1983), Jesmond, Newcastle-upon-Tyne, died in September 2005.

Thomas Primavesi FGA (D.1963), Pointre Claire, Quebec, Canada, died in September 2005.

John Weatherill FGA (D.1957), Cardiff, died in September 2005

MEGA-LOUPE
Dark Field Illumination
at your fingertips

Features optional lighting and a 3-position lens for fast and efficient inclusion detection on loose or mounted stones



2 MODELS

Use it with the new high quality fully corrected 10X master lens

LUMI-LOUPE 15mm lens \$90
MEGA-LOUPE 21mm lens \$115

AHD: \$20 for shipping outside the continental USA
\$8 for shipping inside the continental USA

www.zschubang.com
email: info@zschubang.com

P.O. Box 3356, Redwood City, CA 94064, U.S.A.
Tel 650-369-8966 Fax 650-363-8911

Gem-A
MailTalk

The email-based forum for communication between members

- Share comments and ideas with other members
- Ask or answer questions
- Receive regular news from Gem-A

Have you registered yet?

For instructions on how to register go to www.gem-a.info/information/mailTalk.htm or contact Jack Ogden at jack.ogden@gem-a.info

Forthcoming Events

Tuesday 16 May	London: Private viewing of Fabergé and the Russian Jewellers at Wartski (fully booked)
Tuesday 13 June	Scottish Branch: Gems of Russia, from Karelia to Transbaikal. BRIAN JACKSON
Saturday 17 June	Midlands Branch: Summer supper party
Wednesday 21 June	North West: A review of the garnet family. BRIAN JACKSON
Tuesday 27 June	London: AGM followed by a talks and a private viewing of Sotheby's June sale 'Jewels: Antique, Period and Contemporary'
Thursday 13 July	North East Branch: The Naughty Nineties. BRIAN DUNN
Wednesday 19 July	North West Branch: Thoughts from 'a broad' – a trip around the world of coloured gemstones. TRACEY JUKES
Tuesday 12 September	Scottish Branch: A history of gemmology through the literature. NIGEL ISRAEL
Wednesday 20 September	North West Branch: Colour enhancement of diamond and how it may be detected. PROFESSOR ALAN COLLINS
Wednesday 18 October	North West Branch: Some gemmological and lapidary diversions. DOUG MORGAN
Tuesday 24 October	Scottish Branch: All the colours of diamond. MARTIN VAINER
Sunday 5 November	Gem-A Annual Conference
Monday 6 November	Presentation of Awards and Graduation Ceremony

Contact details

When using e-mail, please give Gem-A as the subject:

London:	Jamie Gould on 020 7404 3334; e-mail jamie.gould@gem-a.info
Midlands Branch:	Paul Phillips on 02476 758 940; e-mail pp.bscfgadga@ntlworld.com
North East Branch:	Mark Houghton on 01904 639761; email sara_e_north@hotmail.com
North West Branch:	Deanna Brady 0151 648 4266 or Ray Rimmer on 0151 525 6066 rr001c8559@blueyonder.co.uk
Scottish Branch:	Catriona McInnes on 0131 667 2199; e-mail scotgem@blueyonder.co.uk
South West Branch:	Richard Slater on 01635 553572; e-mail rslater@dnfa.com

Gem-A Website

For up-to-the-minute information on Gem-A events visit our website on www.gem-a.info

Guide to the preparation of typescripts for publication in The Journal of Gemmology

The Editor is glad to consider original articles shedding new light on subjects of gemmological interest for publication in The Journal. Articles are not normally accepted which have already been published elsewhere in English, and an article is accepted only on the understanding that (1) full information as to any previous publication (whether in English or another language) has been given, (2) it is not under consideration for publication elsewhere and (3) it will not be published elsewhere without the consent of the Editor.

Typescripts Two copies of all papers should be submitted on A4 paper (or USA equivalent) to the Editor. Typescripts should be doubled spaced with margins of at least 25mm. They should be set out in the manner of recent issues of The Journal and in conformity with the information set out below. Papers may be of any length, but long papers of more than 10 000 words (unless capable of division into parts or of exceptional importance) are unlikely to be acceptable, whereas a short paper of 400-500 words may achieve early publication.

The abstract, references, notes, captions and tables should be typed double spaced on separate sheets.

Title page The title should be as brief as is consistent with clear indication of the content of the paper. It should be followed by the names (with initials) of the authors and by their addresses.

Abstract A short abstract of 50-100 words is required.

Key Words Up to six key words indicating the subject matter of the article should be supplied.

Headings In all headings only the first letter and proper names are capitalized.

A This is a first level heading

B This is a second level heading

First and second level headings are ranged left on a separate line.

Third level headings are in italics and are indented within the first line of the text.

Illustrations High resolution digital files, for both colour and black-and-white images, at 300 dpi TIFF or JPEG, and at an optimum size, can be submitted on CD or via email. Vector files (EPS) should, if possible, include fonts. Match proofs are

essential when submitting digital files as they represent the colour balance approved by the author(s).

Transparencies, photographs and high quality printouts can also be submitted. It is recommended that authors retain copies of all illustrations because of the risk of loss or damage either during the printing process or in transit.

Diagrams must be of a professional quality and prepared in dense black ink on a good quality surface. Original illustrations will not be returned unless specifically requested.

All illustrations (maps, diagrams and pictures) are numbered consecutively with Arabic numerals and labelled Figure 1, Figure 2, etc. All illustrations are referred to as 'Figures'.

Tables Must be typed double spaced, using few horizontal rules and no vertical rules. They are numbered consecutively with Roman numerals (Table IV, etc.). Titles should be concise, but as independently informative as possible. The approximate position of the Table in the text should be marked in the margin of the typescript.

Notes and References Authors may choose one of two systems:

(1) The Harvard system in which the authors' names (no initials) and dates (and specific pages, only in the case of quotations) are given in the main body of the text, (e.g. Collins, 2001,341). References are listed alphabetically at the end of the paper under the heading References.

(2) The system in which superscript numbers are inserted in the text (e.g. ... to which Collins refers.³) and referred to in numerical order at the end of the paper under the heading Notes. Informational notes must be restricted to the minimum; usually the material can be incorporated in the text. If absolutely necessary both systems may be used.

References in both systems should be set out as follows, with double spacing for all lines.

Papers Collins, A.T., 2001. The colour of diamond and how it may be changed. *J.Gemm.*, 27(6), 341-59

Books Balfour, I., 2000. Famous diamonds. 4th edn. Christie's, London. p.200

Abbreviations for titles of periodicals are those sanctioned by the World List of scientific periodicals 4th edn. The place of publication should always be given when books are referred to.



The Journal of
Gemmology

Volume 30 No. 1/2
January/April 2006

Contents

The Usambara effect and its interaction with other colour change phenomena A Halvorsen	1	The identification value of the 2293 cm ⁻¹ infrared absorption band in natural and hydrothermal synthetic emeralds J M Duroc-Danner	75
Determination of the origin of blue sapphire using Laser Ablation Inductively Coupled Plasma Mass Spectrometry (LA-ICP-MS) A Abduriyim and H Kitawaki	23	Surface coating of gemstones, especially topaz – a review of recent patent literature K Schmetzer	83
Rubies with lead glass fracture fillings C C Milisenda, Y Horikawa, Y Manaka and U Henn	37	Gem minerals from the Saranovskoye chromite deposit, western Urals E M Spiridonov, M S Alferova and T G Fattykhov	91
A note on a pearl attached to the interior of <i>Crassostrea virginica</i> (Gmelin, 1791) (an edible oyster, common names, American or Eastern oyster) K Scarratt, C Pearce and P Johnson	43	Letters to the Editor	103
A short review of the use of 'keshi' as a term to describe pearls H A Hänni	51	Abstracts	106
A new type of Tairus hydrothermally-grown synthetic emerald, coloured by vanadium and copper K Schmetzer, D Schwarz, H-J Bernhardt and T Häger	59	Book Reviews	114
		Proceedings of the Gemmological Association and Gem Testing Laboratory of Great Britain and Notices	116

Cover Picture: A green Usambara effect (UE) tourmaline turns red when placed on top of another green UE tourmaline.
(See The Usambara effect and its interaction with other colour change phenomena, p.1)

The Gemmological Association and Gem Testing Laboratory of Great Britain

Registered Office: Palladium House, 1-4 Argyll Street, London W1F 7LD